NON-IMMUNE ISLET BETA CELL SUSCEPTIBILITY TO FAILURE IN NOD^{K} MICE

Ainy Khan Hussain

December 2017

A thesis submitted for the degree of Doctor of Philosophy

The Australian National University

Graduate Program in Medicine,
The Medical School,
The Australian National University, Canberra

Statement

The research contained within this thesis was performed in the Endocrinology and Diabetes Research Unit, under the supervision of Professor Christopher Nolan and co-supervision of Dr. Viviane Delghingaro-Augusto. The data presented is my own work, with all contributions from others clearly stated in the acknowledgements and methods.

Contribution

The blind-assessment of pancreas sections for histological sections; H&E and immunohistochemistry was performed by Professor Jane Dahlstrom, Professor of Anatomical Pathology, ANU Medical School and Senior Staff Specialist in Pathology, ACT Pathology at The Canberra Hospital

This thesis is dedicated to Hussain, Haider Hussain and Ali Hussain for their never-ending love, support and encouragement.

Acknowledgements

Thanks to All Mighty Allah that I am able to submit my thesis for the degree of Ph.D.

I would like to recognize from the bottom of my heart the prayers of my mother and my late father who have blessed me always in every walk of my life.

I would like to give my sincere thanks to my supervisor Prof. Christopher Nolan for accepting me as his student, offering me guidance, advice and knowledge to carry on the project and for showing consistent patience throughout the course of supervision. Thanks Chris, for your kind support and help for leading me in the right direction, without your help I could not have finished my research successfully.

I would like to express my deepest gratitude to my co-supervisor, Dr. Viviane Delghingaro-Augusto for teaching me her excellent lab skills and for being a superb mentor during my research candidature. Her exceptional guidance, experienced advice and timely suggestions always helped me in working around difficulties and increased my abilities to become an able and more confident researcher. She is responsible for maintaining a superb atmosphere for doing research in the laboratory. I could have never achieved my research goals without her kind supervision.

I am thankful for the Australian National University for awarding me the Post-graduate Scholarship for the course of Ph.D. I also acknowledge the NHMRC grant, awarded to Prof. Nolan which partly funded this research.

Furthermore, I thank Prof. Christopher Goodnow, for providing NOD^{k} mice for the initial experiments.

Many thanks to my panel members: Dr Charmaine Simeonovic, Department of Immunology, JCSMR, ANU and A/Prof Ross Laybutt, Garvan Institute of Medical Research, NSW; for their active participation in discussions relating to my project and providing their valuable ideas. I appreciate them for making time and for their expert opinions and suggestions from the very beginning of this research journey.

My very special acknowledgement to the diligent and helpful staff of the animal facility at The Canberra Hospital (TCH). Their hard work, dedication, experience and support made it possible for me to work with the mice colonies and spend countless hours in the facility without any difficulty.

My sincere thanks to fabulous facility staff; Ayumi Hosaka, Delia James, Zsuzsa Pasztor and Ken Chau. Thank you guys for taking great care of the mice of this project.

I would also like to convey my special thanks to the Canberra Hospital support staff; Bee Souvannaphong and Ayumi Hosaka for maintaining a very safe and comfortable research environment to work. I would also like to acknowledge the efforts and guidance of Dr. Hannah Clark, Director Research Operations, TCH, for providing and implementing safety guidelines in the research areas.

I would like to take time to pay my gratitude to our previous laboratory technician; Ms. Hana Kaori, who kindly and generously aided me to become comfortable and familiar in the new laboratory setting. Also, she actively assisted me in working with the large cohorts of mice experiments.

For histology, I would like to acknowledge the work of Ms. Elaine Bean from ACT Pathology at TCH for generating the H&E slides for this project.

Additionally, my humble thanks goes to Associate Director of HDR; Assoc. Prof. Krisztina Valter-Kosci for her kind assistance, guidance and availability for my Ph.D candidature. I also very much appreciate the assistance of Dr. Inger Mewburn, Director of Research Training, ANU, who gave me the opportunity to join the 'Thesis Writing Boot Camp'. Her skills and experience in research provided me with the motivation to write and enabled me to finish my thesis in time. Also thanks to Dr. Teresa Neuman and Dr. Bruce Shadbolt for statistical consultation.

I convey special acknowledgement to my research group colleagues; Tenzin Dagpo, Carina Bertoldi Franco and Ayumi Hosaka, who have supported me throughout this journey. They provided me with their very pleasant company and have proved to be wonderful people by all means.

I also acknowledge Dr. Louis Socha (late) who initiated the work on NOD^{k}.insHEL mice, which provided a strong base to continue the work, but in a different direction.

Last but not least, this Ph.D would not have been possible without my life-partner's help and support. I could not have done this degree if he had not have encouraged me to go ahead and finish it. He has always been there whenever I needed him and he understood the demands and commitments of research. He showed persistent confidence in me. Words fail to express my appreciation for my husband Hussain; whose dedication, love and persistent confidence in me, has taken the load off my shoulders. My love goes out to my little boys, Haider Hussain and Ali Hussain, who have spent countless hours without their mother, when she dedicated her time for long hours over the project.

Abstract

Non-immune islet β-cell susceptibility to failure in NOD^{k} mice

NOD^{k} mice are congenic for the protective MHC H2^{k} (*Idd 1* locus) and unlike NOD mice do not develop autoimmune diabetes. The aim of the study was to determine if NOD^{k} β-cells have a non-immune islet β-cell defect that may be revealed by stressing the islets with high fat diet (HFD). B10^{k} (B10.Br mice with H2^{k} haplotype) and Balb/c mice were used as comparator groups.

Male NOD^{k}, B10^{k} and Balb/c mice were fed chow or HF diets from 4 weeks of age for 10 weeks (short-term study) and 20 weeks (long-term study). Body weight and 9 AM fed-state blood glucose levels were measured fortnightly. At 13 and 23 weeks of age intraperitoneal glucose tolerance tests (ipGTT) were performed for both studies. NOD^{k} mice were refreshed by backcrossing on to NOD mice (NOD^{k}-REF) and preliminary experiments were performed to determine the effects of HF-feeding. NOD^{k}-REF mice were also fed chow or HF-diet from weaning, with fortnightly body weight and fed-state blood glucose measurements, and ipGTTs were performed after 9 and 20 weeks on diets. At sacrifice, the pancreases were harvested for histological assessment, including; islet morphology, islet inflammation, β-cell apoptosis, insulin immunohistochemistry and β-cell mass measurement.

Despite excellent glucose tolerance at all ages on chow diet, HF-fed NOD^{k} mice developed diet-induced obesity, profound hyperinsulinemia and diabetes by 13 weeks of age. Severe hyperglycaemia caused several NOD^{k} mice to be euthanased prior to completing the long-term study. B10^{k} mice had poor glucose tolerance on chow diet only, but despite some HF-diet induced excessive weight gain, they did not develop

severe hyperinsulinemia or progress onto diabetes. Balb/c mice maintained excellent glucose tolerance on both diets. Analyses of the pancreas histology does not indicate that diabetes in the HF-fed NOD^{k} mice is due to insulitis. Islet β-cell mass initially increased in HF-fed NOD^{k} mice, but finally began to decrease in the long-term cohort, accompanied by the presence of occasional apoptosis in endocrine cells in the islets of these mice.

The pancreas histological features of the B10^{k} and Balb/c mice did not indicate failure of β-cell mass compensatory effects with HF-feeding.

Many of the effects of HF-feeding of NOD^{k} mice were seen in the HF-fed NOD^{k}-REF mice, except for the development of diabetes. This suggests that the NOD^{k} mice have an additional islet β-cell susceptibility to failure compared to the NOD^{k}-REF mice. These preliminary results indicate that a major diabetes susceptibility factor present in the NOD^{k} mice, important for type 2 diabetes (T2D) development, is not necessary for the development of type 1 diabetes (T1D).

In conclusion, NOD^{k} mice are prone to a severe type 2 diabetes (T2D) phenotype when fed a HF-diet. Underlying non-immune islet susceptibility factors may contribute to the propensity of NOD mice to develop T1D and the NOD^{k} mice to develop T2D. These results are also consistent with the β-cell overwork hypothesis in diabetes pathogenesis as seen in NOD^{k} mice. In addition, these results show that β-cell underwork or "lazy" β-cells in B10^{k} mice may protect them from more severe failure.

Conferences and Meetings attended

Oral Presentations:

- **Non-immune islet β-cell susceptibility to failure in NOD^{k} mice**
  The Australian Society of Medical Research (ASMR), New Investigators Forum (NIF), 3rd June 2014.

- **Non-immune islet β-cell susceptibility to failure in NOD^{k} mice**
  Canberra Health Annual Research Meeting (CHARM), August 12th -15th, 2014.

Poster Presentations:

- ***Ainy K. Hussain,*** Viviane Delghingaro-Augusto, Christopher J. Nolan. The B10^{k} mouse has poor glucose tolerance but is resistant to developing type 2 diabetes: the lazy islet β-cell hypothesis. Canberra Health Annual Research Meeting (CHARM), 9-12 August, 2016-p.100 # L9.

- ***Ainy K. Hussain,*** Viviane Delghingaro-Augusto, Christopher J. Nolan. The B10^{k} mouse has poor glucose tolerance but is resistant to developing type 2 diabetes: the lazy islet β-cell hypothesis. The Australian Society of Medical Research (ASMR), New Investigators Forum (NIF), 8th June, 2016-p.40 #12-P.

- **Ainy *K. Hussain,*** Viviane Delghingaro-Augusto, Christopher J. Nolan. Gliclazide treated B10^{k} mice are protected from high fat diet-induced diabetes. The Australian Society of Medical Research (ASMR), New Investigators Forum (NIF), 3rd June, 2015-p.39 #13-P.

- **Ainy *K. Hussain,*** Tenzin D. Dagpo, Viviane Delghingaro-Augusto, Christopher J. Nolan. NOD^{k} mice develop obesity, hyperinsulinemia and severe hyperglycaemia when fed a high fat diet without evidence of loss of β-cell mass. Islet society and Australian Islet study group, VIII annual scientific meeting,Sydney, Australia - July 19th-21st 2015-p.59,#29-P

- **Ainy *K. Hussain,*** Tenzin D. Dagpo, Viviane Delghingaro-Augusto, Christopher J. Nolan. NOD^{k} mice develop obesity, hyperinsulinemia and severe hyperglycaemia when fed a high fat diet without evidence of loss of β-cell mass- Canberra Health Annual Research Meeting (CHARM), August 11th -14th, 2015-p.93 #72-P

- ***Ainy K. Hussain,*** Viviane Delghingaro-Augusto, Christopher J. Nolan. NOD^{k} mice develop obesity, hyperinsulinemia and severe hyperglycaemia when fed a high fat diet - a new murine model of type 2 diabetes. Australian Diabetes Society (ADS) and the Australian Diabetes Educators Association (ADEA) meeting, Melbourne 27th-29th August 2014.

- Delghingaro-Augusto **V**, Socha LA, ***Khan A***, Chan JY, Laybutt DR, Nolan CJ Susceptibility of NOD^{k} compared to C56BL/10 mice to non-immune islet β-cell failure due to greater susceptibility to endoplasmic reticulum stress. 74th American Diabetes Association Scientific Sessions, San Francisco, USA – June 13th-19th 2014, #2109-P.

- Delghingaro-Augusto V, Socha LA, ***Khan A***, Chan JY, Laybutt DR, Nolan CJ NOD^{k} compared to C56BL/10 mice are more prone to islet β-cell failure due to greater susceptibility to endoplasmic reticulum stress. Australian Diabetes Society & Australian Diabetes Educators Association – Annual Scientific Meeting, Sydney, Australia – 27th-29th August, 2014 – p.132, #102-OR.

Abbreviation

Ach:	acetylcholine
Ach-R:	acetylcholine receptor.
ADP:	adenosine diphosphate
ARC:	Animal Resource Centre
ATP:	adenosine triphosphate
$B10^k$:	B10.BR-H2K2H2-T18a/SgSnJArc
$B10^k$.insHEL:	$B10^k$ transgenic
BETA2:	beta-cell E-box transactivator 2
BSA:	BSA phosphate buffer
CoA:	coenzyme A
C-peptide:	connecting peptide
CTS:	cataract Shionogi sublines
Cyclic AMP:	Cyclic adenosine monophosphate
DAB:	3,3'-Diaminobenzidine
DAG:	diacylglycerides
DPP:	diabetes prevention program
EDTA:	ethylenediaminotetraacetic acid
ER:	endoplasmic reticulum
FA:	fatty acid
FBS:	fetal bovine serum
FFAR1:	free fatty acid receptor 1
GABA:	γ-amino butyric acid
GHS-R1a:	growth hormone secretagogue receptor type 1a
GIP:	gastrointestinal inhibitory polypeptide
GIP-R:	gastric inhibitory polypeptide receptor
GL:	glycerolipid
GLP-1:	glucagon-like peptide 1
GLP-2:	glucagon-like peptide 2

GLUT-4:	insulin-sensitive glucose transporter-4
GSIS:	glucose-stimulated insulin secretion
$H_2O_{2:}$	hydrogen peroxide
HEL:	Hen Egg lysosomal
HFD:	high fat diet
HLA:	Human Leukocyte Antigen
HNF:	hepatocyte nuclear factor
HRP:	horse-radish peroxidase
IAPP:	islet amyloid polypeptide
Idd:	insulin dependent diabetes
IGT:	impaired glucose tolerance
IPF-1:	insulin promoter factor 1
ipGTT:	Intraperitoneal glucose tolerance test
ipITT:	Intraperitoneal insulin tolerance tests
IRS-1:	insulin receptor substrate-1
LC-CoA:	long-chain acyl-CoA
MAG:	monoacylglycerides
Mal-CoA:	malonyl-CoA
MCFs:	metabolic coupling factors
MHC:	major histocompatibility complex
MODY:	maturity onset diabetes of the young
MODY2:	Glucokinase-related MODY
NADPH:	nicotinamide adenine dinucleotide phosphate
NBF:	neutral buffered formalin
NEFA:	Non-esterified fatty acids
NeuroD1:	neurogenic differentiation factor 1
NGT:	normal glucose tolerance
NK:	natural killer
NOD:	Non-Obese Diabetic mouse
NOD^k :	NOD.BR-*H2*^{k}/WickerANU

NOD^k.insHEL:	NOD^k transgenic
NOD^k-REF:	NOD^k-Refreshed
NPY:	neuropeptide Y
OAA:	oxaloacetate
ob/ob:	obese mouse
PBS:	phosphate buffered saline
PC:	prohormone convertases
PC:	pyruvate carboxylase
PDH:	pyruvate dehydrogenase
PEG:	polyethylene glycol-sodium phosphate buffer
PP:	pancreatic polypeptide
PYY:	peptide YY
REF:	Refreshed
rER:	rough endoplasmic reticulum
RIA:	insulin radioimmunoassay
SNPs:	single-nucleotide polymorphisms
SRP:	signal recognition particles
SSN-R:	somatostatin receptor
SST:	somatostatin
SUR1:	sulphonylurea receptor
TG:	triacylglycerides
TMB:	3',5,5'-tetramethylbenzidine
α-ADR-R:	α2-adrenergic receptor
α-cells:	alpha cells
δ-cells:	delta cells
$\Delta\psi m$:	change in plasma membrane potential
β-cell:	beta-cell

TABLE OF CONTENTS

CHAPTER # 1: INTRODUCTION & LITERATURE REVIEW ---------- 19

1.1 INTRODUCTION ---------- 20

1.2. Research hypothesis and objectives ---------- 22
1.2.1. Hypothesis ---------- 22
1.2.2. Objectives of the study ---------- 22
1.2.2.1. Overall objective ---------- 22
1.2.2.2. Specific objectives ---------- 22

1.3. Literature Review ---------- 24
1.3.1. Diabetes: an overview ---------- 24
1.3.1.1. Type 1 Diabetes ---------- 25
1.3.1.1.1. Major histocompatibility complex (MHC) and type 1 Diabetes -- 26
1.3.1.2. Type 2 Diabetes ---------- 27
1.3.1.2.1. Pathophysiology of Type 2 Diabetes ---------- 28
1.3.1.2.2. Genetic factors in type 2 diabetes ---------- 29
1.3.2. Pancreas and its hormones ---------- 31
1.3.2.1. Pancreas ---------- 31
1.3.2.2. Hormones of the pancreas ---------- 32
1.3.2.2.1. Alpha cell hormone: glucagon ---------- 32
1.3.2.2.2. Delta cells hormone: somatostatin ---------- 33
1.3.2.2.3. PP cells hormone: pancreatic polypeptide ---------- 34
1.3.2.2.4. Epsilon cells hormone: ghrelin ---------- 35
1.3.2.2.5. β–cell hormones: insulin and amylin ---------- 35
1.3.3. Insulin structure and function ---------- 36
1.3.3.1. Insulin structure ---------- 36
1.3.3.2. Insulin secretion ---------- 37
13.3.3. Islet β-cell mass ---------- 38
1.3.3.4. The insulin receptor and insulin function ---------- 40
1.3.4. The mechanisms of insulin secretion ---------- 41
1.3.4.1. Mechanisms of nutrient-stimulated insulin secretion ---------- 42
1.3.4.1.1. K+-ATP channel dependent pathway ---------- 42
1.3.4.1.2. The anaplerosis amplification pathway ---------- 43
1.3.4.1.3. The glycerolipid/fatty acid cycling amplification pathway ---------- 44
1.3.4.1.4. Other mediators of insulin secretion ---------- 45

1.3.5. Animal models ---------- 47
1.3.5.1. NOD^{k} congenic mice ---------- 47
1.3.5.2. NOD^{k}.insHEL transgenic mice ---------- 48
1.3.5.3. B10^{k} congenic mice ---------- 49
1.3.5.4. Balb/c ---------- 50

CHAPTER # 2: MATERIALS & METHODS---**51**

2.1. INTRODUCTION ---**52**

2.2. Animal sources, diet and housing ---**52**

2.3. Fortnightly measurement of body weight and blood glucose ---**53**

2.4. Intraperitoneal glucose tolerance test (ipGTT) ---**54**

2.5. Intraperitoneal insulin tolerance test (ipITT) ---**55**

2.6. Euthanasia and tissue harvesting ---**56**
2.6.1. Blood collection ---56
2.6.2. Anaesthesia, cardiac blood collection and euthanasia ---56
2.6.3. Tissue dissection ---57
2.6.3.1. Pancreas ---57
2.6.3.2. Liver ---58
2.6.3.3. Adipose tissue ---58

2.7. Blood Analytical analysis ---**58**
2.7.1. Insulin radioimmunoassay (RIA) ---58
2.7.2. Plasma non-esterified fatty acids (NEFA) ---60
2.7.3. Plasma Triglyceride (TG) ---61
2.7.4. Plasma Proinsulin ---61
2.7.5. Plasma C-peptide ---63
2.7.6. Adiponectin ---63

2.8. Histological analysis---**65**
2.8.1. Haematoxylin and eosin (H&E) staining and scoring ---65
2.8.3. Measurement of β-cell mass ---68

CHAPTER # 3: RESULTS (SHORT TERM STUDY) ---**69**

3.1. INTRODUCTION ---**70**

3.2. Experimental design ---**70**

3.3. Results ---**72**
3.3.1. Body weight measurement---72
3.3.2. Tissue weight measurement ---76
3.3.3. Non-fasting blood glucose measurement ---81
3.3.4. ipGTT ---84
3.3.5 Measurement of plasma insulin levels during ipGTT ---88

3.3.6. Measurement of non-fasting plasma insulin and derivatives ---- 92
3.3.7. Measurement of adiponectin ---- 96
3.3.8. Measurement of Non Esterified Free Fatty Acid (NEFA) ---- 98
3.3.9. Measurement of TG ---- 100

3.4. Discussion ---- **102**
3.4.1 Mouse body and tissue weights ---- 102
3.4.2. Non-fasting blood glucose and glucose tolerance ---- 104
3.4.3. Insulin levels and insulin derivatives ---- 105
3.4.4. Plasma lipid and adiponectin levels ---- 107

3.5. Summary ---- **109**

CHAPTER # 4: RESULTS (LONG TERM STUDY) ---- **110**

4.2. Experimental design ---- **112**

4.3. Results ---- **114**
4.3.1 Body weight measurement ---- 114
4.3.2. Non-fasting blood glucose measurement ---- 118
4.3.3. ipITT ---- 122
4.3.4. ipGTT ---- 126
4.3.5. Measurement of plasma insulin levels during ipGTT ---- 130
4.3.6. Measurement of non-fasting plasma insulin and derivatives ---- 134
4.3.7. Measurement of Non Esterified Free Fatty Acid (NEFA) ---- 140
4.3.8. Measurement of TG ---- 142

4.4. Discussion ---- **144**
4.4.1. Mouse body weights ---- 144
4.4.2. Non-fasting blood glucose and glucose tolerance ---- 145
4.4.3. Insulin levels and insulin derivatives ---- 146
4.4.4. Insulin sensitivity measurements ---- 147
4.4.4. Plasma lipid levels ---- 147
4.4.5. Propensity of different strains to diet-induced diabetes ---- 148

4.5. Summary ---- **150**

CHAPTER # 5: RESULTS (HISTOLOGY) ---- **151**

5.1. INTRODUCTION ---- **151**

5.2. Experimental approach ---- **153**

5.3. Results ---- **154**
5.3.1. Assessment of islet inflammation ---- 154
5.3.2. Pancreatic fat deposits ---- 155

5.3.4. Assessment of pancreas sections immuno-stained for insulin and measurement of islet β-cell mass ---------- 170

5.4. Discussion ---------- **181**
5.4.1 Pancreas inflammation ---------- 182
5.4.2 Islet endocrine cell apoptosis and islet β-cell mass ---------- 183
5.4.3. Pancreatic fat deposits ---------- 184
5.5. Summary ---------- 185

CHAPTER # 6: NOD^{K} REFRESHED (NOD^{K}-REF) MICE ---------- **187**

6.1. INTRODUCTION ---------- **189**

6.2. Experimental plan ---------- **190**

6.3. Results ---------- **192**
6.3.1. Body weight measurement ---------- 192
6.3.2. Non-fasting blood glucose measurement ---------- 194
6.3.4. ipGTT- glucose results ---------- 196
6.3.5. ipGTT-plasma insulin results ---------- 199
6.3.6. Non-fasting insulin measurement ---------- 202

6.4. Discussion ---------- **203**

CHAPTER # 7: FINAL DISCUSSION AND FUTURE DIRECTIONS ---------- **206**

7.2. LIMITATIONS ---------- **211**

7.3. FUTURE DIRECTIONS ---------- **212**

8.0. REFERENCES ---------- **214**

APPENDIX I ---------- **224**

APPENDIX 2 ---------- **225**

APPENDIX 3 ---------- **226**

Chapter#1:

Introduction & Literature Review

1.1 Introduction

Type 1 diabetes results from the destruction of insulin-producing pancreatic islet β-cell by a β-cell-specific autoimmune process. Cytotoxic T cells are believed to be particularly important in this process, but β-cell autoantigens, and other immune effector cells such as macrophages/dendritic cells and B lymphocytes are also involved (Mannering et al., 2016). Genetic susceptibility is believed to be an essential component type 1 diabetes to develop (She and Marron, 1998). The genetic susceptibility is most strongly carried within a restricted set of class II major histocompatibility complex (MHC) alleles (Yoon and Jun, 2005). The autoimmune assault against the β-cell causes progressive β-cell death with 70-80% reduction in the β-cell mass by the time of diagnosis (Thomas et al., 2009). Thus, type 1 diabetes is considered to be primarily a result of dysfunction of the immune system directed at islet β-cells.

The pathogenesis of type 2 diabetes is more variable, with different degrees of β-cell failure along with varying degrees of insulin resistance (Cnop et al., 2005, Nolan et al., 2011). Overweight and obesity results in insulin resistance which needs to be compensated by increased insulin secretion for normoglycaemia to be maintained. If this compensatory islet β-cell response fails, glucose intolerance develops which is later followed by type 2 diabetes (Turner et al., 1995, Nolan et al., 2011).

The mechanisms underlying the development of islet β-cell failure in type 2 diabetes are believed to be very different to those causing type 1 diabetes. It results from a combination of reduced islet β-cell function and loss of β-cell mass (Butler et al., 2003, Nolan et al., 2011). However, there is clearly marked heterogeneity in the pathogenesis of the β-cell failure. This is likely to depend on the effects of both genetic background and life-style factors such as diet and exercise (Nolan et al., 2011). There has also been

recent interest into the potential role of the immune system and islet inflammation in β-cell failure in type 2 diabetes (Donath et al., 2013).

With improved technologies in determining genetic origins of diabetes, there is increasing evidence of marked genetic heterogeneity underlying both type 1 and type 2 diabetes and increased interest in overlap of the two conditions, with the likelihood of some common mechanisms in β-cell failure in both types of diabetes being high (Nolan and Delghingaro-Augusto, 2014, Tuomi et al., 2014, Cnop et al., 2013, Eizirik et al., 2012). It is well recognised that islet β-cells in type 2 diabetes almost certainly have intrinsic non-immune susceptibilities to failure. Unknown is if these same non-immune susceptibility factors contribute to the pathogenesis of type 1 diabetes (Nolan and Delghingaro-Augusto, 2014).

The non-obese diabetic (NOD) mouse has been a key animal model for studying type 1 diabetes. NOD mice develop autoimmune diabetes at a high rate (70-90% in females, 10-40% in males) by 4-6 months of age. Genetic studies in these mice have identified more than 20 insulin dependent diabetes (*Idd*) loci, many of which have been shown to have effects on the immune system. The strongest individual locus in NOD mice is *Idd1* containing the major histocompatibility gene (MHC) complex, *H2* (Wicker et al., 1995, Thayer et al., 2010). Of relevance to this thesis, congenic replacement of the high risk $H2^{g7}$ MHC haplotype with the low risk allele $H2^{k}$ in NOD mice prevents them from developing insulitis and type 1 diabetes (Podolin et al., 1993, Dooley et al., 2016).

From previous work from my laboratory on NOD^{k} mice that are congenic for this low risk $H2^{k}$ MHC (thus the nick-named NOD^{k} mice), we believe that NOD mice do have a non-immune β-cell susceptibility (Dooley et al., 2016). In that work, the effects of stressing the islet β-cells of NOD^{k} and B10.Br mice (nick-named $B10^{k}$, as they have the same low-risk MHC) by islet β-cell specific transgenic expression of modified Hen Egg

lysosomal (HEL) was assessed (insHEL transgenic mice). Expression of the HEL transgene in β-cells driven by the insulin promoter resulted in β-cell stress in all transgenic mice (male and female NOD^k.insHEL and $B10^k$.insHEL), however, diabetes developed in male NOD^k.insHEL mice only. This diabetes was not a consequence of islet autoimmune damage, but islet β-cell apoptosis and loss of β-cell mass was seen in these mice (Dooley et al., 2016). As the $B10^k$ mice did not develop diabetes, despite this β-cell stress, the conclusion was that NOD mice have a non-immune β-cell defect, most likely of genetic origin (Dooley et al. 2016). The work of this thesis takes these findings further.

1.2. Research hypothesis and objectives

1.2.1. Hypothesis

Non-immune β-cell susceptibility factors contribute in the initiation of β-cell damage and pathogenesis of type 1 diabetes in NOD mice.

1.2.2. Objectives of the study

1.2.2.1. Overall objective

The primary objective of the project was to utilise the effects of high fat feeding rather than a molecular islet stressor (HEL transgene) to determine if a susceptibility defect of a non-immune nature is present in islet β-cells of the NOD^k mouse.

1.2.2.2. Specific objectives

In order to achieve the primary objective of the thesis, the following specific objectives or aims were formulated:

1. To study the metabolic characteristics of NOD^k mice, along with two comparison strains (B10^k and Balb/c), after 10 weeks of chow and high fat diet feeding from the time of weaning (short-term study).
2. To study the metabolic characteristics of NOD^k mice, along with two comparison strains (B10^k and Balb/c), after 20 weeks of chow and high fat diet feeding from the time of weaning (long-term study).
3. To study the histology of the pancreases of NOD^k, B10^k and Balb/c mice after 10 and 20 weeks of chow and high fat diet feeding, with particular interest on islet morphology, islet inflammation, β-cell apoptosis and β-cell mass measurement.

This thesis is divided into 7 chapters: Chapter 1 provides an introduction to the research, and literature review on diabetes, role of insulin in the pathogenesis of diabetes, its function, processing and steps involved in the secretion of insulin. This chapter also briefly discusses about the mice models used in the study. Chapter 2 provides a complete description of the procedures and experimental set-ups used in this study. Chapter 3 describes the metabolic results and discussion obtained from the characterisation of mice strains during a short-term study (10 weeks on chow or high fat (HF) diet post-weaning). Chapter 4 describes the metabolic results and discussion obtained from the characterisation of mice strains during a long-term study (20 weeks on chow or high fat (HF) diet post-weaning). Chapter 5 describes the histological analyses of the pancreases at the time of harvest, along with the results of β-cell mass, for mice of both the short and long-term studies. Chapter 6 shows the results from a preliminary study of a refreshed NOD^k mice colony (NOD^k-REF). The final chapter, Chapter 7, is a discussion of the overall findings of the thesis research, highlighting its significance, reflecting on its limitations and finally some concluding remarks and recommendations related to the future research direction.

1.3. Literature Review

Briefly, this literature review is sub-divided into five sections, addressing:

I. Diabetes an overview
II. Pancreas and its hormones
III. Insulin structure and function
IV. The mechanisms of insulin secretion
V. Introduction to the animal models used in this thesis

1.3.1. Diabetes: an overview

Diabetes mellitus (Diabetes) is a chronic condition marked by high levels of glucose in the blood. This condition is caused by the inability of the β-cell of pancreas to produce insulin or of the insulin that is produced to be effective, or both (Assal and Groop, 1999).

Diabetes is undoubtedly one of the most challenging health problems in the 21st century. Diabetes is on the rise in Australia and across the world, and at times it is referred as an epidemic (Barr et al., 2006, Colagiuri et al., 2006). Lifestyle related factors such as eating disorder, obesity and inactive lifestyle play a contributory role in the onset of type 2 diabetes. In recent years, there has been progress in the development of behavioural strategies to modify these lifestyle behaviours for the prevention and treatment of the disease (Wing et al., 2001).

Diabetes mellitus comprises a series of clinically and genetically heterogeneous disorders of carbohydrate, fat and protein metabolism, with the common characteristic of hyperglycaemia. The prevalence of diabetes increases with age, from less than 1% of

western populations affected before age 20 to more than 13% above age 75. Approximately 90% of adult patients with diabetes have type 2 diabetes, previously referred to as non-insulin dependent, in which the hyperglycaemia is caused by a failure of insulin secretion to sustain compensation for insulin resistance. Sustained hyperglycaemia can lead to a number of medical complications broadly classified into macrovascular (coronary artery disease, peripheral arterial disease and stroke) and microvascular categories.

1.3.1.1. Type 1 Diabetes

Type 1 diabetes, previously termed juvenile-onset or insulin-dependent diabetes, is an autoimmune disease and a metabolic disorder characterized by T-cell-mediated destruction of pancreatic β cells, resulting in insulin deficiency and hyperglycaemia. The aetiology of type 1 diabetes is thought to include a genetic predisposition which interacts with environmental factors with distinctive phases of initiation, development and progression of the disease (Burn, 2010).

Type 1 diabetes research is focussed partly by the search for environmental "triggers" of the disease (Todd, 2010). The environmental risk determinants can be classified into three groups: viral infections (e.g. coxsackievirus and cytomegalovirus), early infant diet (e.g. breast feeding versus early introduction of cow's milk components), and toxins (e.g. N-nitroso derivatives) (Atkinson and Eisenbarth, 2001). Treatment for type 1 diabetes is exogenous insulin therapy guided by monitoring of blood glucose levels (Tamborlane et al., 2008). Optimally insulin therapy should be "intensive" consisting of three or more daily injections of insulin or delivery of insulin by an external insulin pump. Dose adjustments are based on at least four self-monitored glucose measurements per day. Intensive diabetes therapy has found to have long-term beneficial effects on type 1 diabetes, particularly microvascular, but with longer-term

follow-up, also macrovascular complications rates (Nathan DM et al., 1993, Nathan DM et al., 2005).

1.3.1.1.1. Major histocompatibility complex (MHC) and type 1 Diabetes

In humans, the MHC is known as the HLA, (Human Leukocyte Antigen) complex and contains over 200 genes. It is located on chromosome 6 and encodes HLA class I and class II molecules. The main function of these molecules, which are heterodimers made up of α and β chains, is to present antigens that have been processed into peptides to antigen-specific receptors on CD4+ and CD8+T lymphocytes. Class I molecules are expressed on most nucleated cells, and are encoded by genes within the HLA-A, B, and C loci, whereas class II molecules, are primarily expressed on antigen presenting cells and are encoded by genes within the HLA-DP, -DQ, and -DR loci (Notkins, 2002). While the MHC class II genotype is one of the strongest factors determining susceptibility to type 1 diabetes, it has long been apparent that susceptibility at MHC class II is a necessary but not sufficient predisposing genetic factor (Bertrams and Baur, 1985).

The NOD mouse spontaneously develops autoimmune type 1 diabetes; it is a key animal model for the study of autoimmune destruction of islet β-cells. Multiple genes are involved in the development of diabetes and the MHC region of the NOD mouse encompasses an *Idd* gene, termed *Iddl.* The NOD allele at *Idd1* is $H2^{g7}$, a dominant gene, which is strongly associated with insulitis and spontaneous diabetes (Wicker et al., 1992, Podolin et al., 1993, Wicker et al., 1995).

Destruction of β-cells in the NOD mouse occurs by penetration of mononuclear infiltrates, primarily of $CD4^+$ T cells, along with $CD8^+$ T cells, however, NK (natural killer) cells, B cells, dendritic cells, and macrophages can also be identified in the

lesions (Makino et al., 1980a). However, NOD disease is primarily dependent on $CD4^+$ and $CD8^+$ T cells (Bach, 1994).

1.3.1.2. Type 2 Diabetes

Type 2 diabetes mellitus is a chronic metabolic disorder that results from defects in both insulin secretion and insulin action (DeFronzo, 1999, Nolan et al., 2011). A steady rise in plasma glucose occurs irrespective of the degree of control or type of treatment (Turner et al., 1998). Type 2 diabetes results from the interaction between environmental risk factors, such as modern life style, abundant nutrient supply and reduced physical activity and also genetic predisposition (Prentki and Nolan, 2006a). Although the genetic basis of type 2 diabetes is yet to be fully elucidated (Tuomilehto et al., 2001), certain environmental and lifestyle factors, such as reduced physical activity poor diet quality, are likely non genetic determining factors (Zimmet, 1988). Diet is known to influence body weight and thus is recognized as a modifiable risk factor for type 2 diabetes (Meyer et al., 2000). There are number of prospective randomised controlled studies such as the Diabetes Prevention Program (DPP) in the USA (Knowler et al., 2002), the 6 years Malmo feasibility study (Eriksson and Lindgärde, 1991), and the Finnish Diabetes Prevention Study (Tuomilehto et al., 2001), that showed that lifestyle modification involving diet and enhanced physical activity helps to delay or prevent the progression of impaired glucose tolerance (IGT) to diabetes. The Nurses' Health Study performed on a large cohort of middle-aged women, suggest that the majority of cases of type 2 diabetes could be prevented by weight loss, regular exercise, modification of diet, abstinence from smoking, and the consumption of limited amounts of alcohol (Hu et al., 2001). Similarly a 6 year follow up study of older Iowa women support inverse associations between total and whole-grain intake and risk of incident diabetes (Meyer et al., 2000). Dietary fibre is reported to improve the

postprandial glycaemic response and insulin concentrations, most likely by slowing the digestion and absorption of food and by regulating several metabolic hormones (Vinik and Jenkins, 1988).

1.3.1.2.1. Pathophysiology of Type 2 Diabetes

Type 2 diabetes is characterised by hyperglycaemia as a consequence of failed islet β-cell compensation for insulin resistance, most often in subjects who are overweight or obese (Nolan et al., 2011). For years the hyperglycaemia was put down relatively simply to a failure of insulin-induced uptake into peripheral tissues such as skeletal muscle and elevated endogenous glucose production by the liver, partly due to insulin resistance and partly due to inadequate insulin secretion (DeFronzo, 2009, Poretsky, 2010). However, now additional mechanisms are thought contributory including pathogenic roles for the brain (appetite regulation and control of hepatic glucose metabolism), kidneys (increased tubular absorption of glucose), gut (incretin secretion and the gut microbiome), alpha-cells in the pancreatic islets (glucagon secretion) and adipose tissue (lipolysis, cytokine release), as well as the traditional roles for islet β-cells, the liver and skeletal muscle (DeFronzo, 2009).

There is much debate about the extent to which insulin resistance or insulin secretion defects are the initiating factors in the development of type 2 diabetes. There is evidence supportive of type 2 diabetes being a consequence of β-cell exhaustion from the need for these cells to compensate for insulin resistance (DeFronzo and Ferrannini, 1991, Kruszynska and Olefsky, 1996, Billings and Florez, 2010). However, reduced β-cell function may also be an early pathogenic feature being demonstrable even when glucose tolerance is still normal, and showing progressive failure with the progression from normal glucose tolerance (NGT) to hyperglycaemia (Porte, 1991, Mitrakou et al., 1992). In reality, type 2 diabetes is more likely a heterogeneous disease, such that both of these

courses may be more correct depending on the individual affected.

As well as defects being present in islet β-cell function, type 2 diabetes gives rise to multiple intracellular deficiencies in insulin activity, being the basis of the insulin resistance. Mostly this occurs due to the impaired signal transduction from the insulin receptor through the intermediary signalling molecules such as insulin receptor substrate (IRS-1) and Akt (Epstein et al., 1994, Hoehn et al., 2008). Increased lipolysis may also contribute in the insulin resistance and failed insulin secretion. Elevated levels of free fatty acids can inhibit insulin secretion and decrease insulin sensitivity in the muscle and liver (Poretsky, 2010).

1.3.1.2.2. Genetic factors in type 2 diabetes

Genome-wide association studies of single-nucleotide polymorphisms (SNPs) have identified over 40 genetic variants that are associated with type 2 diabetes. More have been linked to β-cell function than insulin sensitivity, with each having only a small effect (Nielsen et al., 2003, Billings and Florez, 2010, Wheeler and Barroso, 2011).

Thus, it is likely that a combination of these genetic variants may be required. Furthermore, increasing support is arising for a role for epigenetics, meaning factors that alter the expression of genome that do not involve alterations in genomic DNA, in the pathogenesis of type 2 diabetes (Nolan et al., 2011).

Type 2 diabetes is a phenotypically and genetically heterogeneous disorder and can be divided into early and late form (Hanis et al., 1996). The complexity of type 2 diabetes is related to factors such as genetic heterogeneity, interactions between genes, and the modifying role played by the environment (Busch and Hegele, 2001). The risk of developing type 2 diabetes in a person increases to 2·4 fold with a positive family and 15–25% of first-degree relatives of patients with type 2 diabetes develop impaired

glucose tolerance or diabetes (Stumvoll et al., 2005). Genome-wide screens have led to the localization of susceptibility genes for type 2 diabetes differences between racial groups; including Mexican Americans (Hanis et al., 1996), Pima Indians of the south western United States (Hanson et al., 1998), and in Utah families of Northern European ancestry (Elbein et al., 1999). Each study localized susceptibility to different regions of the genome, suggestive for a combination of different susceptibility genes, which participate in the development of type 2 diabetes in these populations (Horikawa et al., 2000).

Some rare forms of diabetes result from mutations in a single gene, resulting in monogenic diabetes. Monogenic forms of diabetes account for about 1 to 5 percent of all cases of diabetes in young people.

Maturity onset diabetes of the young (MODY) is a group of disorders with an autosomal dominant inheritance, with an early onset before 25 years of age and, almost always, a primary β-cell defect (Jenkins and Campbell, 2004, Hattersley and Patel, 2017). The MODY mutations occur in single genes, which change the structure and function of islet β-cell proteins, some producing non-progressive β-cell dysfunction, others leading to progressive β-cell failure and a more severe phenotype. The classic MODY conditions result from mutations in any one of at least six different genes. One of these genes encodes the glycolytic enzyme glucokinase (Froguel et al., 1993) resulting in a mild abnormality of fasting hyperglycaemia. On the other hand, the other 5 genes encode transcription factors: hepatocyte nuclear factor (HNF) 4α, HNF-1α, insulin promoter factor 1 (IPF-1), HNF-1β and neurogenic differentiation factor 1 (NeuroD1), also known as beta-cell E-box transactivator 2 (BETA2) (Fajans et al., 2001, Hattersley and Patel, 2017). All these genes are expressed in β-cells, and mutation of any of them leads to β-cell dysfunction and diabetes mellitus.

Glucokinase-related MODY (MODY 2) is a common form of this disorder, especially in children with mild hyperglycemia and in women with gestational diabetes and a family history of diabetes. It has been described in persons of all racial and ethnic groups (Desnick, 1973). Polymorphism linkages from the families of glucokinase mutations identified 40 different mutations which generally tend to cluster in exons 5, 6, 7, and 8, which code for the glucose binding site of the enzyme (Vionnet et al., 1992, Gidh-Jain et al., 1993).

1.3.2. Pancreas and its hormones

1.3.2.1. Pancreas

The pancreas is a long, soft organ that lies transversely along the posterior abdominal wall, posterior to the stomach, and extends from the region of the duodenum to the spleen. The human pancreas weighs about 100 grams and is 14-20 cm long (Hruban et al., 2007). The pancreas serves two functions, endocrine and exocrine.

The exocrine function of the pancreas is involved in digestion. The pancreatic acini are clusters of cells that produce digestive enzymes and secretions, and they make up the bulk of the pancreas. The digestive enzymes and secretions are carried through the pancreatic duct system to the duodenum.

The endocrine portion consists of the pancreatic islets, which secrete mainly insulin and glucagon, but also other hormones, that are involved in gluco-regulation. Insulin is the body's only blood glucose-lowering hormone produced by the β-cells of the islets of Langerhans.

A human pancreas contains ~1 million pancreatic islets that are distributed throughout the exocrine parenchyma of the gland. Every pancreatic islet contains ~1,000 endocrine cells of which 75% are insulin-producing β-cells (Rorsman, 2005). These islets are

highly vascularized by an extensive endothelial network and innervated by sympathetic, parasympathetic, and sensory nerves.

1.3.2.2. Hormones of the pancreas

The islets of Langerhans comprised of different endocrine cell types including β-cells (insulin), α-cells (glucagon), and δ-cells (somatostatin) and the PP-cells which secrete pancreatic polypeptide (PP). β-cells make up the majority of islets (around 75-80%), followed by α-cells (about 15%), δ-cells (about 5%) and very few PP-cells (Stefan et al., 1982). These endocrine cells are described briefly in the following sections.

1.3.2.2.1. Alpha cell hormone: glucagon

Glucagon secreting alpha-cells are one of the main endocrine cell populations that coexist in the islet along with insulin-secreting-cells. The most important physiological role of the pancreatic alpha cell is the release of glucose-elevating glucagon in response to hypoglycaemia.

There are three different proposed mechanisms that allow glucose regulation of glucagon secretion; one involves direct effects of glucose on the alpha cell. Another is based on an indirect action mediated by release of insulin, γ-amino butyric acid (GABA), Zn2+or somatostatin. And the third mechanism predicts that glucose sensing occurs in the hypothalamus with altered neural signalling to alpha cells (Vieira et al., 2007).

Insulin and glucagon have opposite effects on glycaemia as well as on the metabolism of nutrients. Insulin acts mainly on muscle, liver and adipose tissue with an anabolic effect, inducing the incorporation of glucose into these tissues and its accumulation as glycogen and fat. In contrast, glucagon induces a catabolic effect, mainly by activating

liver glycogenolysis and gluconeogenesis, which results in the release of glucose into the bloodstream.

The pre-proglucagon-derived peptides glucagon, glucagon-like peptide 1 (GLP-1) and glucagon-like peptide 2 (GLP-2) are all encoded by the pre-proglucagon gene, which is expressed in the central nervous system, intestinal L-cells and pancreatic alpha-cells. A post-translational cleavage by prohormone convertases (PC) is responsible for the maturation of the pre-proglucagon hormone that generates all these peptides. The different expression of PC subtypes in each tissue mediates the production of each different peptide (Mojsov et al., 1987).

An increase in glucagon synthesis along with secretion of epinephrine protects the organism against hypoglycaemia and its potential damaging effects, especially in the brain, which depends on a continuous supply of glucose, its principal metabolic fuel. Additionally, glucose-sensing neurons of the ventromedial hypothalamus further control responses to glycaemia changes. The main action of glucagon occurs in the liver where the insulin/glucagon ratio controls multiple steps of hepatic metabolism. Glucagon stimulates gluconeogenesis and glycogenolysis, which increases hepatic glucose output, ensuring an appropriate supply of glucose to body and brain, and at the same time, it decreases glycogenesis and glycolysis. The glucagon receptor in the liver is highly selective for glucagon, but it exhibits a modest affinity for glucagon-like-peptide 1 (Quesada et al., 2008).

1.3.2.2.2. Delta cells hormone: somatostatin

Somatostatin (SST) is produced by delta cells, which are the third most abundant cell type in pancreatic islets of Langerhans. These cells are typically located on the periphery of the islets, usually between β-cells and the surrounding mantle of alpha cells

(Rhoades and Bell, 2012). Human islets contain about 10% delta cells, which is twice the proportion of mouse islets (Brissova et al., 2005).

SST has a strong and direct inhibitory effect on insulin and glucagon secretion. SST secretion from islet delta-cells is stimulated by increased extracellular glucose, although the threshold concentration for delta-cells to respond to glucose is lower than that for β-cells and ionic events in stimulus-response coupling differ between β and delta-cells. The pancreatic delta-cell and hypothalamus SST consists of two different polypeptides, 14-amino acid and 28-amino acid forms. In delta-cells, the 28-amino acid peptide predominates and, in hypothalamus, the 14-amino acid form predominates (Hauge-Evans et al., 2009).

The peptide hormone SST is also synthesized and secreted by neuroendocrine cells in the central nervous system and the gastrointestinal system, which is the major contributor to circulating SST (Reichlin, 1983). SST has an inhibitory role as well. It acts as an inhibitory regulator of endocrine systems, as a hypothalamic factor to suppress growth hormone secretion from the anterior pituitary, or as a local inhibitor of the release of gastrointestinal peptide hormones (Hauge-Evans et al., 2009).

1.3.2.2.3. PP cells hormone: pancreatic polypeptide

Pancreatic polypeptide (PP) is a 36 amino acid peptide, with a molecular weight of about 4200 Dalton. It produced and secreted by PP cells (originally termed F cells) of the pancreas, primarily located in the islets of Langerhans. These cells also occur scattered through the exocrine parenchyma and occasionally in pancreatic duct epithelium (Lonovics et al., 1981). It is part of a family of peptides that also include peptide YY (PYY) and neuropeptide Y (NPY).

The effects of PP, including inhibition of pancreatic secretion, gall bladder activity, and intestinal motility, are mainly located in the gastrointestinal tract. In addition, PP affects

metabolic functions, including glycogenolysis, and decreases fatty acid levels. It may influence food intake, energy metabolism, and the expression of hypothalamic peptides and gastric ghrelin (Leiter et al., 1985, Berglund et al., 2003).

1.3.2.2.4. Epsilon cells hormone: ghrelin

Ghrelin is a novel 28 amino acid hormone secreted by epsilon (ε-cells), that has many functions in the body. It was first isolated from the stomach and identified as an endogenous ligand for growth hormone secretion from pituitary gland (Pick et al., 1998).

Ghrelin stimulates hunger and feeding behaviour (White, 2003). Circulating ghrelin is produced predominantly in the stomach, while substantially lower amounts are detected in other organs and sites including pancreas. Ghrelin and growth hormone secretagogue receptor type 1a (GHS-R1a) expression have been demonstrated in both human and rodent pancreatic islets (Elleman et al., 2000). Ghrelin inhibits insulin release in mice, rats and humans (Fantl et al., 1993, Lavan et al., 1997, Björnholm et al., 2002). Its role in the pancreatic islets is not well understood.

1.3.2.2.5. β–cell hormones: insulin and amylin

Insulin is discussed in detail in the next section 1.3.3.

Amylin or islet amyloid polypeptide (IAPP) is a small 37-amino acid peptide. It is a second islet β-cell hormone that is normally co-secreted with insulin in response to meals and complements the effects of insulin in postprandial glucose control (Cooper et al., 1987). Amylin is co-secreted with insulin in the ratio of approximately 100:1. The best known functions of amylin are to reduce food intake, to reduce gastric emptying and to inhibit pancreatic glucagon secretion and pancreatic and gastric enzyme secretion. Plasma amylin levels, like insulin are low during fasting and increase during

meals and with glucose administration, and the levels are all directly proportional to body fat (Woods et al., 2006). Amylin is synthesized as a prohormone amyloid polypeptide of 67 amino acids produced by the pancreatic β-cell, and this prohormone undergoes post-translational modifications including protease cleavage to produce amylin (Higham et al., 2000).

1.3.3. Insulin structure and function

Insulin was discovered in 1921-22, by Fredrick Banting, Charles Best, J.J.R. Macleod and James Collip, as one of the great medical breakthroughs of all time (Strakosch, 2004).

1.3.3.1. Insulin structure

Insulin is a small protein, with a molecular weight of about 5808 Daltons (Egea et al., 2005). It was the first protein to have its amino acid sequence sequenced, in 1955 by Fred Sanger (Pillai and Panchagnula, 2001), earning him a Nobel Prize in 1958.

Insulin is built from 51 amino acids and is monomeric when biologically active and in circulation. It is structured with two polypeptide chains, in humans, chain A has 21 amino acids, and chain B has 30 linked by two disulphide bonds, that bridges between the cysteine residues at positions A7 and B7, and A20 and C19. An additional disulphide-bridge connects the cysteine residues at A6 and A11, which is important for determining the tertiary structure and receptor binding of the molecule. There is also a third disulphide bond that connects these same amino acids within Chain A. (Stretton, 2002, Pillai and Panchagnula, 2001).

The insulin gene is only expressed in β-cells of the pancreas (Roy et al., 2003). When this gene is expressed, the messenger RNA transcript is translated into an inactive protein called pre-proinsulin which is composed of 110 amino acids (Wood, 2007). It is

relatively inactive and has to be processed into proinsulin in order to eventually make the insulin hormone. Pre-proinsulin contains a hydrophobic N-terminal signal peptide, which interacts with cytosolic ribonucleoprotein signal recognition particles (SRP). SRP facilitates preproinsulin translocation across the rough endoplasmic reticulum (rER) membrane into the lumen. This process occurs via the peptide-conducting channel where the signal peptide from preproinsulin is cleaved by a signal peptidase to yield proinsulin (Fu et al., 2013). In the endoplasmic reticulum, the single chain proinsulin folds back onto itself, aligning the future A-and B-chain and creating the disulphide bonds in this process. The A-chain and B-chain are still connected by the connecting peptide (C-peptide) (Steiner et al., 1969). In the Golgi-complex, the proinsulin is stored in so-called beta-granules. These contain the proteolytic enzymes that will cleave and remove the C-peptide from proinsulin, resulting in equimolar amounts of insulin and C-peptide in the mature beta-granule (Duckworth et al., 1998).

1.3.3.2. Insulin secretion

Insulin concentrations are normally maintained by a feedback control system that is responsive to the prevailing level of plasma glucose (Bell and Polonsky, 2001). Insulin output must cope with size, composition and appearance rate of meals on one hand and with target tissue sensitivity on the other. Insulin secretion rate must adapt to stimuli both on a minute-by-minute basis, like catecholamines, and in the longer term, like thyroid hormones (Ferrannini and Mari, 2004). First-phase insulin secretion begins within 2 minutes of nutrient ingestion and continues for 10 to 15 minutes. The second phase of prandial insulin secretion follows, and is sustained until normoglycemia is restored (Ferrannini and Mari, 2004). Overt hyperglycemia causes a defect in insulin action, which is called insulin-resistant state. The body compensates against this condition by increasing insulin secretion per cell, consistent with functional

compensation. Islet β-cells can also maintain the compensation by an increase in β-cell mass, particularly seen in rodents, which is achieved by neogenesis of the islet precursor cells in the pancreatic ductal epithelium. (Burks and White, 2001).

13.3.3. Islet β-cell mass

Regulation of blood glucose concentrations requires an adequate number of pancreatic β-cells that respond appropriately to blood glucose concentrations. The collective β-cell numbers are often referred to as the β-cell mass (Matveyenko and Butler, 2008).

Autoimmune destruction of β-cells in type 1 diabetes causes the complete disappearance of β-cells and causes an absolute insulin deficiency (Rahier et al., 2008).

Whereas, type 2 diabetes is characterized by a progressive decline in β-cell function and chronic insulin resistance, where obesity is a major risk factor in the development of the disease. However, most people who are obese and relatively insulin resistant do not develop diabetes as β-cells compensate for the insulin resistance for long periods of time with an increase in secretory capacity and an increase in β-cell mass, or both (Kahn, 1994, DeFronzo, 1997, Polonsky, 2000).

An increase in β-cell mass also happens during pregnancy when maternal metabolism undergoes profound changes and maximum nutrient supply is required for the developing foetus. Detailed rodent studies of β-cell mass and insulin secretion during pregnancy has shown that, there is marked insulin resistance accompanied by a dramatic increase in the insulin response to glucose and an almost doubling of the β-cells mass in rodents, although the latter may not happen to the same extent in human pregnancy. Rat β-cell mass and insulin secretion decreases rapidly after birth reaching pre-pregnancy values at around 10 days postpartum (Edström et al., 1974, Parsons et al., 1992).

Regulation of the β-cell mass involves a balance between β-cell replication and apoptosis, and can include islet neogenesis from exocrine pancreatic ducts. Disruption of any of these pathways of β-cell formation or increased rates of β-cell death could cause a decrease in β-cell mass (Butler et al., 2003).

Rodent models of diabetes, such as the *ob*/*ob* and *db*/*db* mice (Gapp et al., 1983) and the Zucker *fatty* rat (Tokuyama et al., 1995), and hyperinsulienaic humans with obesity and/or type 2 diabetes exhibit mild to marked islet hyperplasia at varying times of their disorders (Pinar et al., 2000). However, the factors contributing to β-cell hyperplasia in insulin-resistant states are not well understood.

Deficits of β-cell mass have been found in various autopsy studies from different European, Asian, and North American populations, where the patients of type 2 diabetes have been reported to have significant reductions in β-cell pancreatic area compared with nondiabetic individuals (Klöppel et al., 1985, Butler et al., 2003). The decrease in β-cell mass in type 2 diabetes individuals has been estimated to be about 40% (Maclean and Ogilvie, 1955).

The number of islet β-cells present at birth is mainly generated by the proliferation and differentiation of pancreatic progenitor cells, a process called neogenesis. Shortly after birth, β-cell neogenesis stops and a small proportion of cycling β-cells can still expand the cell number to compensate for increased insulin demands, although at a slow rate. It appears that in the absence of major external stimuli, the β-cell population has only a very limited potential for regeneration, unlike liver. This is probably due to the limited replication capacity of β-cells and to the fact that neogenesis from precursor cells is not readily reactivated. Yet, under certain conditions where major external stimuli are applied, there can be a quite vigorous regenerative expansion of the β-cell mass (Bouwens and Rooman, 2005).

In NOD mice, β-cells are destroyed by a spontaneous autoimmune reaction leading to a type 1-like diabetes condition. Immune suppression in combination with GLP-1 analog-treatment could restore normoglycaemia and improve islet histology (Ogawa et al., 2004). This involves regeneration as well as increased survival of β-cells. In animal models of type 2 diabetes induced by 90–95% pancreatectomy, daily administration of the GLP-1 analog exendin-4 during 10 days post pancreatectomy decreases the development of diabetes. Where, exendin-4 stimulates the regeneration of the pancreas and expansion of the β-cell mass by the processes of neogenesis and replication of β-cells (Xu et al., 1999).

1.3.3.4. The insulin receptor and insulin function

The insulin receptor belongs to the receptor/tyrosine kinase family, which plays critical roles in development, cell division and metabolism (Fantl et al., 1993). The activation of the receptor/tyrosine kinase family by their cognate ligands causes autophosphorylation and selective protein substrates exclusively on tyrosine residues.

The insulin receptor is composed of two alpha subunits and two β–subunits linked by disulphide bonds. The alpha chains are entirely extracellular and house insulin binding domains, while the linked β-chains penetrate through the plasma membrane. Both receptor-subunits are glycosylated during the process of translation and contain complex N-linked carbohydrate side chains with terminal sialic acid residues, which are necessary for normal folding and function of the receptor (Elleman et al., 2000).

The insulin receptor substrate (IRS) proteins are a family of cytoplasmic adaptor proteins that were first identified for their role in insulin signalling. There are at least four members of the IRS protein family, including IRS-1, -2, -3, and -4. IRS-1 and IRS-2 are expressed in nearly all cells and tissues. Humans express one additional family member, IRS-4, which is more restricted in its expression pattern and is found primarily

in brain, kidney, thymus and liver and IRS-3, is expressed in rodents, but not in humans (Lavan et al., 1997, Björnholm et al., 2002). Most insulin responses are produced or modulated through tyrosine phoshorylation of IRS-1 or IRS-2.

The function of insulin is to control glucose homeostasis by stimulating the clearance of glucose into skeletal muscle and, to a lesser degree, liver and adipose tissue. In muscle and adipocytes, insulin-stimulated glucose uptake is achieved by the translocation of the insulin-sensitive glucose transporter (GLUT-4) from intracellular storage vesicles to the cell surface (James et al., 1988). Insulin also suppresses endogenous glucose production from glycogenolysis and gluconeogenesis in the liver and it inhibits lipolysis in adipose tissue.

1.3.4. The mechanisms of insulin secretion

The blood glucose concentration affects the release of insulin from β-cells. It is a complex and interesting mechanism that shows the complicated nature of glucose regulation. The regulation of insulin secretion by glucose is modulated by various physiological effectors including neural and hormonal factors (Bell and Polonsky, 2001, Muoio and Newgard, 2008). For example, the incretin (intestinal) hormones such as GLP1 and gastrointestinal inhibitory polypeptide (GIP) and the parasympathetic system neurotransmitter acetylcholine (ACh) all potentiate insulin secretion (Muoio and Newgard, 2008).

The clustered β-cells in islets are strategically connected to the vasculature. Capillaries surrounding islets show a remarkable number of small pores called fenestrae that allow for a greater nutrient exchange between the circulation and surrounding tissues. This allows unrestricted nutrient access so that β-cells can sense the nutritional state quickly (Suckale and Solimena, 2008). The islet β-cell is most responsive to glucose as a nutrient secretagogue, and causes glucose-stimulated insulin secretion (GSIS). GSIS is

also potentiated by other metabolic fuels, most notably fatty acids and amino acids. Interaction of amino acids and fatty acid metabolism with glucose metabolism produces metabolic coupling factors (MCFs), which are involved in signalling for insulin exocytosis (Nolan and Prentki, 2008).

1.3.4.1. Mechanisms of nutrient-stimulated insulin secretion

The islet β-cell senses multiple nutrients, hormonal and neural inputs and accordingly secretes insulin appropriately for the requirements of the body at that moment, whether fasted or fed. Essential for insulin secretion is metabolic activation of the β-cell in response to an increased mixed nutrient supply, of which glucose is the most important (Nolan and Prentki, 2008, Prentki et al., 2013).

In order to couple glucose sensing to insulin release, islet β-cell glucose metabolism is essential and this is via three pathways with the production of metabolic coupling factors.

1.3.4.1.1. K+-ATP channel dependent pathway

Glucose enters the β-cell via GLUT2 and after being phosphorylated by glucokinase is metabolized via glycolysis to pyruvate and then acetyl-CoA via pyruvate dehydrogenase with subsequent oxidation in the tricarboxylic acid cycle (Newgard and McGarry, 1995, Suckale and Solimena, 2008). This gives rise to an increased cytosolic ATP/ADP ratio, which closes ATP-sensitive K^+ channels, depolarises the plasma membrane potential, opens voltage-gated Ca^{2+} channels, and Ca^{2+} influx activates insulin granule exocytosis (Fig 1.1) (Rorsman, 2005, Nolan and Prentki, 2008, Prentki et al., 2013). The K^+-ATP channels are composed of two tetramers of two proteins: a pore-forming K^+ channel, Kir 6·2, and a regulatory subunit; the sulphonylurea receptor SUR1. The intercellular ATP binding to Kir 6·2 caused the channel to close whereas binding of ADP to SUR1

opens the channel, therefore the channels are regulated by the intracellular changes of ATP:ADP ratio. Closure of K^+-ATP channels cause membrane depolarization until the threshold potential for opening of voltage-dependent Ca^{2+}-channels is reached. When these channels open, influx of Ca^{2+} into β-cell occurs, down the electrochemical gradient, which results in an increase in $[Ca^{2+}]$ (Henquin et al., 2003).

The K^+-ATP channel-dependent mechanism triggers a release of relatively small proportion (∼10%) of already docked granules at the plasma membrane of β-cell from the immediately-releasable pool. This acute phase of insulin release occurs in the first 10 minutes in response of glucose stimulation (Ashcroft et al., 1984, Jensen et al., 2008). The second phase of glucose-stimulated insulin secretion is due mainly to the K^+-ATP channel-independent pathways acting in interaction with the K^+-ATP channel-dependent pathway, such as the anaplerosis and glycerolipid/fatty acid cycling pathways (Straub and Sharp, 2002).

1.3.4.1.2. The anaplerosis amplification pathway

Pyruvate is the main end product of glycolysis in β-cells, because the cell contains extremely low levels of lactate dehydrogenase, hence there is a limitation of the pyruvate conversion to lactate. The metabolic fate of pyruvate depends on the relative activities of pyruvate carboxylase (PC) and the pyruvate dehydrogenase complex. Pyruvate from glucose that is metabolized via PC enters the anaplerosis/cataplerosis pathway, which can impact on insulin secretion by increasing levels of cataplerosis-derived metabolic coupling molecules such as Nicotinamide adenine dinucleotide phosphate (NADPH) from the malate-, citrate- and isocitrate/α-ketoglutarate-pyruvate shuttles, as well as malonyl-CoA and glutamate (Fig 1.1) (Newgard and McGarry, 1995, Nolan and Prentki, 2008, Prentki et al., 2013). Of note, the anaplerotic enzyme

PC is expressed at very high levels, contributing to 0.4% of the total protein content of islet tissue (MacDonald, 1995).

1.3.4.1.3. The glycerolipid/fatty acid cycling amplification pathway

Non-esterified fatty acids (NEFA) are important to the pancreatic β-cell for its normal function. NEFA deprivation of islet tissue causes loss of GSIS, which can be readily reversed by an exogenous NEFA replacement. However, while elevated NEFA supply can acutely augment GSIS, if chronically in excess particularly in association with elevated glucose, this can reduce insulin biosynthesis, secretion and can induce β-cell cell apoptosis (Lee et al., 1994, Prentki et al., 2002, El-Assaad et al., 2003).

Glycerolipid/fatty acid cycling is one pathway by which NEFA can affect insulin secretion (Prentki and Madiraju, 2012).

To enable glycerolipid/fatty acid cycling, glucose interacts with NEFA by elevating malonyl-CoA, via the anaplerosis pathway, which inhibits partitioning of long chain acyl-CoA to the mitochondrion for fatty acid oxidation (via carnitine palmitoyltransferase-1 inhibition), such that the long chain acyl-CoA are then more available for esterification processes (Nolan et al., 2006, Nolan and Prentki, 2008, Prentki and Madiraju, 2012, Prentki et al., 2013).

Glycerolipids such as diacylglycerol and triacylglycerides formed are rapidly hydrolysed by lipases back to fatty acids and glycerol creating a cycle of newly formed lipids. This cycle produces lipid signaling molecules such as monoacylglycerols and diacylglycerols that are able to enhance GSIS (Fig 1.1) (Nolan and Prentki, 2008, Prentki and Madiraju, 2012, Prentki et al., 2013).

1.3.4.1.4. Other mediators of insulin secretion

Amino acids, such as glutamine and leucine, also interact with the glucose metabolism pathways to enhance the coupling signals produced by glucose alone. The β-cell also responds to other neurohormonal/metabolic extracellular signals by various plasma membrane receptors and their signal transduction pathways (e.g. G-protein coupled signalling for example by cyclic AMP). Relevant to nutrient-induced insulin secretion, islet β-cells have cell surface receptors for fatty acids (e.g. FFAR1) that can modulate GSIS. Effector metabolic coupling factors interact with the insulin granule exocytosis machinery to cause insulin secretion (Fig 1.1) (Nolan and Prentki, 2008, Prentki et al., 2013).

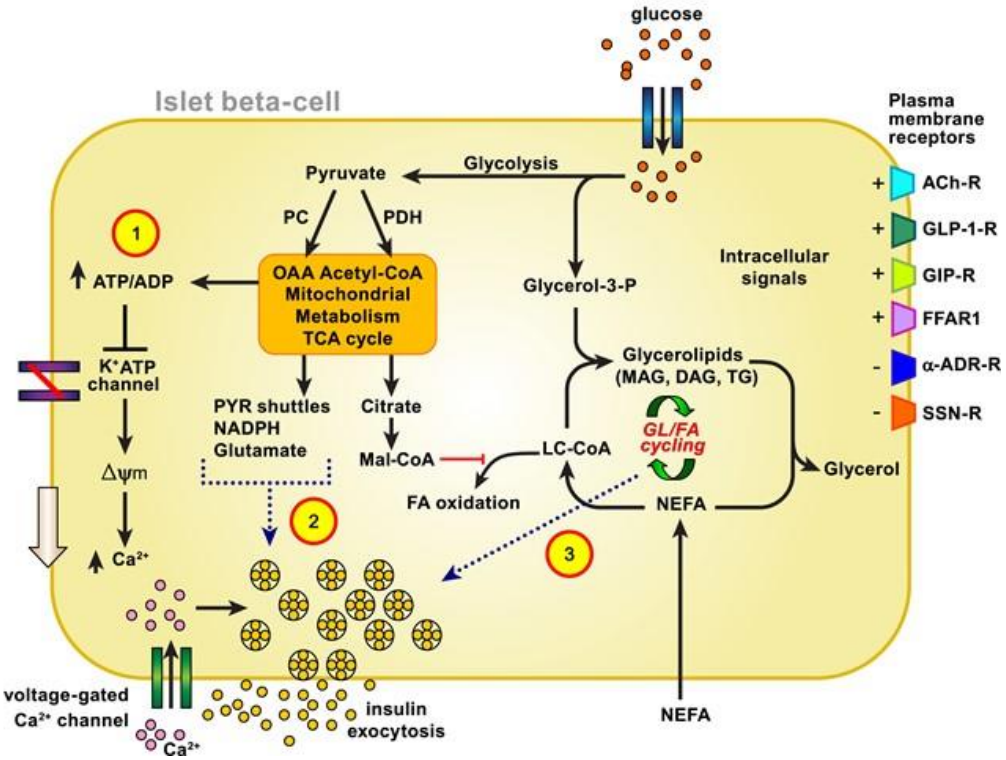

Figure 1.1: Role of islet β-cell metabolic activation by fuels and neuro-hormonal agonists in insulin secretion

Islet β-cell glucose metabolism is essential for glucose to stimulate insulin secretion via three key pathways that produce metabolic coupling factors: (1) The K^+-ATP channel dependent pathway of GSIS. (2) The anaplerosis amplification pathway of GSIS. (3) The glycerolipid/fatty acid cycling amplification pathway (refer to text for details). Amino acids, such as glutamine and leucine, also interact with the glucose metabolism pathways to increase the coupling signals produced by glucose alone. The β-cell also responds to other neurohormonal and metabolic extracellular signals via various plasma membrane receptors.

PC=pyruvate carboxylase. PDH=pyruvate dehydrogenase. Ach-R=acetylcholine receptor. FA=fatty acid. GIP-R=gastric inhibitory polypeptide receptor. GLP-1-R=glucagon-like peptide-1 receptor. FFAR1=free-fatty-acid receptor-1. α-ADR-R= α2-adrenergic receptor. SSN-R=somatostatin receptor. OAA= oxaloacetate. CoA=coenzyme A. MAG=monoacylglycerides. DAG=diacylglycerides. TG=triacylglycerides. Δψm=change in plasma membrane potential. Mal-CoA=malonyl-CoA. LC-CoA=long-chain acyl-CoA. GL=glycerolipid. FA=fatty acid. NEFA=non-esterified fatty acids. Adapted from (Nolan et al., 2011).

1.3.5. Animal models

Many mouse models are used for diabetes research, with most being more relevant to type 2 diabetes. As this thesis is concerned with investigation of possible non-immune susceptibility factors for type 1 diabetes, the key mouse model to be studied was the NOD^{k} mouse, derived from the type 1 diabetes NOD mouse model, with two comparator strains. In this section the background to these three mouse models relevant to, and/or used, in this thesis is provided.

1.3.5.1. NOD^{k} congenic mice

The NOD mouse is the most extensively studied animal model for the development of type 1 diabetes. Experiments conducted in NOD mice have informed immune system modulatory therapies that are being pursued for the prevention of type1 diabetes in humans (Delovitch and Singh, 1997).

The inbred NOD strain was developed in Japan in 1980 by selective breeding of outbred ICR:Jcl mice at Shionogi Research Laboratories. These mice were established by selective mating of the offspring of a female mouse which spontaneously developed diabetes in one of the two sublines of cataract Shionogi (CTS) mice (Makino et al., 1980b).

The development of type 1 diabetes in the NOD mouse is under the control of multiple genes, of which one or more are linked to the MHC. The analysis of NOD mice with the outcross C57BL/10SnJ strain showed at least three non-MHC-linked genes as well, located on chromosomes 1, 3 and 11 (Todd et al., 1991) and one or more genes in the MHC (Hattori et al., 1986). The MHC class II region of the NOD mouse $H2^{g7}$ is strongly linked to the development of diabetes (Podolin et al., 1993, Socha et al., 2003, Dooley et al., 2016).

Within the MHC class II I-A and I-E regions, the NOD mouse was found to express a unique I-A β-chain that could clearly be implicated in the susceptibility of these mice in diabetes. In addition, another feature of the NOD Class II MHC was the absence of I-E α chain production (Todd et al., 1991, Wicker et al., 1987). In order to determine the importance of the absence of the I-E α chain in the propensity of NOD mice to develop diabetes, congenic mice for various I-E^+ and I-E^- MHC haplotypes were created. It was found that I-E^+ NOD mice do develop insulitis and diabetes (Podolin et al., 1993), In this work, a NOD.*H2*^{k} congenic strain was created by outcrossing NOD mice from Taconic Farms (NOD/MrkTac) with B10.BR (congenic for the *H2*^{k} MHC haplotype from C57BR) which were back-crossed with NOD to retain the *H2*^{k} MHC haplotype. The resultant congenic NOD.BR-H2^k/Wicker mice, in which the *H2*^{g7} locus of the MHC Class II of the NOD had been replaced by the *H2*^{k}, have been previously been called NOD^k mice (Dooley et al., 2016), and this abbreviated name is continued to be used for the purpose of this thesis. NOD^k mice do not show the development of spontaneous diabetes for 5-13 months of age (Podolin et al., 1993, Dooley et al., 2016).

NOD^k congenic mice have been shown to contain all auto immune susceptibility loci for NOD except the *H2*^{g7} allele, which is been replaced by the *H2*^{k} allele (Elkon, 2006a).

1.3.5.2. NOD^k.insHEL transgenic mice

A transgenic mouse carries a foreign gene that has been deliberately inserted into its genome. These genes are found in the nucleus of every cell of the body. As mentioned before in Section 1.1, the work of this thesis progresses on from earlier work performed with NOD^k.insHEL transgenic mice (Dooley et al., 2016). The HEL transgene is modified to a cell surface form by addition of coding segments for the transmembrane and cytoplasmic tail of the *H2-Kb* molecule. It is driven by the rat proinsulin gene

promoter (insHEL) such that it is highly expressed in islet β-cells (Dooley et al., 2016). Male NOD^{k}.insHEL, but not female NOD^{k}.insHEL or B10^{k}.insHEL mice of either gender, develop diabetes. Furthermore, the diabetes that develops in the NOD^{k}.insHEL mice appears to have a non-immune pathogenesis, but these mice clearly show evidence of islet β-cell failure indicated by the presence of increased β-cell apoptosis and a decrease in islet β-cell mass (Dooley et al., 2016). Interestingly, all insHEL transgenic mice (male and female NOD^{k}.insHEL and B10^{k}.insHEL) develop hyperinsulinaemia with normal sensitivity to exogenous insulin (Dooley et al., 2016). There was evidence for altered proinsulin processing in the insHEL transgenics, but this was also true for the female NOD^{k}.insHEL and B10^{k}.insHEL of both genders, suggestive of an islet β-cell susceptibility factor NOD^{k}.insHEL mice that is altered by gender (Dooley et al., 2016).

Overexpression of HEL in β-cells of the NOD^{k} provide stress by forcing the cells to produce a foreign highly disulphide bonded protein that can cause endoplasmic reticulum (ER) stress (Dooley et al., 2016). In the work of this thesis we wished to determine if a more usual stressor, such as the HF-diet, could also induce diabetes in the NOD^{k} mouse model

1.3.5.3. B10^{k} congenic mice

A number of glycoproteins are coded at the I region of the mouse MHC complex. The Ia antigens are responsible for initiating an immune response to foreign antigens (McDevitt, 1981). Two different Ia antigen complexes exist, the A complex and the E complex (McDevitt, 1981, Klein et al., 1981). The A complex is generally expressed on B lymphocytes of all mouse haplotypes, yet certain strains fail to assemble the E complex to the cell surface (Mathis et al., 1983). The C57BL/10 strain is one strain that

fails to express an I-E product. C57BL/10 mice do not develop overt diabetes and insulitis (Wicker et al., 1987).

$B10^k$ is the abbreviated name given to B10.BR-$H2^{k/}$SgSnJ mice; a C57BL/10 sub strain congenic for the C57BR $H2^k$ locus (Dooley et al., 2016). This strain was developed in 1965 in Jackson lab, in which the $H2^k$ haplotype was backcrossed from C57BR/cdJ mice onto C57BL/10ScSn mice (Jackson, 1988; April). The $H2^k$ haplotype does express an I-E product. B10.BR also contain diabetic resistant alleles at most non-MHC loci (Elkon, 2006b).

As $B10^k$ mice have the same low risk $H2^k$ MHC haplotype as NOD^k mice, this was selected as a control strain in the insHEL studies (Dooley et al., 2016). We have continued to use it as a control strain in the studies of this thesis, however, while it does not develop insulitis or diabetes, it does develop glucose intolerance (Chapters 3&4).

1.3.5.4. Balb/c

The Balb/c strain is genetically most related to the A/J strain of mice, which is a classic "diabetes-resistant" mouse strain, with low glucose levels (Naggert JK, May 2006). Balb/c, are more glucose tolerant than C57BL/6 and more resistant to the glucotoxic effects of streptozotocin (Cardinal et al., 1998). Balb/c mice have a relatively high β-cell mass due to a large number of islets (Clee and Attie, 2007).

Our laboratory has previously studied Balb/c females on HF-diet for 10 weeks (Delghingaro-Augusto- unpublished). HF-fed Balb/c mice were found to maintain normal glycaemia in both the fed-state and during intra-peritoneal glucose tolerance testing (ipGTT). Considering that early experiments with $B10^k$ mice did not show it to be a suitable control strain due to its poor glucose tolerance even on chow diet (see results chapters), a decision was made to include diabetes resistant Balb/c mice as a third comparator strain for the studies of this thesis.

Chapter#2:

Materials & Methods

2.1. Introduction

This Chapter describes the research design used in the study including: animal sources, experimental set up and procedures, sampling techniques, sample size, instrumentation, data collection, analysis procedures and data presentation.

2.2. Animal sources, diet and housing

Age matched 6 week old male and female B10.BR-H2K2H2-T18a/SgSnJArc mice, called $B10^k$ mice for the purposes of this thesis, were purchased from the Animal Resource Centre (ARC; Perth, WA, Australia). On arrival, the mice were initially caged in groups of 4-5 mice in the Canberra Hospital Animal Facility and fed standard laboratory diet. Sister and brother breeding couples were set up and a colony was maintained at the Canberra Hospital Animal Facility.

NOD.BR-*H2*^{k}/WickerANU, called NOD^k for the purposes of this thesis, were obtained from Prof. Goodnow's laboratory at the John Curtin School of Medical Research at the Australian National University (ANU). Balb/c mice were obtained from ANU Animal Services. Sister and brother breeding couples were also set up for these two strains of mice at the Canberra Hospital Animal Facility.

NOD^k mice were refreshed at ANU, under the management of the Animal Facility staff. Female NOD^k mice (NOD.BR-*H2*^{k}/WickerANU) were crossed with male NOD.ShiLtJArc from ARC and the N1 progeny were further backcrossed twice to the NOD.ShiLtJArc strain. Breeders were selected on the basis of heterozygosity using PCR for *H2k* at the MHC. After two backcrosses, N3 brother and sister *H2*^{k} heterozygotes were intercrossed in order to fix a *H2*^{k} haplotype homozygous progeny (confirmed with PCR). These mice were given the strain name of ASD527:NOD^k.ANU N3F3 (after 3 intercrosses), abbreviated to NOD^k-Refreshed (NOD^k-REF) for the

purposes of this thesis.

For mating of the various mouse colonies, males were put together with the female breeders for 3 consecutive nights. The gestation period was about 21 days for the 3 strains. At 4 weeks of age, mice were weaned on to normal chow diet (unless otherwise stated), containing 59.8% (w/w) carbohydrate, 20% (w/w) protein and 5.4% (w/w) fat; energy content 12MJ/g (Gordon's Speciality Stockfeeds, NSW, Australia) and autoclaved tap water. Mice were accommodated in a temperature-controlled room (21-24^{0}C) with 40-60% humidity on an artificial 12-hour day and 12-hour night cycle.

Only male mice were used for experiments due to their greater propensity to develop diabetes. They remained on normal chow diet from weaning or were placed on to a high fat (HF) diet containing 45% (w/w) sucrose, 19.40% (w/w) protein and 23% (w/w) fat; energy content 20MJ/g (SF03-020 Gordon's Speciality Stockfeeds, NSW, Australia).

The project was approved by the Australian National University Experimental Ethics Committee (Project A2011/027) and all animals received care in compliance with the guidelines prescribed by the committee and the National Health and Medical Research, Australian Code for the Care and Use of Animals for Scientific Purposes (NHMRC, 2013).

2.3. Fortnightly measurement of body weight and blood glucose

Male experimental mice, randomized to either normal chow or HF-diet, were submitted to fortnightly assessment of body weight and fed-tail blood glucose levels. The blood glucose checks were performed between 9 and 10 AM using a glucometer (StatStrip Xpress, Nova Biomedical, Flintshire, UK) calibrated with low (ranging 2.6-4.2mmol/l, 46-76 mg/dl), intermediate (ranging 5.0-7.2 mmol/l, 90-130mg/l) and high (ranging

14.4-18.3 mmol/l, 260-330mg/dl) glucose control solutions. The mice were identified, taken out of cages and quickly placed in a mouse restrainer. With a sterile surgical blade (blade size #15, Swan Morton, Limited, UK), a very small incision (2-3mm) was introduced onto one of the tail veins to produce one drop of blood. The first drop of blood was collected at the glucose test strip and the glucose measurement was then measured automatically by the glucometer. After obtaining the glucose measurement, gentle pressure was applied at the site of the cuts by gauze (Cat# 45849, Cutisoft, BSN Medical Pty. Ltd, Australia), to stop any further bleeding and the tails of the mice were cleaned by fresh gauze. The body weights of the mice were documented by weighing them on a standard laboratory scale (Fx-200i, A&D Company limited, Korea). After the measurements the mice were returned to their respective cages.

2.4. Intraperitoneal glucose tolerance test (ipGTT)

For ipGTTs, mice were fasted for 4 hours so as to be able to obtain baseline glucose and insulin levels, without putting the mice into a significant catabolic state (e.g. by overnight fasting). Food was removed from the original mice cages at 8:00 AM and mice were placed in a new cages with new bedding, without food, but with water during the 4 hours fast. Body weights were measured to calculate the glucose injection dose (2 g glucose/kg body weight).

A 25% working glucose solution was prepared from 50% glucose intravenous infusion (Baxter, Toongabbie, NSW, Australia) by using autoclaved milliQ water.

Mice were restrained in a mouse restrainer and the tail was heated under a heat lamp to induce heat vasodilation, and the blood was collected via a small lateral cut ~5mm at the mouse's tail and gentle massage of the tail. A time 0 min baseline glucose measurement was made as described in Section 2.3. An additional baseline blood sample of 60 µl was collected from each mouse into Eppendorf tubes (Eppendorf South Pacific Pty. Ltd,

NSW, Australia) containing 10µL of 0.5M ethylenediaminotetraacetic acid (EDTA, Cat# E9884, Sigma Aldrich, CA, USA) and the these samples were placed on ice. The intraperitoneal injection of 25% glucose solution (2g/kg body weight) was administered at time 0 h, which started the test. Consecutive measurements of blood glucose levels were taken at 15, 30, 60, 90 and 120 min after the glucose injection from droplets of tail blood by using the glucometer, as described above (Section 2.3). Also, 30-60 µL tail blood samples were collected at 15 and 90 min after the glucose injection for later measurements of insulin, TG and NEFA. On completion of the experiment, mice were returned to their respective cages with food and water. The collected blood samples were centrifuged at 6000 rpm (Rotor # SX4750, Allegra X-15R Centrifuge, Beckman Coulter, CA, USA) for 10 min at 4^0C to separate the plasma. EDTA plasma collected was stored at -80^0C.

2.5. Intraperitoneal insulin tolerance test (ipITT)

Intraperitoneal insulin tolerance tests (ipITT) were performed to assess insulin sensitivity. Insulin causes a fall in glycaemia, such that the mice with the highest insulin sensitivity should have the greatest fall. As for the ipGTTs (Section 2.3), the mice were fasted for 4 hours, housed in individual cages without food, but with bedding and water.

Insulin solution for intraperitoneal injection was prepared freshly by diluting human insulin (0.1 units/ml), from a 100 units/ml insulin stock (Humulin R Cartridges, Lilly-stored at 4˚C) in sterile saline (0.9%). The insulin dose for each mouse was calculated to be 0.75 units/kg body weight.

Baseline blood glucose measurements and 60 µl blood samples into EDTA-treated Eppendorf tubes were taken at time 0 min, as described in Section 2.3 after which the intraperitoneal injection of insulin was given. Consecutive measurements of blood glucose were performed at 15, 30, 45, 60 and 90 minutes after the insulin injection in

droplets of tail blood by the glucometer, as described in Section 2.3. On completion of the experiment, mice were returned to their respective cages with food and water. The time 0 min blood samples were centrifuged at 6000 rpm, (Rotor # SX4750, Allegra X-15R Centrifuge, Beckman Coulter, CA, USA) for 10 min at 4˚C to separate the EDTA plasma which was stored at -80˚C for future analyses.

2.6. Euthanasia and tissue harvesting

2.6.1. Blood collection

On the day of harvest, a 60 µL fed-tail blood sample from each conscious mouse was collected into an EDTA-Eppendorf tube from a lateral cut on the tail, while gently heating and massaging the tail under a heat lamp. Plasma from the blood samples were centrifuged at 6000 rpm (Rotor # SX4750, Allegra X-15R Centrifuge, Beckman Coulter, CA, USA) for 10 min at 4^0C and were stored at -80^0C for further measurement of insulin, pro-insulin, C-peptide and TG and NEFA.

2.6.2. Anaesthesia, cardiac blood collection and euthanasia

After collection of the tail blood samples, the mice were anaesthetized by using ketamine (100 mg/ml, Troy Laboratories, NSW, Australia) at 100mg/kg body weight and xylazine (20 mg/ml, Xylazil, Troy Laboratories, NSW, Australia) at 20 mg/kg of body weight. The anaesthesia was prepared by mixing 1 ml of ketamine and xylazine from stock in 8 ml of saline solution. The dose of anesthesia given to each mouse was 10 µL per gram body weight of the mixed stock and was injected into the peritoneal cavity through the left lower abdominal region using a 25G needle (0.5mm X 25mm, Cat#301807, BD precision glide needle, NJ, USA) with a 1 ml tuberculin syringe (Cat#302100, BD, Biosciences, NJ, USA).

Once each mouse was unconscious, a cardiac puncture was made to collect blood by using a 0.5M EDTA rinsed 1 ml tuberculin syringe (Cat#302100, BD, Biosciences, NJ, USA) and a 25G needle (.05mm X 25mm, Cat#301807, BD precision glide needle, NJ, USA). These cardiac blood samples were collected into 4 ml BD vacutainers (Cat# 366164, BD UK, Polymouth, UK) and immediately placed on ice. Later, these blood samples were centrifuged at 3000 rpm (Rotor # SX4750, Allegra X-15R Centrifuge, Beckman Coulter, CA, USA) for 15 min at 4^0C and were stored at -80^0C for measurement of proinsulin, C-peptide, TG and NEFA.

2.6.3. Tissue dissection

All groups of mice were euthanised still under anaesthesia by cervical dislocation. The abdominal cavity was opened widely and pancreas, liver, adipose tissue; including epididymal and subcutaneous fat were dissected and weighed on laboratory bench scales (FX-200i, Max=220g, d=0.001 g, A&D Company Ltd).

2.6.3.1. Pancreas

After opening the abdominal cavity of each mouse, the pancreas and other abdominal structures were identified prior to removal of the pancreas. The pancreas was carefully held by the spleen and removed by dissection from its bed and attachments, such as to the duodenum, with cleaning of the attached fat. After removal, the pancreas was further cleared of fat and lymph nodes with vision aided by a Stemi 1000 dissecting microscope (Carl Zeiss, Germany). The pancreas was then weighed and recorded on laboratory bench scales (FX-200i, Max=220g, d=0.001 g, A&D Company Ltd) and placed inside a plastic cassette (Embedding cassette, Cat#LID-05, Techno Plas, SA, Australia). The tissue was then fixed in 10% neutral buffered formalin solution (Cat# ANBFB, Biostain, VIC, Australia) and embedded for later histological analyses.

2.6.3.2. Liver

After removal of the pancreas, the whole liver was then quickly dissected. It was weighed and cut in to small pieces and snap-frozen in 7 mL screw cap tubes (Cat#58.536, Sarstedt, Germany) for storage at -80°C for future experiments.

2.6.3.3. Adipose tissue

Epididymal and abdominal subcutaneous adipose tissue depots were dissected from the right side of the mice, because of the site of the anaesthetic injection on the opposite side. The adipose tissue depots were then weighed, cut into small segments and snap-frozen in 7 mL screw cap tubes (Cat#58.536, Sarstedt, Germany) for storage at -80°C for future experiments.

2.7. Blood Analytical analysis

2.7.1. Insulin radioimmunoassay (RIA)

The quantity of insulin in plasma collected from fed-tail blood and during the ipGTTs at times (0, 15 and 90 min) were quantitated using a rat insulin RIA. In this method, a known quantity of radiolabelled tracer antigen (^{125}I-labelled insulin) is mixed with a known dilution of antibody for that antigen, and as a result, the two specifically bind to one another (Abacus, Millipore, MA, USA). When, a sample of unlabelled antigen (sample containing an unknown amount of insulin) is added. This causes a competition between the unlabelled antigens from the plasma to compete with the radiolabelled antigen for antibody binding sites. Thus, an increasing concentration of unlabelled antigen decreases the ratio of antibody-bound tracer to free tracer and *vice versa*. The bound antigens are then separated from the unbound ones, and the radioactivity of the free antigen remaining in the supernatant is measured using a gamma counter.

Test samples and standards were diluted in bovine serum albumin (BSA) phosphate buffer (BSA phosphate buffer; for the constituents see Appendix 1) and were distributed in 12 x 75mm in Polypropylene tubes (Cat # T400A, Simport, represented by Lomb Scientific in Australia) to a volume of 50 µl. A standard curve was generated using purified human insulin at concentrations of 0, 0.0625, 0.125, 0.5, 1, 2, 4, 8, and 16 ng/mL. ^{125}I-insulin (Cat# Abacus, Millipore, MA, USA) and approximately 5µCi/ml was added in aliquots of 50 µl to all tubes, followed by addition of 50 µL of undiluted 1st antibody: Guinea pig anti-rat insulin serum (Cat # ML1013-K, Millipore-Linco cat, Billerica, USA). This was followed by an overnight incubation 4^{0}C. The 1st antibody was not distributed into tubes 1 to 4, as these tubes contain 50µL of the ^{125}I-insulin tracer alone for the determination of the total and non-specific binding, required for data analysis. On the next day, 500 µl of secondary antibody mixture of 335µl of polyethylene glycol-sodium phosphate buffer (PEG; refer to Appendix 1), 85 µl BSA phosphate buffer, 40 µL of 1:5 diluted goat anti-guinea pig immunoglobulin G (Cat#GAGP80-459, Equitech-Bio Inc., TX, USA) and 40 µl of 0.057 mg/ml guinea pig serum (Cat#006-000-120, Jackson ImmunoResearch Laboratories. Inc., PA, USA) were added to all tubes (except total count tubes), followed by a further 2 hours incubation at 4^{0}C.

After the incubation, all tubes (except for the total count tubes) were centrifuged (Rotor # SX4750, Allegra X-15R Centrifuge, Beckman Coulter, CA, USA) at 2,500 rpm for 15 min at 4^{0}C. Supernatant from all (except total count tubes) were discarded by inverting the tubes to remove unbound tracer. The tubes were left inverted on the paper towels to dry for 1 hour. Radioactivity of retained pallets was counted (1 min/tube) using the gamma-counter (Perkin Elmer 2480 Wizard Automatic Gamma Counter, Massachusetts, USA).

2.7.2. Plasma non-esterified fatty acids (NEFA)

The NEFA levels in plasma, collected from mice by cardiac puncture at the time of euthanasia, were measured using the Wako NEFA C kit (Cat#279-75401, Wako Chemicals, Osaka, Japan). Measurement of NEFA is based on the conversion of NEFA to acetyl-CoA, AMP and pyrophosphoric acid by acyl-CoA synthetase in the presence of coenzyme A and ATP. The acyl-CoA thus produced is oxidized by added acyl-CoA oxidase with generation of hydrogen peroxide. The presence of peroxidase permits the oxidative condensation of *3-methy-N-ethyl-N* (β-hydroxyethyl)-aniline with 4-aminoantipyrine to form a purple coloured product, which can be measured calorimetrically at 570 nm.

For the measurement of plasma NEFA, instructions from the Wako kit were followed. Briefly, standards at concentrations of 0, 0.125, 0.25, 0.5, 1, 2 and 3 mmol/l were prepared by using 1 mmol/l of the provided solution. 2.5 µl of the prepared standards and plasma samples were pipetted into duplicate wells of 96-well plates (Cat#167008 Nunce, Thermo Fischer Scientific, Roskilde, Denmark). Fifty µL of Reagent A, previously prepared by combining reagent A with color A, was added by using an Eppendorf repeating manual pipette (Eppendorf 022260201, Hamburg, Germany). Plates were incubated at 37^0C for 10 min. Subsequently, 100 µl of Reagent B, also prepared by mixing reagent B with color reagent B, was added in every used well and incubated at 37^0C for 10 min. After the incubation, the plate was allowed to cool for 5 minutes. The absorbance was read at 570 nm using the FluoStar Optima Spectophotometer (Serial # 413-2046, BMG Labtech, NC, USA).

2.7.3. Plasma Triglyceride (TG)

The TG levels in plasma collected from the cardiac puncture samples was measured using the Wako TG C kit (Cat # 432-40201, Wako Chemicals, Osaka, Japan). This kit is based on the enzymatic hydrolysis of the triglycerides by lipase to glycerol and free fatty acids. The glycerol formed from the initial reaction is then phosphorylated to glycerol-3-phosphate when catalysed by glycerol kinase. The glycerol-3-phosphate is oxidized to hydrogen peroxide in a reaction catalysed by glycerol-3-phosphate oxidase. Peroxidase catalyses the redox-coupled reaction of H_2O_2 with 4-aminoantipyrine and *N-Ethyl-N*-(3-sulfopropyl)-anisidine, to produce a brilliant blue colour which exhibits absorbance at 600 nm.

TG concentrations were measured on a 96 well plate and then read on the FluoStar machine. For TG assay, instructions from Wako kit were followed; briefly working reagent was prepared by mixing one bottle of colour Reagent A with Solvent A.

Plasma samples were thawed on ice for the assay, and 2.5 µl for standards; 0, 1.5, 3, 6, 9, 12, 15, 18 µg/µl and plasma were loaded in a flat bottomed 96 well plate (Cat#167008 Nunce, Thermo Fischer Scientific, Roskilde, Denmark). 150 µl of working reagent was added by the Eppendorf micropipette repeater (Cat# 022260201 Eppendorf, Hamburg, Germany). Then, the plate was incubated at 37°C for 10 min, and cooled for 5 minutes. The absorbance was measured at 600 nm using the FluoStar Optima Spectophotometer (Serial # 413-2046, BMG Labtech, NC, USA).

2.7.4. Plasma Proinsulin

Plasma proinsulin levels were measured from the cardiac plasma collected from the mice at the time of harvest by using the proinsulin ELISA kit, (Cat# 8-PINMS-E01, Alpco; New Hampshire, America). This kit is based on a sandwich type immunoassay where two monoclonal antibodies are directed against separate antigenic determinants

on the proinsulin molecule. A 96-well microplate is coated with a monoclonal antibody specific for proinsulin. After an initial incubation with standards and samples, followed by washing, a horseradish peroxidase enzyme-labeled monoclonal antibody is then added. After a further incubation and washing, 3',5,5'-tetramethylbenzidine (TMB) substrate is added, and the microplate is incubated a third time. Once the third incubation is complete, addition of an acid stop solution stops the reaction giving a colourimetric endpoint, which exhibits absorbance at 450 nm.

The manufacturer protocol was followed to perform the assay. High and low controls and standards at the concentrations of 0, 4, 15, 100 and 300 pM were reconstituted by adding 1.5 ml of deionized water. Ten µl volumes of standards, control and plasma samples were added in duplicates in the 96-well plates. 100 µl of working strength conjugate buffer; prepared earlier from conjugated stock by a $1/10^{th}$ dilution was added into each well and incubated for 2 hours at room temperature with constant shaking (700-900 rpm) on a micro-plate shaker (Multitaskin Ascent, 354 Thermo Labsystems, Finland). Followed by the incubation, the contents of the wells were decanted and the micro-plate was washed 6 times with 350 µL of working strength wash buffer per well (prepared previously by diluting wash buffer concentrate with 20 parts distilled water). During the wash, wells of the micro-plate were filled with working strength wash buffer, and the liquid was discarded; the micro-plate was inverted, and firmly tapped on absorbent paper towels to remove the residual of wash buffer and bubbles. The washing was followed by 100 µl pipetting of TMB substrate with incubation of 30 min at room temperature, with shaking at 700-900 rpm on a micro-plate shaker (Multitaskin Ascent, 354 Thermo Labsystems, Finland). After addition of 100 µl of stop solution, the absorbance of the plate was measured at 450 nm using the Spectophotometer (Multitaskin Ascent, 354 Thermo Labsystems, Finland).

2.7.5. Plasma C-peptide

Plasma C-peptide levels were also measured from the cardiac puncture blood samples using a C-peptide ELISA kit (Cat #80-CPTMS-E01, Alpco; New Hampshire, America). This kit is based on a sandwich type immunoassay in which two monoclonal antibodies are directed against separate antigenic determinants on the C-peptide molecule. C-peptide from the sample reacts with anti-C-peptide antibodies bound to the micro-plate wells. After an initial incubation period and washing, a peroxidase conjugated anti-C-peptide antibody is added. Later, the bound conjugate is detected by reaction with TMB, which then develop a colourimetric pigment, which exhibits absorbance at 450 nm.

The manufacturer protocol was followed to perform the assay. Briefly, high controls, low controls and standards at the concentration of 60, 250, 750, 1,500 and 3,000 pM were prepared by adding 1.5 ml of deionized water for reconstitution. The procedure for this assay is otherwise the same as described in section 2.7.4 of measurement of plasma proinsulin.

2.7.6. Adiponectin

Adiponectin concentrations in cardiac plasma were determined using the Quantikine® ELISA Mouse Adiponectin/Acrp30 Immunoassay (Cat# MRP300, R&D Systems, Minneapolis, MN, USA) according to manufacturer's instructions. This assay uses the quantitative sandwich enzyme immunoassay technique, where plasma samples containing adiponectin were incubated in a 96-well microplate pre-coated with a monoclonal antibody specific for NS0-expressed recombinant mouse adiponectin protein. Addition of enzyme-linked polyclonal antibody specific for mouse adiponectin to the microplate wells causes binding to any mouse adiponectin that had attached to the antibody pre-coated microplate during the incubation period. Hydrogen peroxide and

tetramethylbenzidine addition produced a blue colour. This blue colour is suggested to be proportional to the amount of mouse adiponectin in the well.

Prior to assay performance, plasma samples were diluted 2000-fold in Calibrator Diluent RD5-26 (1X) provided in the kit. Mouse adiponectin standard (lyophilized recombinant mouse adiponectin) was reconstituted in Calibrator Diluent RD5-26 (1X) to produce a stock solution of 10 ng/mL and a 2-fold dilution series in Calibrator Diluent RD5-26 (1X) of 5, 2.5, 1.25, 0.62, 0.31 and 0.16 ng/mL concentrations was prepared. A zero standard of 0 ng/mL adiponectin was created by adding only Calibrator Diluent RD5-26 (1X) without the standard stock solution. A positive control of lyophilized recombinant mouse adiponectin with known concentration range was also assayed.

50 µL of plasma samples, standard dilution series and control was distributed to corresponding wells in the microplate provided by the kit. 50 µL of Assay Diluent RD1W (buffered protein base) was added to all the wells and the plate incubated at room temperature for 2 hours. Wells were then washed five times with 200 µL of wash buffer (provided by the kit) and 100 µL of mouse adiponectin conjugate (enzyme-linked polyclonal antibody specific for mouse adiponectin) was added to all the wells. The plate was then incubated at room temperature for 1 hour. After this incubation period, the plate was flipped over and any unbound enzyme-antibody reagent was removed by washing five times with 200 µL of wash buffer.

100 µL of substrate solution (containing equal parts of hydrogen peroxide and chromogen (tetramethylbenzidine)) was added to all the wells. The microplate was covered with aluminium foil to protect from light and then incubated at room temperature for 30 min producing a blue colour. 100 µL of stop solution containing diluted hydrochloric acid was added to each well to stop the reaction from producing

yellow colour. The optical density of each well was determined within 30 min using a microplate reader (Multiskan Ascent, Thermo Lab systems, USA), reading at 450 nm and then at 540 nm. Optical imperfections in the plate were corrected by subtracting the readings at 540 nm from readings at 450 nm.

2.8. Histological analysis

2.8.1. Haematoxylin and eosin (H&E) staining and scoring

Pancreases removed during the harvest were fixed in formaldehyde for 18 h at room temperature. Formaldehyde serves to stabilize the fine structural details of cells and tissues prior to examination by light or electron microscopy. The standard solution is 10% neutral buffered formalin (NBF), which is approximately 3.7% formaldehyde in phosphate buffered saline. After 18 h the pancreases were transferred to the ACT Pathology Department at The Canberra Hospital for washing in 70% ethanol and then further serial dehydration with xylene followed by embedding into low melting point paraffin (56°C). The paraffin blocks were subjected to sectioning into a series of 4 µm thick sections by microtome (Microm HM200 Ergostar, USA). Sections were stained with H&E according to the standard laboratory protocol (ACT Pathology).

Histological analysis of blinded pancreas sections was performed by Prof Jane Dahlstrom, an experienced pathologist. Islet morphology, presence of exocrine pancreas and islet inflammation, accumulation of pancreas fat deposits, and islet endocrine cell apoptosis were all scored using a scoring sheet as shown in Appendix 2.

2.8.2. Insulin Immunohistochemistry

The pancreas paraffin blocks were subjected to sectioning by microtome (Microm HM200 Ergostar, USA). Three consecutive sections of 5µm at distance of 100 µm were cut and collected on HDS microscopic slides (HD scientific supplies, Australia).

Sections were baked in the oven at 70^0C for 30 min. Before proceeding with the staining protocol; the slides were deparaffinised and rehydrated. Incomplete removal of paraffin could cause poor staining of the section. Slides were placed in a rack and the following washes were performed in a fume hood (Dynasafe control system MK3, Australia): two Xylene (Xylene lab serve-Victoria) washes: 3 minutes each, followed by 2 minutes wash each with 100% ethanol (Cat# BSPEL 9.95.2.5,LabServ, Biolab, (Aust) Ltd, VIC, Australia), 95% ethanol and 70% ethanol. This was followed by washing the slides in running under cold tap water after which they were immersed in 1x phosphate buffer solution (PBS; Cat# 09-8912-100, Medicago AB, Uppsala, Sweden) (Refer Appendix 1). From this step onwards the slides were not be allowed to dry, as drying would cause non-specific antibody binding and could cause high background staining.

The pancreatic sections were targeted by a primary antibody, and subsequently by a secondary antibody, which was conjugated with a horse-radish peroxidase (HRP) enzyme; horseradish peroxidase. The peroxidase binds with 3,3'-Diaminobenzidine (DAB) as a substrate and oxidizes it, producing an easily observable brown colour.

A blocking and dilution buffer was prepared by mixing 5% fetal bovine serum (FBS; Cat# 10082-147, Gibco, Life Technologies Corp., NY, USA) with 1x PBS solution for 15 min. The blocking solution was used to reduce background or unspecific staining.

The slides were stained with the primary antibody: guinea pig anti-insulin (Cat# A0564, Dako, CA, USA) with the dilution of 1:100 with 5% FBS/PBS solution. The combination of primary antibody and FBS/PBS solution was vortexed well and placed on ice until dispensation on sections. The slides were then incubated in a humidity incubation chamber (Lab Scientific, USA) with some water for 1 h.

After the incubation, slides were washed twice with 1x PBS for 2 min each, followed by 20 min incubation with 3% hydrogen peroxide (Cat# H1009, Sigma Aldrich, CA, USA)

made with 1x PBS solution. This acted as endogenous peroxidase blocker. After blocking, the slides were rinsed with 1x PBS twice for 2 minutes. After removing the blocking solution, the surface was dried around the tissue section and the slides were stained with secondary antibody: rabbit anti-Guinea pig IgG-HRP (Cat# P0141, Dako, Glostrup, Denamark) prepared with 5% FBS/PBS solution in 1:40 ratio. The tissue sections on the slides were completely covered with the added volume of HRP conjugated antibody and the slides were incubated for 45 minutes in the humidity incubation chamber at room temperature.

After the staining, the slides were rinsed and washed twice with 1 M PBS for 2 min each. The slides were then stained for 2 min using chromogen 3,3'-Diaminobenzidine tablets (DAB; Cat# D4293, SIGMAFAST™ Sigma-Aldrich, Castle hill, NSW, Australia). The DAB tablets were dissolved by vortex (Cat# BV100 Vortex Mixer, Benchmark Scientific Inc., NJ, USA) in 10mL dH_2O in a 15mL falcon tube. DAB staining was followed by a PBS wash and a quick rinse in running water and immersed in 1x PBS solution.

The slides were counterstained with Harris Hemotoxylin (Cat #HHX2.5L, POCD, Artarmon, NSW, Australia), for 30 seconds and rinsed under running water. The slides were immersed with 1% sodium bicarbonate solution (Cat# S3817, Sigma-Aldrich CA, USA) for 15 seconds and again washed under tap water.

The slides were dehydrated through a series of dips in 75%-90% ethanol, followed by 2 minutes incubation in 100% ethanol and then xylene solution. The slides were mounted by Medite (Cat# 41-4012-00 Pertex-Germany) and cover slipped (Cat# 25X 50#1, Surgipath®Leica, Biosynthesis). Slides for insulin immunohistochemistry were scanned on Aperio ScanScope XT **(**Aperio Technologies, Inc, CA, USA). Analysis of the scanned images was performed on Aperio ImageScope 12.3 (Aperio Technologies, Inc,

CA, USA) slide scanner and analysed by Image J 1.48v software (Wayne Rasband, National Institute of Health, USA).

2.8.3. Measurement of β-cell mass

Pancreatic images for immunohistochemistry were obtained by using the slide scanner; Aperio ScanScope XT (Aperio Technologies, Inc, CA, USA) at 20x magnification. The image was then opened on Image J 1.48v software (Wayne Rasband, National Institute of Health, USA). The images were cleared from presence of any dirty background, fat tissue or lymph node on the software, prior to any measurement. The software was calibrated for images according to number of pixels and length. Threshold adjustments would allow selection of whole pancreas area, as well as areas immuno-stained for insulin (β-cell areas). The process of β-cell area measurement was repeated for each of 3 levels (L1, L2 and L3) from which the average percentage β-cell area per pancreas was calculated. The β-cell mass was calculated, when the % β-cell area per pancreas was divided by 100 and multiplied by the pancreatic weight (mg) registered during harvesting (Refer to Appendix 3).

Chapter # 3:

Results (Short Term Study)

3.1. Introduction

A previous study performed in our laboratory on $B10^k$.insHEL transgenic and NOD^k.insHEL transgenic mice (see section 1.3.5) showed that islet β-cell expression of the HEL transgene resulted in all transgenic mice (male and female NOD^k.insHEL and $B10^k$.insHEL) developing hyperinsulinaemia, but without evidence of impaired sensitivity to exogenous insulin (Dooley et al, 2016). Only male NOD^k.insHEL mice developed non-immune diabetes with a decrease in β-cell mass due to apoptosis. Hence, these gender specific NOD^k mice have the background and propensity to develop islet β-cell failure (Dooley et al, 2016).

To further investigate this propensity to β-cell failure, a more usual diet stressor of islet β-cells was studied in the experiments of this chapter. Male NOD^k and $B10^k$ mice, without the HEL transgene, were stressed by HF-feeding for 10 weeks post-weaning and their metabolic responses were characterized. Unexpectedly, the initial experiment between the NOD^k and $B10^k$ mice showed that the $B10^k$ mice on chow-diet did not have normal glucose tolerance, and for this reason, the $B10^k$ mice couldn't be used as a control strain. Hence, Balb/c mice, known to have normal glucose tolerance on chow-diet, were added to the study as a control third experimental strain.

3.2. Experimental design

This set of experiments was designed to characterise the metabolic phenotype of the three mice strains fed either chow or high fat diet from weaning to the age of 14 weeks. To differentiate from a longer-term study performed later in the thesis, these experiments are described as the "short-term study". This chapter comprises the results of a time course study of body weight and non-fasting blood glucose levels. ipGTTs were also performed at 13 weeks, at which time, fasting plasma TG and NEFA were

also measured. In addition, at 14 weeks, a 9:00 AM non-fasted blood sample was used to measure blood glucose, plasma insulin, TG and NEFA and cardiac plasma was used to measure pro-insulin, C-peptide and adiponectin.

The experimental design for the short-term study is illustrated in Figure 3.1.

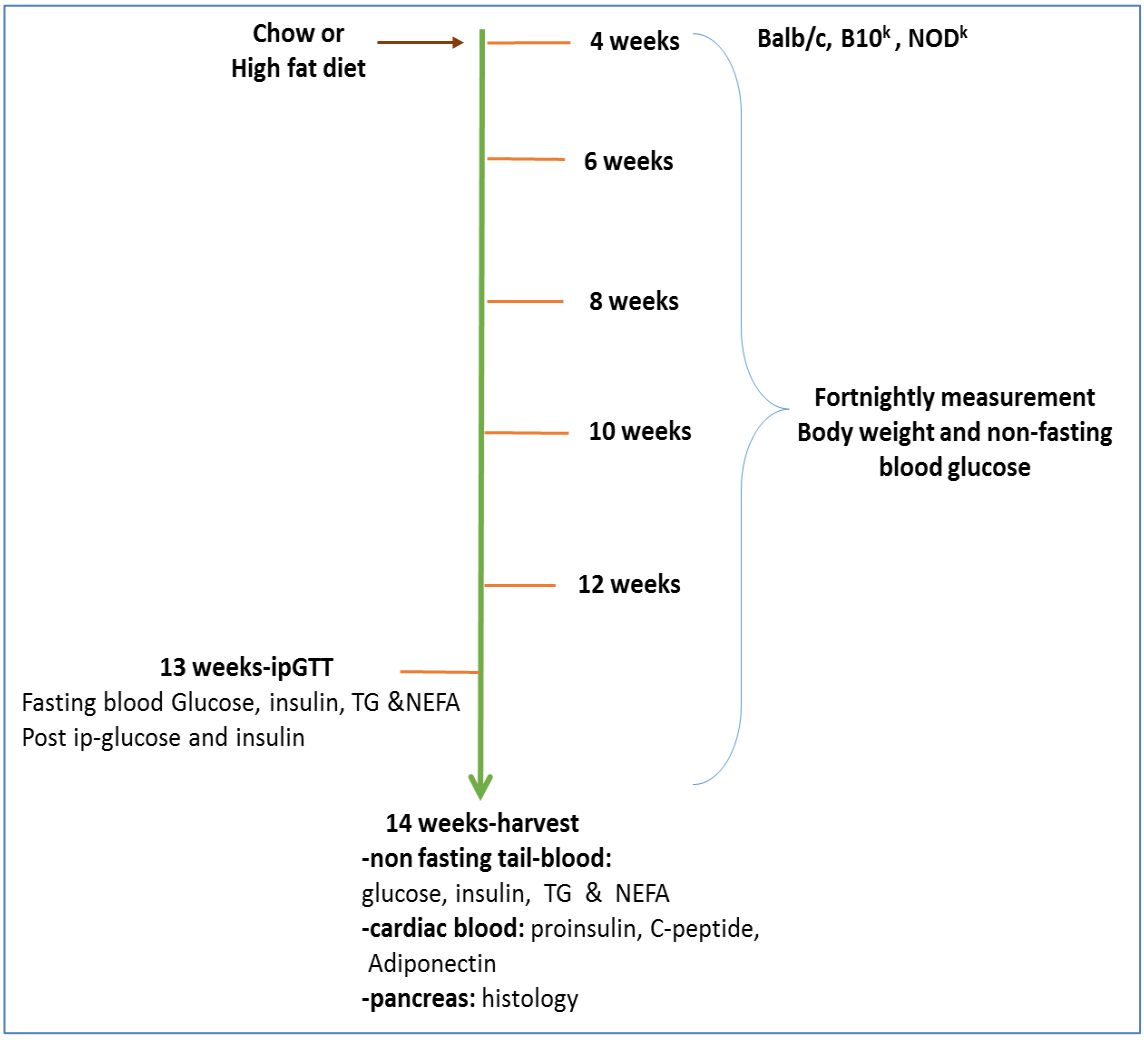

Figure 3.1. Outline of experimental design for the characterization of Balb/c, B10^k and NOD^k mice fed chow or HFD for 10 weeks (post weaning to 14 weeks of age).

Intraperitoneal glucose tolerance test (ipGTT), non-esterified fatty acid (NEFA) and triglycerides (TG).

3.3. Results

3.3.1. Body weight measurement

Body weight of Balb/c, $B10^k$ and NOD^k mice were measured in the non-fasting state between 9:00 and 10:00 AM, every fortnight from 4 weeks of age (i.e. after weaning) until 14 weeks of age. Body weight results are shown in Figure 3.2. The growth curves for body weight over time are shown in Fig 3.2A-D. Fig 3.2E shows the weight at weaning of the 3 different mice strains prior to starting on diet.

NOD^k mice were heavier than the other two strains and this was evident from as early as post weaning at week 4, where the NOD^k mice were 26.9% heavier than Balb/c and 36.5% heavier than $B10^k$ mice (Fig 3.2E). Furthermore, $B10^k$ mice were lighter than Balb/c mice at this time point (Fig 3.2E).

All mice of the respective strains were heavier on the high fat diet compared to chow diet at 14 weeks of age. However, this was only significant for the $B10^k$ and NOD^k mice strains (Fig 3.2A-D). By 14 weeks of age, the chow and HF-fed NOD^k mice were still heavier than the respective chow and HF-fed Balb/c and $B10^k$ mice (Fig 3.2F). Whereas, the increase in body weight of the HF-fed NOD^k mice from weaning to 14 weeks of age was greater than for the HF-fed Balb/c and HF-fed $B10^k$ mice (Fig 3.2G).

On considering the growth curves (Fig 3.2A-D), it is apparent that the HF-fed NOD^k mice develop an earlier and more progressive diet induced obesity in comparison to the other mice strains (Fig 3.2A-C).

Analysis of the data using a general linear model with repeated measures analysis on SPSS statistical program showed a three-way “time*strain*diet”, interaction ($p=0.001$). This is consistent with a different pattern of body weight gain in response to diet

between strains, with a greater propensity of the NOD^{k} mice to develop obesity when stressed by a HF-diet.

Figure 3.2. Body weight measurement during time-course study (age 4-14 weeks) in Balb/c, B10^{k} and NOD^{k} mice fed chow or high fat diet (HFD).

(A) Balb/c chow (n=10) and HFD (n=7) mice. **(B)** B10^{k} chow (n=10) and HFD (n=11) mice. **(C)** NOD^{k} chow (n=11) and HFD (n=10) mice. **(D)** All groups shown. **(E)** Body weight at 4 weeks (baseline measurement) for all mice. **(F)** Body weight measured at 14 weeks for all groups. **(G)** Difference in body weight from 4 to 14 weeks of age in all groups. Means ± SEM. One-way ANOVA of body weight data at 4 weeks shown in table. Two-way ANOVA of body weight data at 14 weeks and difference in body weight shown in table and Bonferroni post-hoc tests: ******$p<0.01$, *******$p<0.001$ vs chow diet of the same strain; $^{\#\#\#}$ $p<0.001$ vs different strain on the same diet.

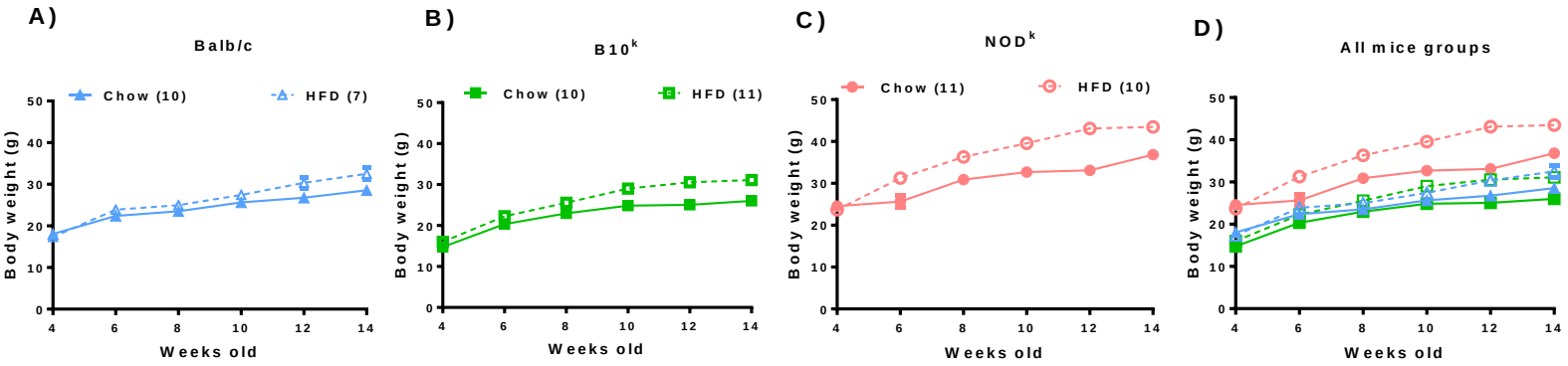

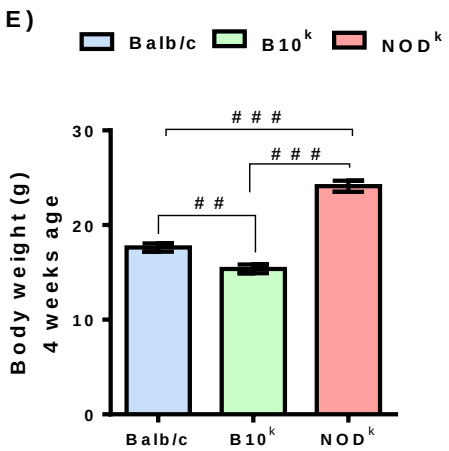

One-way ANOVA	
Strain effect	p<0.0001

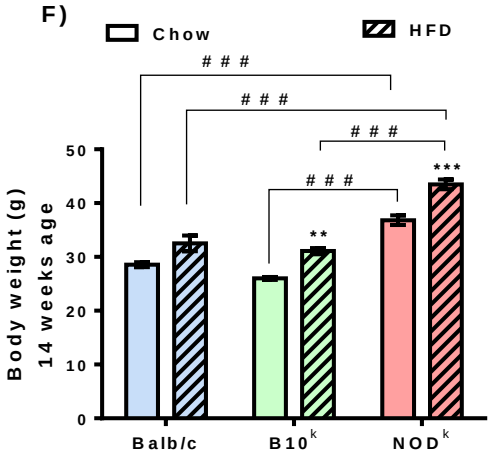

Two-way ANOVA	
Strain effect	p<0.0001
Diet effect	p<0.0001
Strain*Diet interaction	p=0.3196

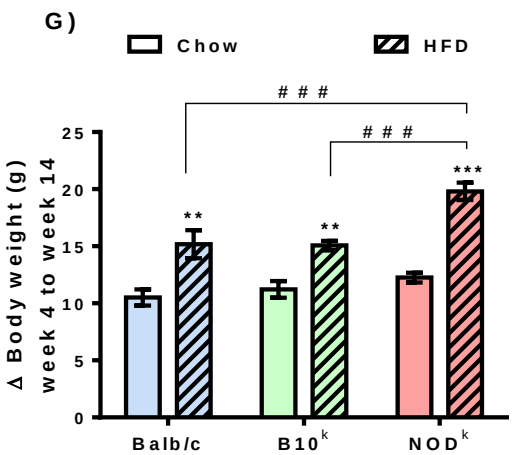

Two-way ANOVA	
Strain effect	p=0.0001
Diet effect	p<0.0001
Strain*Diet interaction	p=0.0430

3.3.2. Tissue weight measurement

Liver, epididymal fat and subcutaneous fat were harvested and weighed from chow and HF-fed Balb/c, $B10^k$ and NOD^k mice at 8 and 12 weeks of age. The graphs with the absolute tissue weights and the relative weight as percentage body weight shown in Figure 3.3 (8 week results in Part 1 and 12 week results in Part 2).

At 8 weeks of age, HF-feeding increased the absolute liver weight in NOD^k mice only (Fig 3.3A), however, this difference was not evident when liver weights were corrected for mouse body weight (Fig 3.3D). By 12 weeks, the effects of HF-feeding on total liver weights was similar to the 8 week time point (Fig 3.3G). Interestingly, with HF-feeding, liver weight of the $B10^k$ mice expressed as a percentage of body weight was significantly reduced (Fig 3.3J).

At 8 weeks of age, the absolute tissue weights of the epididymal fat pads increased in all strains of mice with HF-feeding, but this was greatest in the HF-fed NOD^k mice (Fig 3.3B). Expressed as a percentage of body weight, the effect of HF-feeding to increase this fat depot size was similar in all strains (Fig 3.3E).

The pattern of fat depot weight change in subcutaneous tissues with HF-feeding, however, was different from the epididymal fat depots, as the subcutaneous fat of Balb/c mice did not increase with HF-feeding, expressed as absolute weight or as a percentage of body weight (Fig 3.3C,F).

Interestingly, at 12 weeks of age, the resistance to fat mass expansion of subcutaneous fat of Balb/c mice with HF-feeding was also evident in the epididymal fat depots of this mouse strain (Fig 3.3H,K). By 12 weeks of age, at variance from the Balb/c strain, HF-

feeding of $B10^k$ and NOD^k mice caused expansion of both fat depot sites to a similar degree (Fig 3.3H-L).

Figure 3.3. (Part 1&2) Liver, epididymal fat and subcutaneous fat weights of chow and high fat diet (HFD) fed Balb/c, B10^{k} and NOD^{k} mice at 8 and 12 weeks of age.

(A-F) Tissue weights of mice in all groups at 8 weeks of age. Data are Means ± SEM (n=7-11) mice per group. **(A)** Total liver weight. **(B)** Epididymal fat weight. **(C)** Subcutaneous fat weight. **(D)** Liver weight as percentage of body weight (BW). **(E)** Epididymal fat weight as percentage of BW. **(F)** Subcutaneous fat weight as percentage of BW. **(G-L)** Tissue weights of mice in all groups at 12 weeks of age. Data are Means ± SEM (n=4-6) mice per group. **(G)** Total liver weight. **(H)** Epididymal fat weight. **(I)** Subcutaneous fat weight. **(J)** Liver weight as percentage of BW. **(K)** Epididymal fat weight as percentage of BW. **(L)** Subcutaneous fat weight as percentage of BW. Two-way ANOVA of shown in table and Bonferroni post-hoc tests: *****$p<0.05$, ******$p<0.01$, *******$p<0.001$ vs chow diet of the same strain; $^{\#}$ $p<0.05$, $^{\#\#}$ $p<0.01$, $^{\#\#\#}$ $p<0.001$vs different strain same diet.

PART:1

A)

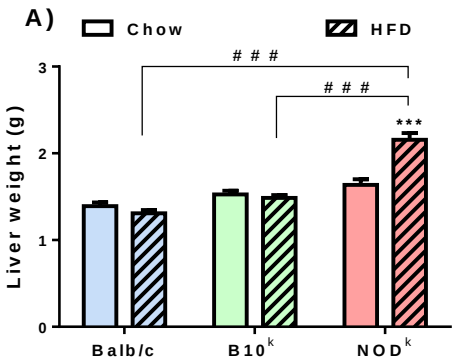

Two-way ANOVA	
Strain effect	p<0.0001
Diet effect	p=0.0041
Strain*Diet interaction	p<0.0001

B)

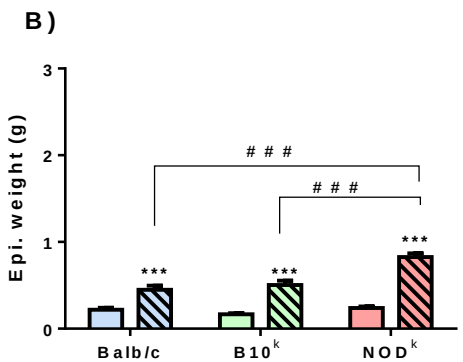

Two-way ANOVA	
Strain effect	p<0.0001
Diet effect	p<0.0001
Strain*Diet interaction	p<0.0001

C)

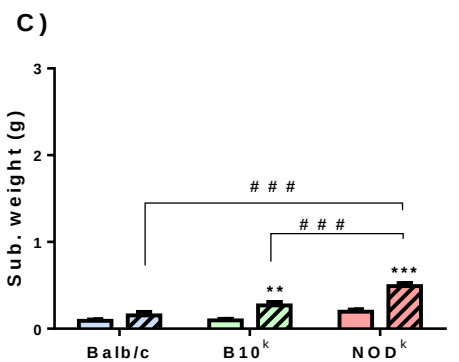

Two-way ANOVA	
Strain effect	p<0.0001
Diet effect	p<0.0001
Strain*Diet interaction	p=0.0019

D)

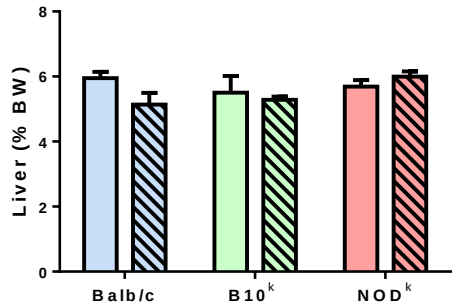

Two-way ANOVA	
Strain effect	p=0.2882
Diet effect	p=0.2997
Strain*Diet interaction	p=0.1316

E)

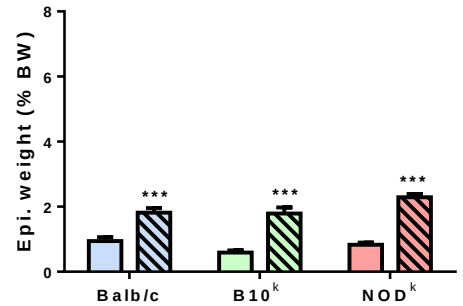

Two-way ANOVA	
Strain effect	p=0.0208
Diet effect	p<0.0001
Strain*Diet interaction	p=0.0579

F)

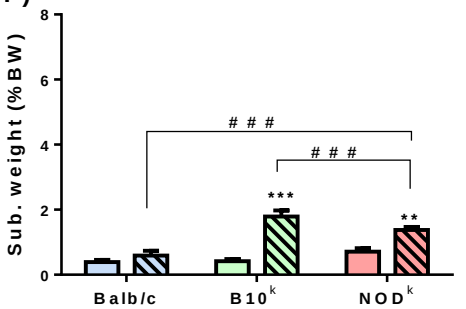

Two-way ANOVA	
Strain effect	p<0.0001
Diet effect	p<0.0001
Strain*Diet interaction	p<0.0001

PART:2

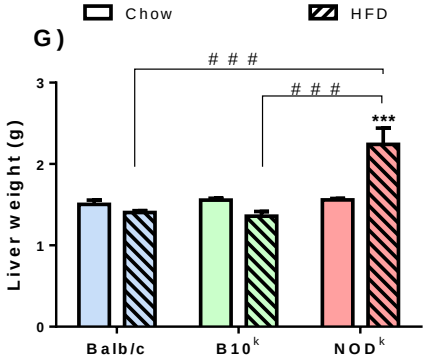

Two-way ANOVA	
Strain effect	p<0.0001
Diet effect	p=0.0707
Strain*Diet interaction	p<0.0001

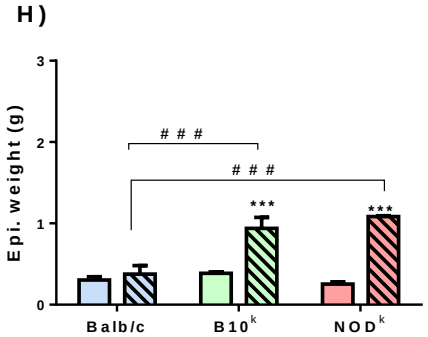

Two-way ANOVA	
Strain effect	p=0.0001
Diet effect	p<0.0001
Strain*Diet interaction	p=0.0001

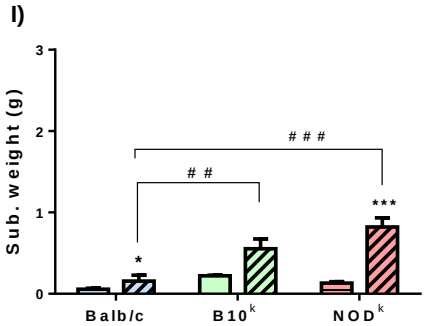

Two-way ANOVA	
Strain effect	p<0.0001
Diet effect	p<0.0001
Strain*Diet interaction	p=0.0011

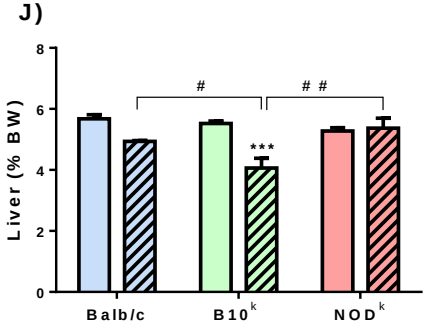

Two-way ANOVA	
Strain effect	p=0.0182
Diet effect	p=0.0002
Strain*Diet interaction	p=0.0030

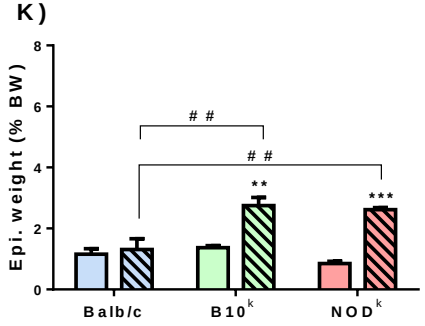

Two-way ANOVA	
Strain effect	p=0.0032
Diet effect	p<0.0001
Strain*Diet interaction	p=0.0027

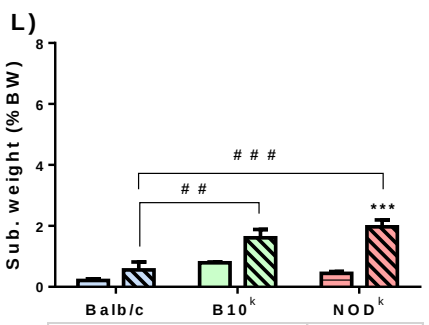

Two-way ANOVA	
Strain effect	p=0.0002
Diet effect	p<0.0001
Strain*Diet interaction	p=0.0114

3.3.3. Non-fasting blood glucose measurement

For determination of the diabetic phenotype, a measurement of non-fasting blood glucose was performed between 9:00 and 10:00 AM fortnightly for 10 weeks during the short-term experiment. A drop of tail-blood was used to obtain the glucose measurement by a glucometer.

The non-fasting blood glucose measurement of $B10^k$ mice at 4 weeks of age (baseline), was mildly but significantly elevated compared to the Balb/c and NOD^k mice (One-way ANOVA) (Fig 3.4E). None of the chow-fed mice had a change in glucose from baseline to 14 weeks of age (Fig 3.4A-D).

The effects of HF-feeding on non-fasting glucose levels was clearly evident in NOD^k mice with the emergence of hyperglycaemia at 10 weeks of age (Fig 3.4 C), such that the HF-fed NOD^k mice were markedly hyperglycaemic by 14 weeks of age (Fig 3.4C,F). In contrast, HF-feeding had no effect on non-fasting glycaemia in Balb/c and $B10^k$ mice (Fig 3.4A, B, D, F, and G).

Using a general linear model with repeated measures to analyse the data, a three-way interaction of strain*diet*time was shown ($p=0.05$). This suggests that the abnormal glucose in NOD^k mice with HF-feeding was time dependent.

Figure 3.4. Non-fasting blood glucose concentration during time-course study (age 4-14 weeks) in Balb/c, B10^{k} and NOD^{k} mice fed chow or high fat diet (HFD).

(A) Balb/c chow (n=10) and HFD (n=7) mice. **(B)** B10^{k} chow (n=10) and HFD (n=11) mice. **(C)** NOD^{k} chow (n=11) and HFD (n=10) mice. **(D)** All groups shown. **(E)** Blood glucose at 4 weeks (baseline measurement) for all groups. **(F)** Blood glucose measurement at 14 weeks for chow and HFD mice for all groups. **(G)** Difference in blood glucose levels from 4 to 14 weeks of age in all groups. Means ± SEM. One-way ANOVA of blood glucose data at 4 weeks shown in table. Two-way ANOVA of blood glucose data at 14 weeks and difference in blood glucose levels shown in table and Bonferroni post-hoc tests: *******$p<0.001$ vs chow diet of the same strain; $^{\#\#}$ $p<0.01$, $^{\#\#\#}$ $p<0.001$ vs different strain on the same diet.

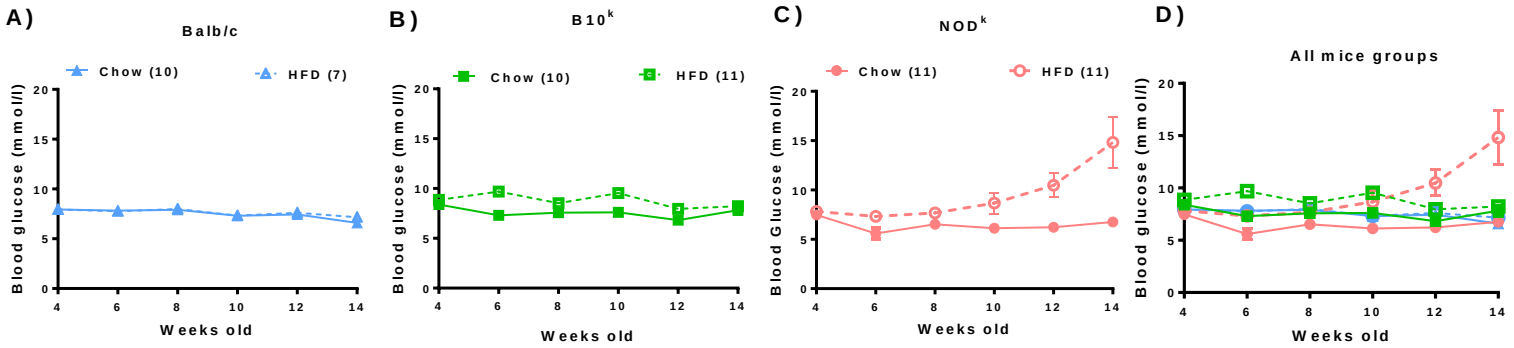

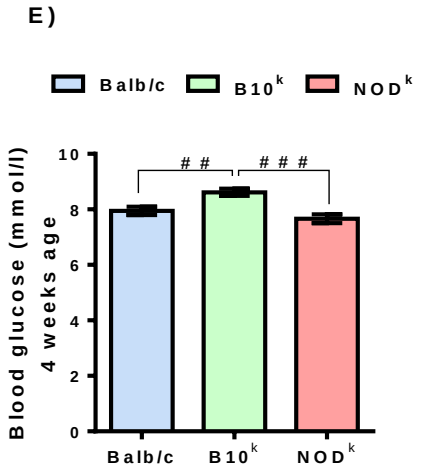

One-way ANOVA	
Strain effect	p<0.0001

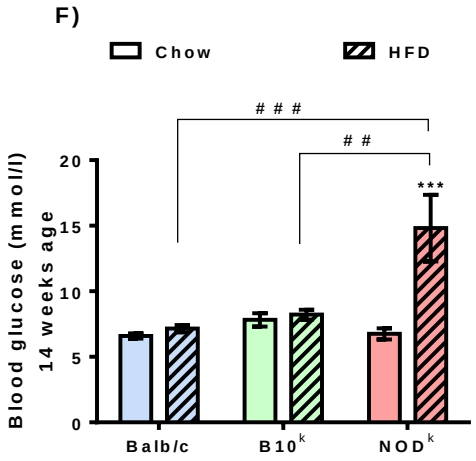

Two-way ANOVA	
Strain effect	p=0.0080
Diet effect	p=0.0043
Strain*Diet interaction	p=0.0028

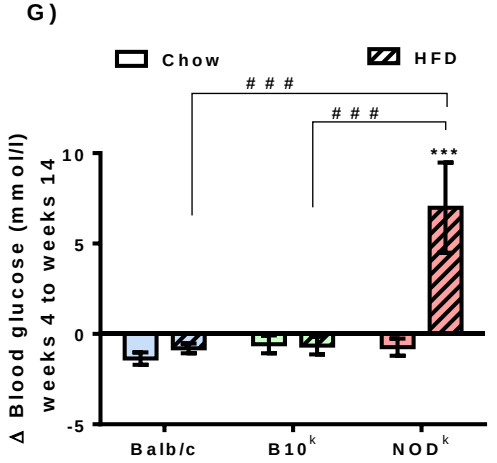

Two-way ANOVA	
Strain effect	p=0.0016
Diet effect	p=0.0085
Strain*Diet interaction	p=0.0028

3.3.4. ipGTT

To determine the effects of HF-feeding on blood glucose regulation and insulin secretion on the three mice strains, ipGTTs were performed in Balb/c, $B10^k$ and NOD^k mice on chow and HF-diet at 13 weeks of age.

The test was performed after 4 hours of fasting and by injecting the mice with 2g/kg body weight of 25 % glucose intraperitoneally.

The 13 weeks of age ipGTT blood glucose results are shown in Figure 3.5, with the glucose curves shown in Fig 3.5A-D.

The fasting glucose concentrations alone are shown in Fig 3.5E, the two hour glucose concentrations alone are shown in Fig 3.5F and the total glucose area under the curve (AUC) results for all groups are shown in Fig 3.5G.

On chow diet, there was a non-significant trend for $B10^k$ mice toward higher fasting glucose levels than the other two groups (Fig 3.5E).

Chow-fed $B10^k$ mice however had impaired glucose tolerance compared to chow-fed NOD^k and Balb/c mice (Fig 3.5D, G).

High-fat feeding resulted in no significant change in glucose tolerance in Balb/c mice, but severe glucose intolerance in both the $B10^k$ and NOD^k mice strains, as evidenced by elevated fasting glucose levels (Fig 3.5E), 2 hour blood glucose levels (Fig 3.5F) and the total area under the ipGTT glucose tolerance curves (Fig 3.5A, B, C, D, G). The worst glucose tolerance was evident in the HF-fed $B10^k$ mice (Fig 3.5D,G).

Two-way ANOVA showed a significant effect of strain ($p<0.0001$) and diet ($p<0.0001$) on glucose tolerance during the ipGTT, with a significant interaction of diet and strain ($p=0.0029$) (Fig 3.5G).

Figure 3.5. Blood glucose concentrations during ipGTT at 13 weeks of age in Balb/c, B10^{k} and NOD^{k} mice fed chow or high fat diet (HFD). Mice fasted for 4 hours were injected with 2g/kg glucose intraperitoneally at time 0.

(A) Balb/c chow (n=10) and HFD (n=7) mice. **(B)** B10^{k} chow (n=10) and HFD (n=11) mice. **(C)** NOD^{k} chow (n=11) and HFD (n=10) mice. **(D)** All groups shown. **(E)** Blood glucose measured at time 0 (fasting) during ipGTT for all groups. **(F)** Blood glucose measured at 2 hours during ipGTT for all groups. **(G)** Total area under the curve (AUC) measured during ipGTT for all groups. Means ±SEM. Two-way ANOVA as shown. Bonferroni post-hoc tests: ***p<0.001 vs chow diet same strain; $^{\#}$ p<0.05, $^{\#\#}$ p<0.01, $^{\#\#\#}$ p<0.001vs different strain same diet.

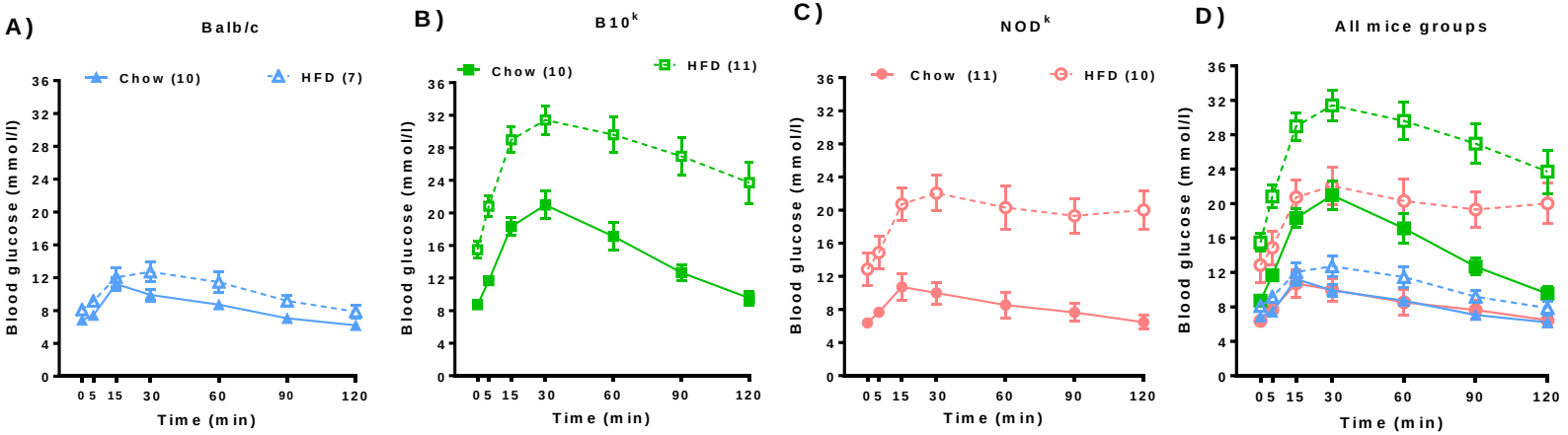

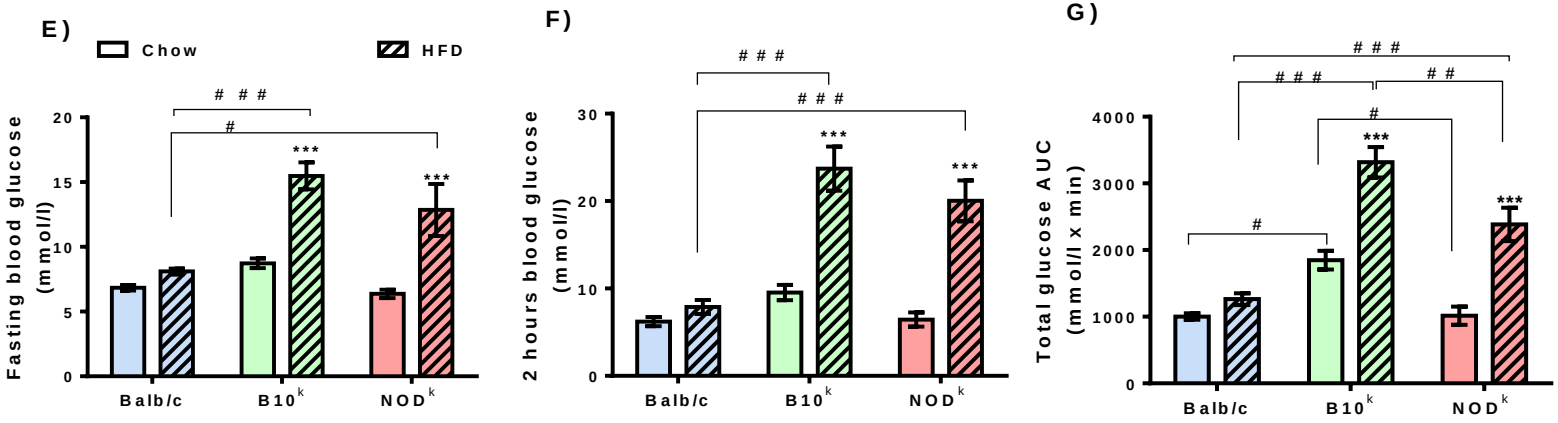

Two-way ANOVA	
Strain effect	p=0.0003
Diet effect	p<0.0001
Strain*Diet interaction	p=0.0253

Two-way ANOVA	
Strain effect	p<0.0001
Diet effect	p<0.0001
Strain*Diet interaction	p=0.0006

Two-way ANOVA	
Strain effect	p<0.0001
Diet effect	p<0.0001
Strain*Diet interaction	p=0.0029

3.3.5 Measurement of plasma insulin levels during ipGTT

Obesity causes insulin resistance. To maintain normoglycaemia, the pancreatic islet β-cells need to compensate for the insulin resistance with insulin hyper-secretion. The generally accepted view is that when the β-cells are not able to sustain this compensatory response to insulin resistance, hyperglycaemia emerges and progresses onto the development of type 2 diabetes. Thus, tail blood plasma was collected during the ipGTT at time 0, 15 and 90 minutes at 13 weeks of age to measure plasma insulin by RIA.

The results are shown in Fig 3.6, with the insulin response over time shown in Fig 3.6A-D, the fasting plasma insulin concentrations shown in Fig 3.6E, the total plasma insulin AUC shown in Fig 3.6F and the change in insulin AUC from the plasma insulin concentration at time 0 min in Fig 3.6G.

On chow-diet, there was a non-significant trend for fasting plasma insulin to be higher in NOD^k mice compared to Balb/c and $B10^k$ mice (Fig 3.6E). Chow-fed $B10^k$ mice did not show a usual increase in plasma insulin at 15 min (Fig 3.6B). The total AUC of the insulin responses however was similar for chow-fed mice, irrespective of strain (Fig 3.6F).

In response to HF-feeding, there was an increase in insulin levels overall, with a marked significant increase in fasting and total insulin AUC in HF-fed NOD^k mice compared to the other strains (Fig 3.6A-F). Of note, the change in plasma insulin AUC from baseline was positive for HF-fed Balb/c and $B10^k$ mice, compared to a marked negative change in plasma insulin AUC in HF-fed NOD^k mice (Fig 3.6G), indicative of dysfunctional insulin secretion in this strain, even though there is an obvious compensatory response to insulin resistance.

Also of note, despite the very severe hyperglycaemia in response to HF-feeding in the $B10^{k}$ mice (Fig 3.6B), a significant increase in total plasma insulin AUC was not seen in this mouse group, indicative of poor β-cell compensation for insulin resistance in this strain.

Figure 3.6. Plasma insulin concentrations during ipGTT at 13 weeks of age in Balb/c, B10^{k} and NOD^{k} mice fed chow or high fat diet (HFD). Mice fasted for 4 hours were injected with 2g/kg glucose intraperitoneally at time 0.

(A) Balb/c chow (n=10) and HFD mice (n=7). **(B)** B10^{k} chow (n=10) and HFD (n=11) mice. **(C)** NOD^{k} chow (n=11) and HFD (n=10) mice. **(D)** All groups shown. **(E)** Plasma insulin measurement at time 0 (fasting) during ipGTT. **(F)** Total area under the curve (AUC) for plasma insulin measurement during ipGTT for all groups. **(G)** Change from basal AUC during ipGTT for all groups. Means ± SEM. Two-way ANOVA as shown. Bonferroni post-hoc tests. **p<0.01 ***p<0.001 vs chow diet same strain; $^{\#\#}$p<0.01, $^{\#\#\#}$ p<0.001vs different strain same diet.

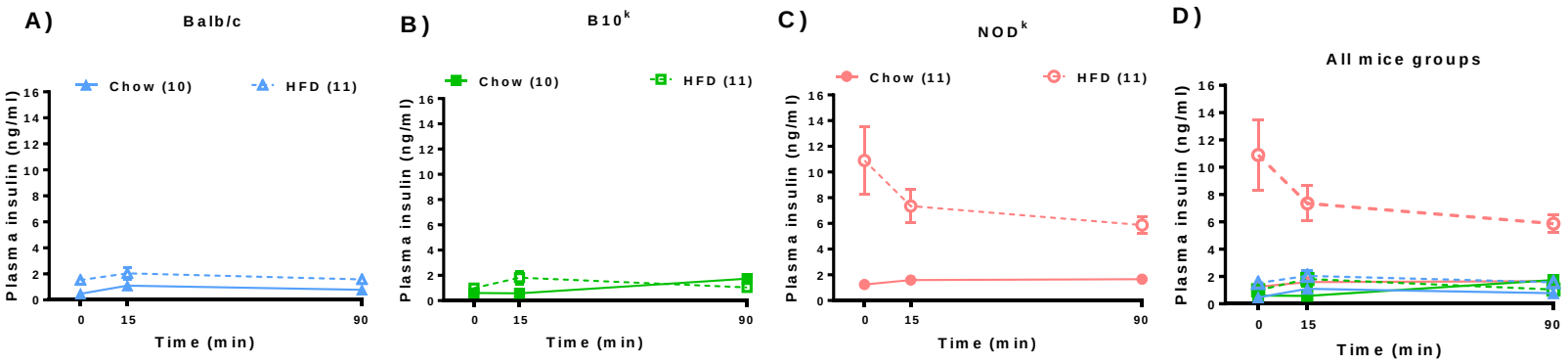

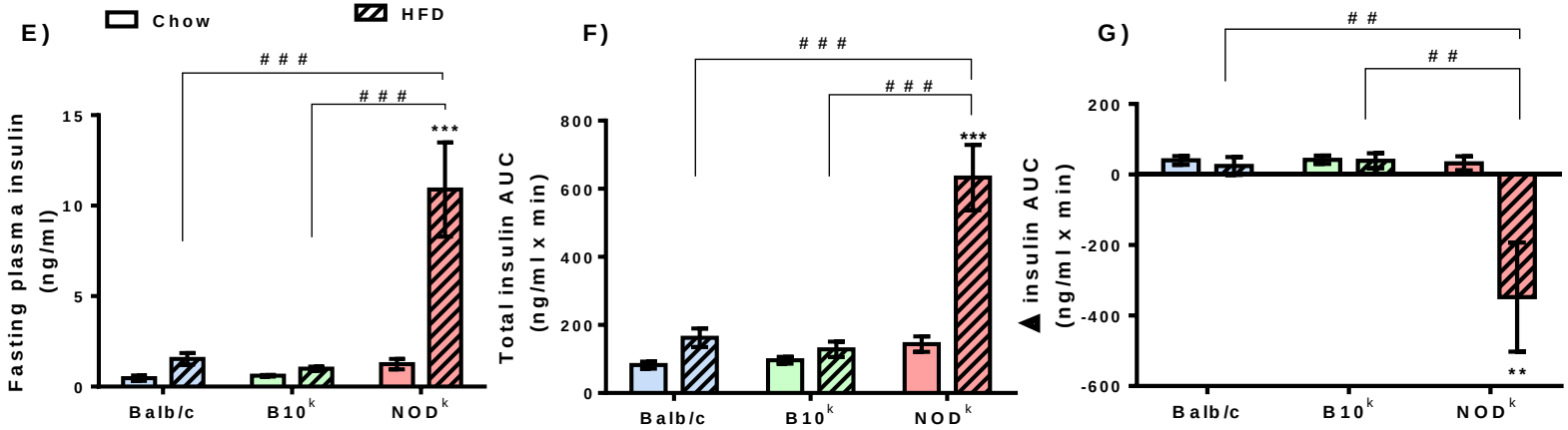

Two-way ANOVA	
Strain effect	p<0.0001
Diet effect	p=0.0005
Strain*Diet interaction	p=0.0003

Two-way ANOVA	
Strain effect	p<0.0001
Diet effect	p<0.0001
Strain*Diet interaction	p<0.0001

Two-way ANOVA	
Strain effect	p=0.0117
Diet effect	p=0.0328
Strain*Diet interaction	p=0.0173

3.3.6. Measurement of non-fasting plasma insulin and derivatives

Non-fasting tail blood was collected immediately before anaesthesia for measurement of plasma insulin from Balb/c, $B10^k$ and NOD^k mice at 14 weeks of age. Further non-fasting blood was collected from cardiac puncture under light anaesthesia. The plasma from the cardiac blood was used to measure C-peptide and proinsulin.

Insulin is synthesized as a precursor molecule, called proinsulin, which is later converted during post-translational modification in the β-cell to insulin. A connecting peptide or C-peptide is an amino acid segment, which connects the insulin A-chain and B-chain together in the proinsulin molecule. Later, the C-peptide is cleaved, leaving the A-chain and B-chain, bound together by disulphide bonds, constituting the mature insulin molecule. An increased level of proinsulin in plasma has been reported in type 2 diabetes in humans and is believed to relate to dysfunction of islet β-cells. C-peptide is secreted in proportion to mature or fully processed insulin. Measurement of insulin, proinsulin and C-peptide in plasma was performed to provide information on the quality of insulin of the three strains of mice on the two different diets.

The non-fasting plasma insulin, proinsulin and C-peptide results in all mice strains are shown in Fig 3.7A-C, with ratios of plasma proinsulin to insulin, proinsulin to C-peptide and insulin to C-peptide are shown in Fig 3.7D-F.

The overall pattern of non-fasting plasma insulin levels as shown in Figure 3.7A is identical to that of fasting insulin levels already shown in Figure 3.6E. Again, a non-significant trend for higher insulin levels was shown in chow-fed NOD^k mice compared to the other two strains. The NOD^k mice again became markedly hyperinsulineamic in response to HF-feeding, which was not evident in the other two strains (Fig 3.7A).

Interestingly, the NOD^{k} mice on chow-diet had significantly higher proinsulin levels than the chow-fed Balb/c and B10^{k} mice, which increased in response to HF-feeding (Fig 3.7 B). HF-feeding, however, had no effect to alter the non-fasting plasma proinsulin concentrations in the Balb/c and B10^{k} mice (Fig 3.7B).

Plasma C-peptide levels were lowest in B10^{k} mice compared to the other two strains, but this was significantly different from NOD^{k} mice only (Fig 3.7C). Unexpectedly, NOD^{k} mice fed HF diet had no further increase in C-peptide levels compared to the effect of HF-feeding, on insulin levels (Fig 3.7A-C).

Of note, the proinsulin/insulin ratio was not increased in NOD^{k} mice on HF-diet suggesting that abnormal insulin processing, resulting in a greater percentage of proinsulin, was not evident in these hyperinsulinaemic mice (Fig 3.7D).

Of particular interest there was a markedly increased insulin/C-peptide ratio in the HF-fed NOD^{k} mice suggestive of impaired clearance of insulin from the blood of these mice (Fig 3.7F). The proinsulin/C-peptide ratio was higher in HF-fed NOD^{k} compared to HF-fed Balb/c mice, but this was not the case in comparison to HF-fed B10^{k} mice.

Figure 3.7. Non-fasting plasma insulin, proinsulin and C-peptide concentrations at 14 weeks of age in Balb/c, B10^{k} and NOD^{k} mice fed chow or high fat diet (HFD).

(A) Non-fasting plasma insulin from all groups from tail-blood. **(B)** Plasma proinsulin from all groups from cardiac blood. **(C)** Plasma C-peptide from all groups from cardiac blood. **(D)** Ratio of proinsulin to insulin. **(E)** Ratio of proinsulin to C-peptide. **(F)** Ratio of insulin to C-peptide. Data are Means ±SEM 7-10 mice per group. Two-way ANOVA as shown. Bonferroni post-hoc tests: **p<0.01, ***p<0.001 vs chow diet same strain; $^{\#}$ p<0.05, $^{\#\#}$ p<0.01, $^{\#\#\#}$ p<0.001 vs different strain same diet.

A)

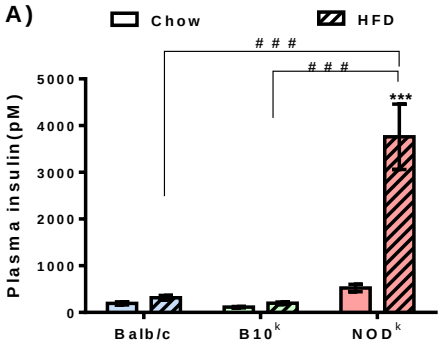

Two-way ANOVA	
strain effect	p<0.0001
Diet effect	p=0.0001
Strain*Diet interaction	p<0.0001

B)

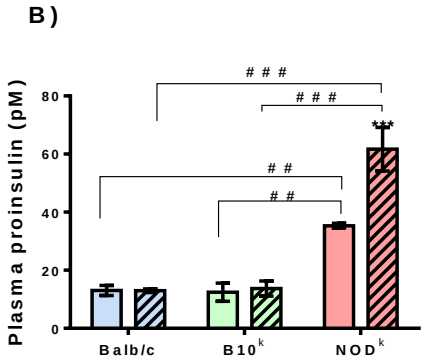

Two-way ANOVA	
strain effect	p<0.0001
Diet effect	p=0.004
Strain*Diet interaction	p=0.0016

C)

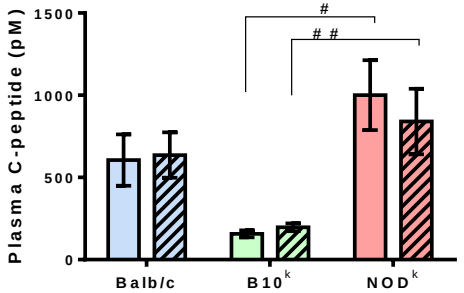

Two-way ANOVA	
Strain effect	p<0.0001
Diet effect	p=0.8060
Strain*Diet interaction	p=0.7396

D)

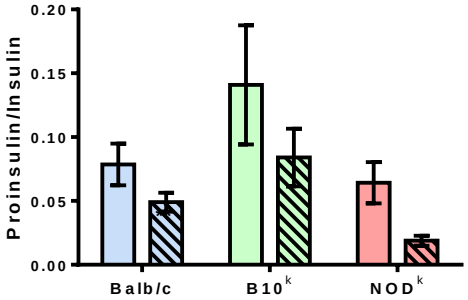

Two-way ANOVA	
Strain effect	p=0.0311
Diet effect	p=0.0553
Strain*Diet interaction	p=0.8771

E)

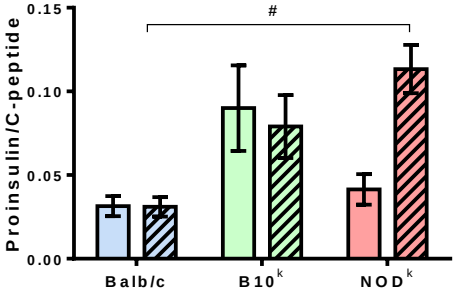

Two-way ANOVA	
Strain effect	p=0.0070
Diet effect	p=0.1623
Strai*Diet interaction	p=0.0470

F)

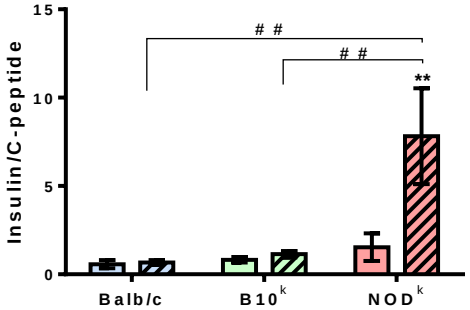

Two-way ANOVA	
Strain effect	p=0.0041
Diet effect	p=0.0416
Strain * Diet interaction	p=0.0298

3.3.7. Measurement of adiponectin

Adiponectin levels were measured from non-fasting cardiac plasma of NOD^k, $B10^k$ and Balb/c mice at 14 weeks. Adiponectin is an adipokine secreted from adipose tissue. Adiponectin levels are inversely proportional to body weight such that they are usually lower in association with obesity and metabolic syndrome.

Unexpectedly, there was a strain effect, but not a diet effect on non-fasting plasma adiponectin levels (Fig 3.8). The increased body weights associated with HF-feeding within each of the strains were not associated with lower adiponectin levels. Plasma adiponectin levels in chow and HF-fed NOD^k mice, however, were significantly lower than the respective diet groups of chow and HF-fed Balb/c and $B10^k$ mice (Fig 3.8).

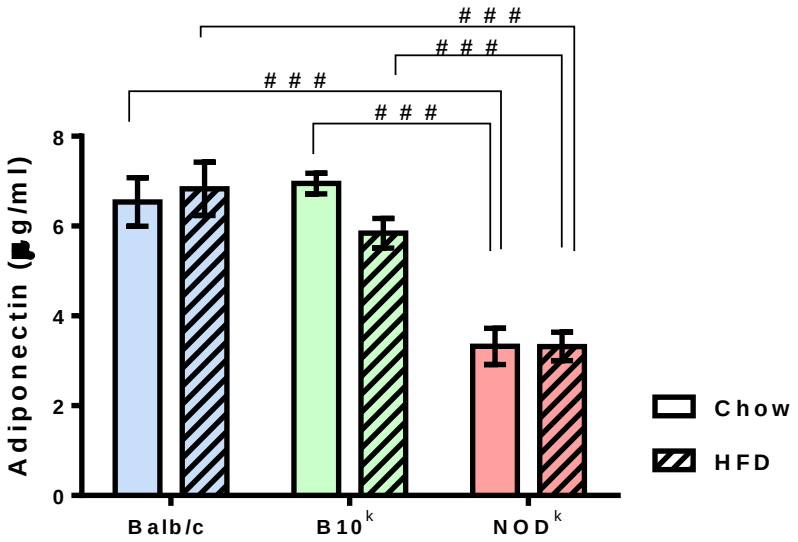

Two-way ANOVA	
Strain effect	p<0.0001
Diet effect	p=0.4269
Strain*Diet interaction	p=0.2039

Figure 3.8. Non-fasting plasma adiponectin concentration from cardiac blood, measured at 14 weeks of age in Balb/c, B10^{k} and NOD^{k} mice fed chow or high fat diet (HFD).

All groups together shown. Data are Means ± SEM 4-10 mice per group. Two-way ANOVA as shown. Bonferroni post-hoc tests: $^{###}$ p<0.001vs different strain same diet.

3.3.8. Measurement of Non Esterified Free Fatty Acid (NEFA)

NEFAs, or FFAs, are released from the hydrolysis of triglyceride in adipose tissues. NEFA reflect body fat mobilization in response to negative energy balance or stress conditions. Obesity and diabetes tend to chronically increase circulating NEFA, which diminishes tissue glucose uptake, while promoting hepatic glucose output. Hence, plasma NEFA was measured in both fasted and non-fasted experimental mice.

Fasting plasma NEFA was measured at time 0 during the ipGTT at 13 weeks. The results show a main strain effect, with lowest levels in $B10^k$ mice and highest levels in NOD^k mice, but no main diet effect on NEFA levels (Fig 3.9A).

Fed 9:00 AM NEFA was measured from tail blood collected before anaesthesia and mice harvest at 14 weeks of age. There was again a main strain effect, but there was not a significant main diet effect. (Fig 3.9B). Of note, in contrast to the fasted state, the Balb/c mice had the lowest levels and the NOD^k mice, the highest fed-state NEFA levels. Following Bonferroni post-hoc testing, fed-state NEFA levels in HF-fed NOD^k were higher compared to HF-fed Balb/c mice (Fig 3.9B).

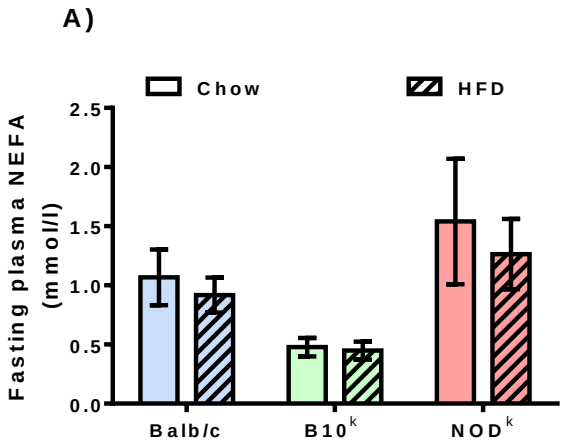

Two-way ANOVA	
Strain effect	p<0.0042
Diet effect	p<0.5183
Strain*Diet interaction	p=0.9002

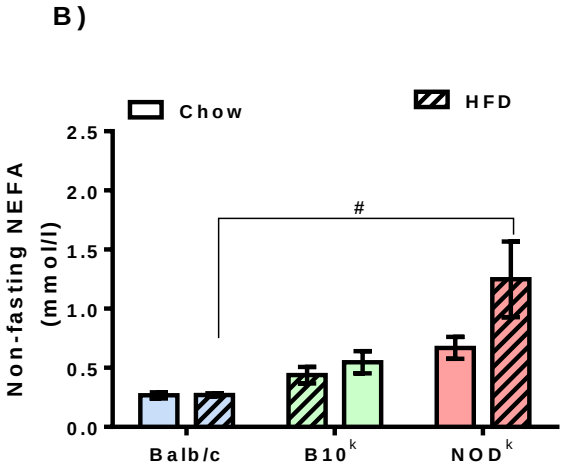

Two-way ANOVA	
Strain effect	p=0.0074
Diet effect	p=0.1992
Strain*Diet interaction	p=0.3239

Figure 3.9. Plasma NEFA concentrations of Balb/c, B10^{k} and NOD^{k} mice fed chow or high fat diet (HFD).

(A) Fasting plasma NEFA from tail-blood at 13 weeks of age, all groups shown. **(B)** Non-fasting NEFA from tail-blood at 14 weeks of age, all groups shown. Data are Means ±SEM 5-10 mice per group. Two-way ANOVA as shown. Bonferroni post-hoc tests: $^{\#}$ $p<0.05$ vs different strain same diet.

3.3.9. Measurement of TG

Elevated TG levels are characteristic of the metabolic syndrome and type 2 diabetes. TG levels are affected by insulin sensitivity, the fed-fasted state transition, dietary content and physical activity.

TG was measured from fasting plasma collected from Balb/c, $B10^k$ and NOD^k mice at time 0, at 13 weeks of age.

Fasting plasma TG was lowest in chow fed Balb/c mice, similar in chow-fed $B10^k$ and NOD^k, and increased after HF-feeding in NOD^k mice only (Fig 3.10A). Bonferroni post-hoc test showed that fasting TG levels were significantly 2 fold higher in HF-fed NOD^k mice compared to HF-fed $B10^k$ mice and >10 fold higher compared to HF-fed Balb/c mice.

Fed (9:00 AM) non-fasting TG was measured from blood collected before anaesthesia and mice harvest at 14 weeks age. The pattern of non-fasting TG concentrations was essentially the same as the fasting TG levels (Fig 3.10A, B), with a very strong main strain effect and a strain-diet interaction, with the NOD^k mice having the only significant TG concentration increase with the HF-diet. Clearly, the NOD^k mice are most prone to developing hypertriglyceridemia that is aggravated by HF-feeding.

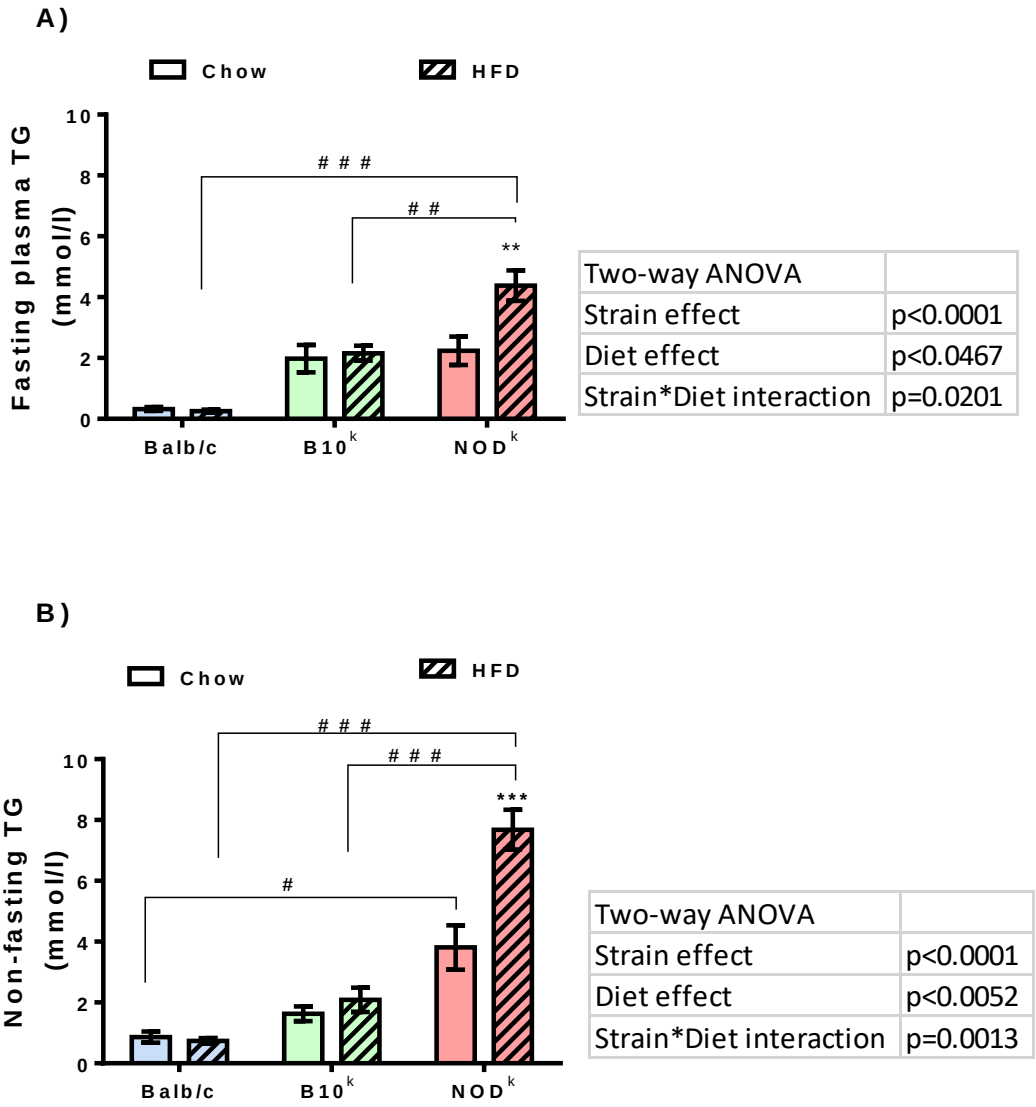

Figure 3.10. Plasma TG concentrations in Balb/c, B10^{k} and NOD^{k} mice fed chow or high fat diet (HFD).

(A) Fasting plasma TG from tail-blood at 13 weeks of age, all groups shown. **(B)** Non-fasting TG from tail-blood at 14 weeks of age, all groups shown. Data are Means ± SEM 5-10 mice per group. Two-way ANOVA as shown. Bonferroni post-hoc tests: **p<0.01, ***p<0.001 vs chow diet same strain; $^{\#}$ p<0.05, $^{\#\#}$ p<0.01, $^{\#\#\#}$ p<0.0001 vs different strain same diet.

3.4. Discussion

The major finding of the experiments of this Chapter is that NOD^k mice, despite having excellent glucose tolerance on a standard chow diet, develop a severe type 2 diabetes phenotype with high fat diet feeding. The HF-fed NOD^k mice have rapid weight gain, become profoundly hyperinsulienaic, dyslipidaemic and by 14 weeks of age are markedly hyperglycaemic. Thus, the NOD^k mouse derived from the type 1 diabetes model NOD; is prone to develop diabetes if stressed by overexpression of a foreign protein in its β-cells (Dooley et al., 2016) or by a high fat diet. These findings are in keeping with the hypothesis of this thesis, that non-immune islet β-cell susceptibilities to dysfunction may contribute to the pathogenesis of both type 1 and type 2 diabetes.

The second major and unexpected finding was that B10^k mice have very poor glucose tolerance, even when fed on standard chow. But most interesting is that, despite this poor glucose tolerance on chow diet, with HF-feeding B10^k mice do not develop diabetes by 14 weeks of age, as determined by elevation of 9 AM fed-state blood glucose levels.

The Balb/c mice had excellent glucose tolerance on chow diet and was relatively resistant to the development of HF-diet induced obesity and completely resistant to the development of HF-diet induced glucose intolerance and diabetes.

3.4.1 Mouse body and tissue weights

Male NOD^k mice weighed more at weaning and were more prone to develop HF-diet induced obesity by 14 weeks of age than the other two strains. However, increases in adipose tissue depots of NOD^k and B10^k mice, expressed as percent of body weight,

were not different in response to HF-feeding at 8 and 12 weeks of age. The Balb/c mice, however, were quite resistant to HF-diet induced expansion of adipose depot mass, particularly evident at 12 weeks of age. It has been reported that multiple genes and/or alleles contribute in the variation in body weight, feeding and drinking pattern, when 28 strains were studied for the preference of food and water intake and spout side preference (Bachmanov et al., 2002), also to the pre-disposition to type 2 diabetes (Doria et al., 2008; Montgomery et al. 2013). Interestingly, Jackson Laboratories reported similar findings of diet-induced obesity and the development of hyperglycaemia in male "non-obese non-diabetic mice (NON mice)", a mouse strain with the NOD background, but like the NOD^{k} mice studied in this thesis, a low risk MHC ($H2^{nb1}$) for autoimmune diabetes (Jackson, 2006). There are few studies of HF-feeding of C57BL/10 mice, however, consistent with the findings here in $B10^{k}$ mice, they are prone to diet-induced obesity (Radley-Crabb et al., 2011). The resistance of Balb/c mice to diet-induced

obesity and adipose tissue expansion is consistent with previous reports (Fearnside et al., 2008, Marcelin et al., 2013).

Total liver weight increased with HF-feeding in NOD^{k} mice, but this was not seen in the other two strains. This is could be due to an increase in hepatic triglyceride content, or hepatosteatosis. However, expressed as a percentage of body weight, the increase in liver size was proportional to the increase in total body weight. Of interest, is the decrease in liver weight, expressed as a percentage of body weight in $B10^{k}$ mice. This could be indicative of this mouse strain being less prone to hepatosteatosis than NOD^{k} mice. For confirmation of the extent to which the strains develop hepatosteatosis in response to HF-feeding, assessment of liver triglyceride content, liver histological analysis and liver metabolic gene expression would be necessary.

Food intake measurements were not performed during this experiment due to difficulties with crumbling of the HF diet and activity was not measured, as we had no access to the equipment required. Balb/cByJ mice, a substrain of Balb/c, however, have previously been shown to eat less fat than C57BL/6, when provided free access to fat, protein or carbohydrate. This is likely to be at least part of the reason for Balb/c mice being more resistant to diet-induced obesity (Qiu et al., 2001).

3.4.2. Non-fasting blood glucose and glucose tolerance

In Balb/c mice, HF-feeding had no effect at all on the 9AM fed-state glucose levels, consistent with the resistance of this strain to develop diet-induced obesity and hyperglycaemia. The $B10^k$ mice, as early as weaning (4 weeks of age), had slightly higher 9 AM fed glucose levels than the other two strains. However, in this strain, HF-feeding did not significantly increase the 9 AM fed-state glucose levels, even though there seemed to be a minor increases at 6 and 10 weeks of age, not progressing to 14 weeks of age. In contrast, the HF-fed NOD^k mice developed marked fed-state hyperglycaemia by 14 weeks of age (14.8±2.5 mmol/l), consistent with the development of diabetes, with the increase beginning by about 10 weeks of age. This was clearly an effect of HF-feeding, as chow fed NOD^k mice maintained excellent fed-state glucose levels for the duration of this time course (6.8±0.4 mmol/l).

Intraperitoneal glucose tolerance was examined at 13 weeks of age. Again, the Balb/c mice showed resistance to the effects of HF-feeding on glucose metabolism, as glucose tolerance was not significantly worsened. The results in $B10^k$ mice were unexpected. On chow diet, these mice had very poor glucose tolerance compared to the other two strains. Furthermore, despite this strain not developing diabetes as determined by the 9 AM fed-state glucose levels, HF-feeding led to severe worsening of glucose tolerance with frankly diabetic curves. Also, in contrast to the fed-state glucose levels, fasting

blood glucose was elevated to a diabetic level (15.5±1.0 mmol/l). Consistent with the 9 AM fed-state glucose levels, chow-fed NOD^k mice displayed excellent glucose tolerance at 13 weeks of age and HF-fed NOD^k mice had diabetic glucose tolerance tests curves. It should be noted that glucose bolus injections were calculated according to the mouse body weight, which may have partially contributed to the differences in glucose tolerance between the chow-fed and HF-fed states.

The development of hyperglycaemia after only 4 hours of fasting was also unexpected in the $B10^k$ mice. This may be indicative of an exaggerated stress response to fasting, or the development of an imbalance of the glucagon/insulin ratio. This phenomenon could also be indicative of an important role of the liver in gluco-regulation in this mouse, as it is likely that dysregulated hepatic glycogenolysis and gluconeogenesis will have contributed to this fasting effect (Basu et al., 2005). To explore this further, glucagon and the other counter-regulatory hormones such as the catecholamines and glucocorticoids would need to be measured, and endogenous glucose production could also be measured using metabolic-tracer methodologies, which are beyond the scope of this thesis.

3.4.3. Insulin levels and insulin derivatives

The hyperglycaemia of diabetes can be a consequence of predominant insulin deficiency (e.g. from islet β-cell destruction in type 1 diabetes) or a failure of islet β-cells to compensate for the presence of insulin resistance (as occurs in type 2 diabetes). Hence, in order to determine the cause of hyperglycaemia in the NOD^k and $B10^k$ mice, it was essential to measure insulin levels, particularly in response to a glucose load.

The ipGTT plasma insulin levels of Balb/c mice showed a normal pattern of increase at 15 min and a returning to basal at 90 min. Furthermore, there appeared to be the

expected increase in levels as would be expected from feeding the mice a HF-diet. The ipGTT insulin levels of the chow and HF-fed $B10^k$ mice were very similar to those of the respective Balb/c mice, but this was unexpected considering the hyperglycaemic glucose tolerance curves of both the chow and HF-fed $B10^k$ mice. Furthermore, the chow-fed $B10^k$ mice did not show the normal increase in insulin that is expected at the 15 min time point. Thus, a failure of insulin secretion to respond to hyperglycaemia is likely to be a factor contributing to the severely abnormal glucose tolerance of $B10^k$ mice. Again, in marked contrast, the insulin levels of the NOD^k mice were profoundly increased in the HF-fed compared to the chow-fed NOD^k mice. Insulin secretion in the chow-fed NOD^k mice appeared to be normal at which time glucose tolerance was normal. Fasting levels of insulin, however, increased by about 9 fold in response to them being on HF-diet. Furthermore, the pattern of secretion was very abnormal in the HF-fed NOD^k, which showed a fall rather than increase in levels at 15 min compared to the fasting levels. This is indicative of the islet β-cells of the NOD^k mice at least trying to compensate for HF-diet induced insulin resistance compared to the apparent lack of effort of the $B10^k$ mice. But the results also show evidence of β-cells dysfunction in the NOD^k mice, as they were not able to increase plasma insulin levels in response to a glucose load.

As explained in the introduction, insulin is the result of post-translational modification, including the cleaving of C-peptide from proinsulin, to form mature insulin. Type 2 diabetes is associated with an increase in the ratio of proinsulin to insulin which could be indicative of islet β-cell stress, and it has been proposed that an elevated proinsulin to insulin ratio can be an indicator of β-cells dysfunction (Saisho et al., 2007). After the release of insulin and C-peptide into the extracellular space from the secretory vesicles, the insulin has a relatively shorter serum half-life ~2–3 min and C-peptide has a longer half-life of ~30 min, as it escapes from the first-pass metabolism by the liver (Faber et

al., 1978, Wahren et al., 2012). As C-peptide is stable in plasma for longer, it is used clinically as a marker of β-cells function (Yosten and Kolar, 2015).

For the above reasons, we measured fed-state insulin, proinsulin and C-peptide from the mice at the time of mice euthanasia and tissue sampling. The marked increase in total insulin of HF-fed NOD^k mice was again demonstrated. However, the ratio of proinsulin to insulin was reduced, rather than increased, in these hyperinsulinaemic mice. This suggests that proinsulin processing is not an issue in NOD^k mice. Surprising, however, was the C-peptide results. Despite total insulin levels being 7 fold higher in HF-fed compared to chow-fed NOD^k mice, the C-peptide levels were not different. This raises the possibility that the profound hyperinsulinaemia of NOD^k is a consequence of reduced clearance rather than increased secretion. Insulin clearance in the liver has been reported in subjects with glucose intolerance (Bonora et al., 1983). Also worth noting is the finding that C-peptide levels of $B10^k$ mice are generally much lower than in the other strains, which would be consistent with $B10^k$ mice being an insulin hypo-secreting strain.

The appropriateness of insulin secretion and levels needs to take into account the degree of insulin resistance, which was not measured in the short-term studies of this Chapter. The marked hyperinsulinaemia of the HF-fed NOD^k mice could be reflective of greater insulin resistance developing in this strain in response to the diet. Insulin tolerance tests were performed in the cohort of animals of the long-term study reported in Chapter 4.

3.4.4. Plasma lipid and adiponectin levels

Plasma lipid levels and adipokine levels reflect the complex metabolic relationships between organs including the adipose tissue (Reaven, 1995). Adiponectin is a protein that is synthesized and released from adipocytes. Plasma adiponectin levels are

generally decreased in obesity and other insulin-resistant states (Weyer et al., 2001), and its concentration falls with weight increase (Yang et al., 2001). Interestingly, the plasma adiponectin concentrations were reduced in NOD^k mice compared to the other two mouse strains, irrespective of the diet they were on. This would be consistent with a constitutive difference in the behaviour of adipose tissue in NOD^k mice from the other two strains. Unexpected, was an absence of effect of HF-diet on adiponectin levels in any of the three strains of mice.

With respect to plasma lipid levels, fasting and non-fasting NEFA and TG were measured and metabolic differences between the three mouse stains were again found. NEFAs, are released from the hydrolysis of triglyceride in adipose tissue. NEFA concentrations in plasma fall after each meal, as insulin suppresses adipose tissue lipolysis (Paolisso and Howard, 1998, McGarry, 2002). Plasma NEFA appeared to follow the physiological rules of the fasting-feeding transition best, as NEFA levels showed suppression in the fed-state. NEFA levels were intermediate in $B10^k$ mice, with little evidence of effect of the nutritional state. NEFA levels tended to be highest in NOD^k mice, with an effect of HF-diet to reduce suppression of levels in the fed-state. With respect to TG levels, Balb/c mice had the lowest levels and NOD^k mice the highest levels, even on chow diet as shown in the fed-state.

Although, the measurements of plasma lipid and adipokine levels are minimal, there is a suggestion from this data, particularly of chow-fed mice, that the adipose tissue of NOD^k mice may be more prone to the abnormalities that are typical of the metabolic syndrome and type 2 diabetes (McGarry, 2002). Certainly the adipose of Balb/c mice is not prone to develop characteristics of metabolic syndrome. It has been shown that the acute elevated plasma FFA by intravenous infusion of heparinized triglyceride emulsions causes a >80% inhibition of insulin-stimulated whole-body glucose uptake in skeletal muscles and disappears approximately 4 h after normalization of plasma FFA

(Boden, 2008). An elevated fasting TG has also been identified in predicting the future of type 2 diabetes (Tirosh et al., 2008).

3.5. Summary

The analysis of metabolic physiology of Balb/c, $B10^k$ and NOD^k mice strain in response to HF diets, clearly shows marked variability across multiple parameters of body weight, relative tissues weight, fed-state and fasting glucose levels, glucose tolerance, insulin secretion and plasma lipid and adipose tissues measures. Of relevance to our hypothesis, NOD^k mice develop a severe phenotype in response to HF-feeding suggestive of a propensity of this mouse to have non-immune susceptibility to failure. This mouse fed a HF-diet, however, develops a phenotype typical of type 2 diabetes, with profound hyperinsulinemia and a suggestion that the latter is due to reduced insulin clearance. Unexpected, were very interesting results for $B10^k$ mice which have very poor glucose tolerance, but are resistant to diabetes development. They seem to be poor secretors of insulin, which raises the possibility that insulin hypo-secretion could be a protection from progression to frank diabetes. The reason for the resistance to obesity and diabetes of the Balb/c mice is also intriguing with the results being consistent with previous reports suggesting less over-eating and the adipose tissue are less prone to features typical of the metabolic syndrome.

Further studies are required to determine the mechanisms underlying the profound differences between these three mouse strains.

Chapter # 4: Results
(Long Term Study)

4.1. Introduction

From earlier work in our laboratory, it was shown that the expression of the HEL transgene in β-cells of male NOD^k mice developed non-immune diabetes, but that expression of HEL in the β-cells of $B10^k$ mice did not have this effect (Dooley et al., 2016). The diabetes in the male NOD^k HEL mice was associated with a decrease in β-cell mass due to β-cell apoptosis.

In the work of Chapter 3, the aim was to determine if a more usual β-cell stressor, high fat diet, could also cause non-immune β-cell failure in the NOD^k mouse. Basically, we showed that high fat feeding of male NOD^k mice from weaning for a period of 10 weeks did cause excess weight gain, severe hyperinsulinemia and diabetes. The male Balb/c mice fed HF-diet for 10 weeks had less weight gain and were able to maintain excellent glycaemic control with modest increases in insulinaemia. The findings of the $B10^k$ mice were unexpected and of particular interest. The $B10^k$ mice after 10 weeks of post-weaning chow diet displayed very poor glucose tolerance which did worsen if the diet was HF; however, neither chow-fed nor HF-fed $B10^k$ mice developed diabetes, as determined by 9 AM fed blood glucose levels. The $B10^k$ mice did gain weight on the HF diet, but less quickly than the NOD^k mice. Of particular note, they failed to respond with an increase in insulin levels to compensate for the insulin resistance induced by HF- feeding.

This very interesting finding in $B10^k$ mice, of poor glucose tolerance, but resistance to the development of diabetes after 10 weeks of HF diet, prompted the longer-term experiments of this Chapter. The aim was to see if $B10^k$ mice maintain their resistance to diabetes development or later do develop diabetes. Hence, Balb/c, $B10^k$ and NOD^k mice were fed chow or HF diets for 20 weeks post-weaning (long-term experiment) for

further characterization of their glucose tolerance and diabetes status, with particular interest in the $B10^k$ mice. It was anticipated that the NOD^k mice on HF-diet would develop overt diabetes necessitating them to be euthanized early and the Balb/c mice would continue to compensate well to the longer period of HF-feeding.

4.2. Experimental design

This set of experiments called the "long-term study" was designed to characterise the metabolic phenotype of the three mice strains fed either chow or HF-diet from weaning to the age of 24 weeks. As performed in Chapter 3 but for a shorter time, a time course of measurement of body weight and non-fasting blood glucose levels was undertaken. An ipITT was performed to assess insulin sensitivity at 13 weeks of age, and an ipGTT was performed at 23 weeks of age to assess glucose tolerance and *in vivo* insulin secretion in response to glucose. Fasting plasma TG and NEFA were also measured at time 0 of the ipGTT. Prior to anaesthesia for terminal pancreas tissue harvesting, tail blood was obtained for non-fasting blood glucose, plasma insulin, TG and NEFA measurements. Under anaesthesia, prior to tissue harvest, cardiac blood was obtained for the measurement of plasma proinsulin and C-peptide. Blood sampling and pancreas harvest and their processing are described in Chapter 2.

As overt diabetes was expected in the NOD^k mice, a protocol was set for early experimental termination of mice according to 9 AM non-fasting blood glucose measurements. If a mouse had blood glucose measurements of 20 mmol/l or above for two consecutive measurements, that mouse would be diagnosed as having overt diabetes and would be culled early, but with termination bloods and tissue harvest as for the other mice of this study. The experimental design for the long-term study is illustrated in Figure 4.1.

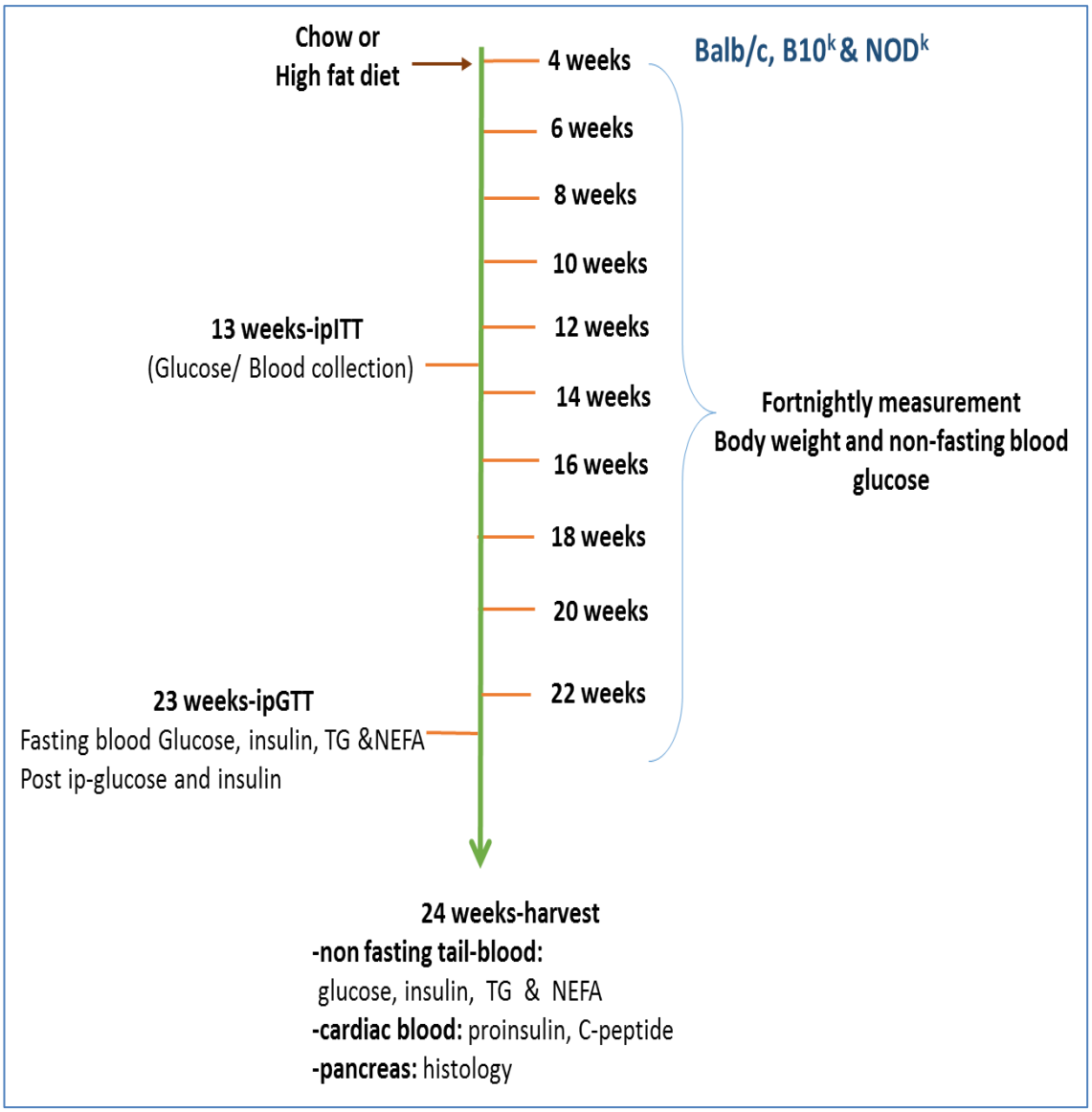

Figure 4.1: Outline of experimental design for the characterization of Balb/c, B10^k and NOD^k mice fed chow or HFD for 20 weeks (post weaning to 24 weeks of age).

Intraperitoneal insulin tolerance test (ipITT), Intraperitoneal glucose tolerance test (ipGTT), non-esterified fatty acid (NEFA) and triglycerides (TG).

4.3. Results

4.3.1 Body weight measurement

Body weight of Balb/c, $B10^k$ and NOD^k mice were measured in the non-fasting state between 9:00 and 10:00 AM, every fortnight from 4 weeks of age (i.e. after weaning) until 24 weeks of age. Body weight results are shown in Figure 4.2.

The growth curves for body weight over time are shown in Fig 4.2A-D. Fig 4.2E shows the weight at weaning of the 3 different mice strains prior to starting on diet. Body weight at 24 weeks is shown in Fig 4.2F and the difference in body weight from 4 weeks to 24 weeks in the mice groups is shown in Fig 4.2G.

At 4 weeks of age (i.e. at weaning) the NOD^k mice were significantly heavier than the $B10^k$ and Balb/c mice (Fig 4.2E). Furthermore the Balb/c mice were also significantly heavier than the $B10^k$ mice at this same age, prior to commencement of high fat feeding (Fig 4.2E). Diabetes did develop in 5 of the 6 HF-fed NOD^k mice, requiring ethical culling prior to 24 weeks of age, as indicated in Fig 4.2C. For this reason, results for body weight at 24 weeks of age (Fig 4.2F) and the change in body weight from 4 to 24 weeks (Fig 4.2G) for NOD^k mice are not shown. However, it is clearly demonstrated in Fig 4.2C that HF-diet feeding of the NOD^k rapidly increased the body weight of this strain of mice compared to its chow-fed controls.

Analysis of the data up to 12 weeks of age using a general linear model with repeated measured analysis on SPSS statistical program showed a three-way "time*strain*diet", interaction ($p<0.0005$), indicative of greater early effect of HF-diet on body weight in NOD^k compared to the other two strains (Fig 4.2A-D).

$B10^k$ and Balb/c mice were heavier on the HF-diet compared to their respective chow fed groups at 24 weeks of age, however, there was not a diet-strain interaction for body

weight or the change in body weight from 4 to 24 weeks of age between these two mice strains (Fig 4.2F-G).

Figure 4.2. Body weight measurement during time-course study (age 4-24 weeks) in Balb/c, B10^{k} and NOD^{k} mice fed chow or high fat diet (HFD).

(A) Balb/c chow (n=6) and HFD (n=6) mice. **(B)** B10^{k} chow (n=6) and HFD (n=6) mice. **(C)** NOD^{k} chow (n=6) and HFD (n=6) mice. Several HF-fed NOD^{k} mice were euthanized before 24 weeks due to severe hyperglycemia. Numbers in brackets refer to the number of mice remaining **(D)** All groups shown. **(E)** Body weight at 4 weeks (baseline measurement) for all mice. **(F)** Body weight measured at 24 weeks for B10^{k} and Balb/c mice only. **(G)** Change in body weight from 4 to 24 weeks of age for B10^{k} and Balb/c mice only. Means ± SEM. One-way ANOVA of body weight data at 4 weeks shown in table (E). Two-way ANOVA of body weight data at 24 weeks and change in body weight shown (F&G). Bonferroni post-hoc tests: ******$p<0.01$, *******$p<0.001$ vs chow diet of the same strain; $^{\#\#}$ $p<0.01$, $^{\#\#\#}$ $p<0.001$ vs different strain on the same diet.

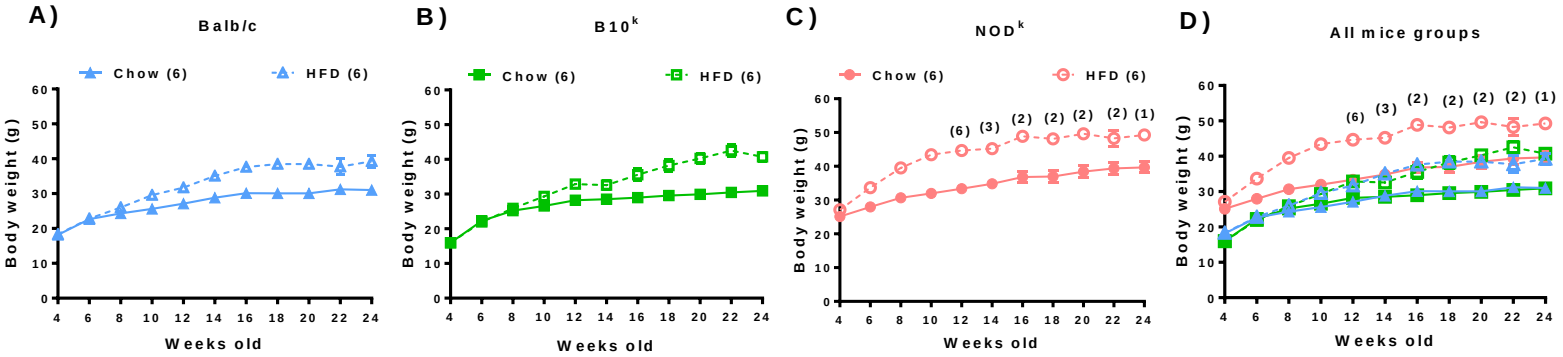

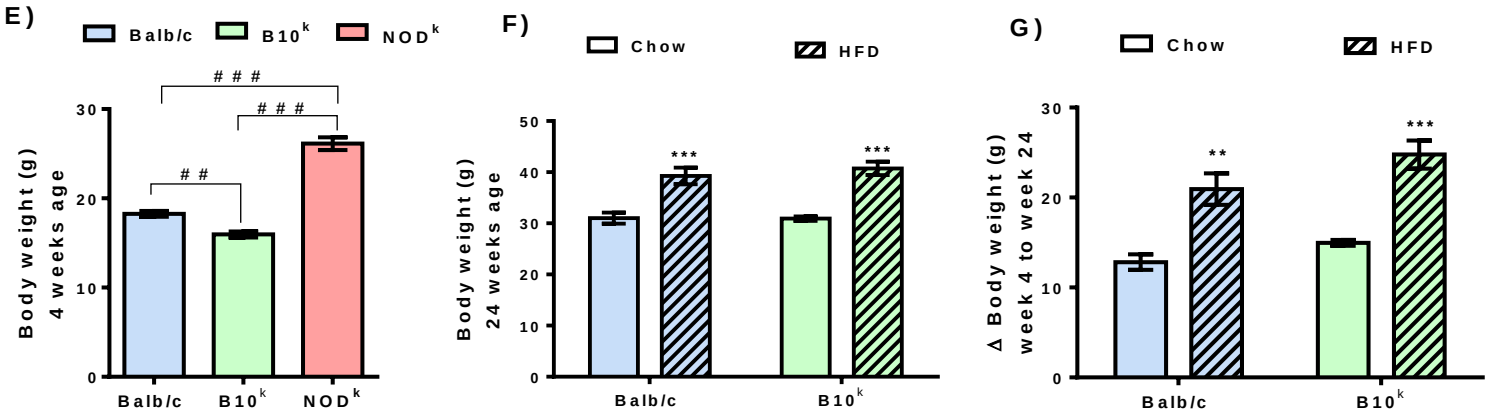

One-way ANOVA	
Strain effect	p<0.0001

Two-way ANOVA	
Strain effect	p=0.5714
Diet effect	p<0.0001
Strain*Diet interaction	p=0.5219

Two-way ANOVA	
Strain effect	p=0.0275
Diet effect	p<0.0001
Strain*Diet interaction	p=0.5064

4.3.2. Non-fasting blood glucose measurement

For determination of the diabetic phenotype, a measurement of non-fasting blood glucose was performed between 9:00 and 10:00 AM fortnightly up to 24 weeks of age during the long-term experiment. A drop of tail-blood was used to obtain the glucose measurement by a glucometer. Fed-blood glucose concentrations are shown in Figure 4.3.

At 4 weeks of age (weaning), there were no differences between the non-fasting glucose levels of the three mice strains (Fig 4.3E). On chow-diet until 24 weeks of age, Balb/c, $B10^k$ and NOD^k mice all maintained normal fed-state glycaemia (Fig 4.3A-D).

With HF-feeding, non-fasting blood glucose did not change in Balb/c mice, but there was a minimal increase in HF-fed $B10^k$ glucose levels, which was significantly different from their chow fed counterparts at 24 weeks of age (Fig 4.3A, B, D, F& G). Similarly, the change in fed-state blood glucose concentrations from 4 to 24 weeks was positive in the HF-fed $B10^k$ mice compared to no change in the HF-fed Balb/c mice and chow-fed mice of both strains (Fig 4.3G).

HF-fed NOD^k mice, however, did develop fed-state hyperglycaemia and diabetes, requiring 5 of the 6 animals to be culled before the completion of the experiment (Fig 4.3 C, D&H). The percentage of non-diabetic NOD^k mice is shown in the survival curve (Fig 4.3H), where 100% chow-fed NOD^k mice survived and were non-diabetic by 24 weeks of age.

Whereas, only 1 of 6 HF-fed NOD^k mice survived during the long-term experiment and could be regarded non-diabetic. Analysis of the data by log-rank test showed the diabetes free survival of HF-fed NOD^k to be significantly less than the chow-fed NOD^k mice ($p=0.0039$).

Analysis by general linear model of the blood glucose data using repeated measures to 12 weeks of age showed a three-way interaction between strain, diet and time ($p<0.05$). This suggests that the effect of HF diet to induce hyperglycaemia in NOD^k mice is time dependent.

Figure 4.3. Non-fasting blood glucose concentration during time-course study (age 4-24 weeks) in Balb/c, B10^{k} and NOD^{k} mice fed chow or high fat diet (HFD).

(A) Balb/c chow (n=6) and HFD (n=6) mice. **(B)** B10^{k} chow (n=6) and HFD (n=6) mice. **(C)** NOD^{k} chow (n=6) and HFD (n=6) mice. Several HF-fed NOD^{k} mice were euthanized before 24 weeks due to severe hyperglycemia. Numbers in brackets refer to the number of mice remaining **(D)** All groups shown. **(E)** Blood glucose at 4 weeks (baseline measurement) for all groups. **(F)** Blood glucose measurement at 24 weeks for B10^{k} and Balb/c mice only. **(G)** Change in blood glucose concentration from 4 weeks to 24 weeks in B10^{k} and Balb/c mice only. **(H)** Percentage of NOD^{k} mice non-diabetic over time course. Means ± SEM. One-way ANOVA of blood glucose data at 4 weeks shown in table (E). Two-way ANOVA of blood glucose concentration at 24 weeks and change in blood glucose concentrations in tables (F&G). Bonferroni post-hoc tests: *****$p<0.05$ vs chow diet of the same strain; $^{\#}$ $p<0.05$, vs different strain on the same diet. Survival curve log-rank (Mantel-Cox) test (H).

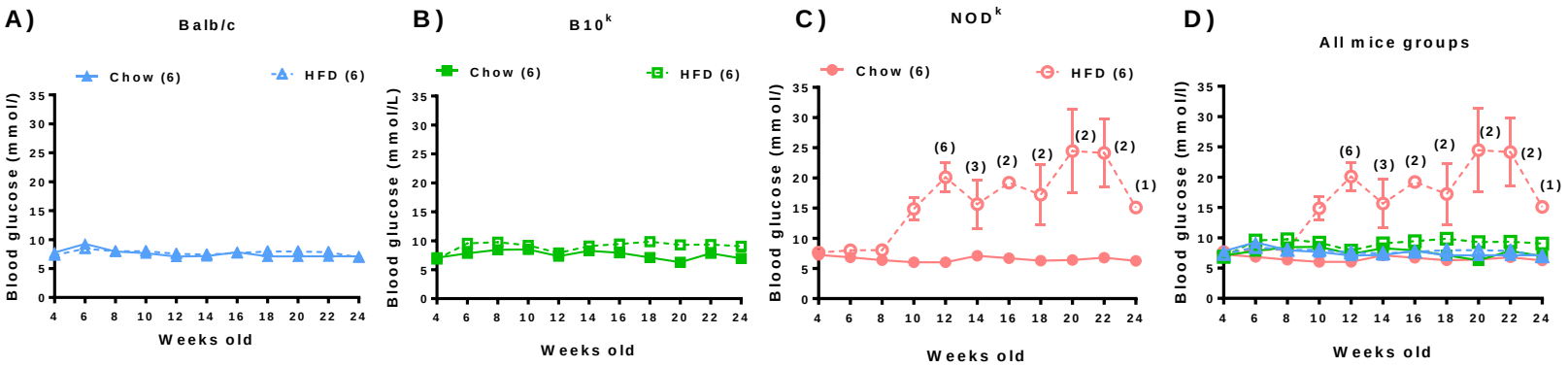

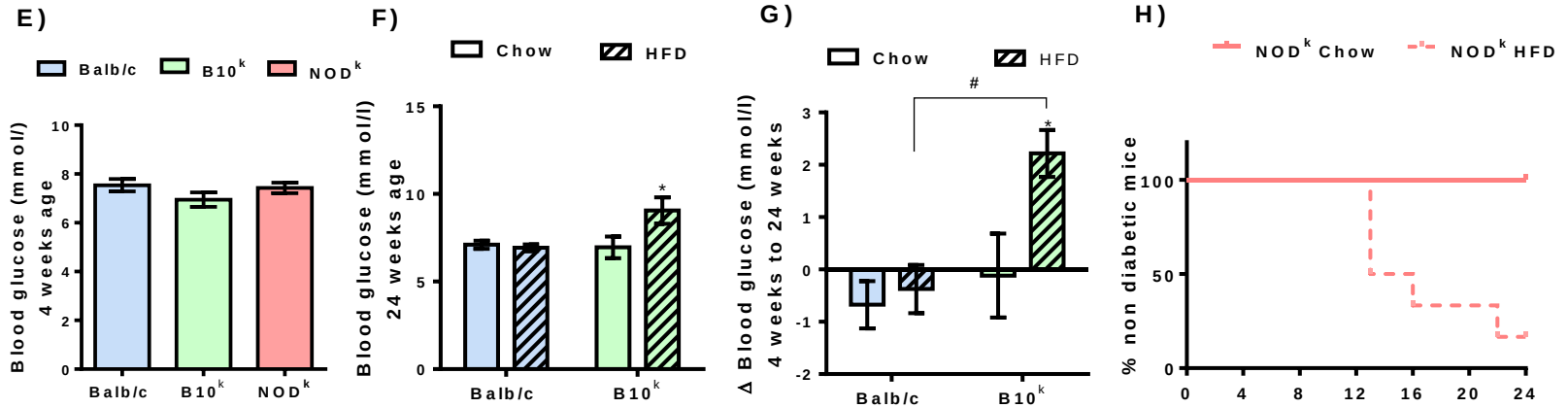

One-way ANOVA	
Strain effect	p=0.2459

Two-way ANOVA	
Strain effect	p=0.0667
Diet effect	p=0.0711
Strain*Diet interaction	p=0.0370

Two-way ANOVA	
Strain effect	p=0.0110
Diet effect	p=0.0295
Strain*Diet interaction	p=0.0854

Log-rank(Mantel-Cox)Test	
Survival curve	p=0.0039

4.3.3. ipITT

At 13 weeks of age ipITTs were performed to measure insulin sensitivity in Balb/c, $B10^k$ and NOD^k mice on chow or HF-diet. Mice were fasted for 4 hours and the test was conducted after intraperitoneal injection of human insulin with a dose of 0.75 U/kg body weight.

Blood glucose concentrations were measured before insulin injection and 15, 30, 45, 60 and 90 min post insulin injection. Results for the ipITTs are shown in Figure 4.4.

The blood glucose concentrations during the ipITTs for Balb/c, $B10^k$ and NOD^k mice are shown in Fig 4.4A-D. The blood glucose results expressed as % of baseline glucose are shown in Fig 4.4E. The blood glucose percentage fall at the nadir is presented in Fig 4.4F.

The fasting blood glucose concentrations of chow-fed Balb/c, $B10^k$ and NOD^k mice were similar, but the fasting blood glucose levels of the HF-fed $B10^k$ and NOD^k mice were elevated (Fig 4.4A-D).

The chow fed mice of the three strains had similar reductions of blood glucose in response to the exogenous insulin injection (Fig 4.4 D-F). It should be noted that ipITT studies were performed in only 3 of 6 HF-fed NOD^k mice, as 3 mice had developed diabetes by the time of this test.

The glucose fall in HF-fed Balb/c mice did not suggest the presence of insulin resistance (Fig 4.4A, D-F). Following an initial trend for blood glucose to increase after the ip insulin injection in HF-fed $B10^k$ mice, glucose levels did fall, with the percentage fall to nadir being not different between chow and HF-fed $B10^k$ mice (Fig 4.4B, D-F). Whereas, the ipITT results of the chow and HF-fed NOD^k mice were suggestive of HF

diet induction of insulin resistance in this strain, particularly when assessed by the percentage fall in blood glucose from baseline to nadir (Fig 4.4C-F). Due to the reduced number of HF-fed NOD^k mice tested, however, the insulin resistance caused by HF diet in NOD^k mice could not be statistically shown.

Figure 4.4. Blood glucose concentrations during ipITTs at 13 weeks in Balb/c, B10^{k} and NOD^{k} mice fed chow or high fat diet (HFD). Mice were fasted for 4 hours and were injected with 0.75 units/kg insulin (diluted to 0.1 units/ml) intraperitoneally at time 0 minutes.

(A) Balb/c chow (n=6) and HFD (n=6) mice. **(B)** B10^{k} chow (n=6) and HFD (n=6) mice. **(C)** NOD^{k} chow (n=6) and HFD (n=3) mice. Three HF-fed NOD^{k} mice were euthanized before the ipITTs were to be performed due to the development of diabetes. **(D)** All groups shown. **(E)** Percentage of baseline glucose concentration shown for all mice groups during ipITT. **(F)** Blood glucose fall at nadir, expressed as percentage fall from baseline; all groups shown. Means ±SEM. Two-way ANOVA as shown (F).

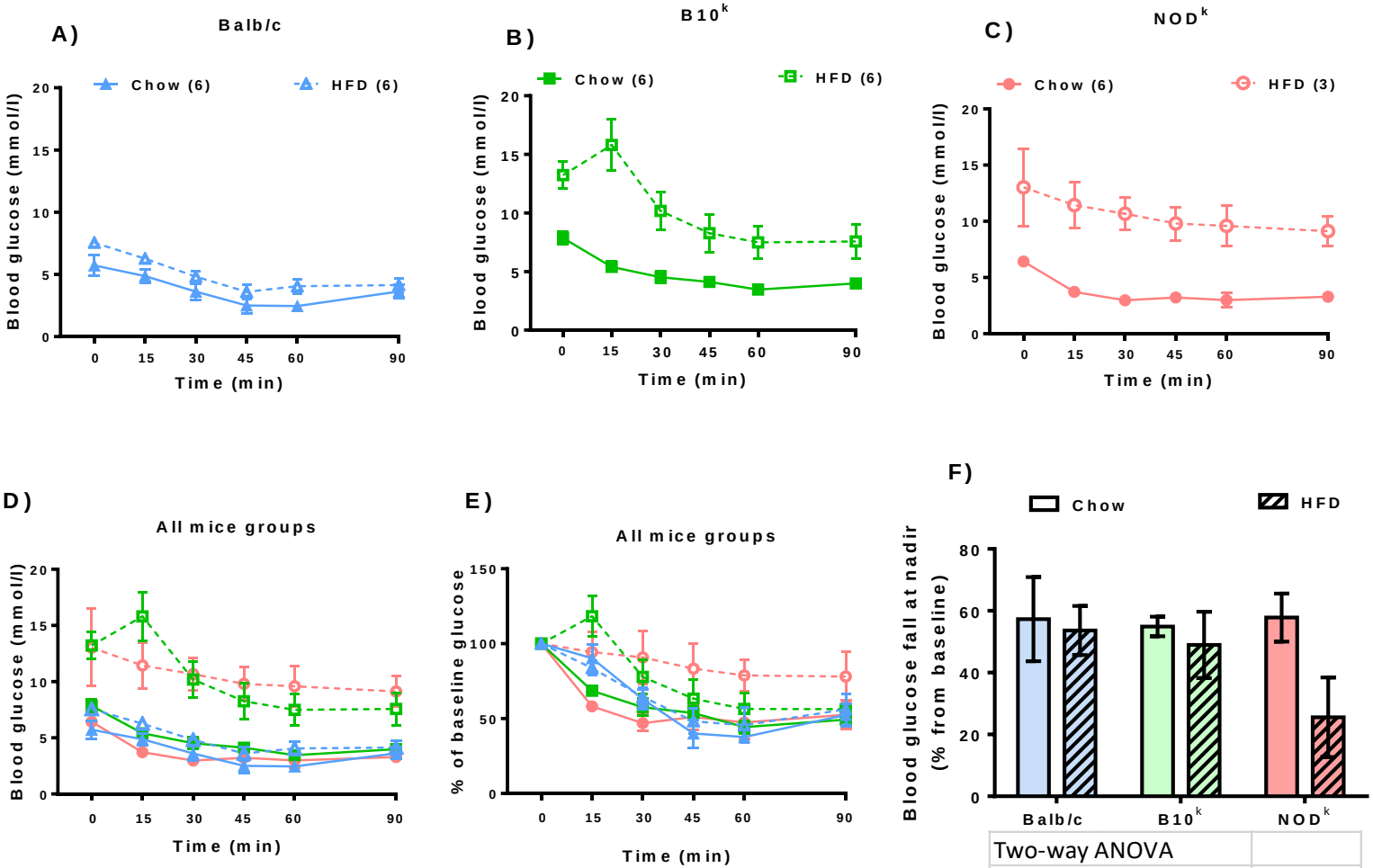

Two-way ANOVA	
Strain effect	p=0.4292
Diet effect	p=0.1039
Strain*Diet interaction	p=0.3637

4.3.4. ipGTT

ipGTTs were performed at 23 weeks of age in chow-fed and HF-fed Balb/c, $B10^k$ and NOD^k mice. These tests were performed to determine the effects of longer-term HF-feeding on blood glucose regulation and insulin secretion of the three mice strains.

The test was performed after 4 hours of fasting and by injecting mice 2g of 25% glucose per kg body weight intraperitoneally. Of note, an ipGTT was only performed in one mouse from the HF-fed NOD^k group, as 5 of the 6 mice from this group had been culled earlier because of the development diabetes with severe hyperglycaemia.

The ipGTT results are shown in Figure 4.5, with the glucose curves shown in Fig 4.5 A-D. The total glucose area under the curve (AUC) results for chow-fed Balb/c, $B10^k$ and NOD^k are shown in Fig 4.5E.

The fasting and the 2 h post-glucose load blood glucose levels, and the total blood glucose AUC results, are for chow and HF-fed Balb/c and $B10^k$ mice are shown in Fig 4.5F-H.

In keeping with the results of the short-term study, glucose tolerance of chow-fed $B10^k$ mice was significantly impaired compared to chow-fed Balb/c and NOD^k mice (Fig 4.5 B,D-E). Furthermore, the total glucose AUC results showed that chow-fed NOD^k mice even have better glucose tolerance than chow-fed Balb/c mice (Fig 4.5E).

Even after this much longer period of HF-feeding, Balb/c mice showed no deterioration in glucose tolerance (Fig 4.5E).

As already mentioned, HF-feeding of NOD^k mice caused diabetes in 5 of the 6 mice studied, such that it was not a surprise that severe glucose tolerance was evident in the one HF-fed NOD^k mouse that underwent the ipGTT (Fig 4.5C). HF-feeding of $B10^k$

mice caused elevated fasting blood glucose and severely abnormally glucose tolerance, as was also seen in the short term study (Fig 4.5 C, F-H).

Figure 4.5. Blood glucose concentrations during ipGTTs at 23 weeks of age in Balb/c, B10^{k} and NOD^{k} mice fed chow or high fat diet (HFD). Mice were fasted for 4 hours and injected with 2g/kg glucose intraperitoneally at time 0 minutes.

(A) Balb/c chow (n=6) and HFD (n=6) mice. **(B)** B10^{k} chow (n=6) and HFD (n=6) mice. **(C)** NOD^{k} chow (n=6) and HFD (n=1) mice. Five HF-fed NOD^{k} mice were euthanized before the ipGTTs were to be performed due to the development of diabetes. **(D)** All groups shown. **(E)** Total glucose area under the curve (AUC) measured during ipGTT for chow-fed mice of all groups. **(F)** Fasting blood glucose concentrations during ipGTT for Balb/c and B10^{k} mice only. **(G)** 2 hours blood glucose concentrations during ipGTT for Balb/c and B10^{k} mice only. **(H)** Total glucose area under the curve (AUC) during ipGTT for Balb/c and B10^{k} mice only. Means ±SEM. One-way ANOVA of total glucose AUC for chow mice only shown (E). Two-way ANOVA shown (F-H). Bonferroni post-hoc tests: ******$p<0.01$, *******$p<0.001$ vs chow diet of the same strain; $^{\#\#}$ $p<0.01$, $^{\#\#\#}$ $p<0.001$vs different strain same diet.

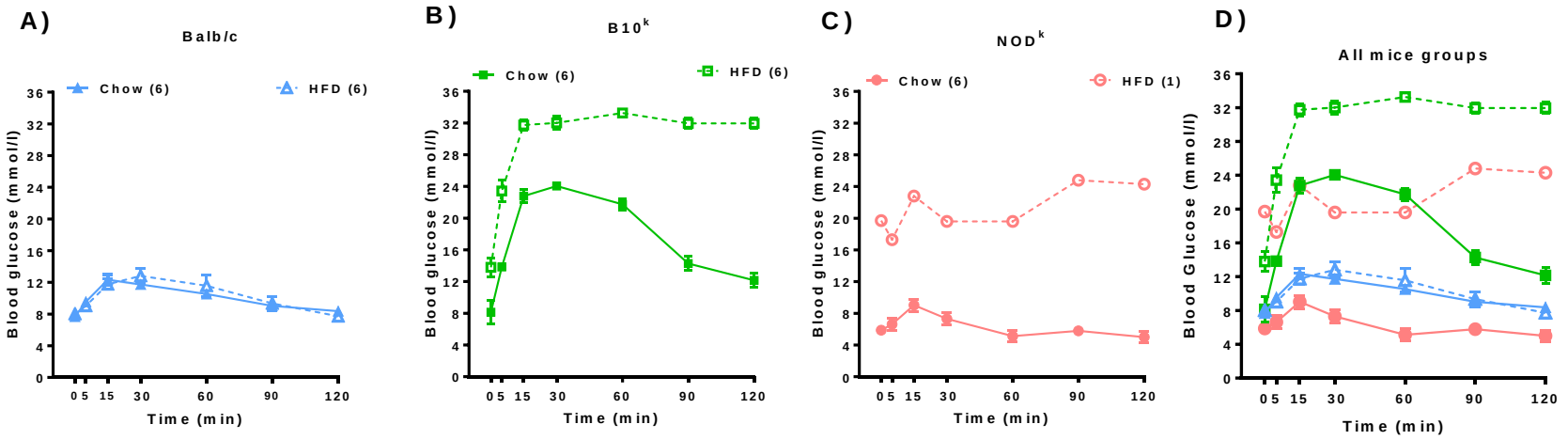

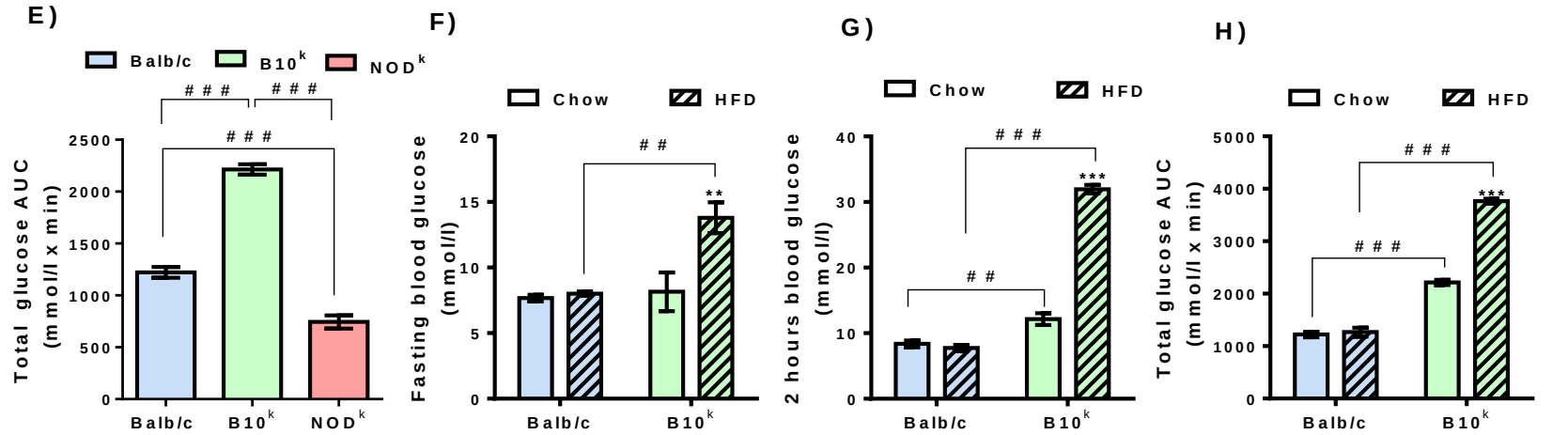

One-way ANOVA	
Strain effect	p<0.0001

Two-way ANOVA	
Strain effect	p=0.0038
Diet effect	p=0.0057
Strain*Diet interaction	p=0.0117

Two-way ANOVA	
Strain effect	p<0.0001
Diet effect	p<0.0001
Strain * Diet interaction	p<0.0001

Two-way ANOVA	
Strain effect	p<0.0001
Diet effect	p<0.0001
Strain * Diet interaction	p<0.0001

4.3.5. Measurement of plasma insulin levels during ipGTT

Despite severe glucose intolerance in chow and HF-fed in $B10^k$ mice, in the short-term study, these mice failed to respond with increased insulin secretion. NOD^k mice, however, responded to 9 weeks of HF-feeding with increased basal insulin, but abnormal insulin responses (no increase) following ip glucose. Insulin responses to ipGTTs were again assessed in the three mice groups on chow and HF-diets after the longer period of 19 weeks on diet. As discussed in Section 4.3.2, only one HF-diet treated NOD^k mouse underwent the ipGTT within this longer-term cohort.

The results are shown in Figure 4.6, with the insulin response over time shown in Fig 4.6A-D, the fasting plasma insulin concentrations for chow groups shown in Fig 4.6E, the total insulin AUC shown in Fig 4.6F and the change in insulin AUC from the plasma insulin concentration at time 0 min in Fig 4.6G.

Fasting plasma insulin values for the chow-fed NOD^k mice trended higher compared the other two strains ($p=0.052$; strain effect with one way ANOVA) (Fig 4.6E). The pattern of insulin response to ip glucose was normal (increase at 15 min followed by fall back towards baseline) in chow-fed Balb/c mice only (Fig 4.6A-D).

Of note, despite excellent glucose tolerance in chow-fed NOD^k mice (see Fig 4.5C), the pattern of insulin secretion was not normal in these mice. Despite the glucose intolerance, chow-fed $B10^k$ mice again had low insulin levels and no increase in response to the glucose load (Fig 4.6B).

In response to HF-feeding, Balb/c mice did show a compensatory increase in plasma insulin levels, while maintaining a normal pattern of insulin release following the ip glucose load (Fig 4.6A, F-G). Again $B10^k$ mice did not mount a compensatory increase in insulin levels in response to HF-diet, and this mouse strain did not show the normal

increase in insulin levels that should occur after an ip glucose load. Data from the one - NOD^k mouse that underwent the ipITT needs to be interpreted carefully, but again showed an abnormal pattern in response to ip glucose (Fig 4.6C).

Figure 4.6. Plasma insulin concentrations during ipGTTs at 23 weeks of age in Balb/c, B10^{k} and NOD^{k} mice fed chow or high fat diet (HFD). Mice were fasted for 4 hours and were injected with 2g/kg glucose intraperitoneally at time 0 minutes.

(A) Balb/c chow (n=6) and HFD mice (n=6). **(B)** B10^{k} chow (n=6) and HFD (n=6) mice. **(C)** NOD^{k} chow (n=6) and HFD (n=1) mice. Five HF-fed NOD^{k} mice were euthanized before the ipGTTs were to be performed due to the development of diabetes. **(D)** All groups shown. **(E)** Fasting insulin concentration during ipGTTs of chow-fed mice of all groups. **(F)** Total area under the curve (AUC) for plasma insulin concentrations during ipGTTs of Balb/c and B10^{k} mice only. **(F)** Change from basal plasma insulin AUC during ipGTTs for Balb/c and B10^{k} mice only. Means ±SEM. One-way ANOVA of total glucose AUC for chow-fed mice (E). Two-way ANOVA shown (F-G). Bonferroni post-hoc tests. ***$p<0.001$ vs chow diet same strain.

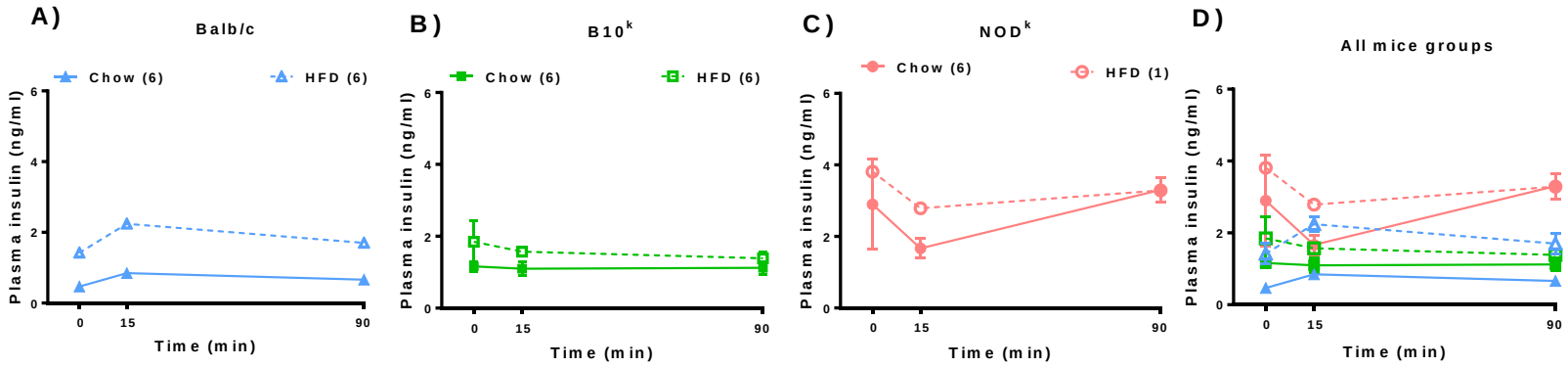

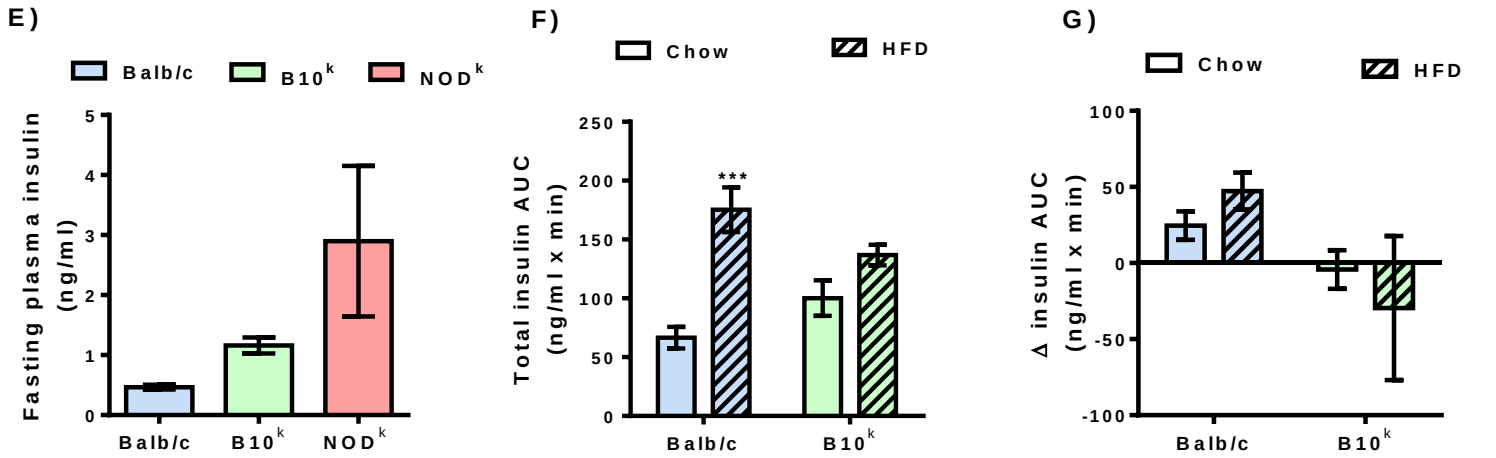

One-way ANOVA	
Strain effect	p=0.0522

Two-way ANOVA	
Strain effect	p=0.8576
Diet effect	p<0.0001
Strain*Diet interaction	p=0.0157

Two-way ANOVA	
Strain effect	p=0.0526
Diet effect	p=0.9616
Strain*Diet interaction	p=0.3600

4.3.6. Measurement of non-fasting plasma insulin and derivatives

Tissues of Balb/c, $B10^k$ and NOD^k mice were harvested at 24 weeks of age. Prior to anaesthesia non-fasting tail blood was obtained for measurement of plasma insulin and fed NEFA and TG. Under light anaesthesia and prior to organ harvest, cardiac blood was collected from the mice for the measurement of plasma proinsulin and C-peptide levels.

The non-fasting insulin, proinsulin and C-peptide results of all mice strains are shown in Fig 4.7A-C. As the age at which tissue harvest was performed was earlier in 5 of the 6 HF-fed NOD^k mice, the fed insulin, proinsulin and C-peptide results of the NOD^k mice on chow-diet and HF-diet, according to age at the time of sampling, are also shown in (Fig 4.7D-F).

In the chow-fed mice, the non-fasting plasma insulin of NOD^k mice was higher than for the other two strains, being significantly higher to the insulin of the $B10^k$ group with post hoc testing (Fig 4.7A). Plasma proinsulin was also significantly higher in chow-fed NOD^k compared to chow-fed Balb/c and $B10^k$ mice (Fig 4.7B). A similar trend was observed for non-fasting C-peptide levels to be highest in chow-fed NOD^k mice (Fig 4.7 C).

In contrast to the short-term studies, HF-fed NOD^k mice did not show a massive increase in non-fasting plasma insulin compared to their respective chow-fed mice (Fig 4.7A&D), which would be consistent with islet β-cell failure to compensate in these mice at the time of diabetes development. None of the strains at this age showed an effect of HF-feeding to increase non-fasting plasma insulin, pro-insulin or C-peptide levels (Fig 4.7A-C). The age of harvest had little effect on levels in the HF-fed NOD^k mice (Fig 4.7D-F).

The ratios of fed proinsulin/insulin, proinsulin/C-peptide and insulin/C-peptide of the data shown in Fig 4.8A-C. For the same reason as in Figure 4.7, the fed proinsulin/insulin, proinsulin/C-peptide and insulin/C-peptide ratios for the NOD^k mice on chow-diet and HF-diet, according to age at the time of sampling, are also shown in Fig 4.8D-F. The same pattern of a higher proinsulin/C-peptide in $B10^k$ mice compared to Balb/c mice, as seen at 14 weeks of age (Fig 3.7), was again seen at 24 weeks of age (Fig 4.8B). The markedly increased proinsulin/C-peptide and insulin/C-peptide ratios in plasma of fed HF-fed compared to chow-fed NOD^k mice seen at 14 weeks of age, was not seen in older NOD^k mice at the time of harvest (Fig 4.8B, C, E, F).

Figure 4.7. Non-fasting plasma insulin, proinsulin and C-peptide concentrations at 24 weeks of age (or end of study if before 24 weeks) in Balb/c, B10^{k} and NOD^{k} mice fed chow or high fat diet (HFD).

Non-fasting **(A)** plasma insulin concentrations from all groups, measured from tail-blood. **(B)** Plasma proinsulin concentrations from all groups, measured from cardiac blood. **(C)** Plasma C-peptide concentrations from all groups, measured from cardiac blood. **(D)** Plasma insulin concentrations from chow-fed NOD^{k} and HF-fed NOD^{k} mice only, based on the age at sampling. **(E)** Plasma proinsulin concentrations from chow-fed NOD^{k} and HF-fed NOD^{k} mice only, based on the age at sampling. **(F)** Plasma C-peptide concentrations from chow-fed NOD^{k} and HF-fed NOD^{k} mice only, based on the age at sampling. Means ±SEM. Two-way ANOVA shown (A-C). Bonferroni post-hoc tests: $^{\#}$ $p<0.05$, $^{\#\#}$ $p<0.01$ vs different strain same diet.

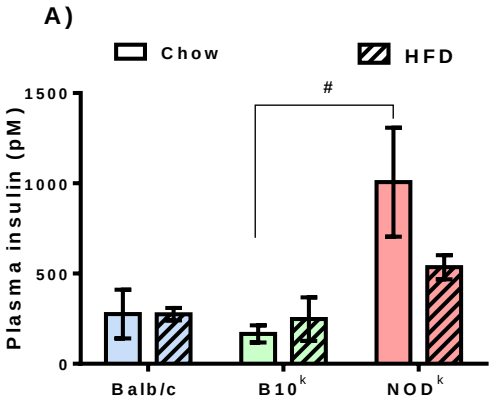

Two-way ANOVA	
Strain effect	p=0.0061
Diet effect	p=0.3778
Strain*Diet interaction	p=0.2445

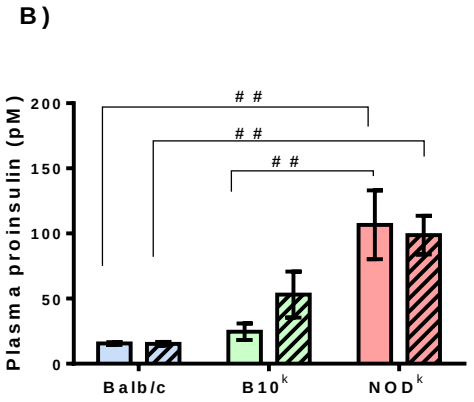

Two-way ANOVA	
Strain effect	p<0.0001
Diet effect	p=0.5725
Strain*Diet interaction	p=0.4281

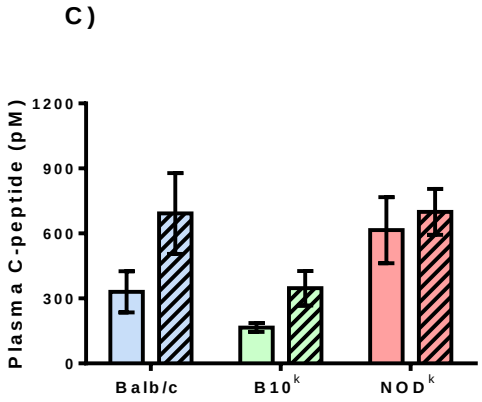

Two-way ANOVA	
Strain effect	p=0.0275
Diet effect	p=0.0685
Strain*Diet effect	p=0.5388

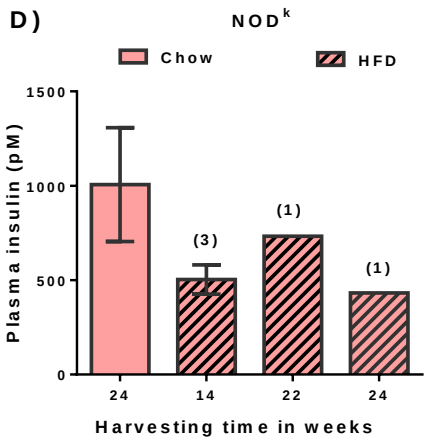

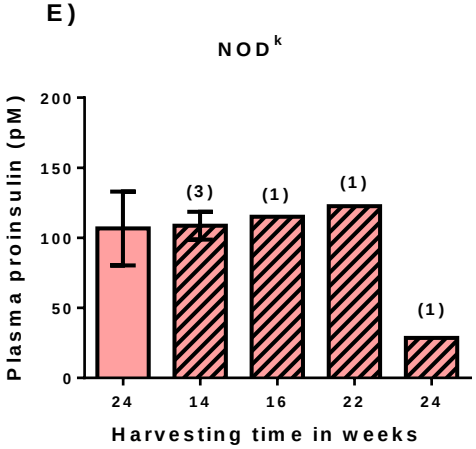

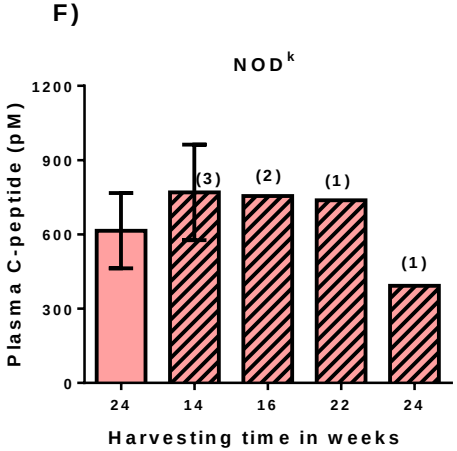

Figure 4.8. Ratios of non-fasting proinsulin to insulin, proinsulin to C-peptide and insulin to C-peptide at 24 weeks of age (or end of study if before 24 weeks) in Balb/c, B10^{k} and NOD^{k} mice fed chow or high fat diet (HFD).

(A) Ratio of proinsulin to insulin in all groups. **(B)** Ratio of proinsulin to C-peptide in all groups. **(C)** Ratio of insulin to C-peptide in all groups. **(D)** Ratio of proinsulin to insulin in chow-fed NOD^{k} and HF-fed NOD^{k} mice only, based on the age of sampling. **(E)** Ratio of proinsulin to C-peptide in chow-fed NOD^{k} and HF-fed NOD^{k} mice only, based the age of sampling. **(F)** Ratio of insulin to C-peptide chow-fed NOD^{k} and HF-fed NOD^{k} mice only, based on the age of sampling. Means ±SEM. Two-way ANOVA shown (A-C).

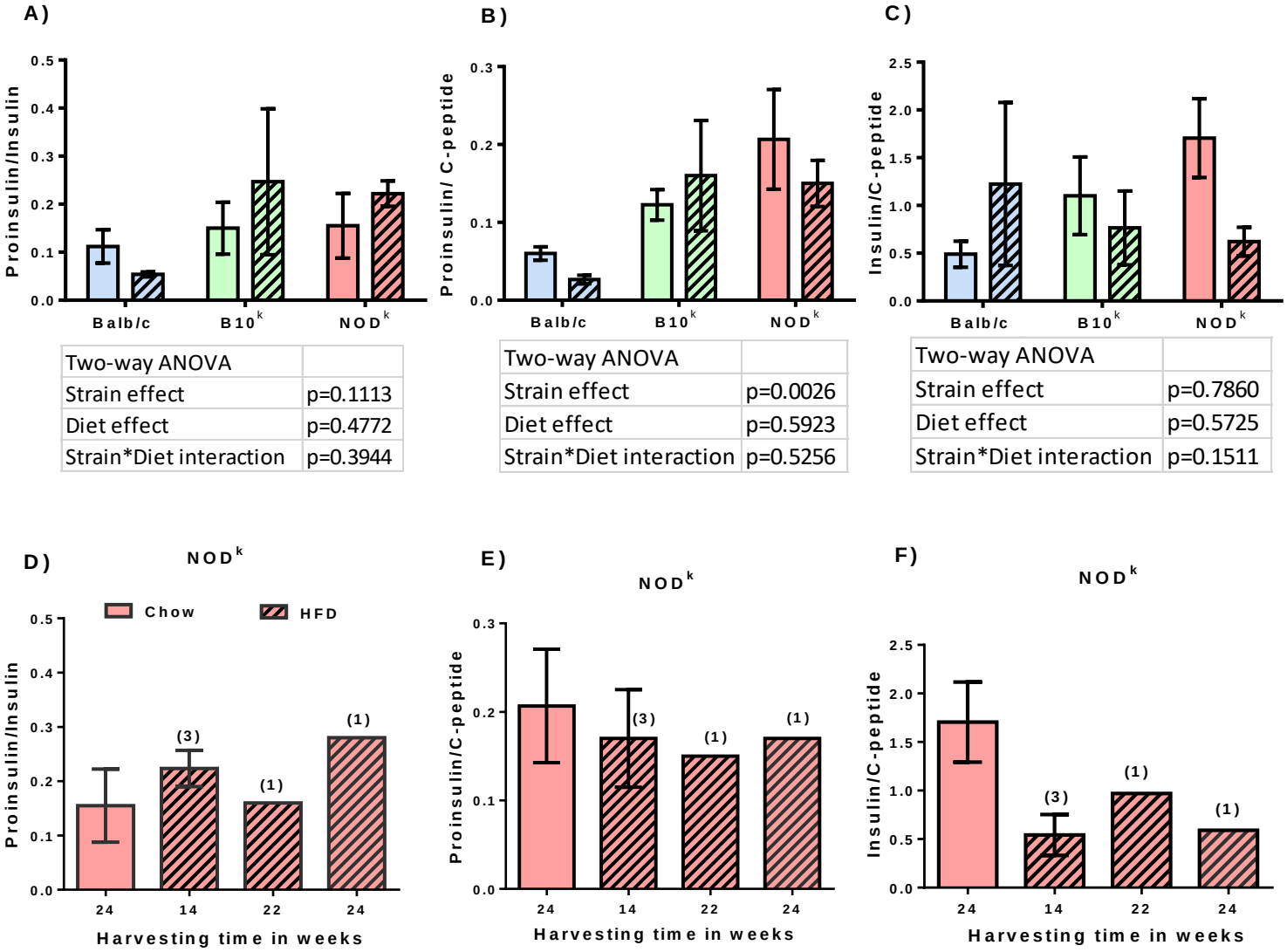

Two-way ANOVA	
Strain effect	p=0.1113
Diet effect	p=0.4772
Strain*Diet interaction	p=0.3944

Two-way ANOVA	
Strain effect	p=0.0026
Diet effect	p=0.5923
Strain*Diet interaction	p=0.5256

Two-way ANOVA	
Strain effect	p=0.7860
Diet effect	p=0.5725
Strain*Diet interaction	p=0.1511

4.3.7. Measurement of Non Esterified Free Fatty Acid (NEFA)

Fasting plasma NEFA levels were measured at time 0 min during the ipGTT test at 23 weeks of age and the results are shown for Balb/c and $B10^k$ mice in Fig 4.9A. An ipGTT was performed in only one HF-fed NOD^k mouse, hence the NOD^k mice results are shown separately in Fig 4.9C. The fasting NEFA levels were higher in the Balb/c compared to $B10^k$ mice, however, the NEFA levels of these two strains of mice, at this age, was not affected by diet (Fig 4.9A). The NEFA levels of the chow-fed NOD^k mice were also similar to the chow-fed Balb/c mice (Fig 4.9C).

Non-fasting NEFA levels were measured from tail vein blood collected prior to anaesthesia on the day of tissue harvesting at 24 weeks of age. There was a significant strain effect, with the highest levels in NOD^k mice, again without a significant effect of diet (Fig 4.9B). The non-fasting NEFA concentrations HF-fed NOD^k mice according to the age of blood sampling are shown separately in (Fig 4.9D).

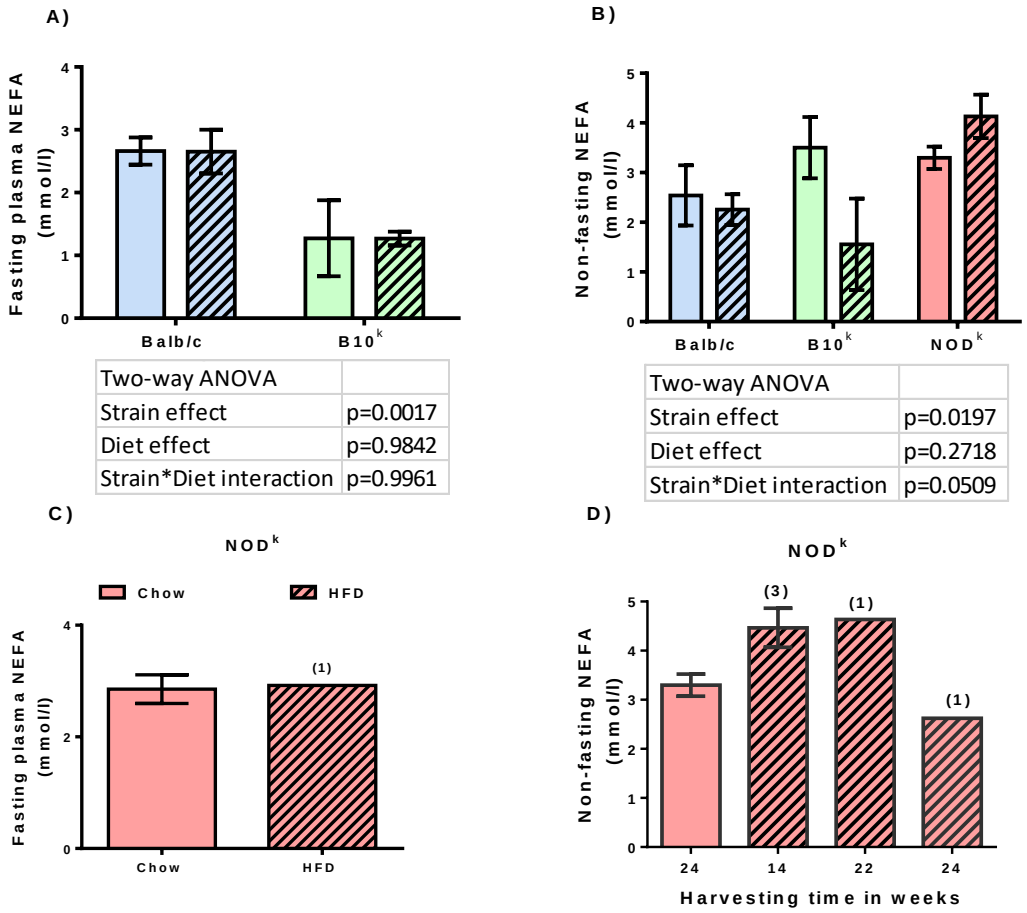

Figure 4.9. Plasma NEFA concentrations in Balb/c, B10^k and NOD^k mice fed chow or high fat diet (HFD).

(A) Fasting plasma NEFA from tail-blood at 23 weeks of age, Balb/c and B10^k mice groups shown only. **(B)** Non-fasting NEFA from tail-blood at 24 weeks of age (or end of study if before 24 weeks), all groups shown. **(C)** Fasting plasma NEFA concentrations from chow-fed NOD^k and HF-fed NOD^k mice only, based on age of blood sampling. **(D)** Non-fasting plasma NEFA concentrations from chow-fed NOD^k and HF-fed NOD^k mice only, based on age of blood sampling. Data are Means ±SEM 1-6 mice per group. Two-way ANOVA shown (A-B).

4.3.8. Measurement of TG

Fasting plasma TG concentrations were measured from blood collected from the tail vein of Balb/c, $B10^k$ and NOD^k mice at time 0 min of the ipGTT at 23 weeks of age. The results are shown for Balb/c and $B10^k$ mice in Fig 4.10A. An ipGTT was performed in only one HF-fed NOD^k mouse, hence the NOD^k mice results are shown separately in Fig 4.10C. The fasting plasma TG concentrations of Balb/c and $B10^k$ mice were not significantly different and were not affected according to chow or HF-feeding (Fig 4.10A). The NEFA levels of the chow-fed NOD^k mice were also similar to the other two strains of mice (Fig 4.10C).

Non-fasting TG levels were measured from tail vein blood collected prior to anaesthesia on the day of tissue harvesting, at 24 weeks of age. Non-fasting TG concentrations of NOD^k mice were the highest, with $B10^k$ mice having the lowest levels (Fig 4.10B). Again there was no evidence for diet effect in the TG levels (Fig 4.10B). The non-fasting NEFA concentrations of HF-fed NOD^k mice, according to the age of blood sampling, are shown separately in Fig 4.10D.

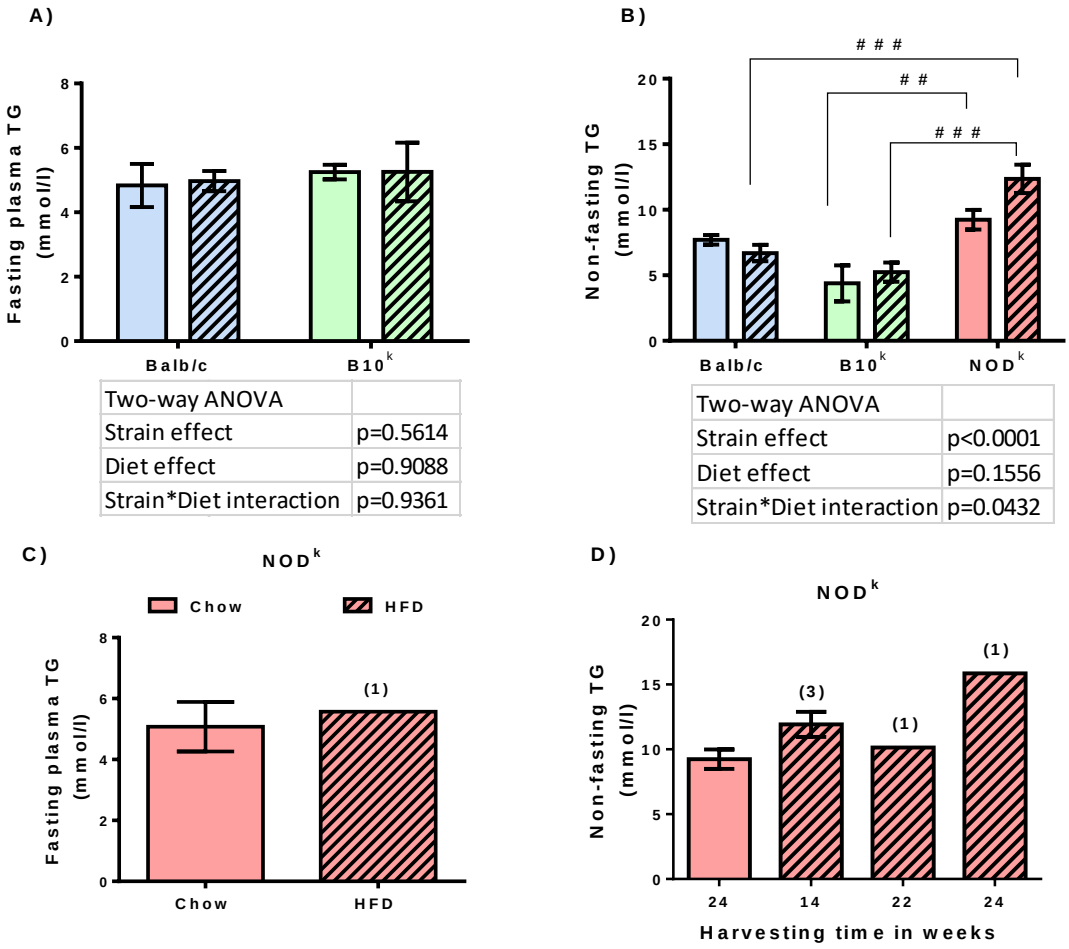

Figure 4.10. Plasma TG concentrations in Balb/c, B10^k and NOD^k mice fed chow or high fat diet (HFD).

(A) Fasting plasma TG concentrations from tail-blood at 23 weeks of age, Balb/c and B10^k mice groups shown only. **(B)** Non-fasting plasma TG concentrations from tail-blood at 24 weeks of age (or end of study if before 24 weeks), all groups shown. **(C)** Fasting plasma TG concentrations from chow-fed NOD^k and HF-fed NOD^k mice only, based on age of blood sampling. **(D)** Non-fasting plasma TG concentrations from chow-fed NOD^k and HF-fed NOD^k mice only, based on age of blood sampling. Data are Means ±SEM 1-6 mice per group. Two-way ANOVA shown (A-B). Bonferroni post-hoc tests: $^{\#\#}$ p<0.01, $^{\#\#\#}$ p<0.001 vs different strain same diet.

4.4. Discussion

The long-term study in part is confirmatory of the findings of the short-term study reported in Chapter 3, again showing markedly different metabolic responses to HF-feeding of the three mice strains. In short, out to 24 weeks of age, Balb/c mice again showed resistance to the development of diabetes, the $B10^k$ mice did not progress to diabetes despite extremely poor glucose tolerance and insulin secretion, and the NOD^k mice again developed a severe type 2 diabetes phenotype in response to the HF-diet that required early ethical culling due to the severity of hyperglycaemia.

Additionally in the long-term study (not assessed in the short term study), insulin resistance was assessed by ipITTs at 13 weeks of age. There was not an obvious difference in insulin sensitivity between the three strains on chow-diet. HF-feeding, however, did appear to worsen insulin sensitivity in the NOD^k mice, although the results were not significant due to limited numbers of mice studies (only 3 in the HF-fed NOD^k mice). The findings also need to be interpreted with caution due to the significant limitations of this method.

At variance in the long-term from the short-term study was the lesser degree of hyperinsulinaemia in HF-fed NOD^k mice in blood taken from conscious mice prior to anaesthetic for tissue harvesting. This would be consistent with a severe degree of islet β-cell failure having developed by the time of HF-diet induced diabetes development in the NOD^k mice.

4.4.1. Mouse body weights

Again the NOD^k mice were heavier than the other 2 strains at the weaning age of 4 weeks. Furthermore, the NOD^k mice appeared to be most susceptible to HF-diet induced obesity, with HF-fed NOD^k mice being 33% heavier than their chow-fed NOD^k

counterparts at 10 weeks of age compared to the Balb/c and B10k mice that were only 15% and 10% heavier than their chow-fed counterparts at the same age.

4.4.2. Non-fasting blood glucose and glucose tolerance

According to the non-fasting glucose levels, HF-feeding resulted in a severe diabetic phenotype in the NOD^k mice and this developed between the age of 12-24 weeks. Only one HF-fed NOD^k mouse made it to the end of the study and had an ipGTT. This ipGTT showed severe glucose intolerance, such that the mouse was also likely to develop diabetes. Non-fasting glucose levels and glucose tolerance of the chow-fed NOD^k mice, however, remained normal. This is consistent with a propensity for NOD^k mice to develop diabetes only when stressed, this time by HF-feeding. This is again consistent with the previous report from the Jackson Laboratories of a propensity for "NON mice", NOD mice congenic for low risk MHC haplotypes, to develop diet-induced obesity and hyperglycaemia (Jackson, 2006).

The main reason for doing this extended study was to determine if $B10^k$ mice would develop diabetes with an extra 10 weeks on HF-diet. The results again were remarkable, as despite very poor glucose tolerance even on chow diet, the HF-fed $B10^k$ mice did not develop diabetes, as assessed by 9 AM fed-glucose levels, and although a minor increase in non-fasting glucose was observed. Again, in response to 4 h of fasting the HF-fed $B10^k$ mice had markedly elevated fasting glucose levels and severely impaired glucose tolerance. As discussed in Chapter 3, the mechanisms underlying this variance between fed-state and fasted state glucose homeostasis is not known, but is of interest.

Again in Balb/c mice, non-fasting 9 AM glucose levels and ipGTT glucose levels remained unaffected by HF-feeding out to the older age of 24 weeks, indicative of the resistance of this strain of mice to diet-induced hyperglycaemia.

4.4.3. Insulin levels and insulin derivatives

HF-fed Balb/c mice increased their insulin levels during ipGTT testing, consistent with this strain of mice being able to compensate appropriately for HF-diet induced obesity and insulin resistance. Furthermore, this was the only strain than maintained a normal pattern of insulin secretion in the ipGTT, having a glucose-induced rise in insulin at the 15 min time point.

Interestingly, the non-fasting insulin levels of the normoglycaemic chow-fed NOD^k mice at 24 weeks of age were higher than the other 2 strains, suggesting some degree of insulin resistance in these mice. This trend was also present in the short-term study. However, in contrast to the marked non-fasting hyperinsulinemia in response to HF-feeding of NOD^k seen in the short-term study, marked hyperinsulinemia was not evident in the HF-fed NOD^k mice of the long-term study. This would be consistent with failure of islet β-cell compensation in these mice with the development of a type 2 diabetes phenotype (Nolan et al., 2006, Weir and Bonner-Weir, 2004). Also worth noting are the C-peptide levels which were similar between the chow-fed and HF-fed NOD^k mice, which is against a marked reduction of insulin clearance in HF-fed compared to chow-fed NOD^k mice, as was suggested by the equivalent measures in NOD^k mice at 14 weeks of age.

It is not possible to comment much about the insulin levels during the ipGTT of HF-fed NOD^k mice during the long-term study, as only one mouse had this procedure. The pattern of insulin response in NOD^k mice on chow diet at 24 weeks of age, however, was not normal, with failure of the mice to increase insulin levels at the 15 min time point. This would also be consistent with this mouse having an underlying defect in glucose-stimulated insulin secretion even though glucose tolerance remained normal on chow diet.

The $B10^k$ insulin results of the long-term study were very similar to those of the short-term study. Again, despite very poor glucose tolerance, the $B10^k$ mice failed to mount a compensatory islet β-cell response either in the non-fasting blood sample prior to animal harvesting or in response to the ipGTT. Again, the $B10^k$ mice showed the lowest C-peptide levels across the 3 strains consistent with this strain being an insulin hypo-secretor.

4.4.4. Insulin sensitivity measurements

The gold standard measure of insulin sensitivity is the euglycaemic hyperinsulinaemic clamp (Bowe et al., 2014). However, this procedure was beyond the scope of this thesis, in which the focus was more on islet β-cell function. For this reason, ipITTs were performed in the long-term cohort of mice at 13 weeks of age (Bowe et al., 2014). Despite relative non-fasting hyperinsulinaemia in chow-fed NOD^k mice, insulin sensitivity (as determined by the % fall in blood glucose from time 0 min) was not different between the three mouse strains. However, in response to HF-feeding the insulin sensitivity of the HF-fed NOD^k mice appeared to be reduced, but this difference was not significant, possibly due to the small number of HF-fed NOD^k mice (n=3 only) that had this test. The interpretation of ipITT's is difficult here, however, due to the differences between groups on the baseline glucose levels (the HF-fed $B10^k$ and NOD^k mice were hyperglycaemic) and due to differences in mouse weights (higher in NOD^k mice), as the insulin dose is in proportion to the weight of the mice.

4.4.4. Plasma lipid levels

As the majority of NOD^k mice did not have an ipGTT, fasting lipid levels were not available for the HF-fed NOD^k mice. In the non-fasting results, however, the previous finding of higher non-fasting NEFA and TG levels in NOD^k mice was found in the

longer-term study. These results are again consistent with the NOD^{k} mice being prone to a type 2 diabetes phenotype, including dyslipidaemia, with HF-feeding.

4.4.5. Propensity of different strains to diet-induced diabetes

The Balb/c mice were again found to be resistant to the development of diabetes consistent with previous reports (Montgomery et al., 2013). The reason for this resistance is unclear, but this mouse strain is not as prone to develop diet-induced obesity. Of note, Balb/c mice have been reported to be relatively resistant to the development of hepatic accumulation of lipid with HF-feeding (Montgomery et al., 2013), and hepatic lipid is known to be associated with dysfunctional hepatic glucose regulation (Williams et al., 2012). Of importance, the response of pancreatic islets of Balb/c mice to HF-feeding appears to be a normal compensatory response.

The relative hyperinsulinaemia and the failure of a normal insulin response to ip glucose in the chow-fed NOD^{k} mice is supportive of the view that this strain of mice has an underlying islet β-cell defect. The failure to sustain marked hyperinsulinaemia by the time of diabetes development is also consistent with the dogma that type 2 diabetes is a consequence of islet β-cell failure to sustain a compensatory response to insulin resistance (Prentki and Nolan, 2006).

The findings of the long-term HF-feeding of B10^{k} mice are of most interest in this Chapter, as the results do suggest that poor islet responsiveness may protect them from failure, as has been previously argued (Andrikopoulos, 2010). A normally functioning β-cell responds to an increased nutrient load with mitochondrial metabolism and the production of metabolic coupling factors that promote insulin exocytosis (Nolan and Prentki, 2008). However, this reliance on mitochondrial metabolism increases the production of reactive oxygen species and the potential for oxidative stress, endoplasmic reticulum stress and β-cell damage. Hence, it has been argued that the

most fuel responsive β-cell cells may be the most vulnerable (Nolan and Prentki, 2008, Andrikopoulos, 2010).

The hypothesis of slowing down metabolism to protect β-cells was tested by overexpressing the Foxo1 transcription factor in INS832/13 β-cells. Foxo-1 overexpression protected them against oxidative stress by strong suppression of genes responsible for glucose oxidation and insulin secretion (Buteau et al., 2007).

The metabolic deceleration theory is also supported by studies of C57BL/6J and DBA/2 mouse models. Obesity due to the leptin (*ob*) or leptin receptor (*db*) causes diabetes depending on the mouse background, with C57BL/6J mice being diabetes resistant and DBA/2 mice being diabetes prone. The DBA/2 mouse has been shown to have the propensity to hyper-secrete insulin in both *in vivo* and *in vitro*. Furthermore, a genome wide search reported that the glucose-induced insulin hyper-secretion phenotype of the DBA/2 mouse was likely due to a five-fold higher expression of the nicotinamide nucleotide transhydrogenase (*Nnt*) gene in DBA/2 compared to C57BL/6J mice (Aston-Mourney et al., 2007, Andrikopoulos, 2010). Nicotinamide nucleotide transhydrogenase (*Nnt*) is involved in mitochondrial metabolism and cellular redox and energy homeostasis (Murphy, 2015).

Glucolipotoxicity has been proposed as a mechanism to induce islet β-cell failure in subjects at risk of type 2 diabetes (Prentki and Nolan, 2006b, Poitout and Robertson, 2008, Zraika et al., 2004). The NOD^{k} mice that did develop diabetes in response to HF-feeding has higher circulating lipid levels, as shown in both the short and long-term studies. The contribution of the dyslipidaemia of this mouse strain to islet β-cell compensatory responses and then failure under HF-diet conditions also warrants attention in further studies.

4.5. Summary

The results of the long-term study essentially confirmed the findings of the short-term study, but provides strength to the view that a hyper-responsiveness of islet β-cell to stress is associated with a greater risk for β-cell failure (e.g. NOD^k mice) and that a hypo-responsiveness of the islet β-cell to stress is protective of complete β-cell failure (e.g. $B10^k$ mice).

The next chapter (Chapter 5) reports findings of the histological examination of the pancreases of both the short- and long-term studies.

Chapter # 5:

Results (Histology)

5.1. Introduction

In Chapters 3 and 4, we have presented results that characterize the metabolic phenotype of the chow and HF-fed Balb/c, $B10^k$ and NOD^k male mice after 10 and 20 weeks on the diets post weaning (short and long-term studies). The three mice strains have remarkably different phenotypes. The Balb/c mice are relatively resistant to diet-induced obesity and are diabetes resistant. The $B10^k$ mice have very poor glucose tolerance on chow diet, are prone to diet-induced obesity, but despite worsening of glucose tolerance on HF-diet, do not progress onto diabetes even out to 24 weeks of age. The NOD^k mice have excellent glucose tolerance on chow diet, are the most prone to diet-induced obesity and they develop a severe type 2 diabetes phenotype when fed a HF-diet. Some understanding of the pathophysiology can be deduced from the physiological testing with ipGTTs and ipITTs and measurements of insulin, proinsulin and C-peptide, but mechanisms have not been explored further than this.

In this Chapter, in order to further understand the mechanisms involved, we present the results of histological assessment of pancreatic islets from H&E pancreas sections and of β-cell mass calculated from insulin immuno-stained pancreas sections and computer assisted morphometric analysis.

From the H&E sections, particular interest was placed on the presence of inflammatory cells in both the pancreas, peri-islet regions and in islets (insulitis). From the previous work on the NOD^k.insHEL transgenic mouse, there was no evidence for an immune mechanism contributing to the diabetes (Dooley et al., 2016). Considering that the NOD^k mouse is derived from the NOD mouse, an animal model of autoimmune type 1 diabetes that is characterized by insulitis, it was again important to determine the presence or absence of insulitis in this study.

In several of the H&E sections, apoptotic endocrine cells were observed and these were formally assessed. With HF-feeding, it was also noted that some, but not all strains of mice were prone to develop intra-pancreatic fats depots. This was also formally assessed.

From the immuno-stained sections, the main interest was measurement of islet β-cell mass, as the classic changes in type 2 diabetes are firstly, an increase in islet β-cell mass, in the islet β-cell compensation phase, followed by loss of β-cell mass corresponding to the time that blood glucose levels reach the diabetic range (Prentki and Nolan, 2006a).

5.2. Experimental approach

The histological and immunohistochemistry methodologies are presented in Chapter 2. Briefly, at the time of euthanasia and tissue harvest, the pancreases were rapidly removed, weighed and fixed in formalin and processed into paraffin blocks. Sections were cut for H&E staining and insulin immunohistochemistry.

A very experienced and senior anatomical pathologist, Professor Jane Dahlstrom from ANU Medical School, scored blinded H&E pancreas sections for acute and chronic inflammation, presence of fat deposits in exocrine pancreas and endocrine cell apoptosis.

Islet β cell mass was also assessed by blinded assessment of insulin immuno-stained sections (3 sections per pancreas). These sections were analyzed on Image J and from the total stained area, as a percentage of pancreas area, and the pancreas weight, islet β-cell mass was calculated. Complete description of the procedure for the measurement of islet β-cell mass is detailed in Chapter 2.

The results of both the short-term and long-term experiments are described below.

5.3. Results

5.3.1. Assessment of islet inflammation

Representative microscopic images of H&E stained pancreatic sections showing typical inflammatory infiltrates in chow and HF-fed mice at 14 weeks and 24 weeks of age are shown in Fig 5.1, and Fig 5.2, respectively. Average blinded scores for inflammatory infiltrates are presented in Fig 5.6 and Table 5.1.

Exocrine pancreatic tissue acute inflammation, if seen, was always within a single focus of mild severity. It was seen in a small number of pancreases only, without evidence of clear differences between mouse strains or diet use (Table 5.1).

Chronic inflammation, however, was more frequently seen and this was more likely to be present in $B10^k$ mice and NOD^k mice than Balb/c mice (Fig 5.6 and Table 5.1). The chronic inflammation was at worst moderate. It was not seen to invade islets (i.e. insulitis was not seen), but was predominantly present as peri-ductal collections, with at times extension into peri-islet regions and occasionally into exocrine tissue lobules (Fig 5.1 and 5.2). Pancreatic inflammatory infiltrates were not seen at all in Balb/c mice on chow or HF-diet in the short-term study or in chow-fed Balb/c mice in the long-term study (Fig 5.1, Fig 5.2, Fig 5.6 and Table 5.1) however, mild inflammatory infiltrates were evident in the long-term HF-fed Balb/c mice (Fig 5.2, Fig 5.6 and Table 5.1). The majority of $B10^k$ mice pancreases had some evidence of peri-ductal/peri-islet infiltrates with possible worsening of severity with ageing, but not high-fat feeding (Fig 5.1, Fig 5.2, Fig 5.6 and Table 5.1), although greater mouse number would be required to confirm this finding. Inflammatory infiltrates were also commonly seen in NOD^k mice,

perhaps with greater severity with HF-feeding, particularly in the older age group (Fig 5.1, Fig 5.2, Fig 5.6 and Table 5.1). Again greater numbers would be needed to confirm these trends in severity. Importantly, invasive insulitis was not seen in the HF-fed NOD^k mice, even in the long-term study in which they invariably had diabetes at the time of pancreas harvest.

5.3.2. Pancreatic fat deposits

Many of the pancreases displayed fat deposits in the H&E sections. On fixation, the lipid dissolves leaving a classic rounded 'empty' appearance. The presence or absences of these fat deposits are shown in lower power representative images in Figures 5.3 and 5.4 for the short and longer-term studies, respectively.

Minor fat deposits were present in chow-fed Balb/c mice, particularly in those from the longer-term study, but the deposits were clearly greater with HF-feeding (Fig 5.3, Fig 5.4, Fig 5.6 and Table 5.1). Interestingly, chow-fed $B10^k$ mice had minimal intra-pancreatic fat and this minimally increased with HF-feeding (Fig 5.3, Fig 5.4, Fig 5.6 and Table 5.1). Also unexpected was the finding of fat deposits in the pancreases of most chow-fed NOD^k mice, with some evidence of worsening with HF-feeding in the short-term study mice. In the HF-fed NOD^k mice of the long-term study, the accumulation of fat deposits did not seem worse than the corresponding mice on chow diet, however, these HF-fed NOD^k mice had diabetes at the time of harvest, which may have reduced these deposits due to induction of a catabolic state (Fig 5.3, Fig 5.4, Fig 5.6 and Table 5.1).

Figure 5.1. Representative images of pancreas sections stained with H&E showing inflammation in chow and high fat diet (HFD) fed Balb/c, $B10^k$ and NOD^k at 14 weeks of age (Short-term study).

(A) Chow-fed Balb/c mouse pancreas with no inflammation in the pancreatic section. **(B)** Chow-fed $B10^k$ mouse showing minimal peri-ductal inflammation. **(C)** Chow-fed NOD^k mouse showing mild peri-ductal inflammation. **(D)** HF-fed Balb/c mouse with no evidence of inflammation. **(E)** HF-fed $B10^k$ mouse with mild peri-ductal inflammation. **(F)** HF-fed NOD^k mouse with moderate peri-ductal and peri-islet inflammation. Scale bar, 50 μm. Arrows point to area of inflammation.

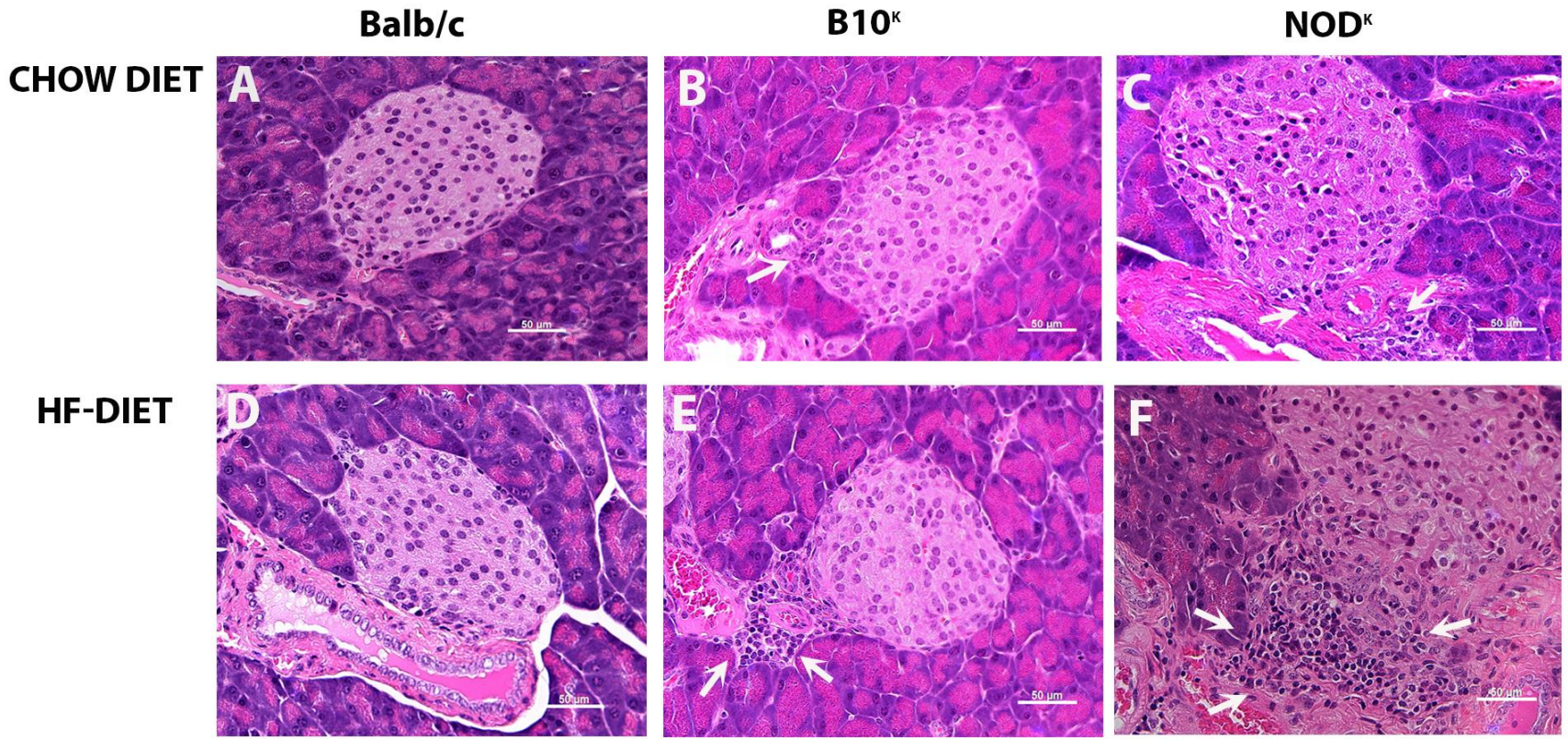
Balb/c
B10K
NODK
CHOW DIET
HF-DIET
A
B
C
D
E
F
50 µm

Figure 5.2. Representative images of pancreas sections stained with H&E showing inflammation in chow and high fat diet (HFD) fed Balb/c, $B10^k$ and NOD^k at 24 weeks of age (Long-term study).

(A) Chow-fed Balb/c mouse pancreas with no inflammation. **(B)** Chow-fed $B10^k$ mouse showing minimal periductal and peri-islet inflammation. **(C)** Chow-fed NOD^k mouse showing minimal peri-islet inflammation. **(D)** HF-fed Balb/c mouse with mild peri-ductal inflammation. **(E)** HF-fed $B10^k$ mouse with mild peri-ductal and peri-islet inflammation. **(F)** HF-fed NOD^k mouse with moderate peri-ductal and peri-islet inflammation. This mouse harvested at 24 weeks. Scale bar, 50 μm. Areas point to arrows of inflammation.

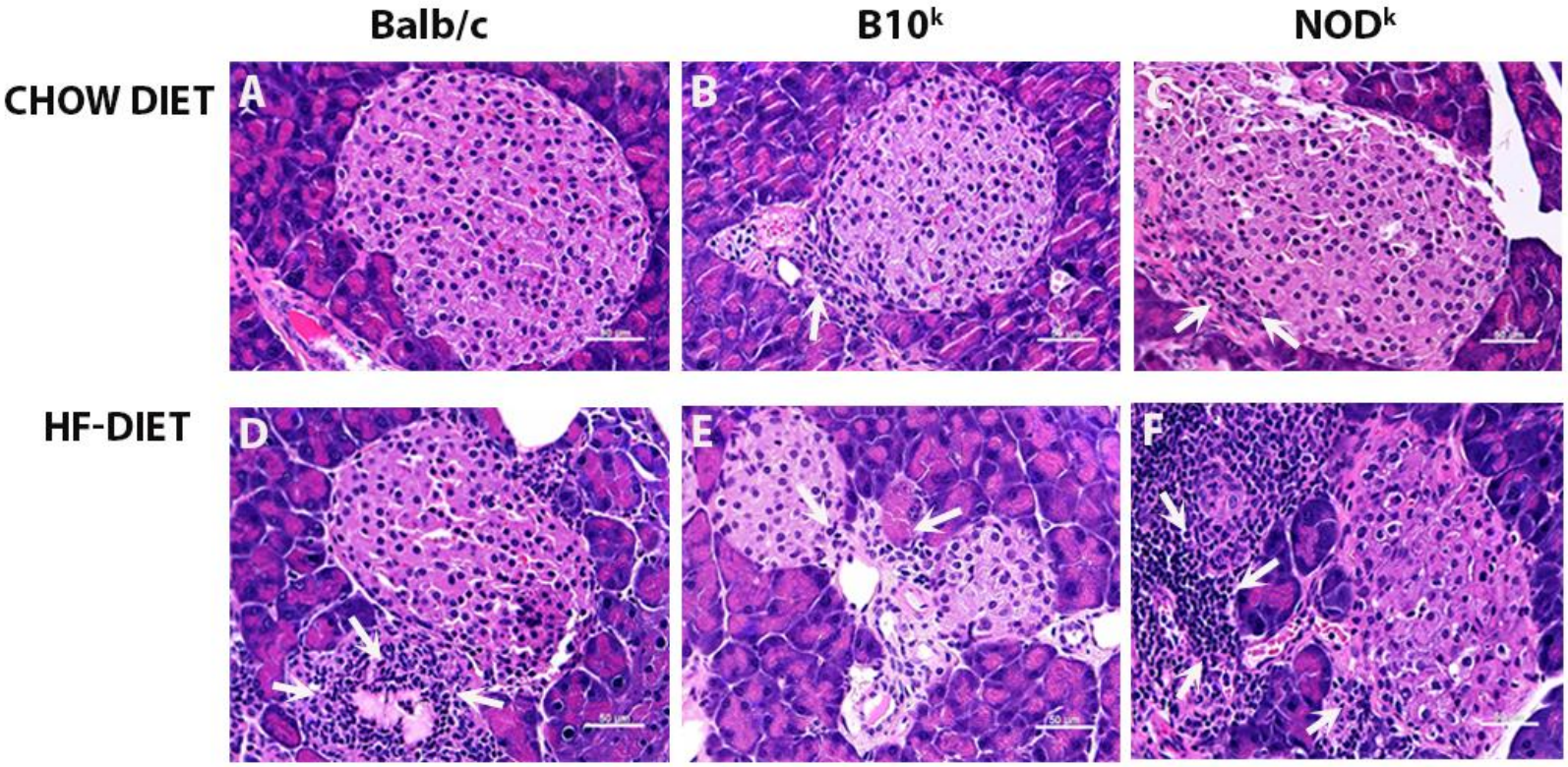
Balb/c
B10k
NODk
CHOW DIET
HF-DIET
A
B
C
D
E
F

Figure 5.3. Representative images of pancreas sections stained with H&E showing presence of fat deposits in chow and high fat diet (HFD) fed Balb/c, B10^{k} and NOD^{k} at 14 weeks (Short-term study).

(A) Chow-fed Balb/c mouse pancreas showing negligible fat deposits. **(B)** Chow-fed B10^{k} mouse showing no presence of fat. **(C)** Chow-fed NOD^{k} mouse showing negligible fat deposits. **(D)** HF-fed Balb/c mouse showing mild accumulation of fat deposits. **(E)** HF-fed B10^{k} mouse showing infrequent fat deposits. **(F)** HF-fed NOD^{k} mouse with moderate accumulation of fat deposits in exocrine pancreas. Scale bar, 500 μm. Arrows point to fat deposits.

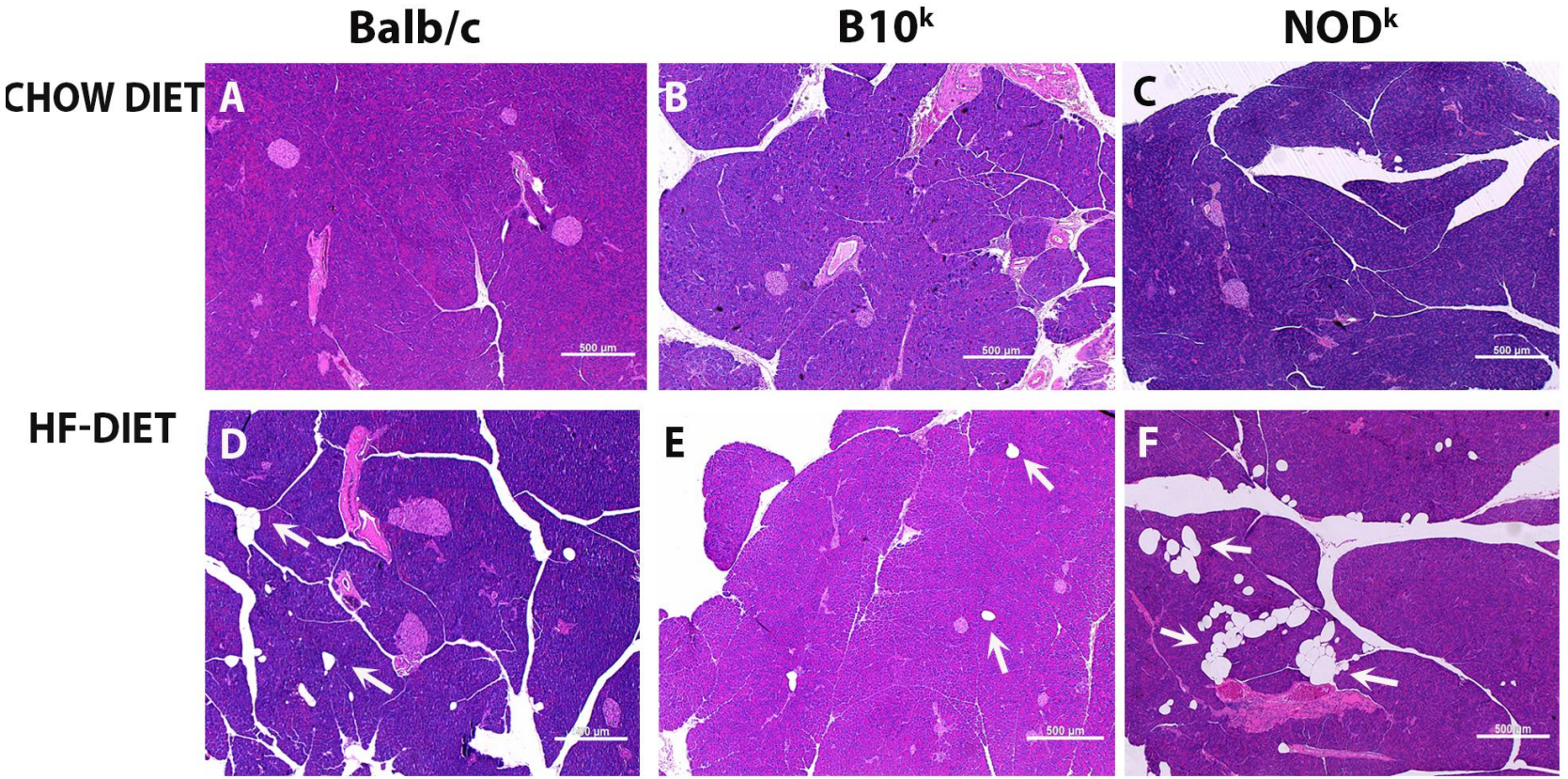
Balb/c
B10k
NODk
CHOW DIET
HF-DIET
A
B
C
D
E
F
500 µm

Figure 5.4. Representative images of pancreatic sections stained with H&E showing presence of fat deposits in chow and high fat diet (HFD) fed Balb/c, B10^{k} and NOD^{k} at 24 weeks (Long-term study).

(A) Chow-fed Balb/c mouse pancreas showed negligible fat deposits. **(B)** Chow-fed B10^{k} with negligible fat deposits. **(C)** Chow-fed NOD^{k} mouse showing infrequent fat deposits. **(D)** HF-fed Balb/c mouse showing moderate accumulation of fat deposit in the exocrine pancreas. **(E)** HF-fed B10^{k} mouse showing negligible fat presence. **(F)** HF-fed NOD^{k} mouse showing infrequent fat presence in exocrine pancreas. Scale bar, 500 μm. Arrows point to fat deposits.

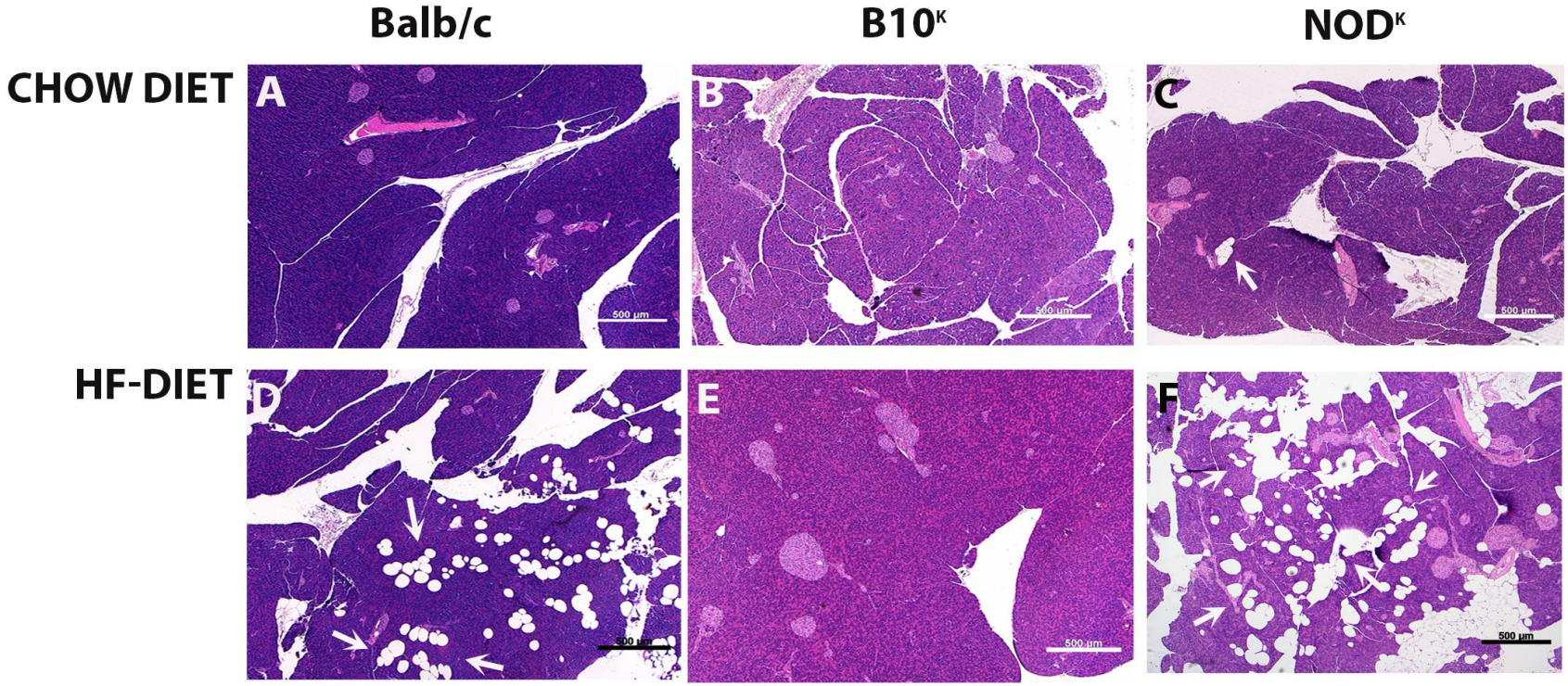
Balb/c
B10K
NODK
CHOW DIET
HF-DIET
A
B
C
D
E
F
500 µm

5.3.3. Islet endocrine cell apoptosis

Islet endocrine cell apoptosis was observed by Professor Dahlstrom in some of the blinded sections and this was scored. Representative images of apoptotic endocrine cells are shown in Fig 5.5. Other than one apoptotic cell being seen in a chow-fed $B10^k$ mice, apoptotic endocrine cells were only seen in HF-fed NOD^k mice (3 of 11 mice in the short-term study and 5 of 6 mice in the long-term study) (Fig 5.5 and Table 5.1). Although, it is most likely that the apoptosis is in islet β-cells, this cannot be concluded from these H&E sections.

Figure 5.5. Representative image of H&E sections of pancreas for apoptosis in high fat diet (HFD) fed Balb/c, B10^{k} and NOD^{k} at the time of harvest on the long-term study.

(A) HF-fed Balb/c mice at 24 weeks of age. **(B)** HF-fed B10^{k} mice at 24 weeks of age. **(C)** HF-fed NOD^{k} mice at 24 weeks of age. In these images apoptotic endocrine cells are evident in the HF-fed NOD^{k} mouse section only, as shown by the circling of apoptotic cells.

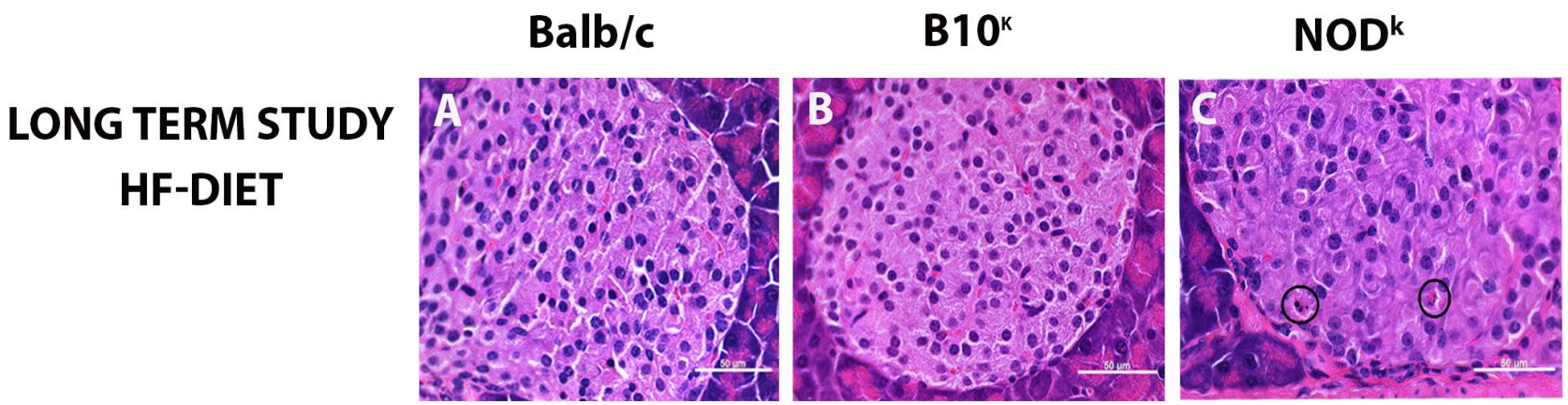

Figure 5.6. Blinded scoring of pancreas H&E sections for grade of chronic inflammation (A&C) and grade of pancreatic exocrine fat presence (B&D) in chow and high fat fed Balb/c, B10^{k} and NOD^{k} mice harvested from the short-term experiment at 14 weeks of age (A&B) and from the long-term experiment at 24 weeks of age or earlier in some HF-fed NOD^{k} mice (C&D).

Results presented as percentages of all mice pancreases examined (n=9-11 mice short term study, n=5-6 long term study).

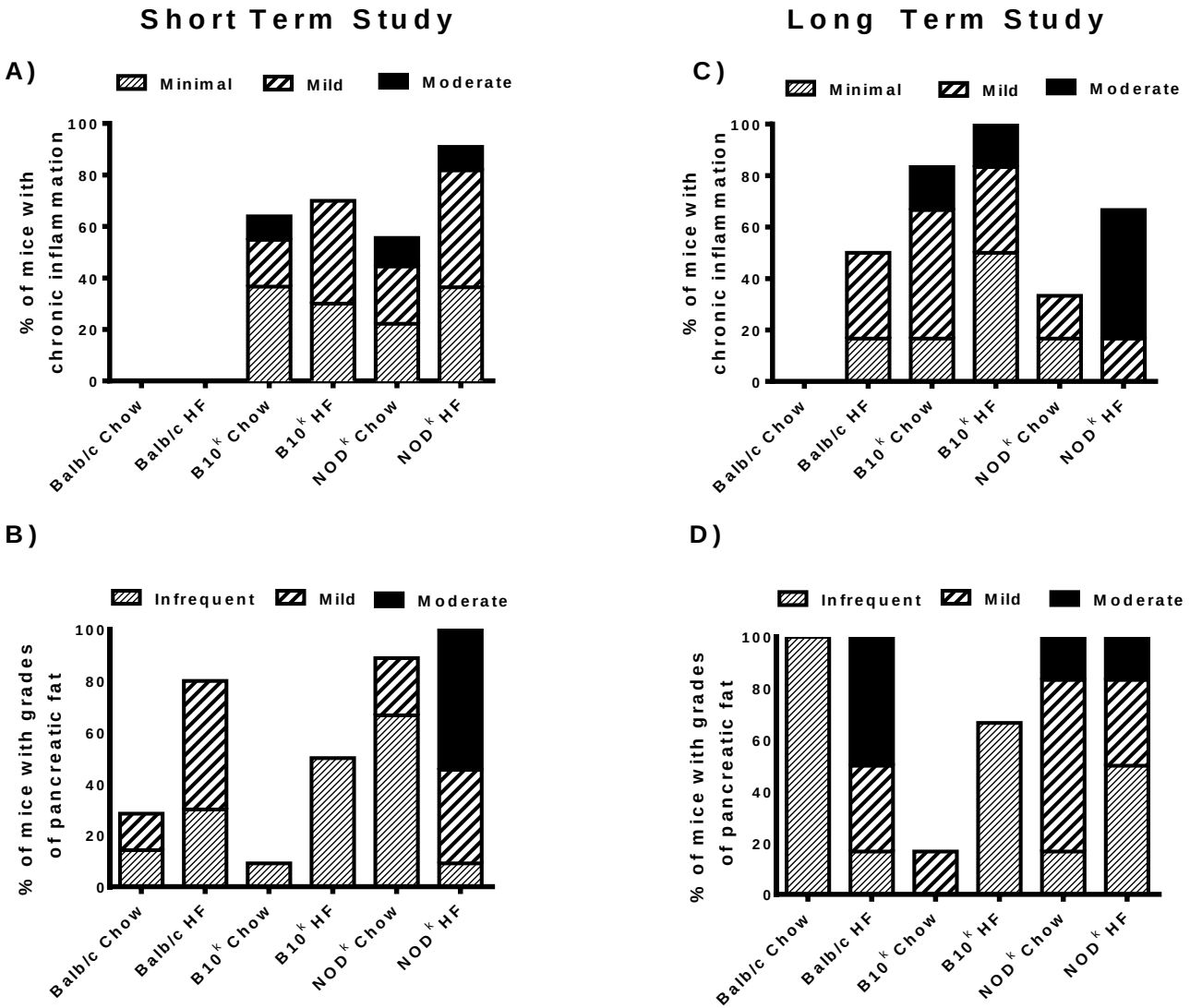
Short Term Study
Long Term Study
A)
C)
B)
D)
Minimal
Mild
Moderate
Infrequent
% of mice with chronic inflammation
% of mice with grades of pancreatic fat
0
20
40
60
80
100
Balb/c Chow
Balb/c HF
B10K Chow
B10K HF
NODK Chow
NODK HF

Table 5.1: Summary of blinded scoring of pancreatic H&E sections for presence of acute inflammation, chronic inflammation, apoptosis and exocrine tissue fat deposits in chow and high fat fed Balb/c, B10^{k} and NOD^{k} mice harvested at 14 weeks of age (short-term study) and at 24 weeks of age (long-term study).

Several HF-fed NOD^{k} mice were euthanized before 24 weeks due to severe hyperglycaemia. The results shown include the total number of pancreases assessed in each mouse group and the number of pancreases within each group in which the particular histological features were found to be present. Chi-Square statistical analysis was performed and p-values are shown.

Table 5.1

SHORT-TERM STUDY

	Balb/c Chow diet	Balb/c HF-diet	B10^{k} Chow diet	B10^{k} HF-diet	NOD^{k} Chow diet	NOD^{k} HF-diet	Chi-square P-value
Total (n)	**7**	**10**	**11**	**10**	**9**	**11**	
Acute inflammation present (n)	0	0	2	2	0	1	0.22
Chronic Inflammation present (n)	0	0	7	7	6	10	<0.0001
Apoptosis present (n)	0	0	1	0	0	3	0.08
Pancreatic fat present (n)	2	8	1	5	8	11	<0.0001

LONG-TERM STUDY

	Balb/c Chow diet	Balb/c HF-diet	B10^{k} Chow diet	B10^{k} HF-diet	NOD^{k} Chow diet	NOD^{k} HF-diet	Chi-square P-value
Total (n)	**5**	**6**	**6**	**6**	**6**	**6**	
Acute inflammation present (n)	0	2	1	1	0	0	0.54
Chronic Inflammation present (n)	0	4	5	6	2	4	0.01
Apoptosis present (n)	0	0	1	0	0	5	0.003
Pancreatic fat present (n)	5	6	1	4	6	6	0.0006

5.3.4. Assessment of pancreas sections immuno-stained for insulin and measurement of islet β-cell mass

Representative images of pancreas sections immuno-stained for insulin from chow and HF-fed Balb/c, $B10^k$ and NOD^k mice from the short-term and long-term study are shown in Figures 5.7 and 5.8, respectively. Mouse pancreas weight, number of islets per section, islet β-cell area and islet β-cell mass results, including corrections for body weight, are shown in Fig. 5.9 and 5.10, for the short-term and long-term studies, respectively.

In the short-term study, pancreas weights were higher in $B10^k$ and NOD^k mice compared to Balb/c mice, but were not affected by diet (Fig 5.9A). Pancreas weight, corrected for body weight as a percentage, however, was reduced by HF-feeding, indicative of the effect of HF-diet to increase weight in tissues other than pancreas (Fig 5.9B). At variance with this though, HF-diet appeared to increase pancreas weight in $B10^k$ mice proportional to whole body weight in the longer-term study (Fig 5.10A, B). In the long-term study, HF-fed NOD^k mice were harvested earlier than 24 weeks of age in most mice due to the development of diabetes, such that it was expected that their pancreas weights would be lower (Fig 5.10A); however, after adjustment for body weight, some of the HF-fed NOD^k mice pancreases were still clearly small (Fig 5.10B,E).

From the insulin immuno-stained sections and pancreas weights, islet number per pancreas section and islet area per section were measured, and β-cell mass was calculated. On viewing the representative images of the short-term studies, it appears that HF-feeding increased the size of the islets in all strains, but that the intensity of insulin staining was reduced in the HF-fed NOD^k islets (Fig 5.7). The representative insulin immuno-stained section of the long-term HF-fed NOD^k mouse pancreas again

showed less intense, but also irregular, insulin staining compared to the other mice, and the islets appeared smaller (Fig 5.8). The morphometric analysis of the insulin stained areas of all of the pancreases confirmed changes in β-cell mass between strains caused by HF-feeding (Fig 5.9 and 5.10) as presented in the following paragraphs.

In the short-term study, there was no effect of diet to change islet number per pancreas and there was no significant difference across strains (Fig 5.9C). There was, however, an across strain effect of HF-feeding to increase β-cell area, which in the Balb/c mice was more than two-fold (Fig 5.9C, D). Islet β-cell mass was greatest in the larger NOD^k mice, but this was not found after correction for body weight (Fig 5.9E, F). Also, HF-feeding had an across strain effect to increase β-cell mass, but again this effect was not significant after correcting for body weight of the mice (Fig 5.9E,F).

In the long-term study, the fact that most of the HF-fed NOD^k pancreases were harvested before 24 weeks of age needs to be taken into consideration (Fig 5.10). Panels J-L of Fig 5.10 show the data according to age at harvest. However, the measurements of β-cell area per pancreas section and β-cell mass corrected for body weight should be less affected by the age of harvest. In these older mice, there was now a difference in the number of islets/section across the strains, with the NOD^k mice having the fewest (Fig 5.10D). With β-cell area, there was a strain-diet interaction, with β-cell area increasing in Balb/c mice and falling in NOD^k mice with HF-feeding (Fig 5.10G). A strain-diet interaction was also evident for β-cell mass, with a fall in β-cell mass in the NOD^k mice with HF-feeding compared to the other two strains, but this interaction was not significant after correction for body weight (Fig 5.10H,I). Consistent with the representative image, however, β-cell area and mass was reduced rather than increased with HF-feeding in the longer-term HF-fed NOD^k mice.

Figure 5.7. Representative images of pancreas sections with insulin immunohistochemistry in chow and HF-fed Balb/c, B10^{k} and NOD^{k} at 14 weeks of age (Short-term study).

The insulin immune-stain is brown in colour and is shown within the pancreatic islets. **(A)** Chow-fed Balb/c mouse pancreas section. **(B)** Chow-fed B10^{k} mouse pancreas section **(C)** Chow-fed NOD^{k} mouse pancreas section. **(D)** HF-fed Balb/c mouse pancreas section. **(E)** HF-fed B10^{k} mouse pancreas section. **(F)** HF-fed NOD^{k} mouse pancreas section. Scale bar, 500 μm. Arrows point to insulin-staining within pancreatic islets.

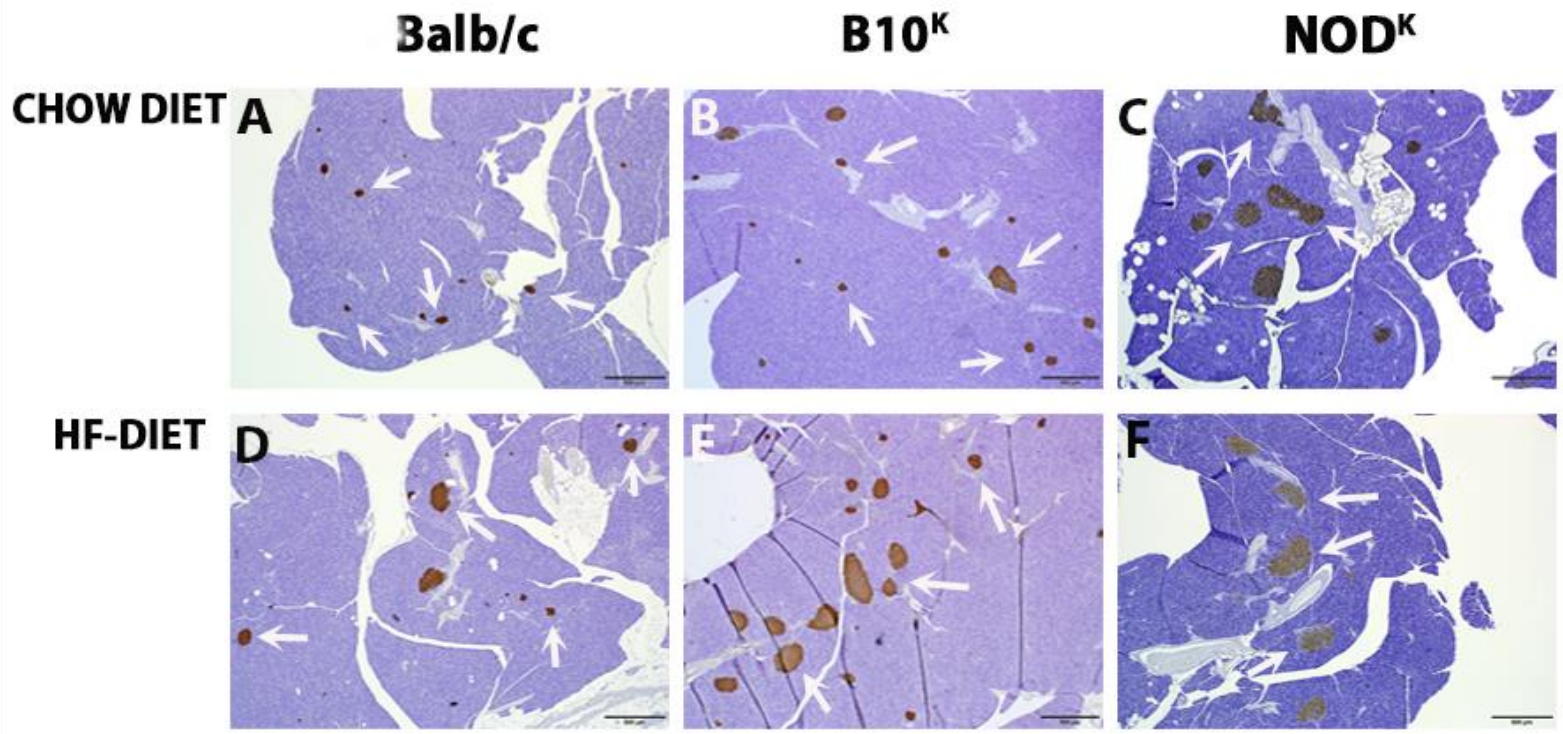
Balb/c
B10K
NODK
CHOW DIET
HF-DIET
A
B
C
D
E
F

Figure 5.8. Representative images of pancreas sections with insulin immunohistochemistry in chow and HF-fed Balb/c, B10^{k} and NOD^{k} at 24 weeks of age (Long-term study).

The insulin immune-stain is brown in colour and is shown within the pancreatic islets. **(A)** Chow-fed Balb/c mouse pancreas section. **(B)** Chow-fed B10^{k} mouse pancreas section. **(C)** Chow-fed NOD^{k} mouse pancreas section. **(D)** HF-fed Balb/c mouse pancreas section. **(E)** HF-fed B10^{k} mouse pancreas section. **(F)** HF-fed NOD^{k} mouse pancreas section. Scale bar, 500 μm. Arrows point to insulin-staining within pancreatic islets.

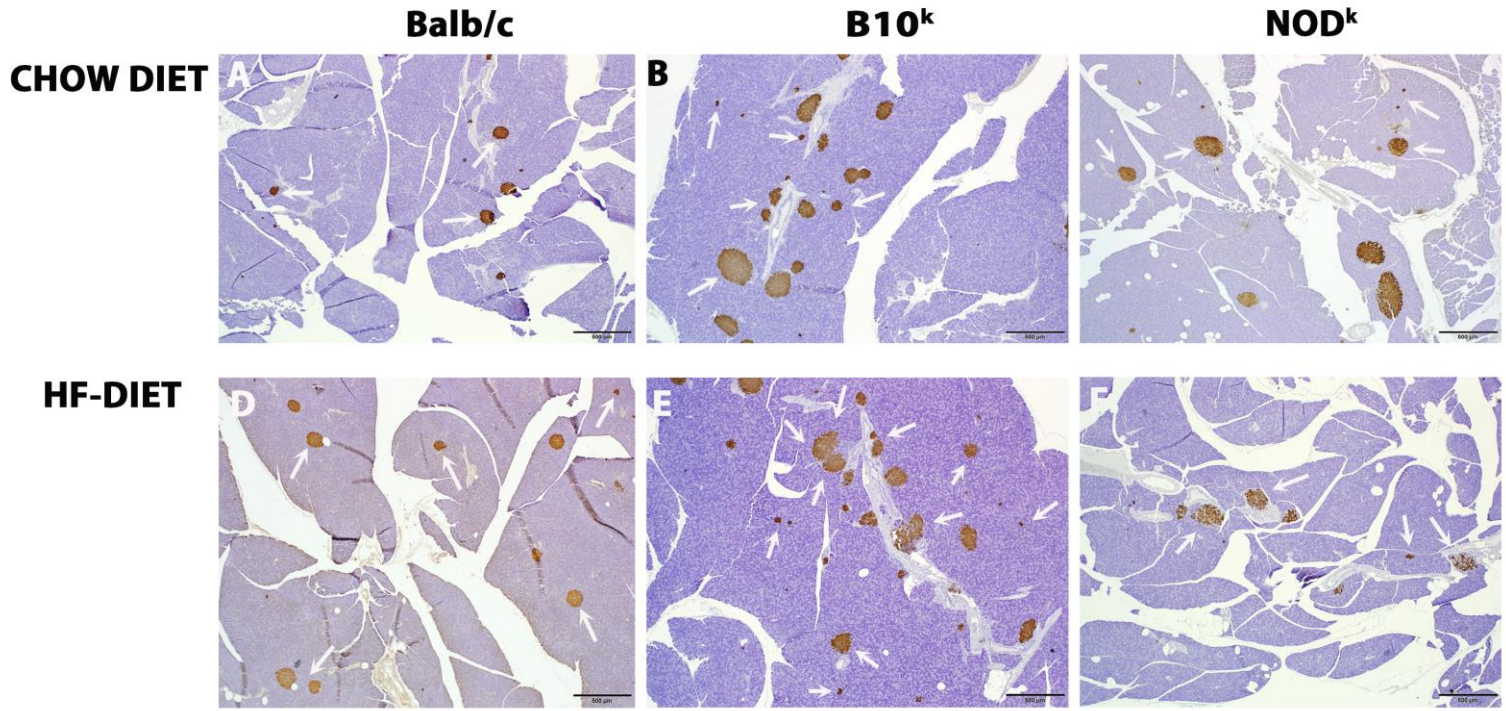
Balb/c
B10k
NODk
CHOW DIET
HF-DIET
A
B
C
D
E
F

Figure 5.9. Summary of morphometric analysis of insulin immuno-stained pancreas sections, including measurement of islet β-cell mass, of Balb/c, B10^{k} and NOD^{k}, fed on chow or high fat diet (HFD), harvested at the end of the short-term study (14weeks of age).

(A) Pancreatic weight for all groups. **(B)** Pancreatic weight as percentage of body weight (BW) for all groups. **(C)** Average number of islets per section for all groups. **(D)** β-cell area as percentage of total pancreas area for all groups. **(E)** β-cell mass per mouse for all groups. **(F)** β-cell mass per BW of mice for all groups. Data are Means ± SEM of 4-5 mice per group. Two-way ANOVA shown in tables below graphs. Bonferroni post-hoc tests: *****$p<0.05$ vs chow diet of the same strain; $^{\#}$ $p<0.05$ vs different strain on the same diet.

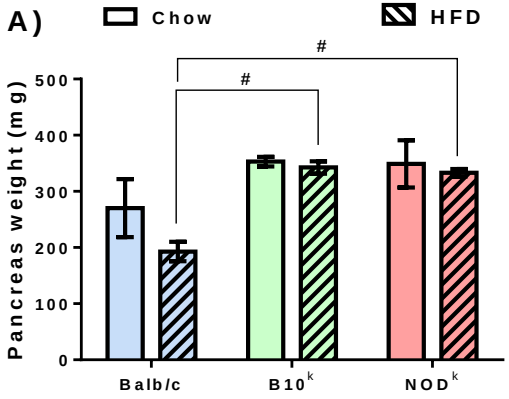

Two-wayANOVA	
Strain effect	p=0.0013
Diet effect	p=0.1651
Strain* Diet interaction	p=0.4760

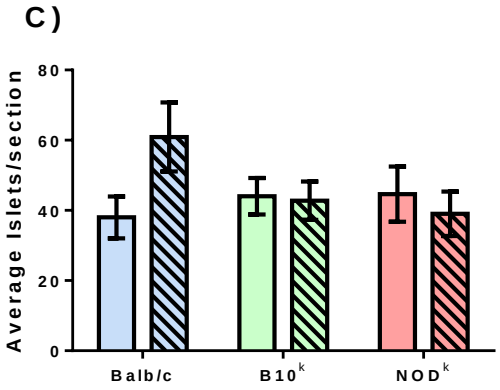

Two-wayANOVA	
Strain effect	p=0.5359
Diet effect	p=0.3667
Strain* Diet interaction	p=0.1233

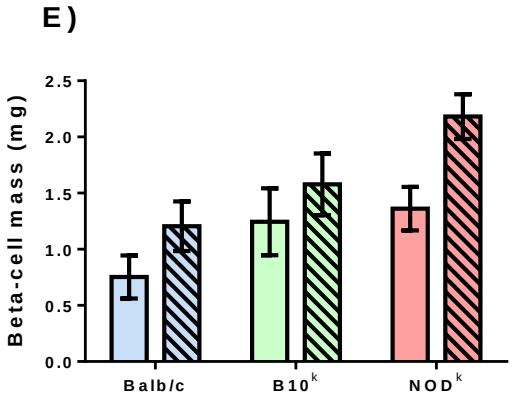

Two-wayANOVA	
Strain effect	p=0.0083
Diet effect	p=0.0100
Strain* Diet interaction	p=0.5319

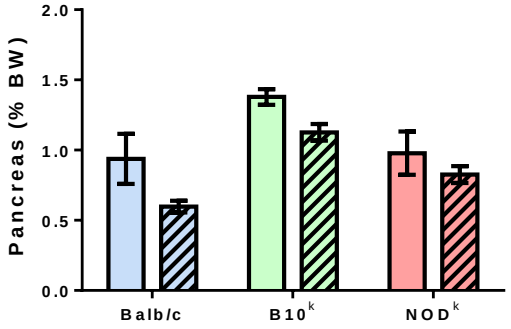

Two-wayANOVA	
Strain effect	p=0.0011
Diet effect	p=0.017
Strain* Diet interaction	p=0.6816

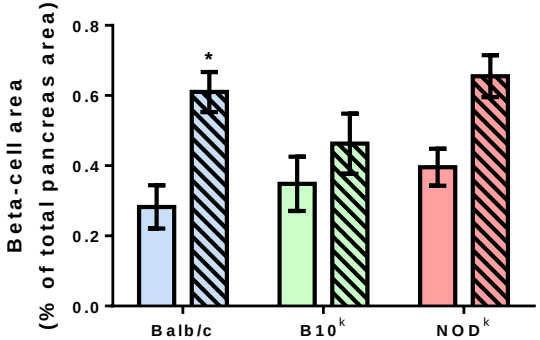

Two-wayANOVA	
Strain effect	p=0.1880
Diet effect	p=0.0003
Strain* Diet interaction	p=0.2977

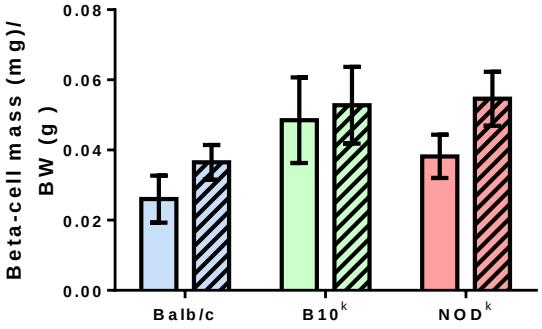

Two-wayANOVA	
Strain effect	p=0.0845
Diet effect	p=0.1445
Strain* Diet interaction	p=0.7635

Figure 5.10. (Part 1&2) Summary of the morphometric analysis of insulin immuno-stained pancreas sections, including measurement of islet β-cell mass, of Balb/c, B10^{k} and NOD^{k}, fed on chow or high fat diet (HFD), harvested at the end of the long-term study (24 weeks of age).

Part 1 (A) Pancreatic weight for all groups. **(B)** Pancreatic weight as percentage of body weight (BW) for all groups. **(C)** Average number of islets per section for all groups. **(D-F)** As several HF-fed NOD^{k} mice were euthanized before 24 weeks due to severe hyperglycaemia, data for NOD^{k} mice are also shown according to age at pancreas harvest. **(D)** Pancreatic weight for chow and HF-fed NOD^{k} mice only, according to the age at pancreas harvest. **(E)** Pancreatic weight as percentage of body for chow and HF-fed NOD^{k} mice only, according to the age at pancreas harvest. **(F)** Average number of islets per section for chow and HF-fed NOD^{k} mice only, according to the age at pancreas harvest.

Part 2 (G) β-cell area as percentage of total pancreas area for all groups. **(H)** β-cell mass per mouse for all groups. **(I)** β-cell mass per BW of mice for all groups. **(J-L)** As several HF-fed NOD^{k} mice were euthanized before 24 weeks due to severe hyperglycaemia, data for NOD^{k} mice are also shown according to age at pancreas harvest. **(J)** β-cell area as percentage of total pancreas area for chow and HF-fed NOD^{k} mice only, according to the age at pancreas harvest. **(K)** β-cell mass per mouse for chow and HF-fed NOD^{k} mice only, according to the age at pancreas harvest. **(L)** β-cell mass per BW for chow and HF-fed NOD^{k} mice only, according to the age at pancreas harvest. Data are Means ± SEM (n=4) mice per group. Two-way ANOVA shown in tables below graphs. Bonferroni post-hoc tests: $^{\#}$ $p<0.05$, $^{\#\#}$ $p<0.01$, vs different strain same diet.

PART:1

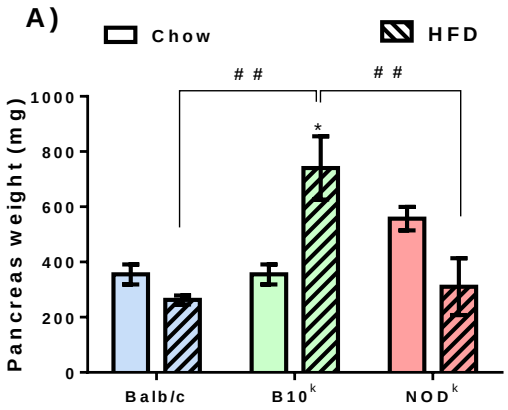

Two-way ANOVA	
Strain effect	p=0.0064
Diet effect	p=0.7697
Diet* Strain interaction	p=0.0004

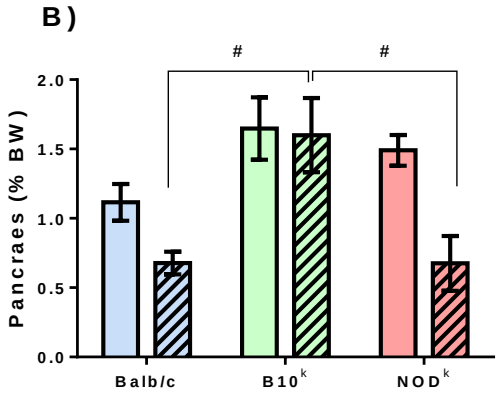

Two-way ANOVA	
Strain effect	p=0.0023
Diet effect	p=0.0090
Diet* Strain interaction	p=0.1353

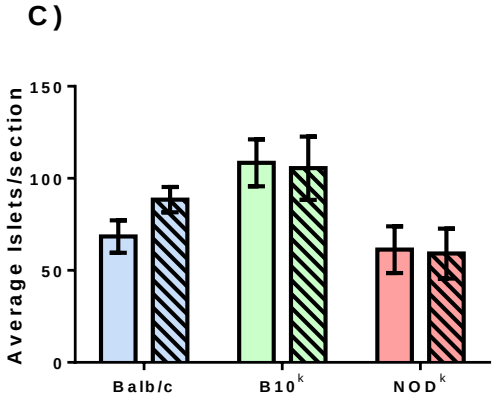

Two-way ANOVA	
Strain effect	p=0.0049
Diet effect	p=0.6197
Diet* Strain interaction	p=0.5621

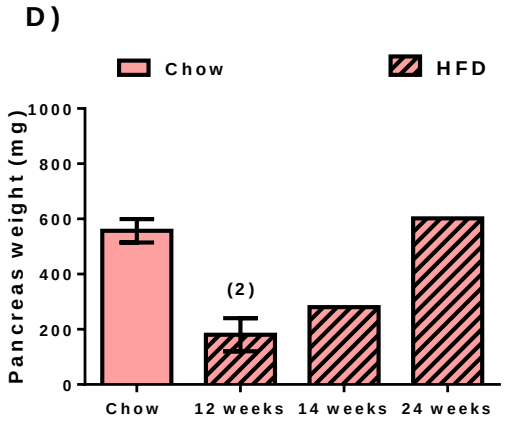

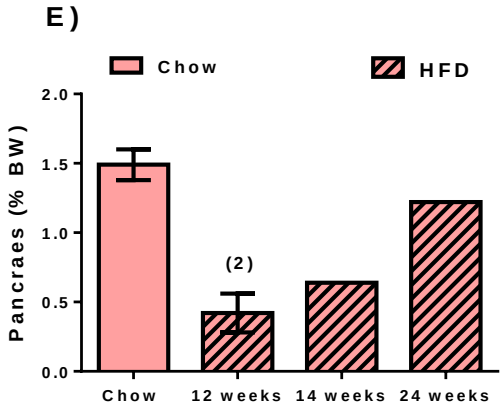

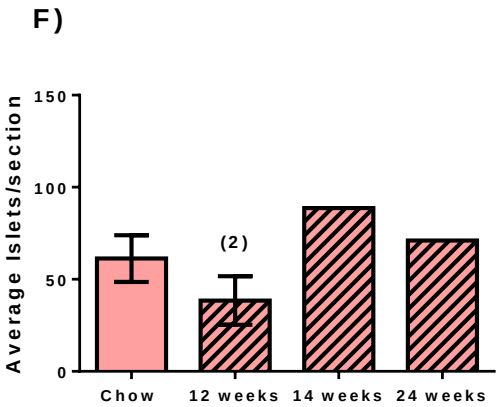

PART : 2

G)

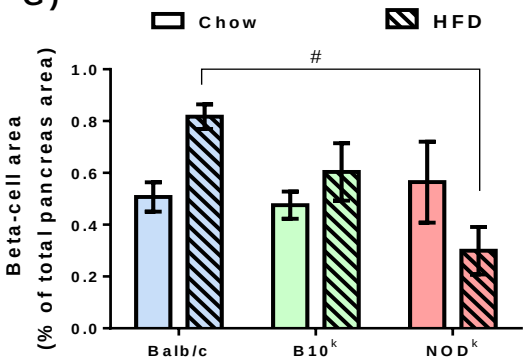

Two-way ANOVA	
Strain effect	p=0.0670
Diet effect	p=0.4613
Diet* Strain interaction	p=0.0178

H)

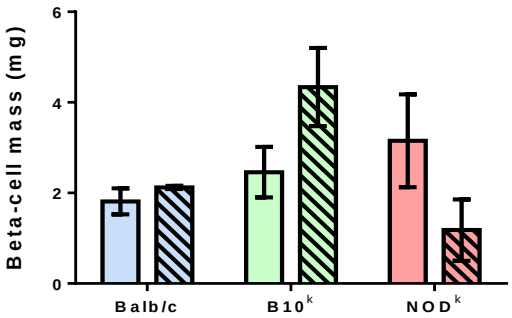

Two-way ANOVA	
Strain effect	p=0.0957
Diet effect	p=0.8943
Diet* Strain interaction	p=0.0294

I)

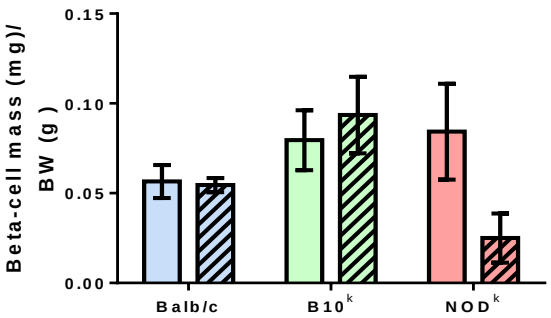

Two-way ANOVA	
Strain effect	p=0.1307
Diet effect	p=0.2712
Diet* Strain interaction	p=0.1044

J)

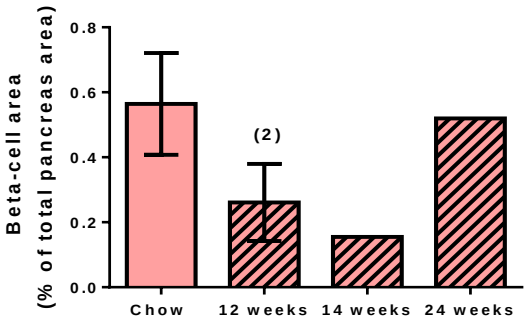

K)

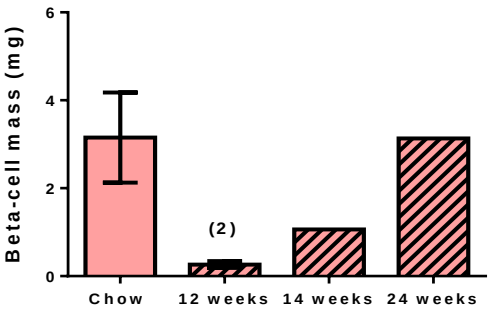

L)

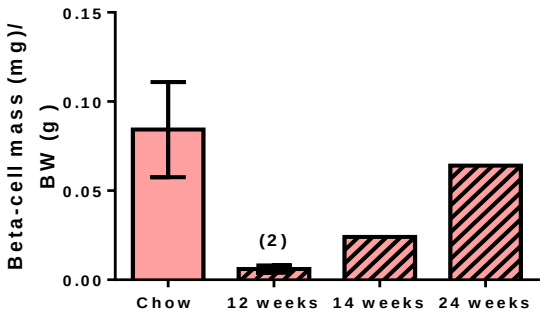

5.4. Discussion

Type 1 diabetes is caused by an immunological destruction of islet β-cells by invasion of islets by cytotoxic T-lymphocytes and to a lesser extent other immune cell types such as macrophages, B-lymphocytes and plasma cells, a process called insulitis (Tuomi et al., 2014, Mannering et al., 2016). The histological features of this process have been very well described in the NOD mouse model of type 1 diabetes (Delovitch and Singh, 1997, Kay et al., 1997). The histological characteristics of the islets in type 2 diabetes are more variable, but the process of β-cell mass expansion to compensate for insulin resistance followed by loss of β-cell mass has been well described. Depending on genetic background, however, type 2 diabetes can also be a consequence of dysfunction of islet β-cell cells, with and without, loss of β-cell mass (Jeffery and Harries, 2016). More controversial is the role of inflammation in causing islet failure in type 2 diabetes, but there is increasing evidence to support this (Donath et al., 2013). Thus the histological examination of the pancreas, with attention to the presence or absence of inflammation and the measurement of islet β-cell mass are important in determining the mechanisms by which diabetes may develop.

β-cell mass decreases in type 1 diabetes, where total loss of β-cells occur due to insulitis (Maclean and Ogilvie, 1955). Whereas, in type 2 diabetes, certain stimuli could trigger apoptotic pathway in β-cells, including elevated glucose, NEFA, cytokines, accumulation of islet amyloid polypeptide and ER stress (Cnop et al., 2005).

From the previous work on the NOD^{k}.insHEL mouse model, particular efforts were made to exclude immune mechanisms in the development of diabetes (Dooley et al., 2016). The experiments included study of the effects of β-cell expression of the HEL protein on the immune incompetent NOD^{k}.*Prkdc*^{scid} and NOD^{k}.*Rag1*$^{-/-}$ lines (Dooley et

al., 2016). These studies did suggest that NOD^{k} mice have an underlying non-immune pre-disposition to β-cell failure. In the work of this thesis, we hypothesized that such non-immune susceptibility to β-cell failure would occur in NOD^{k} mice in response to HF-feeding. For this reason, it was important for us to examine the mice pancreases for islet inflammation.

Also in the NOD^{k}.insHEL mouse model, islet β-cell mass was reduced and apoptotic β-cells were found to be increased (Dooley et al., 2016). Thus the NOD^{k} islet β-cells stressed by this molecular mechanism are prone to apoptosis. We wished to determine if the β-cells of NOD^{k} islets are also susceptible to apoptosis by the more physiological stressor of HF-feeding. For this reason islet endocrine cell apoptosis was looked for and β-cell mass was measured.

In addition, the histological responses of the other two strains of mice to HF-feeding was important to enable comparison, but also to provide some further insight in the failure of B10^{k} mice to compensate with increased insulin secretion in response to HF-feeding.

5.4.1 Pancreas inflammation

Within the three strains of mice, the Balb/c mice were least prone to inflammation in the pancreases, with the degrees of inflammation being similar between B10^{k} and NOD^{k} mice. While HF-feeding did not seem to aggravate the degree of inflammation in B10^{k} mice, some aggravation could have been occurring within the NOD^{k} mice, but this would require more mice to be certain. Nevertheless, the inflammation was usually of mild to moderate severity only and was not seen to cause insulitis in any of the strains. Most of the inflammation in the B10^{k} and NOD^{k} mice was peri-ductal, with some occurrences of the peri-ductal inflammation spilling over to the peri-islet region.

Uncertain is whether any of this inflammatory infiltrates are pathogenic with respect to islet health. In previous experiments, peri-islet inflammatory infiltrates do not seem to be harmful to the islets unless the leukocyte penetrate the extracellular matrix of the peri-islet capsule, which is composed of the peri-islet basement membrane and subjacent interstitial matrix (Ziolkowski et al., 2012). Importantly, insulitis was not seen in any of three strains of mice, such that the glucose intolerance and diabetes within the $B10^k$ and NOD^k mice is not caused by aggressive immune destruction of β-cells. An effect of inflammatory cytokines having an effect on islet function, however, cannot be excluded.

5.4.2 Islet endocrine cell apoptosis and islet β-cell mass

There was an across strain increase in β-cell area and mass in response to HF-feeding at the 14 week time-point, however, when corrected by mouse weights, this effect did not quite reach statistical significance. In the long-term study, however, this same response of β-cell area and mass to increase with HF-feeding, while evident in Balb/c and $B10^k$ mice, was no longer evident in the NOD^k mice. Islet β-cell mass of HF-fed NOD^k mice, after correction for body weight considering the different ages the mice were harvested, was reduced rather than increased.

β-cells mass is maintained by a well-organized regulation of β-cell replication and apoptosis and also by the development of new islets from exocrine pancreatic ducts (Finegood et al., 1995, Bonner-Weir, 2000). Any disturbance causing a decrease in β-cell replication or an increase in the rate of β-cells death will result in a decrease in β-cells mass.

Of interest was the finding of scattered apoptotic endocrine cells almost exclusively in the islets of HF-fed NOD^k mice. They were more frequently seen in the mice of the

long-term study, but could also be seen in HF-fed NOD^k mice from the short-term study. As stated above, it is likely that this apoptosis is within islet β-cells, but this needs to be confirmed with another imaging method, such as dual immunohistochemistry for insulin and activated caspase-3 as was performed in the NOD^k.insHEL islets (Dooley et al., 2016). The apoptotic cells correspond to a reduction in β-cell area and mass in the NOD^k islets by the time of diabetes development.

5.4.3. Pancreatic fat deposits

Pancreatic steatosis or "non-alcoholic fatty pancreas disease (NAFLD)" refer to the occurrence of increased pancreatic fat (Catanzaro et al., 2016). It occurs in association with obesity and the metabolic syndrome and has been implicated as a possible factor in the pathogenesis of type 2 diabetes, including islet β-cell dysfunction, although the available evidence is far from clear (van der Zijl et al., 2010, Chen et al., 2015, Heni et al., 2010, Della Corte et al., 2015). It could also be that intrapancreatic fat reflects the increased fat accumulation of the whole body only and is not at all locally pathogenic or diabetogenic (Catanzaro et al., 2016).

On this background, the results of intra-pancreatic fat deposit accumulation in this study are interesting. Even though Balb/c mice have been reported to be resistant to the development of fatty liver (Montgomery et al., 2013), in this study HF-feeding did promote intra-pancreatic fat accumulation. Clearly, the fat content of the liver in these mice need to be examined though. This intra-pancreatic fat accumulation was not associated with abnormal glucose tolerance, such that in this model it is benign.

The NOD^k mice, even on chow diet with perfectly normal glucose tolerance, had evidence of increased fat content in the pancreases and this worsened with HF-feeding.

This would favor a role of intra-pancreatic fat in diabetes development, but this finding could also be a non-causative association.

The $B10^k$ mice, that had poor glucose tolerance, had few pancreatic fat deposits, even with long-term HF-feeding. Of course these mice did not progress onto develop diabetes, and it could be argued that having little pancreatic fat protected them from complete β-cell failure, but again this is purely speculation.

Elevated TG and FFA causes abnormal fat deposition in the liver, heart, muscles, and pancreas, which is called steatosis, known to be related to obesity and/or insulin resistance (Yin et al., 2004). The HF-fed NOD^k mice, in short-term study, displayed raised plasma TG and FFA concentrations in fasting and non-fasting state. They were significantly obese from the Balb/c and $B10^k$ on HF-diet in both studies and were insulin resistance during ipITT in long-term study.

5.5. Summary

In the HF-fed NOD^k mice, the diabetes was not caused by insulitis, however, a role for the mild to moderate peri-islet inflammatory infiltrates cannot be fully excluded. Such infiltrates were also present in the chow-fed mice that didn't develop diabetes, although with HF-feeding there may have been some increase in their number and size. Diabetes in this mouse did seem to correspond to a reduction in β-cell mass due to β-cell apoptosis, however, the latter needs to be confirmed by further imaging with dual staining immunohistochemistry for insulin and activated caspase 3.

The poor glucose tolerance of the chow-fed and HF-fed $B10^k$ mice was not a consequence of reduced β-cell mass compared to the other strains. This suggests that the islet defect has to be a functional one.

The various findings of fat content in the different models suggest that it is associated with adiposity, but the greater propensity to develop is dependent on genetic background. While a pathogenic role for pancreatic fat cannot be excluded, its presence in HF-fed Balb/c mice suggest that under some circumstances it can be benign in nature.

Overall, these histological findings are helpful in determining the differences in metabolic phenotype between the various mice strains on the two diets, further studies will be required to determine the molecular determinants of these differences.

Chapter # 6:

NOD^{k} Refreshed (NOD^{k}-REF) Mice

6.1. Introduction

NOD^{k} mice from John Curtin Medical Research Centre at ANU (from Prof Chris Goodnow) were used in this project to investigate the hypothesis that NOD^{k} mice have the propensity to develop islet β-cell failure when stressed by HF-feeding. They originated from NOD.BR-*H2*^{k}/Wicker mice dating back to 1993 (Podolin et al., 1993). We found that male chow-fed NOD^{k} mice maintain normoglycaemia, but with mild hyperinsulinemia and an abnormal pattern of insulin secretion to an ipGTT at age 24 weeks. With HF feeding, male NOD^{k} mice develop a type 2 diabetes phenotype after only 10 weeks on HF-diet, characterised by diet-induced obesity, dyslipidaemia, hyperinsulinemia and hyperglycaemia. HF diet for more than 10 weeks results in severe diabetes in NOD^{k} mice associated with islet β-cell dysfunction and apoptosis, almost certainly with loss of β-cell mass, but without evidence of insulitis. All of this is highly suggestive that the islet β-cells of the NOD mouse have a non-immune susceptibility to failure. This is demonstrable in NOD^{k} mice, as they are protected from islet β-cell destruction from autoimmunity through carrying the autoimmune low-risk MHC *H2*^{k} haplotype, such that other mechanisms of β-cell failure are more easily delineated (Dooley et al., 2016).

Through this project, some difficulty in breeding and maintaining the NOD^{k} colony was experienced. The frequency of litters was reduced and some male NOD^{k} mice were unexpectedly dying around 180-210 days, with autopsy suggesting this may have been related to obstruction of the urethra by gelatinous material and prostatitis. As there were no records of this mouse colony being refreshed since 1993, genetic drift with additional mutations was suspected as a possible contributor to these difficulties maintaining the colony. Genetic drift have previously been reported in NOD mice substrains (Simecek et al., 2015). For this reason a decision was made to refresh the

NOD^{k} colony.

The NOD^{k} mice were refreshed at ANU as discussed in the experimental plan (Section 6.2). In order to determine if the refreshed NOD^{k} mice would develop the same type 2 diabetes phenotype as the original ANU NOD^{k} mice, two separate cohorts of refreshed male NOD^{k} mice were placed on chow or HF-diet from soon after weaning and were followed up to the age of 24-25 weeks.

6.2. Experimental plan

The NOD^{k} mice were refreshed at ANU, under the management of the animal facility staff. The female NOD^{k} mice (from the original ANU colony) were crossed with male NOD.ShiLtJArc from the Animal Resource Centre WA and the N1 progeny were backcrossed to the NOD.ShiLtJArc strain a further two times. Breeders were selected on the basis of heterozygosity using PCR for *H2k* at the MHC. After two backcrosses, N3 male and female (brother and sister) *H2*^{k} heterozygotes were intercrossed in order to fix a *H2*^{k} haplotype homozygous progeny (confirmed with PCR) for continued inbreeding. These mice were given the strain name of ASD527:NOD^{k}.ANU N3F3 (after 3 intercrosses) and we have given this refreshed strain the nick name of NOD^{k}-Refreshed (NOD^{k}-REF) for the purposes of this chapter.

Male NOD^{k}-REF mice were placed on chow or HF-diet after weaning to characterise the phenotype of the mice. The experiment was conducted in two separate cohorts. For practical reasons, the first cohort of NOD^{k}-REF mice were placed on chow or HF-diet from 5 weeks of age and the second cohort from 4 weeks of age. All mice (both cohorts) remained on diet for 21 weeks. Body weight and non-fasting blood glucose levels were measured over time and ipGTT tests were performed after 9 and 20 weeks on diet. The experimental design for this study is illustrated in Figure 6.1.

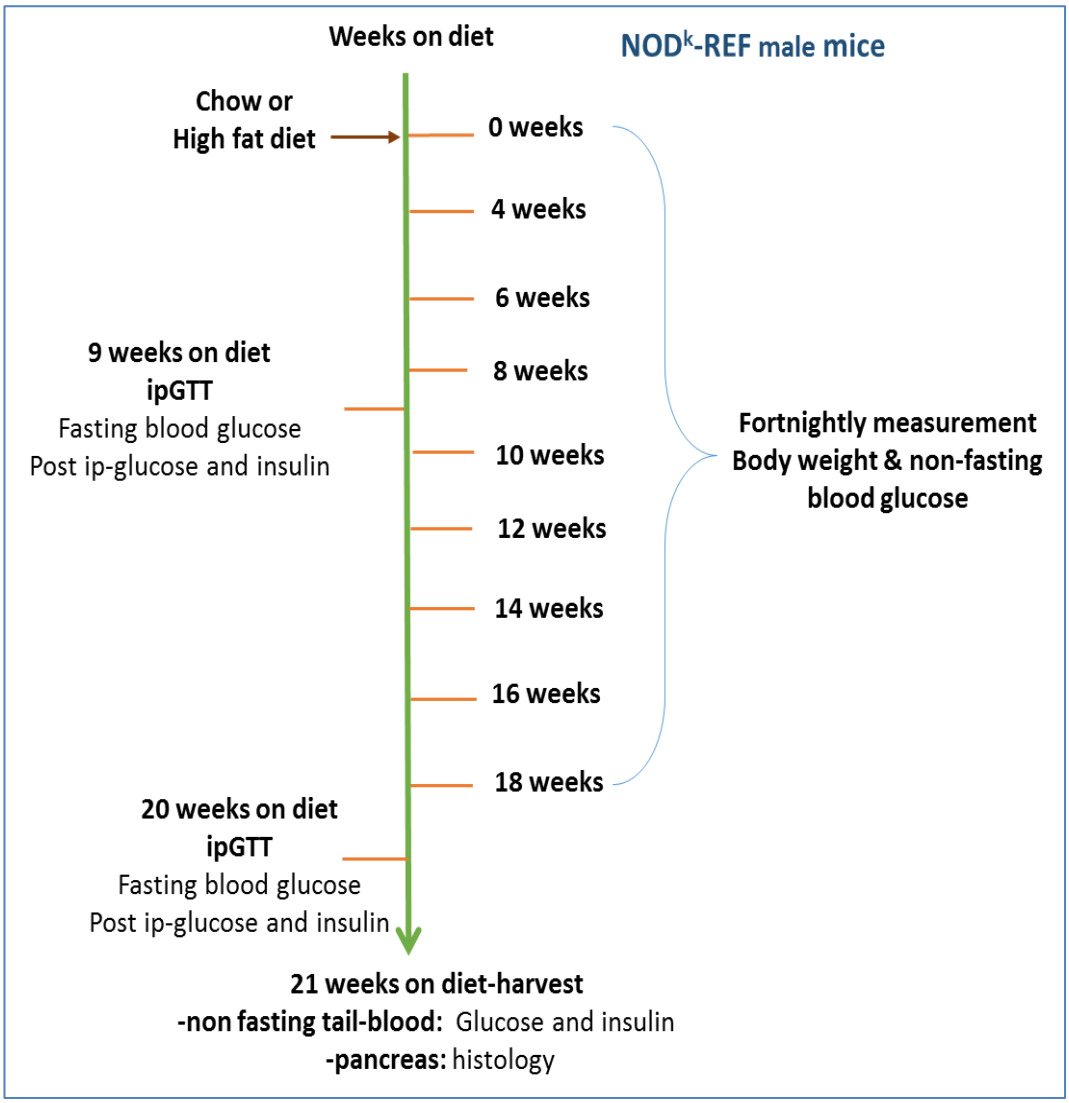

Figure 6.1: Outline of experimental design for the characterization of NOD^{k}-REF mice fed chow or HF-diet for 21 weeks (post weaning to harvesting).

6.3. Results

6.3.1. Body weight measurement

The body weight measurements for male NOD^{k}-REF mice over time are shown in (Fig 6.2). Although the NOD^{k}-REF mice tended to be slightly smaller to the NOD^{k} mice, they were susceptible to HF-diet induced obesity as shown by a 70% greater gain in body weight from weaning than their chow-fed counterparts (Fig 6.2A,D).

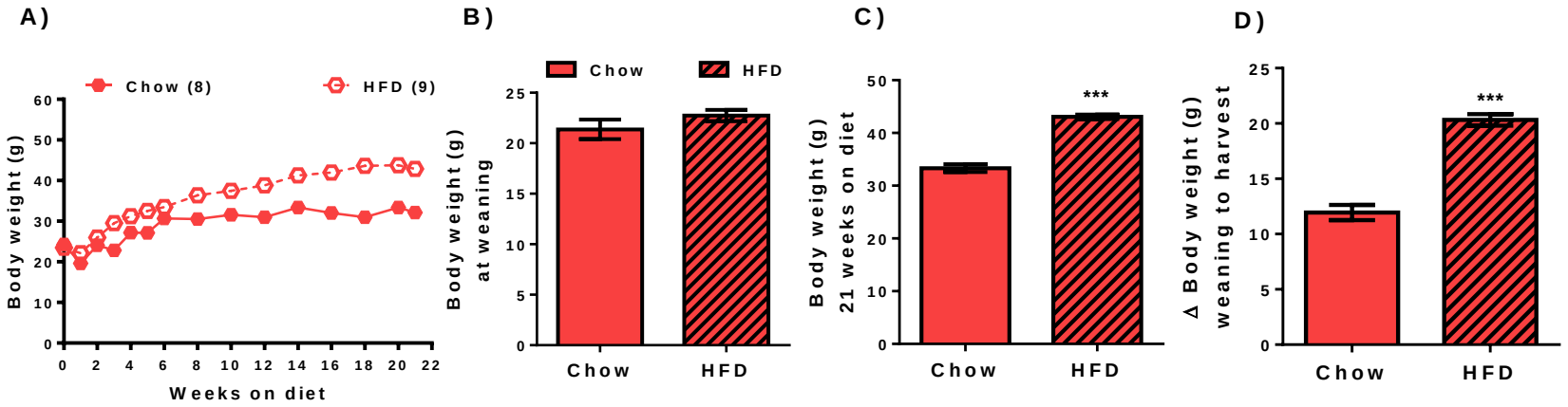

Figure 6.2. Body weight measurement during time-course study according to weeks on diet (from weaning to harvest) in NOD^{k}-REF mice fed chow or high fat diet (HFD). NOD^{k}-REF chow (n=8) and HFD (n=9) mice. **(A)** Chow and HF-fed NOD^{k}-REF groups shown. **(B)** Body weight at weaning (baseline measurement) for NOD^{k}-REF mice. **(C)** Body weight measured at 21 weeks for NOD^{k}-REF mice **(D)** Change in body weight from weaning to harvest in NOD^{k}-REF mice group. Means ± SEM. Student's unpaired t-test: ***p<0.001 vs chow diet.

6.3.2. Non-fasting blood glucose measurement

Non-fasting glucose was measured at 9AM from tail vein blood at 2 weekly intervals from the time of weaning. The results are shown in Fig 6.3. As expected, the chow fed NOD^k mice maintained normal blood glucose levels through the course of the feeding study (Fig 6.3). Unexpectedly, the HF-fed NOD^k mice also maintained normal blood glucose levels through the entirety of the study (Fig 6.3). Thus, unlike the NOD^k mice, the NOD^k-REF mice are resistant to the development of a type 2 diabetes phenotype.

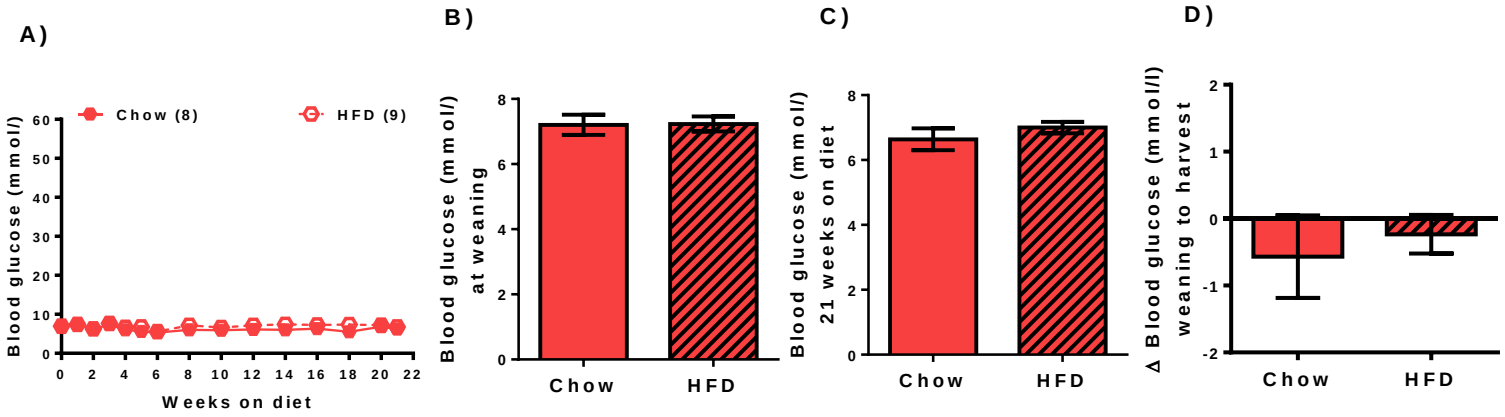

Figure 6.3. Non-fasting blood glucose measurement during time-course study according to weeks on diet (from weaning to harvest) in NOD^{k}-REF mice fed chow or high fat diet (HFD). NOD^{k}-REF chow (n=8) and HFD (n=9) mice. **(A)** Chow and HF-fed NOD^{k}-REF groups shown. **(B)** Blood glucose concentrations at weaning (baseline measurement) for NOD^{k}-REF mice. **(C)** Blood glucose measurement at 21 weeks for NOD^{k}-REF mice **(D)** Difference in blood glucose levels from weaning to harvest in NOD^{k}-REF mice group.

6.3.4. ipGTT- glucose results

ipGTTs were performed in the chow and HF-fed NOD^{k}-REF mice after 9 weeks and 20 weeks on diet (at 13-14 weeks and 24-25 weeks of age, respectively). The results of the glycaemic responses are shown in Fig 6.4. The HF-diet induced a marginal increase in fasting glycaemia, which reached significance in the older mice only (Fig 6.4E,F). HF-feeding caused a moderate degree of glucose intolerance after 9 weeks (Fig 6.4A,C,D) and moderately severe glucose intolerance after 20 weeks on diet, (Fig 6.4E,G,H), but it did not cause the extremely severe glucose intolerance that was seen after only 10 weeks of HF feeding in the orginal NOD^{k} mice (data presented in Chapter 3).

Figure 6.4: Blood glucose concentrations during ipGTT after 9 and 20 weeks on diet (from weaning to harvest) in NOD^{k}-REF mice fed chow or high fat diet (HFD). Mice fasted for 4 hours were injected with 2g/kg glucose intraperitoneally at time 0 min. **(A-D)** ipGTT performed after 9 weeks on diet, NOD^{k}-REF chow (n=5) and HFD (n=6) mice. **(A)** Blood glucose levels during course of ipGTT. **(B)** Blood glucose measured at time 0 h (fasting) during ipGTT. **(C)** Blood glucose measured at 2 hours during ipGTT. **(D)** Total Area under the curve (AUC) measured during ipGTT. **(E-H)** ipGTT performed after 20 weeks on diet, NOD^{k} -REF chow (n=8) and HFD (n=9) mice. **(E)** Blood glucose levels during course of ipGTT. **(F)** Blood glucose measured at time 0 h (fasting) during ipGTT. **(G)** Blood glucose measured at 2 hours during ipGTT. **(H)** Total Area under the curve (AUC) measured during ipGTT. Means ± SEM. Student's unpaired t-test: *****$p<0.05$, ******$p<0.01$, *******$p<0.001$ vs chow diet.

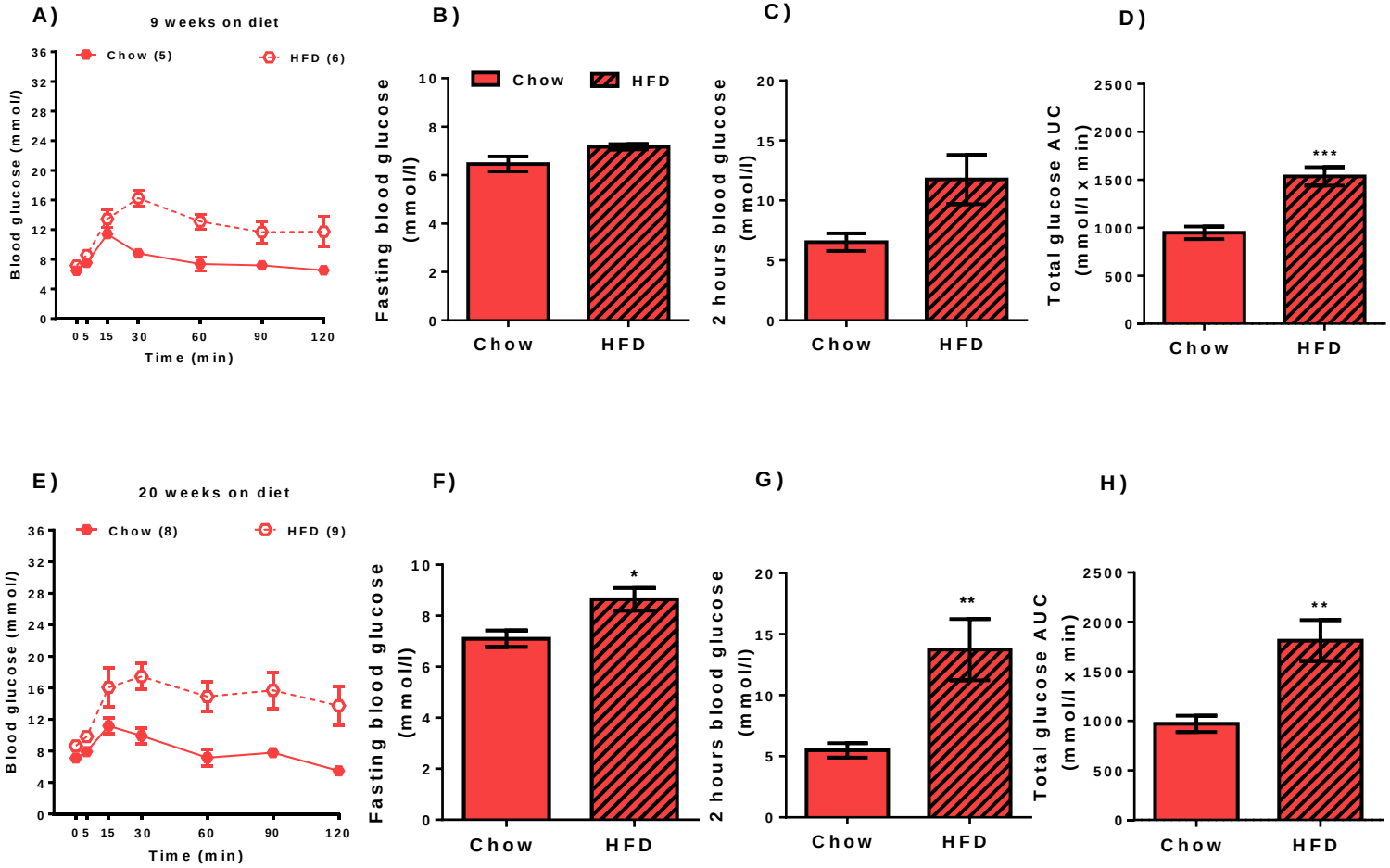
A)
9 weeks on diet
Chow (5)
HFD (6)
Blood glucose (mmol/l)
Time (min)
B)
Fasting blood glucose (mmol/l)
Chow
HFD
C)
2 hours blood glucose (mmol/l)
D)
Total glucose AUC (mmol/l x min)
***
E)
20 weeks on diet
Chow (8)
HFD (9)
F)
*
G)
**
H)
**

6.3.5. ipGTT-plasma insulin results

The results of plasma insulin levels of the ipGTT studies performed in the chow and HF-fed NOD^{k}-REF mice after 9 weeks and 20 weeks on diet, corresponding to the ipGTT glucose (Fig 6.4) are presented in Fig 6.5. The insulin results after 9 weeks on diet are shown in Fig 6.5 A-D. And Fig 6.5E-H, shows plasma insulin results after 20 weeks of diet.

In the chow fed NOD^{k}-REF mice, insulin levels showed a reasonably normal response to the ip glucose, with no obvious change from after 9 weeks on diet to after 20 weeks on diet (Fig 6.5). In response to HF-diet, hyperinsulinemia developed, and the abnormal pattern of insulin response, with a tendency for levels to fall rather than increase at 15 min, was seen at both times (Fig 6.5). The degree of hyperinsulinemia was greater after 20 compared to 9 weeks on the HF-diet.

Figure 6.5: Plasma insulin concentrations during ipGTT after 9 and 20 weeks on diet (from weaning to harvest) in NOD^{k}-REF mice fed chow or high fat diet (HFD). Mice fasted for 4 hours were injected with 2g/kg glucose intraperitoneally at time 0 min. **(A-D)** Plasma insulin measurement after 9 weeks on diet, NOD^{k} -REF chow (n=5) and HFD (n=6) mice. **(A)** Plasma insulin levels during course of ipGTT. **(B)** Plasma insulin measured at time 0 h (fasting) during ipGTT. **(C)** Total Area under the curve (AUC) for plasma insulin measurement during ipGTT. **(D)** Change from basal AUC during ipGTT. **(E-H)** Plasma insulin measurement after 20 weeks on diet, NOD^{k} -REF chow (n=8) and HFD (n=9). **(E)** Plasma insulin levels during course of ipGTT. **(F)** Plasma insulin measured at time 0 h (fasting) during ipGTT. **(G)** Total Area under the curve (AUC) for plasma insulin measurement during ipGTT. **(H)** Change from basal AUC during ipGTT. Means ± SEM. Student's unpaired t-test: *****$p<0.05$, ******$p<0.01$, *******$p<0.001$ vs chow diet.

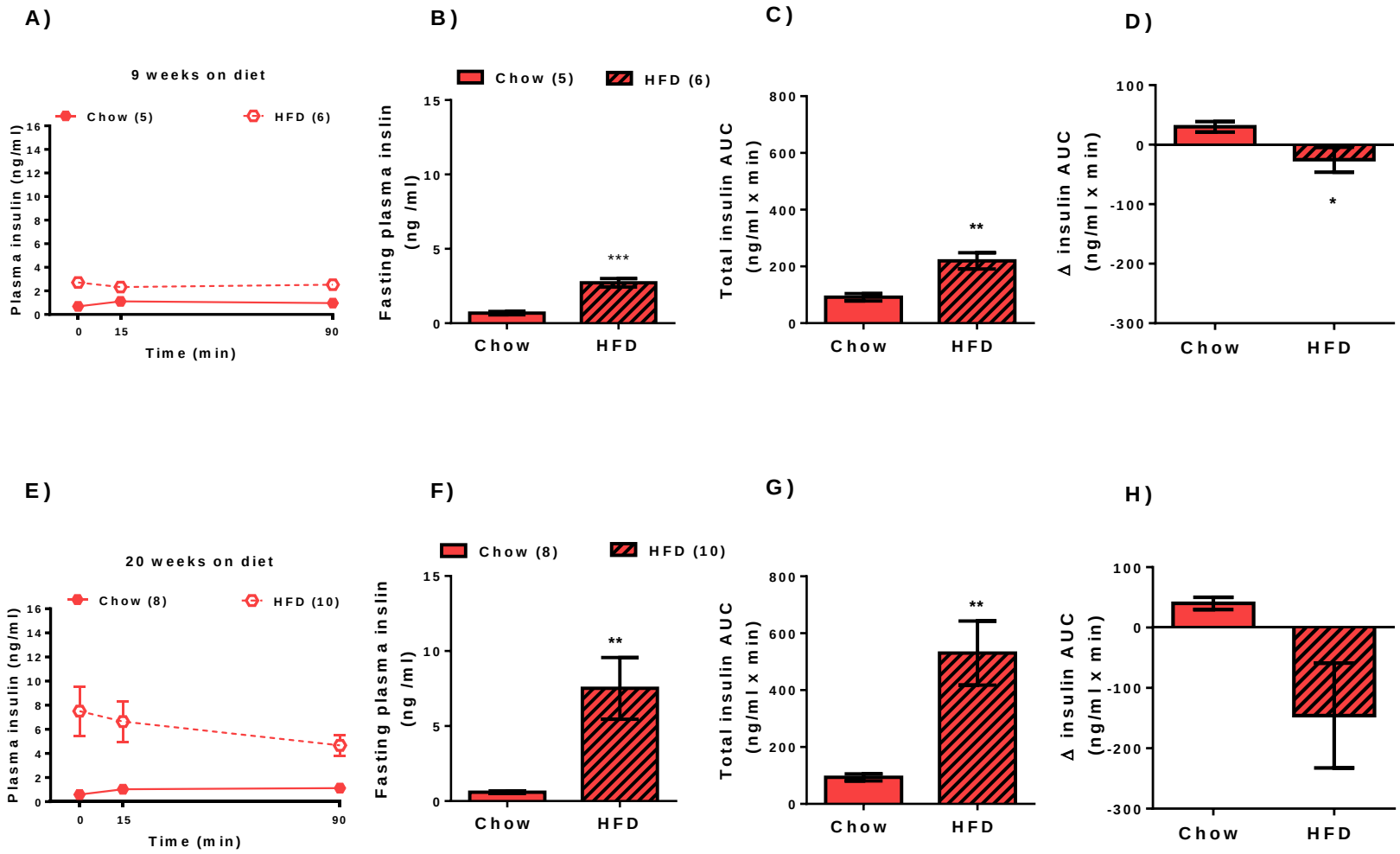
A)
9 weeks on diet
Chow (5)
HFD (6)
Plasma insulin (ng/ml)
Time (min)
B)
Chow (5)
HFD (6)
Fasting plasma inslin (ng /ml)
***
Chow
HFD
C)
Total insulin AUC (ng/ml x min)
**
Chow
HFD
D)
Δ insulin AUC (ng/ml x min)
*
Chow
HFD
E)
20 weeks on diet
Chow (8)
HFD (10)
Plasma insulin (ng/ml)
Time (min)
F)
Chow (8)
HFD (10)
Fasting plasma inslin (ng /ml)
**
Chow
HFD
G)
Total insulin AUC (ng/ml x min)
**
Chow
HFD
H)
Δ insulin AUC (ng/ml x min)
Chow
HFD

6.3.6. Non-fasting insulin measurement

Non-fasting tail blood was collected immediately before anaesthesia for measurement of plasma insulin from chow and HF-fed NOD^{k}-REF after 21 weeks on diet. The non-fasting insulin concentration was significantly elevated in HF-fed NOD^{k}-REF mice from the chow-fed NOD^{k}-REF group (Figure 6.6).

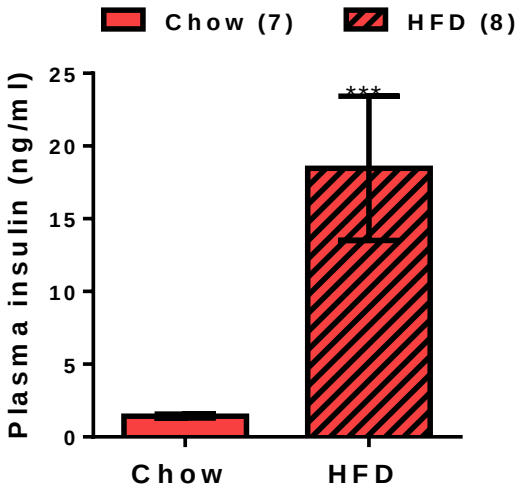

Figure 6.6: Non-fasting plasma insulin concentrations after 21 weeks of diet (from weaning) in NOD^{k}-REF mice fed chow or high fat diet (HFD). Data are Means ± SEM. Student's unpaired t-test: ******p<0.001 vs chow diet.

6.4. Discussion

This experiment was set up to ascertain whether the refreshed NOD^{k} colony (NOD^{k}-REF) had the same metabolic phenotype as the NOD^{k} mice that have been used for the main body of this thesis. The initial plan was for a 10 week dietary study, but this was extended to 20 weeks due to the resistance of the NOD^{k}-REF mice to develop diabetes. The results were remarkable, in that 9 AM non-fasting glucose levels remained normal in the NOD^{k}-REF mice, even after 20 weeks on HF-diet. This is in stark contrast to the HF-NOD^{k} mice that developed a severe diabetes phenotype after 10-20 weeks of HF feeding which resulted in a need for them to be ethically culled.

This unexpected finding is of particular interest, as it raises very interesting hypotheses about what might be happening, and has important implications on the overall conclusions that can be made from the work of this thesis, as is discussed below.

There are also limitations on the interpretation that can be made from the available data from these experiments. Due to the need to complete experiments for this thesis, analyses of plasma lipids, proinsulin and C-peptide have not been completed and pancreas histology has not yet been performed. These results, if available, would have been useful to be able to make a complete comparison between the NOD^{k}-REF and the original NOD^{k} mice. Also, an experimental design in which the NOD^{k} and NOD^{k}-REF mice were studied in parallel would have been much better in order to be able to directly compare the phenotypes.

Nevertheless, the differences between the two NOD^{k} strains are remarkable, one developing a profound type 2 diabetes phenotype and the other obesity and glucose intolerance, but a resistance to diabetes development.

There was a trend for the NOD^{k}-REF mice to be a little smaller at 4-5 weeks of age and perhaps for the weight gain to be less rapid with HF-feeding, but this would need to be confirmed in comparing the two strains at the same time, under exactly the same environmental conditions. However, the NOD^{k}-REF mice did develop HF-diet induced obesity. They also developed HF-diet induced hyperinsulinemia and glucose intolerance, but with an apparent lesser severity after 9 weeks on diet compared to 20 weeks on diet. The degree of hyperinsulinemia in the NOD^{k}-REF after 20 weeks on HF-diet was similar to that of the NOD^{k} mice after only 10 weeks on HF-diet, but the NOD^{k} mice had significant fasting hyperglycaemia after only 10 weeks on diet, as opposed to a very minimal increase in the NOD^{k}-REF mice after twice as long on HF-diet.

Thus, the major difference between the two strains is that the NOD^{k} mice of Chapter 3, 4 and 5 are prone to develop diabetes and the NOD^{k}-REF mice of this chapter are diabetes resistant, at least up to 20 weeks after starting HF feeding from weaning age.

Recently, environmental factors have been shown to be particularly important in determining the metabolic characteristics of mice, with interactions being present between mice genetic background, diet and the gut microbiome (Ussar et al., 2015, Perry et al., 2016). Differences in the gut microbiome between the strains is possible because of a different history of environments, but the environment including diets of the NOD^{k} and NOD^{k}-REF mice should have been the same through the respective time course studies (same animal facility, same diets), however, the experiments were performed at different times of about a year apart (this study and the long-term study).

We are more in favour of there being a genetic difference between the two mouse strains, as genetic drift is known to occur in NOD mice (Simecek et al., 2015). The original NOD mice strains from Japan were dispensed to various laboratories around

the world in the 1980s. The NOD^{k} used in this study were originally from a gift of the Wicker laboratory from mice received by Taconic Laboratories. Taconic received their strain from Japan in 1985 (Podolin et al., 1993). The NOD.ShiLtJArc mice used to refresh our NOD^{k} colony creating the NOD^{k}-REF mice originate from a NOD substrain sent to the Joslin Diabetes Centre in 1984 and from there set up at Jackson Laboratories from where ARC obtain their NOD mice (Laboratory, 2014).

The question arises as to what implications these findings have on the original hypothesis and objectives of this thesis. If for example a mutation has come into the NOD^{k} mice, that is not present in the NOD^{k}-REF mice, then this additional mutation is not required by NOD mice for type 1 diabetes pathogenesis, as NOD.ShiLtJArc (which will not have this mutation) do develop type 1 diabetes. However, it was apparent in NOD^{k}-REF mice, which they do have abnormal glucose tolerance on HF-feeding and the insulin responses of these mice to ip glucose is not normal. It could be that there is an important islet β-cell non-immune susceptibility factor in both strains of NOD^{k} mice, but that both (± others) susceptibility factors interact to cause a more profound islet β-cell phenotype.

The interpretation of the results of the published NOD^{k}.insHEL study also needs to be interpreted in the light of the findings of the NOD^{k} and NOD^{k}-REF findings of this thesis for the same reasons (Dooley et al., 2016), as a specific genetic defect in the NOD^{k} background of the T2D diabetes prone NOD^{k}.insHEL mice, may not be present in the they NOD .

Chapter # 7: Final discussion and Future Directions

7.1. Final discussion

The majority of research into preventing type 1 diabetes is focused on modulating immunological aspects of the disease. The main hypothesis of this thesis underlying the objectives, however, was that non-immune β-cell susceptibility factors contribute to the initiation of islet β-cell damage, followed by immune attack, in the pathogenesis of type 1 diabetes in NOD mice. If correct, the importance would be that alternative or "adjuvant" non-immunological approaches to type 1 diabetes prevention could also be developed.

The main research tool used to explore the main aim was the NOD^{k} mouse model, which is congenic for *H2*^{k}, a low risk MHC allele for type 1 diabetes. On a chow diet, NOD^{k} mice have excellent glucose tolerance and clearly are resistant to the development of insulitis and type 1 diabetes, as has previously been reported and was confirmed in experiments within this thesis (Podolin et al., 1993, Dooley et al., 2016). This on its own would suggest that islet β-cells of NOD^{k} are completely normal within non-immune diabetes susceptibility factors. However, this is not the case as stressing their islet β-cells by (i) overexpressing the HEL gene specifically in the β-cells (from previous work from our laboratory) or (ii) by feeding the mice a HF-diet does induce diabetes, at least in males, with clear evidence of β-cell failure (Dooley et al., 2016). In the study of HEL overexpression, the potential role for islet autoimmune attack as the cause of the diabetes within male NOD^{k}.insHEL mice was excluded through extensive experimentation, including experiments with immune-incompetent mice (Dooley et al., 2016). The histological experiments in this thesis are also supportive of this conclusion, however, the presence of some peri-islet inflammatory collections in HF-fed NOD^{k} does not permit a strong conclusion with respect to absence of autoimmune attack as

was possible from the previous work (Dooley et al., 2016). Thus, taken together, the previous work on male NOD^{k}.insHEL mice and the current work on male HF-fed NOD^{k} mice are supportive of the hypothesis.

The most striking feature of diabetic male HF-fed NOD^{k} mice was how well they resemble the phenotype of human type 2 diabetes (DeFronzo, 2009, Nolan et al., 2011). These mice developed diet-induced obesity, profound hyperinsulinemia, dyslipidemia and became frankly diabetic. Thus, this mouse model is closely related to the NOD mouse model of type 1 diabetes, with just a change in its MHC such that it is resistant to autoimmune islet attack, develops type 2 diabetes when challenged with a poor diet. Thus, this work is also supportive of the hypothesis of there being overlap in islet β-cell susceptibility to type 1 and type 2 diabetes (Nolan and Delghingaro-Augusto, 2014, Tuomi et al., 2014).

The studies of the NOD^{k}-REF strain of mice, however, showed a very different phenotype with HF-feeding. These mice were resistant to the development of diabetes, even though they had many of the same features of the NOD^{k} mice. The NOD^{k}-REF mice did develop diet-induced obesity, hyperinsulinemia and at least moderately severe glucose intolerance, albeit, not to the same degree and as quickly as the NOD^{k} mice. The pattern of insulin response to intraperitoneal glucose in male HF-fed NOD^{k}-REF mice was very similar to that of the NOD^{k} mice consistent with an abnormal response of islet β-cells. The major difference between NOD^{k} mice and NOD^{k}-REF mice was that, with HF-feeding, the latter maintain perfectly normal fed-state blood glucose levels out to 24 weeks of age (i.e. after 20 weeks of HF-feeding).

This hints that the NOD^{k} mice have at least one additional diabetes susceptibility factor compared to NOD^{k}-REF mice. Obviously, this creates an opportunity to explore this extra factor through further experiments, but it also clouds the interpretation of the main

objective of the thesis. Considering that NOD.ShiLtJArc, that were used to refresh our NOD^k mice, do develop type 1 diabetes, then the additional susceptibility factor in NOD^k mice cannot be necessary for type 1 diabetes development. This also illustrates the challenges in interpreting results from murine models of diabetes due to the marked interactions between genome and environment, with an indication that the gut microbiome in particular is a significant component in these interactions (Ussar et al., 2015). Also, the pathophysiology of all forms of diabetes, other than the infrequent monogenic forms, is invariably a consequence of the interaction of multiple genetic risk factors (Tuomi et al., 2014). It is certainly possible that in NOD^k mice, there are multiple non-immune islet β-cell susceptibility factors, and that one additional factor (or other environmental factor) interacts making this particular mouse more susceptible to β-cell failure.

The histological analyses of the NOD^k mice provide some clues to why diabetes develops. As in the NOD^k.insHEL studies in which increased β-cell apoptosis was seen, the HF-fed NOD^k mice had evidence of islet endocrine cell apoptosis (Dooley et al., 2016). This was seen on the H&E sections, such that it is not proven that it was in β-cells, however, the reduction in islet β-cell mass seen in the insulin immuno-stained sections of the HF-fed NOD^k mice pancreases from the long-term study is consistent with it being β-cell apoptosis. Further investigation of the apoptosis with immuno-staining for activated caspase-3 is planned. The mechanisms underlying this increased likelihood of β-cell apoptosis in NOD^k mice is of importance, but was beyond the scope of this thesis.

The results of the $B10^k$ mice were also much unexpected, but extremely interesting. They had very poor glucose tolerance, even on chow diet. For this reason we included Balb/c mice in the work of the thesis, as a more normal comparator strain. The $B10^k$

mice developed much worse glucose tolerance when stressed with the HF-diet, but the remarkable finding was they did not develop diabetes as determined by the 9 AM fasting blood glucose level. As glucose tolerance was so severe after 10 weeks of HF-feeding, the long-term study was performed to determine if they would be still non-diabetic after 20 weeks of HF-feeding. The results were the same, the $B10^k$ mice have poor glucose tolerance, but are very diabetes resistant. The $B10^k$ mice did not seem to have a reduction in β-cell mass, but they failed to secrete insulin well. In fact, they showed a minimal compensatory response to HF-feeding. It is almost as if this poor β-cell response is protective of the mice developing complete islet β-cell failure. It is reasonable to conclude that this strain is a insulin hypo-secreting strain compared to the NOD^k mice which insulin hyper-secrete. The islet β-cell has been described as being fuel responsive and vulnerable (Nolan and Prentki, 2008). As the islet β-cells of the $B10^k$ mice are poorly fuel responsive, they may be less vulnerable. There has been much interest in the hypothesis that insulin hyper-secretion is a risk factor for islet β-cell failure (Andrikopoulos, 2010). The $B10^k$ mouse could be used in future to further evaluate this hypothesis.

Another peculiarity of the $B10^k$ mice, was their propensity to develop fasting hyperglycaemia (as on the day of the ipGTT), when fed-state glycaemia was normal. This could have been due to different effects of stress or perhaps an effect on the insulin/glucagon ratio.

The Balb/c mice were remarkable in their maintenance of normal glucose tolerance even after 20 weeks of HF-feeding. In comparing the three mice strains, it is of interest to see the differences in sites of fat accumulation. The Balb/c mice were less likely to accumulate subcutaneous fat, but avidly developed intra-pancreatic fat deposits. There has been recent interest in the potential pathogenic effects of intra-pancreatic fat, but

these results suggest that it could be much more benign (van der Zijl et al., 2010, Chen et al., 2015, Heni et al., 2010, Della Corte et al., 2015). The reason Balb/c mice are diabetes resistant compared to many other mouse strains is also of interest and warrants further research.

7.2. Limitations

The completed work of thesis includes detailed physiological phenotyping of the three strains of mice on chow and high fat diet. With respect to determining mechanisms between the strains, we did demonstrate differences in pancreatic islet histological features and β-cell mass. Of particular interest was the increased rates of islet endocrine cell apoptosis in HF-fed NOD^k mice. Unfortunately, due to lack of time, mechanistic experiments on isolated pancreatic islets, that were originally planned, could not be performed. The experiments we did plan are included in the future directions section.

In the physiological studies, some limitations in interpretation come from the ipGTT and ipITT assessments that were performed. The ipGTT, as compared to the oGTT, does not assess the effects of the incretin hormone system on glucose-stimulated insulin secretion. Furthermore, we did not measure incretin hormones due to an inability to sample more blood volume. An advantage of the ipGTT, however, was consistency in testing compared to variable glucose absorption rates and animal stress with the oGTT. The intravenous GTT would also provide additional information of islet β-cell function. Also the hyperinsulinemia euglycaemic clamp, if performed, would have given a more gold standard assessment of insulin sensitivity. Again, this test was not performed because of the technical challenges associated with this test and the large number of experimental groups.

One of the unexpected findings was the very abnormal glucose tolerance of the $B10^k$ mice, but their resistance to the development of diabetes, as determined by the morning

fed glucose. We hypothesize that this is due to resistance of the β-cells to failure. We would have liked to age these mice further to determine if they do eventually develop diabetes.

7.3. Future directions

There is more work to be performed to determine the mechanisms of the findings of this thesis. Islets were harvested for the assessment of islet gene expression at the mRNA level, including genes of islet differentiation, islet function, endoplasmic reticulum stress, mitochondrial stress and inflammation. This work needs to be completed. The dual immunohistochemistry for insulin and activated caspase-3 needs to be performed. The pancreases of the NOD^{k}-REF need to be assessed histologically to determine if the difference between this strain and the NOD^{k} is on islet β-cell mass.

All the insulin secretion data of this thesis is from *in vivo* experiments using the ipGTT. It is important that the differences in insulin secretion of the three strains is investigated in freshly isolated islets *in vitro.* Particular interest will need to focus on whether the islet β-cell of the NOD^{k} mice are hyper-secretors as opposed to the B10^{k} mice being hypo-secretors. At which part of the nutrient sensing, insulin secretion coupling processes and insulin exocytosis pathways of β-cell function will need to be explored.

The very unexpected finding of the B10^{k} resistance to diabetes development is of particular interest. If the reason for this resistance can be determined, this may lead to quite novel approaches to the prevention of type 2 diabetes in particular.

The NOD^{k}-REF findings were also very unexpected. This provides a real opportunity to determine what must be a very strong diabetogenic factor in NOD^{k} mice. It is likely to be related to an increased propensity for β-cell apoptosis. As the genetic background of NOD^{k}-REF and NOD^{k} should be fairly similar, an approach to determine the potential

genetic factor causing this difference should not be too difficult with modern gene sequencing approaches.

Finally, the work of this thesis is supportive of the NOD^{k} mice having perhaps multiple non-immune susceptibility factors. This is really exciting for future research into type 1 diabetes, as combining therapies to modulate immunological and non-immunological factors for diabetes prevention are clearly possible. More focus on the non-immune mechanisms of β-cell susceptibility in mouse models and importantly also in humans is a very worthy direction for future research.

8.0. References

ANDRIKOPOULOS, S. 2010. Obesity and Type 2 diabetes: Slow down!—Can metabolic deceleration protect the islet beta cell from excess nutrient-induced damage? *Molecular and cellular endocrinology,* 316**,** 140-146.

ASHCROFT, F. M., HARRISON, D. E. & ASHCROFT, S. J. 1984. Glucose induces closure of single potassium channels in isolated rat pancreatic β-cells. *Nature,* 312**,** 446-448.

ASSAL, J. & GROOP, L. 1999. Definition, diagnosis and classification of diabetes mellitus and its complications.

ASTON-MOURNEY, K., WONG, N., KEBEDE, M., ZRAIKA, S., BALMER, L., MCMAHON, J., FAM, B., FAVALORO, J., PROIETTO, J. & MORAHAN, G. 2007. Increased nicotinamide nucleotide transhydrogenase levels predispose to insulin hypersecretion in a mouse strain susceptible to diabetes. *Diabetologia,* 50**,** 2476-2485.

ATKINSON, M. A. & EISENBARTH, G. S. 2001. Type 1 diabetes: new perspectives on disease pathogenesis and treatment. *The Lancet,* 358**,** 221-229.

BACH, J.-F. 1994. Insulin-dependent diabetes mellitus as an autoimmune disease. *Endocrine reviews,* 15**,** 516-542.

BACHMANOV, A. A., REED, D. R., BEAUCHAMP, G. K. & TORDOFF, M. G. 2002. Food intake, water intake, and drinking spout side preference of 28 mouse strains. *Behavior genetics,* 32**,** 435-443.

BARR, E., MAGLIANO, D., ZIMMET, P., POLKINGHORNE, K., ATKINS, R., DUNSTAN, D., MURRAY, S. & SHAW, J. 2006. The Australian Diabetes, Obesity and Lifestyle Study: tracking the accelerating epidemic: its causes and outcomes. *Melbourne: International Diabetes Institute*.

BASU, R., CHANDRAMOULI, V., DICKE, B., LANDAU, B. & RIZZA, R. 2005. Obesity and type 2 diabetes impair insulin-induced suppression of glycogenolysis as well as gluconeogenesis. *Diabetes,* 54**,** 1942-1948.

BELL, G. I. & POLONSKY, K. S. 2001. Diabetes mellitus and genetically programmed defects in β-cell function. *Nature,* 414**,** 788-791.

BERGLUND, M. M., HIPSKIND, P. A. & GEHLERT, D. R. 2003. Recent developments in our understanding of the physiological role of PP-fold peptide receptor subtypes. *Experimental Biology and Medicine,* 228**,** 217-244.

BERTRAMS, J. & BAUR, M. 1985. Insulin-dependent diabetes mellitus. *Histocompatibility testing 1984.* Springer.

BILLINGS, L. K. & FLOREZ, J. C. 2010. The genetics of type 2 diabetes: what have we learned from GWAS? *Annals of the New York Academy of Sciences,* 1212**,** 59-77.

BJÖRNHOLM, M., HE, A., ATTERSAND, A., LAKE, S., LIU, S., LIENHARD, G., TAYLOR, S., ARNER, P. & ZIERATH, J. 2002. Absence of functional insulin receptor substrate-3 (IRS-3) gene in humans. *Diabetologia,* 45**,** 1697-1702.

BODEN, G. 2008. Obesity and free fatty acids. *Endocrinology and metabolism clinics of North America,* 37**,** 635-646.

BONNER-WEIR, S. 2000. Islet growth and development in the adult. *Journal of molecular endocrinology,* 24**,** 297-302.

BONORA, E., ZAVARONI, I., COSCELLI, C. & BUTTURINI, U. 1983. Decreased hepatic insulin extraction in subjects with mild glucose intolerance. *Metabolism,* 32**,** 438-446.

BOUWENS, L. & ROOMAN, I. 2005. Regulation of pancreatic beta-cell mass. *Physiological reviews,* 85**,** 1255-1270.

BOWE, J. E., FRANKLIN, Z. J., HAUGE-EVANS, A. C., KING, A. J., PERSAUD, S. J. & JONES, P. M. 2014. Metabolic phenotyping guidelines: assessing glucose homeostasis in rodent models. *Journal of Endocrinology,* 222**,** G13-G25.

BRISSOVA, M., FOWLER, M. J., NICHOLSON, W. E., CHU, A., HIRSHBERG, B., HARLAN, D. M. & POWERS, A. C. 2005. Assessment of human pancreatic islet architecture and composition by laser scanning confocal microscopy. *Journal of Histochemistry & Cytochemistry,* 53**,** 1087-1097.

BURKS, D. J. & WHITE, M. F. 2001. IRS proteins and beta-cell function. *Diabetes,* 50**,** S140.

BURN, P. 2010. Type 1 diabetes. *Nature Reviews Drug Discovery,* 9**,** 187-188.
BUSCH, C. & HEGELE, R. 2001. Genetic determinants of type 2 diabetes mellitus. *Clinical genetics,* 60**,** 243-254.
BUTEAU, J., SHLIEN, A., FOISY, S. & ACCILI, D. 2007. Metabolic diapause in pancreatic β-cells expressing a gain-of-function mutant of the forkhead protein Foxo1. *Journal of Biological Chemistry,* 282**,** 287-293.
BUTLER, A. E., JANSON, J., BONNER-WEIR, S., RITZEL, R., RIZZA, R. A. & BUTLER, P. C. 2003. β-cell deficit and increased β-cell apoptosis in humans with type 2 diabetes. *Diabetes,* 52**,** 102-110.
CARDINAL, J. W., ALLAN, D. J. & CAMERON, D. P. 1998. Differential metabolite accumulation may be the cause of strain differences in sensitivity to streptozotocin-induced β cell death in inbred mice. *Endocrinology,* 139**,** 2885-2891.
CATANZARO, R., CUFFARI, B., ITALIA, A. & MAROTTA, F. 2016. Exploring the metabolic syndrome: Nonalcoholic fatty pancreas disease. *World Journal of Gastroenterology,* 22**,** 7660.
CHEN, D., LIESS, C., POLJAK, A., XU, A., ZHANG, J., THOMA, C., TRENELL, M., MILNER, B., JENKINS, A. & CHISHOLM, D. 2015. Phenotypic characterization of insulin-resistant and insulin-sensitive obesity. *The Journal of Clinical Endocrinology & Metabolism,* 100**,** 4082-4091.
CLEE, S. M. & ATTIE, A. D. 2007. The genetic landscape of type 2 diabetes in mice. *Endocrine reviews,* 28**,** 48-83.
CNOP, M., ABDULKARIM, B., BOTTU, G., CUNHA, D. A., IGOILLO-ESTEVE, M., MASINI, M., TURATSINZE, J.-V., GRIEBEL, T., VILLATE, O. & SANTIN, I. 2013. RNA-sequencing identifies dysregulation of the human pancreatic islet transcriptome by the saturated fatty acid palmitate. *Diabetes***,** DB_131383.
CNOP, M., WELSH, N., JONAS, J.-C., JÖRNS, A., LENZEN, S. & EIZIRIK, D. L. 2005. Mechanisms of pancreatic β-cell death in type 1 and type 2 diabetes many differences, few similarities. *Diabetes,* 54**,** S97-S107.
COLAGIURI, R., COLAGIURI, S., YACH, D. & PRAMMING, S. 2006. The answer to diabetes prevention: science, surgery, service delivery, or social policy? *American journal of public health,* 96**,** 1562-1569.
COOPER, G., WILLIS, A., CLARK, A., TURNER, R., SIM, R. & REID, K. 1987. Purification and characterization of a peptide from amyloid-rich pancreases of type 2 diabetic patients. *Proceedings of the National Academy of Sciences,* 84**,** 8628-8632.
DEFRONZO, R. A. 1997. Pathogenesis of type 2 diabetes: metabolic and molecular implications for identifying diabetes genes.
DEFRONZO, R. A. 1999. Pharmacologic therapy for type 2 diabetes mellitus. *Annals of internal medicine,* 131**,** 281-303.
DEFRONZO, R. A. 2009. From the triumvirate to the ominous octet: a new paradigm for the treatment of type 2 diabetes mellitus. *Diabetes,* 58**,** 773-795.
DEFRONZO, R. A. & FERRANNINI, E. 1991. Insulin resistance: a multifaceted syndrome responsible for NIDDM, obesity, hypertension, dyslipidemia, and atherosclerotic cardiovascular disease. *Diabetes care,* 14**,** 173-194.
DELLA CORTE, C., MOSCA, A., MAJO, F., LUCIDI, V., PANERA, N., GIGLIONI, E., MONTI, L., STRONATI, L., ALISI, A. & NOBILI, V. 2015. Nonalcoholic fatty pancreas disease and Nonalcoholic fatty liver disease: more than ectopic fat. *Clinical endocrinology,* 83**,** 656-662.
DELOVITCH, T. L. & SINGH, B. 1997. The nonobese diabetic mouse as a model of autoimmune diabetes: immune dysregulation gets the NOD. *Immunity,* 7**,** 727-738.
DESNICK, R. J. 1973. α - Galactosidase A. *Encyclopedia Of Molecular Medicine*.
DONATH, M. Y., DALMAS, É., SAUTER, N. S. & BÖNI-SCHNETZLER, M. 2013. Inflammation in obesity and diabetes: islet dysfunction and therapeutic opportunity. *Cell metabolism,* 17**,** 860-872.
DOOLEY, J., TIAN, L., SCHONEFELDT, S., DELGHINGARO-AUGUSTO, V., GARCIA-PEREZ, J. E., PASCIUTO, E., DI MARINO, D., CARR, E. J., OSKOLKOV, N. & LYSSENKO, V. 2016.

Genetic predisposition for beta cell fragility underlies type 1 and type 2 diabetes. *Nature genetics*.
DUCKWORTH, W. C., BENNETT, R. G. & HAMEL, F. G. 1998. Insulin degradation: progress and potential 1. *Endocrine reviews,* 19**,** 608-624.
EDSTRÖM, K., CERASI, E. & LUFT, R. 1974. Insulin response to glucose infusion during pregnancy. A prospective study of high and low insulin responders with normal carbohydrate tolerance. *Acta endocrinologica,* 75**,** 87-104.
EGEA, P. F., STROUD, R. M. & WALTER, P. 2005. Targeting proteins to membranes: structure of the signal recognition particle. *Current opinion in structural biology,* 15**,** 213-220.
EIZIRIK, D. L., SAMMETH, M., BOUCKENOOGHE, T., BOTTU, G., SISINO, G., IGOILLO-ESTEVE, M., ORTIS, F., SANTIN, I., COLLI, M. L. & BARTHSON, J. 2012. The human pancreatic islet transcriptome: expression of candidate genes for type 1 diabetes and the impact of pro-inflammatory cytokines. *PLoS Genet,* 8**,** e1002552.
EL-ASSAAD, W., BUTEAU, J., PEYOT, M.-L., NOLAN, C., RODUIT, R., HARDY, S., JOLY, E., DBAIBO, G., ROSENBERG, L. & PRENTKI, M. 2003. Saturated fatty acids synergize with elevated glucose to cause pancreatic β-cell death. *Endocrinology,* 144**,** 4154-4163.
ELBEIN, S. C., HOFFMAN, M. D., TENG, K., LEPPERT, M. F. & HASSTEDT, S. J. 1999. A genome-wide search for type 2 diabetes susceptibility genes in Utah Caucasians. *Diabetes,* 48**,** 1175-1182.
ELKON, K. B. 2006a. *Apoptosis and its relevance to autoimmunity*, S Karger Ag.
ELKON, K. B. 2006b. *Apoptosis and Its Relevance to Autoimmunity: 2 Tables*, Karger Publishers.
ELLEMAN, T., FRENKEL, M., HOYNE, P., MCKERN, N., COSGROVE, L., HEWISH, D., JACHNO, K., BENTLEY, J., SANKOVICH, S. & WARD, C. 2000. Mutational analysis of the N-linked glycosylation sites of the human insulin receptor. *Biochem. J,* 347**,** 771-779.
EPSTEIN, F. H., ATKINSON, M. A. & MACLAREN, N. K. 1994. The pathogenesis of insulin-dependent diabetes mellitus. *New England Journal of Medicine,* 331**,** 1428-1436.
ERIKSSON, K.-F. & LINDGÄRDE, F. 1991. Prevention of Type 2 (non-insulin-dependent) diabetes mellitus by diet and physical exercise The 6-year Malmö feasibility study. *Diabetologia,* 34**,** 891-898.
FABER, O. K., KEHLET, H., MADSBAD, S. & BINDER, C. 1978. Kinetics of human C-peptide in man. *Diabetes,* 27**,** 207-209.
FAJANS, S. S., BELL, G. I. & POLONSKY, K. S. 2001. Molecular mechanisms and clinical pathophysiology of maturity-onset diabetes of the young. *New England Journal of Medicine,* 345**,** 971-980.
FANTL, W. J., JOHNSON, D. E. & WILLIAMS, L. T. 1993. Signalling by receptor tyrosine kinases. *Annual review of biochemistry,* 62**,** 453-481.
FEARNSIDE, J. F., DUMAS, M.-E., ROTHWELL, A. R., WILDER, S. P., CLOAREC, O., TOYE, A., BLANCHER, C., HOLMES, E., TATOUD, R. & BARTON, R. H. 2008. Phylometabonomic patterns of adaptation to high fat diet feeding in inbred mice. *PLoS One,* 3**,** e1668.
FERRANNINI, E. & MARI, A. 2004. Beta cell function and its relation to insulin action in humans: a critical appraisal. *Diabetologia,* 47**,** 943-956.
FINEGOOD, D. T., SCAGLIA, L. & BONNER-WEIR, S. 1995. Dynamics of β-cell mass in the growing rat pancreas: estimation with a simple mathematical model. *Diabetes,* 44**,** 249-256.
FROGUEL, P., ZOUALI, H., VIONNET, N., VELHO, G., VAXILLAIRE, M., SUN, F., LESAGE, S., STOFFEL, M., TAKEDA, J. & PASSA, P. 1993. Familial hyperglycemia due to mutations in glucokinase--definition of a subtype of diabetes mellitus. *New England Journal of Medicine,* 328**,** 697-702.
FU, Z., GILBERT, E. R. & LIU, D. 2013. Regulation of insulin synthesis and secretion and pancreatic Beta-cell dysfunction in diabetes. *Current diabetes reviews,* 9**,** 25.
GAPP, D., LEITER, E., COLEMAN, D. & SCHWIZER, R. 1983. Temporal changes in pancreatic islet composition in C57BL/6J-db/db (diabetes) mice. *Diabetologia,* 25**,** 439-443.

GIDH-JAIN, M., TAKEDA, J., XU, L., LANGE, A., VIONNET, N., STOFFEL, M., FROGUEL, P., VELHO, G., SUN, F. & COHEN, D. 1993. Glucokinase mutations associated with non-insulin-dependent (type 2) diabetes mellitus have decreased enzymatic activity: implications for structure/function relationships. *Proceedings of the National Academy of Sciences,* 90**,** 1932-1936.

HANIS, C., BOERWINKLE, E., CHAKRABORTY, R., ELLSWORTH, D., CONCANNON, P., STIRLING, B., MORRISON, V., WAPELHORST, B., SPIELMAN, R. & GOGOLIN-EWENS, K. 1996. A genome–wide search for human non–insulin–dependent (type 2) diabetes genes reveals a major susceptibility locus on chromosome 2. *Nature genetics,* 13**,** 161-166.

HANSON, R. L., EHM, M. G., PETTITT, D. J., PROCHAZKA, M., THOMPSON, D. B., TIMBERLAKE, D., FOROUD, T., KOBES, S., BAIER, L. & BURNS, D. K. 1998. An autosomal genomic scan for loci linked to type II diabetes mellitus and body-mass index in Pima Indians. *The American Journal of Human Genetics,* 63**,** 1130-1138.

HATTERSLEY, A. T. & PATEL, K. A. 2017. Precision diabetes: learning from monogenic diabetes. *Diabetologia***,** 1-9.

HATTORI, M., BUSE, J. B., JACKSON, R., GLIMCHER, L., DORF, M., MINAMI, M., MAKINO, S., MORIWAKI, K., KUZUYA, H. & IMURA, H. E. A. 1986. The NOD mouse: recessive diabetogenic gene in the major histocompatibility complex. *Science,* 231**,** 733-735.

HAUGE-EVANS, A. C., KING, A. J., CARMIGNAC, D., RICHARDSON, C. C., ROBINSON, I. C., LOW, M. J., CHRISTIE, M. R., PERSAUD, S. J. & JONES, P. M. 2009. Somatostatin secreted by islet δ-cells fulfills multiple roles as a paracrine regulator of islet function. *Diabetes,* 58**,** 403-411.

HENI, M., MACHANN, J., STAIGER, H., SCHWENZER, N. F., PETER, A., SCHICK, F., CLAUSSEN, C. D., STEFAN, N., HÄRING, H. U. & FRITSCHE, A. 2010. Pancreatic fat is negatively associated with insulin secretion in individuals with impaired fasting glucose and/or impaired glucose tolerance: a nuclear magnetic resonance study. *Diabetes/metabolism research and reviews,* 26**,** 200-205.

HENQUIN, J.-C., RAVIER, M., NENQUIN, M., JONAS, J.-C. & GILON, P. 2003. Hierarchy of the β‐cell signals controlling insulin secretion. *European journal of clinical investigation,* 33**,** 742-750.

HIGHAM, C. E., HULL, R. L., LAWRIE, L., SHENNAN, K. I., MORRIS, J. F., BIRCH, N. P., DOCHERTY, K. & CLARK, A. 2000. Processing of synthetic pro‐islet amyloid polypeptide (proIAPP) ‘amylin’by recombinant prohormone convertase enzymes, PC2 and PC3, in vitro. *European Journal of Biochemistry,* 267**,** 4998-5004.

HOEHN, K. L., HOHNEN-BEHRENS, C., CEDERBERG, A., WU, L. E., TURNER, N., YUASA, T., EBINA, Y. & JAMES, D. E. 2008. IRS1-independent defects define major nodes of insulin resistance. *Cell metabolism,* 7**,** 421-433.

HORIKAWA, Y., ODA, N., COX, N. J., LI, X., ORHO-MELANDER, M., HARA, M., HINOKIO, Y., LINDNER, T. H., MASHIMA, H. & SCHWARZ, P. E. 2000. Genetic variation in the gene encoding calpain-10 is associated with type 2 diabetes mellitus. *Nature genetics,* 26**,** 163-175.

HRUBAN, R., PITMAN, M. & KLIMSTRA, D. 2007. AFIP atlas of tumor pathology, fourth series, fascicle 6: tumors of the pancreas. *American Registry of Pathology, Washington, DC in collaboration with the Armed Forces Institute of Pathology, Washington, DC*.

HU, F. B., MANSON, J. E., STAMPFER, M. J., COLDITZ, G., LIU, S., SOLOMON, C. G. & WILLETT, W. C. 2001. Diet, lifestyle, and the risk of type 2 diabetes mellitus in women. *New England Journal of Medicine,* 345**,** 790-797.

JACKSON, L. 1988; April. H-2 Haplotypes of Mice from Jackson Laboratory Production Colonies. . *JAX® Mice database*.

JACKSON, L. 2006. NON/ShiLtJ males: a new model of diet-induced obesity and diabesity. JAX Notes online: The Jackson Laboratory, News and Insights.

JAMES, D. E., BROWN, R., NAVARRO, J. & PILCH, P. F. 1988. Insulin-regulatable tissues express a unique insulin-sensitive glucose transport protein.

JEFFERY, N. & HARRIES, L. W. 2016. Beta cell differentiation status in type 2 diabetes. *Diabetes, Obesity and Metabolism*.
JENKINS, A. & CAMPBELL, L. 2004. The genetics and pathophysiology of diabetes mellitus type II. *Journal of inherited metabolic disease,* 27**,** 331-347.
JENSEN, M. V., JOSEPH, J. W., RONNEBAUM, S. M., BURGESS, S. C., SHERRY, A. D. & NEWGARD, C. B. 2008. Metabolic cycling in control of glucose-stimulated insulin secretion. *American Journal of Physiology-Endocrinology and Metabolism,* 295**,** E1287-E1297.
KAHN, C. R. 1994. Insulin action, diabetogenes, and the cause of type II diabetes. *Diabetes,* 43**,** 1066-1085.
KAY, T., CHAPLIN, H., PARKER, J., STEPHENS, L. & THOMAS, H. 1997. CD4+ and CD8+ T lymphocytes: clarification of their pathogenic roles in diabetes in the NOD mouse. *Research in immunology,* 148**,** 320-327.
KLEIN, J., JURETIĆ, A., BAXEVANIS, C. N. & NAGY, Z. A. 1981. The traditional and a new version of the mouse H–2 complex.
KLÖPPEL, G., LÖHR, M., HABICH, K., OBERHOLZER, M. & HEITZ, P. 1985. Islet pathology and the pathogenesis of type 1 and type 2 diabetes mellitus revisited. *Pathology and Immunopathology Research,* 4**,** 110-125.
KNOWLER ET AL. 2002. Reduction in the incidence of type 2 diabetes with lifestyle intervention or metformin. *The New England journal of medicine,* 346**,** 393.
KRUSZYNSKA, Y. T. & OLEFSKY, J. M. 1996. Cellular and molecular mechanisms of non-insulin dependent diabetes mellitus. *Journal of investigative medicine,* 44**,** 413-428.
LABORATORY, T. J. 2014. Mouse Strain Datasheet 001976. 05-AUG-14 ed. https://www.jax.org/strain/001976: The Jackson Laboratory.
LAVAN, B. E., LANE, W. S. & LIENHARD, G. E. 1997. The 60-kDa phosphotyrosine protein in insulin-treated adipocytes is a new member of the insulin receptor substrate family. *Journal of Biological Chemistry,* 272**,** 11439-11443.
LEE, Y., HIROSE, H., OHNEDA, M., JOHNSON, J., MCGARRY, J. D. & UNGER, R. H. 1994. Beta-cell lipotoxicity in the pathogenesis of non-insulin-dependent diabetes mellitus of obese rats: impairment in adipocyte-beta-cell relationships. *Proceedings of the National Academy of Sciences,* 91**,** 10878-10882.
LEITER, A., MONTMINY, M., JAMIESON, E. & GOODMAN, R. 1985. Exons of the human pancreatic polypeptide gene define functional domains of the precursor. *Journal of Biological Chemistry,* 260**,** 13013-13017.
LONOVICS, J., DEVITT, P., WATSON, L. C., RAYFORD, P. L. & THOMPSON, J. C. 1981. Pancreatic polypeptide: A review. *Archives of Surgery,* 116**,** 1256-1264.
MACDONALD, M. J. 1995. Influence of glucose on pyruvate carboxylase expression in pancreatic islets. *Archives of biochemistry and biophysics,* 319**,** 128-132.
MACLEAN, N. & OGILVIE, R. F. 1955. Quantitative estimation of the pancreatic islet tissue in diabetic subjects. *Diabetes,* 4**,** 367-376.
MAKINO, S., KUNIMOTO, K., MURAOKA, Y., MIZUSHIMA, Y., KATAGIRI, K. & TOCHINO, Y. 1980a. Breeding of a non-obese, diabetic strain of mice. *Jikken dobutsu. Experimental animals,* 29**,** 1-13.
MAKINO, S. A., KUNIMOTO, K., MURAOKA, Y., MIZUSHIMA, Y., KATAGIRI, K. & TOCHINO, Y. 1980b. Breeding of a non-obese, diabetic strain of mice. *Jikken dobutsu. Experimental animals,* 29**,** 1-13.
MANNERING, S., PATHIRAJA, V. & KAY, T. 2016. The case for an autoimmune aetiology of type 1 diabetes. *Clinical & Experimental Immunology,* 183**,** 8-15.
MARCELIN, G., LIU, S.-M., SCHWARTZ, G. J. & CHUA, S. C. 2013. Identification of a loss-of-function mutation in Ube2l6 associated with obesity resistance. *Diabetes,* 62**,** 2784-2795.
MATHIS, D. J., BENOIST, C., WILLIAMS, V. E., KANTER, M. & MCDEVITT, H. O. 1983. Several mechanisms can account for defective E alpha gene expression in different mouse haplotypes. *Proceedings of the National Academy of Sciences,* 80**,** 273-277.
MATVEYENKO, A. & BUTLER, P. 2008. Relationship between β - cell mass and diabetes onset. *Diabetes, Obesity and Metabolism,* 10**,** 23-31.

MCDEVITT, H. 1981. THE ROLE OF H‐2 I REGION GENES IN REGULATION OF THE IMMUNE RESPONSE. *International Journal of Immunogenetics,* 8**,** 287-295.
MCGARRY, J. D. 2002. Banting lecture 2001 Dysregulation of fatty acid metabolism in the etiology of type 2 diabetes. *Diabetes,* 51**,** 7-18.
MEYER, K. A., KUSHI, L. H., JACOBS, D. R., SLAVIN, J., SELLERS, T. A. & FOLSOM, A. R. 2000. Carbohydrates, dietary fiber, and incident type 2 diabetes in older women. *The American journal of clinical nutrition,* 71**,** 921-930.
MITRAKOU, A., KELLEY, D., MOKAN, M., VENEMAN, T., PANGBURN, T., REILLY, J. & GERICH, J. 1992. Role of reduced suppression of glucose production and diminished early insulin release in impaired glucose tolerance. *New England Journal of Medicine,* 326**,** 22-29.
MOJSOV, S., WEIR, G. & HABENER, J. 1987. Insulinotropin: glucagon-like peptide I (7-37) co-encoded in the glucagon gene is a potent stimulator of insulin release in the perfused rat pancreas. *Journal of clinical investigation,* 79**,** 616.
MONTGOMERY, M. K., HALLAHAN, N. L., BROWN, S., LIU, M., MITCHELL, T. W., COONEY, G. J. & TURNER, N. 2013. Mouse strain-dependent variation in obesity and glucose homeostasis in response to high-fat feeding. *Diabetologia,* 56**,** 1129-1139.
MUOIO, D. M. & NEWGARD, C. B. 2008. Molecular and metabolic mechanisms of insulin resistance and β-cell failure in type 2 diabetes. *Nature reviews Molecular cell biology,* 9**,** 193-205.
MURPHY, M. P. 2015. Redox Modulation by Reversal of the Mitochondrial Nicotinamide Nucleotide Transhydrogenase. *Cell metabolism,* 22**,** 363-365.
NAGGERT JK, S. K., SMITH RV, PAIGEN B, PETERS LL May 2006. Diet effects on bone mineral density and content, body composition, and plasma glucose, leptin, and insulin levels. *MPD,* 143.
NATHAN DM ET AL. 1993. The effect of intensive treatment of diabetes on the development and progression of long-term complications in insulin-dependent diabetes mellitus. *N Engl j Med,* 1993**,** 977-986.
NATHAN DM ET AL. 2005. Intensive diabetes treatment and cardiovascular disease in patients with type 1 diabetes. *N Engl J Med,* 2005**,** 2643-2653.
NEWGARD, B. & MCGARRY, J. D. 1995. Metabolic coupling factors in pancreatic β-cell signal transduction. *Annual review of biochemistry,* 64**,** 689-719.
NHMRC 2013. Australian code for the care and use of animals for scientific purposes. 8th edition.
NIELSEN, E.-M. D., HANSEN, L., CARSTENSEN, B., ECHWALD, S. M., DRIVSHOLM, T., GLÜMER, C., THORSTEINSSON, B., BORCH-JOHNSEN, K., HANSEN, T. & PEDERSEN, O. 2003. The E23K variant of Kir6. 2 associates with impaired post-OGTT serum insulin response and increased risk of type 2 diabetes. *Diabetes,* 52**,** 573-577.
NOLAN, C., LEAHY, J., DELGHINGARO-AUGUSTO, V., MOIBI, J., SONI, K., PEYOT, M.-L., FORTIER, M., GUAY, C., LAMONTAGNE, J. & BARBEAU, A. 2006. Beta cell compensation for insulin resistance in Zucker fatty rats: increased lipolysis and fatty acid signalling. *Diabetologia,* 49**,** 2120-2130.
NOLAN, C. J., DAMM, P. & PRENTKI, M. 2011. Type 2 diabetes across generations: from pathophysiology to prevention and management. *The Lancet,* 378**,** 169-181.
NOLAN, C. J. & DELGHINGARO-AUGUSTO, V. 2014. RNA sequencing of all transcripts and how islet β-cells fail. *Diabetes,* 63**,** 1823-1825.
NOLAN, C. J. & PRENTKI, M. 2008. The islet β-cell: fuel responsive and vulnerable. *Trends in Endocrinology & Metabolism,* 19**,** 285-291.
NOTKINS, A. L. 2002. Immunologic and genetic factors in type 1 diabetes. *Journal of Biological Chemistry,* 277**,** 43545-43548.
OGAWA, N., LIST, J. F., HABENER, J. F. & MAKI, T. 2004. Cure of overt diabetes in NOD mice by transient treatment with anti-lymphocyte serum and exendin-4. *Diabetes,* 53**,** 1700-1705.
PAOLISSO, G. & HOWARD, B. 1998. Role of non‐esterified fatty acids in the pathogenesis of Type 2 diabetes mellitus. *Diabetic medicine,* 15**,** 360-366.

PARSONS, J. A., BRELJE, T. C. & SORENSON, R. L. 1992. Adaptation of islets of Langerhans to pregnancy: increased islet cell proliferation and insulin secretion correlates with the onset of placental lactogen secretion. *Endocrinology,* 130**,** 1459-1466.
PERRY, R. J., PENG, L., BARRY, N. A., CLINE, G. W., ZHANG, D., CARDONE, R. L., PETERSEN, K. F., KIBBEY, R. G., GOODMAN, A. L. & SHULMAN, G. I. 2016. Acetate mediates a microbiome–brain–β-cell axis to promote metabolic syndrome. *Nature,* 534**,** 213-217.
PICK, A., CLARK, J., KUBSTRUP, C., LEVISETTI, M., PUGH, W., BONNER-WEIR, S. & POLONSKY, K. 1998. Role of apoptosis in failure of beta-cell mass compensation for insulin resistance and beta-cell defects in the male Zucker diabetic fatty rat. *Diabetes,* 47**,** 358-364.
PILLAI, O. & PANCHAGNULA, R. 2001. Insulin therapies–past, present and future. *Drug discovery today,* 6**,** 1056-1061.
PINAR, H., PINAR, T. & SINGER, D. B. 2000. Beta-cell hyperplasia in macrosomic infants and fetuses of nondiabetic mothers. *Pediatric and Developmental Pathology,* 3**,** 48-52.
PODOLIN, P. L., PRESSEY, A., DELARATO, N. H., FISCHER, P. A., PETERSON, L. B. & WICKER, L. S. 1993. I-E+ nonobese diabetic mice develop insulitis and diabetes. *The Journal of experimental medicine,* 178**,** 793-803.
POITOUT, V. & ROBERTSON, R. P. 2008. Glucolipotoxicity: fuel excess and β-cell dysfunction. *Endocrine reviews,* 29**,** 351-366.
POLONSKY, K. 2000. Dynamics of insulin secretion in obesity and diabetes. *International Journal of Obesity,* 24**,** S29-S31.
PORETSKY, L. 2010. *Principles of diabetes mellitus*, Springer.
PORTE, D. 1991. β-cells in type II diabetes mellitus. *Diabetes,* 40**,** 166-180.
PRENTKI, M., JOLY, E., EL-ASSAAD, W. & RODUIT, R. 2002. Malonyl-CoA Signaling, Lipid Partitioning, and Glucolipotoxicity Role in β-Cell Adaptation and Failure in the Etiology of Diabetes. *Diabetes,* 51**,** S405-S413.
PRENTKI, M. & MADIRAJU, S. M. 2012. Glycerolipid/free fatty acid cycle and islet β-cell function in health, obesity and diabetes. *Molecular and cellular endocrinology,* 353**,** 88-100.
PRENTKI, M., MATSCHINSKY, F. M. & MADIRAJU, S. M. 2013. Metabolic signaling in fuel-induced insulin secretion. *Cell metabolism,* 18**,** 162-185.
PRENTKI, M. & NOLAN, C. J. 2006a. Islet β cell failure in type 2 diabetes. *Journal of Clinical Investigation,* 116**,** 1802.
PRENTKI, M. & NOLAN, C. J. 2006b. Islet β cell failure in type 2 diabetes. *The Journal of clinical investigation,* 116**,** 1802-1812.
QIU, J., OGUS, S., MOUNZIH, K., EWART-TOLAND, A. & CHEHAB, F. 2001. Leptin-deficient mice backcrossed to the BALB/cJ genetic background have reduced adiposity, enhanced fertility, normal body temperature, and severe diabetes. *Endocrinology,* 142**,** 3421-3425.
QUESADA, I., TUDURÍ, E., RIPOLL, C. & NADAL, Á. 2008. Physiology of the pancreatic α-cell and glucagon secretion: role in glucose homeostasis and diabetes. *Journal of Endocrinology,* 199**,** 5-19.
RADLEY-CRABB, H. G., FIOROTTO, M. L. & GROUNDS, M. D. 2011. The different impact of a high fat diet on dystrophic mdx and control C57Bl/10 mice. *PLOS Currents Muscular Dystrophy*.
RAHIER, J., GUIOT, Y., GOEBBELS, R., SEMPOUX, C. & HENQUIN, J.-C. 2008. Pancreatic β-cell mass in European subjects with type 2 diabetes. *Diabetes, Obesity and Metabolism,* 10**,** 32-42.
REAVEN, G. 1995. The fourth musketeer—from Alexandre Dumas to Claude Bernard. *Diabetologia,* 38**,** 3-13.
REICHLIN, S. 1983. Somatostatin. *The New England journal of medicine,* 309**,** 1495-1501.
RHOADES, R. A. & BELL, D. R. 2012. *Medical Phisiology: Principles for Clinical Medicine*, Lippincott Williams & Wilkins.

RORSMAN, P. 2005. Insulin secretion: function and therapy of pancreatic beta-cells in diabetes: review. *South African Journal of Diabetes and Vascular Disease,* 2**,** p. 109-113.
ROY, S. S., MUKHERJEE, M., BHATTACHARYA, S., MANDAL, C., KUMAR, L. R., DASGUPTA, S., BANDYOPADHYAY, I. & WAKABAYASHI, K. 2003. A new cell secreting insulin. *Endocrinology,* 144**,** 1585-1593.
SAISHO, Y., MARUYAMA, T., HIROSE, H. & SARUTA, T. 2007. Relationship between proinsulin-to-insulin ratio and advanced glycation endproducts in Japanese type 2 diabetic subjects. *Diabetes research and clinical practice,* 78**,** 182-188.
SHE, J.-X. & MARRON, M. P. 1998. Genetic susceptibility factors in type 1 diabetes: linkage, disequilibrium and functional analyses. *Current opinion in immunology,* 10**,** 682-689.
SIMECEK, P., CHURCHILL, G. A., YANG, H., ROWE, L. B., HERBERG, L., SERREZE, D. V. & LEITER, E. H. 2015. Genetic analysis of substrain divergence in non-obese diabetic (NOD) mice. *G3: Genes| Genomes| Genetics,* 5**,** 771-775.
SOCHA, L., SILVA, D., LESAGE, S., GOODNOW, C. & PETROVSKY, N. 2003. The role of endoplasmic reticulum stress in nonimmune diabetes: NOD. k iHEL, a novel model of β cell death. *Annals of the New York Academy of Sciences,* 1005**,** 178-183.
STEFAN, Y., ORCI, L., MALAISSE-LAGAE, F., PERRELET, A., PATEL, Y. & UNGER, R. H. 1982. Quantitation of endocrine cell content in the pancreas of nondiabetic and diabetic humans. *Diabetes,* 31**,** 694-700.
STEINER, D., CLARK, J., NOLAN, C., RUBENSTEIN, A., MARGOLIASH, E., ATEN, B. & OYER, P. 1969. Proinsulin and the biosynthesis of insulin. *Recent progress in hormone research,* 25**,** 207.
STRAKOSCH, C. 2004. The discovery of insulin. *University Endocrine Department. Greenslopes Private Hospital: Brisbane,* 20.
STRAUB, S. G. & SHARP, G. W. 2002. Glucose‐stimulated signaling pathways in biphasic insulin secretion. *Diabetes/metabolism research and reviews,* 18**,** 451-463.
STRETTON, A. O. 2002. The first sequence: Fred Sanger and insulin. *Genetics,* 162**,** 527-532.
STUMVOLL, M., GOLDSTEIN, B. J. & VAN HAEFTEN, T. W. 2005. Type 2 diabetes: principles of pathogenesis and therapy. *The Lancet,* 365**,** 1333-1346.
SUCKALE, J. & SOLIMENA, M. 2008. Pancreas islets in metabolic signaling-focus on the beta-cell. *Front. Biosci,* 13**,** 7156-7171.
TAMBORLANE, W. V., BECK, R. W., BODE, B. W., BUCKINGHAM, B., CHASE, H. P., CLEMONS, R., FIALLO-SCHARER, R., FOX, L. A., GILLIAM, L. K. & HIRSCH, I. B. 2008. Continuous glucose monitoring and intensive treatment of type 1 diabetes. *The New England journal of medicine,* 359**,** 1464-1476.
THAYER, T. C., WILSON, S. B. & MATHEWS, C. E. 2010. Use of nonobese diabetic mice to understand human type 1 diabetes. *Endocrinology and metabolism clinics of North America,* 39**,** 541-561.
THOMAS, H. E., MCKENZIE, M. D., ANGSTETRA, E., CAMPBELL, P. D. & KAY, T. W. 2009. Beta cell apoptosis in diabetes. *Apoptosis,* 14**,** 1389-1404.
TIROSH, A., SHAI, I., BITZUR, R., KOCHBA, I., TEKES-MANOVA, D., ISRAELI, E., SHOCHAT, T. & RUDICH, A. 2008. Changes in triglyceride levels over time and risk of type 2 diabetes in young men. *Diabetes Care,* 31**,** 2032-2037.
TODD, J. A. 2010. Etiology of type 1 diabetes. *Immunity,* 32**,** 457-467.
TODD, J. A., AITMAN, T. J., CORNALL, R. J., GHOSH, S., HALL, J. R., HEARNE, C. M., KNIGHT, A. M., LOVE, J. M., MCALEER, M. A. & PRINS, J.-B. 1991. Genetic analysis of autoimmune type 1 diabetes mellitus in mice. *Nature,* 351**,** 542-547.
TOKUYAMA, Y., STURIS, J., DEPAOLI, A. M., TAKEDA, J., STOFFEL, M., TANG, J., SUN, X., POLONSKY, K. S. & BELL, G. I. 1995. Evolution of β-cell dysfunction in the male Zucker diabetic fatty rat. *Diabetes,* 44**,** 1447-1457.
TUOMI, T., SANTORO, N., CAPRIO, S., CAI, M., WENG, J. & GROOP, L. 2014. The many faces of diabetes: a disease with increasing heterogeneity. *The Lancet,* 383**,** 1084-1094.

TUOMILEHTO, J., LINDSTRÖM, J., ERIKSSON, J. G., VALLE, T. T., HÄMÄLÄINEN, H., ILANNE-PARIKKA, P., KEINÄNEN-KIUKAANNIEMI, S., LAAKSO, M., LOUHERANTA, A. & RASTAS, M. 2001. Prevention of type 2 diabetes mellitus by changes in lifestyle among subjects with impaired glucose tolerance. *New England Journal of Medicine,* 344**,** 1343-1350.

TURNER ET AL. 1995. UK Prospective Diabetes Study 16: overview of 6 years' therapy of type II diabetes: a progressive disease. *Diabetes,* 44**,** 1249-1258.

TURNER ET AL. 1998. Intensive blood-glucose control with sulphonylureas or insulin compared with conventional treatment and risk of complications in patients with type 2 diabetes (UKPDS 33). *The Lancet,* 352**,** 837-853.

USSAR, S., GRIFFIN, N. W., BEZY, O., FUJISAKA, S., VIENBERG, S., SOFTIC, S., DENG, L., BRY, L., GORDON, J. I. & KAHN, C. R. 2015. Interactions between gut microbiota, host genetics and diet modulate the predisposition to obesity and metabolic syndrome. *Cell metabolism,* 22**,** 516-530.

VAN DER ZIJL, N. J., GOOSSENS, G. H., MOORS, C. C., VAN RAALTE, D. H., MUSKIET, M. H., POUWELS, P. J., BLAAK, E. E. & DIAMANT, M. 2010. Ectopic fat storage in the pancreas, liver, and abdominal fat depots: impact on β-cell function in individuals with impaired glucose metabolism. *The Journal of Clinical Endocrinology & Metabolism,* 96**,** 459-467.

VIEIRA, E., SALEHI, A. & GYLFE, E. 2007. Glucose inhibits glucagon secretion by a direct effect on mouse pancreatic alpha cells. *Diabetologia,* 50**,** 370-379.

VINIK, A. I. & JENKINS, D. J. 1988. Dietary fiber in management of diabetes. *Diabetes Care,* 11**,** 160-173.

VIONNET, N., STOFFEL, M., TAKEDA, J., YASUDA, K., BELL, G., ZOUALI, H., LESAGE, S., VELHO, G., IRIS, F. & PASSA, P. 1992. Nonsense mutation in the glucokinase gene causes early-onset non-insulin-dependent diabetes mellitus.

WAHREN, J., KALLAS, Å. & SIMA, A. A. 2012. The clinical potential of C-peptide replacement in type 1 diabetes. *Diabetes,* 61**,** 761-772.

WEIR, G. C. & BONNER-WEIR, S. 2004. Five stages of evolving beta-cell dysfunction during progression to diabetes. *Diabetes,* 53**,** S16-S21.

WEYER, C., FUNAHASHI, T., TANAKA, S., HOTTA, K., MATSUZAWA, Y., PRATLEY, R. E. & TATARANNI, P. A. 2001. Hypoadiponectinemia in obesity and type 2 diabetes: close association with insulin resistance and hyperinsulinemia. *The Journal of Clinical Endocrinology & Metabolism,* 86**,** 1930-1935.

WHEELER, E. & BARROSO, I. 2011. Genome-wide association studies and type 2 diabetes. *Briefings in functional genomics,* 10**,** 52-60.

WHITE, M. F. 2003. Insulin signaling in health and disease. *Science,* 302**,** 1710-1711.

WICKER, L., APPEL, M., DOTTA, F., PRESSEY, A., MILLER, B., DELARATO, N., FISCHER, P., BOLTZ, R. & PETERSON, L. 1992. Autoimmune syndromes in major histocompatibility complex (MHC) congenic strains of nonobese diabetic (NOD) mice. The NOD MHC is dominant for insulitis and cyclophosphamide-induced diabetes. *The Journal of experimental medicine,* 176**,** 67-77.

WICKER, L. S., MILLER, B. J., COKER, L. Z., MCNALLY, S. E., SCOTT, S., MULLEN, Y. & APPEL, M. 1987. Genetic control of diabetes and insulitis in the nonobese diabetic (NOD) mouse. *The Journal of experimental medicine,* 165**,** 1639-1654.

WICKER, L. S., TODD, J. A. & PETERSON, L. B. 1995. Genetic control of autoimmune diabetes in the NOD mouse. *Annual review of immunology,* 13**,** 179-200.

WILLIAMS, K., SHACKEL, N., GORRELL, M., MCLENNAN, S. & TWIGG, S. 2012. Diabetes and nonalcoholic fatty liver disease: a pathogenic duo. *Endocrine reviews,* 34**,** 84-129.

WING, R. R., GOLDSTEIN, M. G., ACTON, K. J., BIRCH, L. L., JAKICIC, J. M., SALLIS, J. F., SMITH-WEST, D., JEFFERY, R. W. & SURWIT, R. S. 2001. Behavioral science research in diabetes lifestyle changes related to obesity, eating behavior, and physical activity. *Diabetes care,* 24**,** 117-123.

WOOD, E. 2007. The Oxford dictionary of biochemistry and molecular biology. Wiley Online Library.

WOODS, S. C., LUTZ, T. A., GEARY, N. & LANGHANS, W. 2006. Pancreatic signals controlling food intake; insulin, glucagon and amylin. *Philosophical Transactions of the Royal Society B: Biological Sciences,* 361**,** 1219-1235.

XU, G., STOFFERS, D. A., HABENER, J. F. & BONNER-WEIR, S. 1999. Exendin-4 stimulates both beta-cell replication and neogenesis, resulting in increased beta-cell mass and improved glucose tolerance in diabetic rats. *Diabetes,* 48**,** 2270-2276.

YANG, W.-S., LEE, W.-J., FUNAHASHI, T., TANAKA, S., MATSUZAWA, Y., CHAO, C.-L., CHEN, C.-L., TAI, T.-Y. & CHUANG, L.-M. 2001. Weight reduction increases plasma levels of an adipose-derived anti-inflammatory protein, adiponectin. *The Journal of Clinical Endocrinology & Metabolism,* 86**,** 3815-3819.

YIN, W., LIAO, D., KUSUNOKI, M., XI, S., TSUTSUMI, K., WANG, Z., LIAN, X., KOIKE, T., FAN, J. & YANG, Y. 2004. NO-1886 decreases ectopic lipid deposition and protects pancreatic beta cells in diet-induced diabetic swine. *Journal of endocrinology,* 180**,** 399-408.

YOON, J.-W. & JUN, H.-S. 2005. Autoimmune destruction of pancreatic β cells. *American journal of therapeutics,* 12**,** 580-591.

YOSTEN, G. L. & KOLAR, G. R. 2015. The physiology of proinsulin C-peptide: unanswered questions and a proposed model. *Physiology,* 30**,** 327-332.

ZIMMET, P. Z. 1988. Primary prevention of diabetes mellitus. *Diabetes Care,* 11**,** 258-262.

ZIOLKOWSKI, A. F., POPP, S. K., FREEMAN, C., PARISH, C. R. & SIMEONOVIC, C. J. 2012. Heparan sulfate and heparanase play key roles in mouse β cell survival and autoimmune diabetes. *The Journal of clinical investigation,* 122**,** 132.

ZRAIKA, S., DUNLOP, M. E., PROIETTO, J. & ANDRIKOPOULOS, S. 2004. Elevated SNAP-25 is associated with fatty acid-induced impairment of mouse islet function. *Biochemical and biophysical research communications,* 317**,** 472-477.

Appendix I

The constituents and preparation of solution mentioned in the Materials and Methods Chapter are shown.

General Solutions

Phosphate Buffered Saline (PBS)

For preparation of 1 L, the following was added:

1 L of MilliQH_2O

2 PBS tablets (Medicago AB, Uppsala, Sweden)

Solution was sterile-filtered using 0.22µm filter and stored at 4°C.

HEPES 1M

HEPES 238.4g (Sigma Aldrich, CA, USA)

dH2O 1000ml

Phosphate buffer

Final volume (1 litre)

9.3 g of EDTA (Sigma Aldrich, CA, USA)

6.9 g of NaH_2PO_4 (Cat# S5011, Sigma Aldrich, St.Leus,, USA)

0.1g Thimerosal (0.01%) (Cat# T5125, Sigma Aldrich, St.Leus,, USA)

(Light sensitive product)

Solution was pH adjusted to 7.5 using NaOH 10mmol/L to 1 L using dH_2O then was sterile-filtered using 20µm filter. The bottle containing the solution was wrapped in aluminium foil and stored at 4°C.

PEG phosphate buffer (Phosphate buffer + PEG 3%)

30g of PEG 8000 (polyethylene glycol) (Cat #P2139, Sigma Aldrich, CA, USA)

1000 ml phosphate buffer

Keep at 4°C.

BSA phosphate buffer (Phosphate buffer + 1% BSA)

10 g BSA- RIA grade (Sigma: A-7888)

1000 ml phosphate buffer

Keep at 4

Appendix 2

H& E Scoring sheet

mouse ID	Diet	Blinded ID	Scoring parameter					
			pancreas (0=normal 1= abnormal)					
			pancreas (0 =none;1= acute inflammation ;2 - saponification and acute inflammation 3= chronic inflammation; 4=1 and 3)					
			pancreas - severity of acute inflammation (1= minimal 2=mild 3= moderate 4= severe)					
			pancreas - severity of chronic inflammation (1= minimal 2=mild 3= moderate 4= severe)					
			location of inflammation (1-lobule; 2= periductal; 3= perislet; 4=1 and 2; 5= 2 and 3; 6= all					
			periductal inflammation (1=<10% of ducts affects ; 2=10=50%; 3= >50%)					
			pancreas fat (0= absent 1= present)					
			fat in exocrine pancreas (1= infrequent 2 = mild (some) 3= moderate 4=severe)					
			islets (0=normal; 1= abnormal)					
			H&E Islet structure (1 normal, 2 some islets mildly dysmorphic, 3 some islets moderately dysmorphic, 4 some islets severely dysmorphic 5= small)					

Appendix 3

Calculation of beta-cell mass:

1. % β-cell area per pancreas= $\frac{\text{Islet Sum Area x 100}}{\text{Pancreas Area}}$

2. Average number of the % β-cell area per pancreas (L1,L2 and L3)

3. $\frac{\text{\% β-cell (average from all levels)}}{100}$ X weight of the pancreas (mg)